



<https://theses.gla.ac.uk/>

Theses Digitisation:

<https://www.gla.ac.uk/myglasgow/research/enlighten/theses/digitisation/>

This is a digitised version of the original print thesis.

Copyright and moral rights for this work are retained by the author

A copy can be downloaded for personal non-commercial research or study,
without prior permission or charge

This work cannot be reproduced or quoted extensively from without first
obtaining permission in writing from the author

The content must not be changed in any way or sold commercially in any
format or medium without the formal permission of the author

When referring to this work, full bibliographic details including the author,
title, awarding institution and date of the thesis must be given

Enlighten: Theses

<https://theses.gla.ac.uk/>
research-enlighten@glasgow.ac.uk

TRACER STUDIES ON THE SOLID STATE
- DIFFUSION IN HYDROGEN BONDED SOLIDS

A Thesis submitted for the degree of

Doctor of Philosophy

of the

University of Glasgow

by

Andrew Roxburgh Mc Ghie. B.Sc. A.R.C.S.T.

December 1965

ProQuest Number: 10647004

All rights reserved

INFORMATION TO ALL USERS

The quality of this reproduction is dependent upon the quality of the copy submitted.

In the unlikely event that the author did not send a complete manuscript and there are missing pages, these will be noted. Also, if material had to be removed, a note will indicate the deletion.



ProQuest 10647004

Published by ProQuest LLC (2017). Copyright of the Dissertation is held by the Author.

All rights reserved.

This work is protected against unauthorized copying under Title 17, United States Code
Microform Edition © ProQuest LLC.

ProQuest LLC.
789 East Eisenhower Parkway
P.O. Box 1346
Ann Arbor, MI 48106 – 1346

ABSTRACT

Ubbelohde has proposed a proton transfer mechanism to explain electrical conductivity studies on a series of crystalline organic acids and it has been suggested that conductivity increases with the degree of co-operative hydrogen bonding in the crystal. Experiments have been carried out to test this hypothesis by studying the conductivity and the rate of proton diffusion, using tritium as tracer, in the same single crystals of two organic acids exhibiting different degrees of co-operative hydrogen bonding; benzoic acid which exists as a cyclic dimer in the solid state and acetic acid which has linear chains of co-operative hydrogen bonds extending through the crystal.

The acids were purified by distillation, sublimation and zone refining techniques and single crystals were grown from the melt in a Bridgman oven. Diffusion was studied by a sectioning technique using tritium labelled benzoic and acetic acids to obtain the hydrogen diffusion rates and carbon-14 labelled benzoic acid was used to measure the diffusion coefficient of the bulk molecule.

The electrical conductivity of benzoic acid was found to be very low in single crystals, being less than $10^{-14} \text{ ohm}^{-1} \text{ cm}^{-1}$ 70° below the melting point, contrary to measurements by Ubbelohde but agreeing with more recent measurements by Eley. A proton conductivity was found, however, in oxalic acid dihydrate, a co-operatively hydrogen bonded acid, which was comparable to

that found in other hydrogen bonded systems.

A tritium diffusion was observed in benzoic acid which was considerably faster than the bulk diffusion and which could not be explained by a proton diffusion mechanism. This tritium diffusion was found to vary with the water content in the diffusion cell but a lower limit was obtained which satisfied the Arrhenius equation

$$D = 0.5^{+2.0}_{-0.4} \cdot \exp \left[- \frac{20,000 \pm 1,300}{RT} \right]$$

Diffusion studies in p-terphenyl doped benzoic acid crystals, deuterio benzoic acid and polycrystalline benzoic acid have helped to elucidate the mechanism which is believed to be the diffusion of water molecules trapped in the crystals through interstitial defects. The carbon-14 bulk diffusion in benzoic acid was found to obey the following Arrhenius equation.

$$D = (1.8^{+7.6}_{-1.78} \times 10^2) \times 10^{12} \cdot \exp \left[- \frac{44,000 \pm 4,400}{RT} \right]$$

and can be explained in terms of a relaxed vacancy diffusion mechanism.

Conductivity and diffusion studies in acetic acid were both found to be greatly affected by the presence of moisture and no definite conclusion could be reached regarding proton conductivity in this system.

ACKNOWLEDGMENTS.

The author wishes to express his sincere thanks to his supervisor, Dr. J. N. Sherwood, for his guidance, help and encouragement throughout this period of research.

The author also wishes to thank Mrs. R. Fergie for typing the manuscript and his wife, Anne, for tracing all diagrams.

Thanks are also due to the Scientific Research Council for the award of a maintenance grant during this course of study.

CONTENTS

PAGE

INTRODUCTION - - - - - 1

CHAPTER I PURIFICATION AND CRYSTAL GROWTH

1. Introduction - - - - - 12

2. Purification of Benzoic Acid - - - - - 17

 a) Distillation - - - - - 18

 b) Zone Refining - - - - - 20

3. Design of Benzoic Acid Crystals Growing Ovens - - - 27

4. Growth of Doped Benzoic Acid Crystals - - - - - 35

5. Purity of Benzoic Acid - - - - - 40

6. Growth of Acetic Acid Crystals - - - - - 45

CHAPTER II DIFFUSION AND CONDUCTIVITY EXPERIMENTS

1. Introduction to Diffusion - - - - - 49

2. Preparation of Radioactive Isotopes - - - - - 54

3. Deposition Systems - - - - - 59

4. Diffusion Anneal Conditions - - - - - 64

5. The Sectioning Technique - - - - - 67

6. Determination of Radioactivity in the Crystal Sections
77

7. Preparation of Diffusion Samples - - - - - 83

8. The Diffusion Experiments - - - - - 84

9. The Exchange Experiments - - - - - 85

10. Conductivity Studies - - - - - 87

CHAPTER III THE RESULTS AND THEIR INTERPRETATION

PAGE

a Tritium and Carbon 14 Diffusion in Benzoic Acid Single Crystals	91
b Tritium and Carbon 14 Diffusion in Polycrystalline Benzoic Acid.	104
c Tritium Exchange between Benzoic Acid/Water Vapour	109
d Tritium Diffusion in Acetic Acid - - - - -	111
e The Conductivity Studies - - - - -	113
f Tabulated Results - - - - -	117

CHAPTER IV DISCUSSION OF THE RESULTS

a Proton Transport in Hydrogen Bonded Solids.	
1 Previous Work - - - - -	118
11 Conductivity Results - - - - -	123
b Diffusion in Benzoic Acid	
1 Summary of Results - - - - -	128
11 Molecular Diffusion - - - - -	130
111 Grain Boundary Diffusion - - - - -	135
IV Tritium Diffusion - - - - -	137
c Diffusion in Acetic Acid - - - - -	144
d Conclusion - - - - -	145
e Future Work - - - - -	146

REFERENCES

APPENDICES

LIST OF FIGURES

FIGURE

- 1 a Unit cell of benzoic acid.
b Unit cell of acetic acid.
- 2 Principle of single crystal growth.
- 3 Distillation of benzoic acid into growing tube.
- 4 Automatic zone refiner No. 1.
- 5 Automatic zone refiner No. 2.
- 6 Benzoic acid crystal growing oven No. 1.
- 7 Temperature gradients in crystal growing ovens.
- 8 Crystal growing oven No. 2.
- 9 Crystal growing vessels.
- 10 U.V. spectra of p-Terphenyl and benzoic acid.
- 11 Purification and crystal growth of deuterobenzoic acid.
- 12 Freezing point apparatus.
- 13 Water determination in benzoic acid.
- 14 Tritiation of benzoic acid.
- 15 Vacuum sublimation apparatus.
- 16 Tritiation of acetic acid.
- 17 Benzoic acid evaporator.
- 18 Acetic acid deposition system.
- 19 Diffusion cells.
- 20 Thermistor controller circuit.
- 21 Fine adjustment chuck.
- 22 Suction apparatus.
- 23 U.V. calibration of benzoic acid in cyclohexane.
- 24 a Effect of scintillator volume on tritium counting efficiency.
b Effect of benzoic acid on tritium counting efficiency.
- 25 Conductivity cells.
- 26 Graph of $\log_{10} A$ VS $\frac{1}{L}$ for tritium diffusion \perp (001) plane in benzoic acid (large vessels).

- 27 Arrhenius plots for tritium and C^{14} diffusion in benzoic acid single crystals.
- 28 a, b. Graph $\log_{10} A$ VS \bar{X}^2 for tritium diffusion \perp^r (001) plane in benzoic acid small vessels.
- 29 Graph $\log_{10} A$ VS \bar{X}^2 for tritium diffusion \perp^r (001) plane in benzoic acid under dry conditions.
- 30 Graph $\log_{10} A$ VS \bar{X}^2 for tritium diffusion \perp^r (001) plane in deuterobenzoic acid and p-Terphenyl doped benzoic acid.
- 31 Graph $\log_{10} A$ VS \bar{X}^2 for tritium diffusion \perp^r (001) plane in benzoic and deuterobenzoic acid simultaneously.
- 32 Graph $\log_{10} A$ VS \bar{X}^2 for tritium diffusion \perp^r (001) plane in benzoic acid from THO vapour.
- 33 a, b. Graph $\log_{10} A$ VS \bar{X}^2 for C^{14} diffusion \perp^r (001) plane in benzoic acid.
- 34 Graph of $\log_{10} A$ VS \bar{X}^2 for C^{14} diffusion parallel to (001) plane in benzole acid.
- 35 Graph of $\log_{10} A$ VS \bar{X} for C^{14} diffusion in benzoic acid compacts.
- 36 Graph of $\log_{10} A$ VS \bar{X} for tritium diffusion in benzoic acid compacts.
- 37 Arrhenius plots for grain boundary diffusion in benzoic acid compacts.
- 38 Graph R_2 VS \sqrt{t} for exchange reaction between tritiated benzoic acid and water vapour.
- 39 Arrhenius plot for tritium exchange H_2O /benzoic acid.
- 40 Graph $\log_{10} A$ VS \bar{X}^2 for tritium diffusion \perp^r (100) plane in acetic acid.
- 41 A.C. conductivity in benzoic acid compacts.
- 42 Time variation of A.C. conductivity in acetic acid single crystals
- 43 a, b. A.C. and D.C. conductivity in oxalic acid dihydrate.
- 44 Schematic view of hydrogen bonded chains in crystals.

INTRODUCTION

Investigation of the physical and chemical properties of solids has, until recently, been principally confined to those materials of potential industrial importance e.g. metals, semiconducting and ionic crystals. This work has lead to a fairly well developed theory of the solid state in these systems.¹

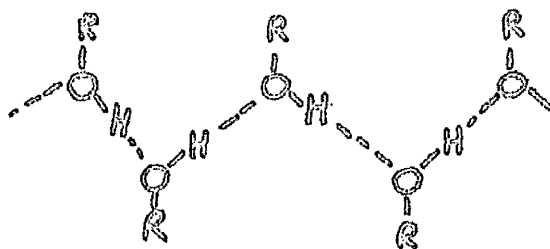
A recent upsurge in interest in organic and molecular solids has evolved, however, from the discovery of interesting semiconducting and photoconducting properties in these systems.^{2,3} Electrical and optical properties have been studied in a large number of organic solids ranging from well characterised aromatic solids like anthracene⁴ and naphthalene⁵ to more complicated, biologically interesting protein-like structures.⁶ In all systems it has been found that properties are frequently very dependent on the degree of purification and hence the crystalline perfection of the solids. The imperfections in the crystals, whether natural imperfections due to impurity molecules or non equilibrium line defects like dislocations, can greatly affect the property being studied and give rise to extrinsic properties which may completely mask the intrinsic property being investigated.

Organic solids differs from metallic and ionic solids in that their binding forces are primarily Van der Waals interactions and the molecules crystallise in the system which gives the greatest packing density⁷ except where other factors such as hydrogen bonding have an effect. There have been relatively few studies on organic solids other than electrical/optical

properties and in order to understand the basic molecular reactions occurring in these solids an extensive study is required on the properties of both 'perfect' crystals and crystals having a known and controlled defect structure.

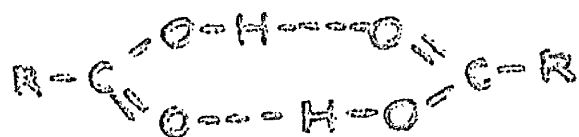
A class of organic solids which has important chemical properties and has not undergone extensive study is that in which the formation of intermolecular hydrogen bonds controls the structural arrangement of the molecules in the crystal. Hydrogen bonded organic crystals can be divided into two principle categories, co-operative and non co-operative, although some structures may contain a mixture of both. These have been reviewed by Ubbelohde and Gallacher.

Co-operative hydrogen bonding is exhibited by crystals which contain infinite chains of hydrogen bonds extending through the crystal. Typical examples of such a structure are the alcohols whose configuration can be represented schematically as



where R is a hydrocarbon group. Such co-operative assemblies can be further sub-divided into chains, sheets and three dimensional networks depending on the spatial arrangement of the hydrogen bonds.

Non co-operative systems as their name suggests are composed of closed cyclic structures e.g.



cyclic dimers as exhibited by almost all carboxylic acids.

In all cases, however, the configuration is achieved which leaves the system in its lowest potential energy configuration.

Interest has been aroused in the possible role of co-operative hydrogen bonded systems as protonic conductors. It has been suggested that hydrogen bonded hydration structures are present in protein membranes which are favourable to protonic control systems and that fast proton transport may play an important role in biological reaction kinetics.¹⁰ Fe(II) - Fe(III) oxidation has been observed in iron salts dissolved in ice and a mechanism involving proton transport along hydrogen bonded chains has been suggested.¹¹ Some experimental studies have been made to test the validity of a proton transport mechanism in co-operatively hydrogen bonded solids.

12

In 1951 Kakiuchi et al. demonstrated that current flow through cetyl alcohol occurred almost entirely by proton charge transport. They did this by observing the spectra of hydrogen discharged at the cathode after passing a current through the solid alcohol. Smyth¹³ has also proposed a proton transfer

mechanism associated with molecular rotation to explain high conductivity and dielectric loss in the higher alcohols, n-tetradecyl and hexadecyl.

The effect of the degree of co-operation on conductivity has been studied by Pollock and Ubbelohde¹⁴ in a series of organic acids and they found that as the degree of co-operation increased the conductivity increased and the activation energy decreased, the conductivity being greater in acids containing water of crystallisation. They interpreted their results as substantiating a proton conduction mechanism in hydrogen bonded solids.

A comprehensive conductimetric study has been made by Eley and his co-workers¹⁵ on systems containing the (C=O --- H - N) hydrogen bonded unit ranging from simple molecules like glycine and oxamide to polyamides and naturally occurring proteins. Only in polyamides was the conductivity due to proton migration and in all other systems the conductivity was 10^4 times lower and electronic in origin. Eley also found that the presence of adsorbed moisture on proteins greatly affect the conductivity.¹⁶ This has been shown to give proton conduction in keratin¹⁷ but electronic conduction in haemoglobin.¹⁸

Conductivity studies in ice which, though not an organic solid, is equivalent to an alcohol R-OH with $R \equiv H$, has been exhaustively studied^{10, 19, 20} and proton transport verified by this and electrolysis measurements.²¹

With the exception of ice all the above studies showing proton conductivity were made on polycrystalline compacts. It has frequently been shown, however, that compacts often give misleading results as intergranular and surface effects may occur due to the presence of adsorbed impurities e.g. oxygen and water.²² It would be preferable, therefore, to examine this proposed proton conduction in single crystals of materials in which the crystallographic orientation is known and the chemical impurity concentration and non-equilibrium defect structure can be reduced to a minimum.

As no intrinsic proton conductivity has yet been conclusively proved in hydrogen bonded organic crystals it was thought that a useful contribution could be made to organic solid state theory by attempting such an investigation in single crystals of a series of molecules exhibiting different types of co-operative hydrogen bonding.

An independent method of verifying charge transport mechanisms in ionic crystals is to measure both the bulk conductivity and the diffusion coefficient of the ion which is believed to be the charge carrier in the same single crystal over a range of temperature. If the same mechanism is responsible for both phenomena they will be related through the well known Nernst - Einstein equation.²³

$$\frac{\sigma}{D} = \frac{Ne^2}{kT}$$

which correlates the specific conductivity, σ , at temperature T with the measured diffusion coefficient, D . N is the total number of ions of the conducting species per unit volume, e the electronic charge and k Boltzmann's constant.

The Nernst-Einstein equation has been experimentally verified for ionic solids by the work of Mepother, Crooks and Maurer²⁴ who studied D.C. conductivity and Na^{24} diffusion in the same single crystals of sodium chloride. They found that the Nernst-Einstein equation was obeyed exactly in the intrinsic temperature region but not in the extrinsic region. This proved that in the intrinsic region the conductivity was due solely to the migration of sodium ions. This type of measurement has not been attempted in hydrogen bonded organic solids which are proton conductors and it was thought that such a study might yield interesting information about the nature of the charge carriers in these systems. Ubbelohde's study of organic acids¹⁴ gave specific conductivities of 10^{-6} to 10^{-7} $\text{ohm}^{-1}\text{cm}^{-1}$ for co-operatively bonded acids at temperatures well below their melting points. If this is due to proton conduction alone then the diffusion coefficient of the proton calculated from the Nernst - Einstein equation is 10^{-11} to 10^{-13} $\text{cm}^2 \text{sec}^{-1}$ which is measureable by tracer techniques.

Before embarking on such a study, however, it is essential that a suitable isotope of hydrogen is available for a diffusion study and should satisfy the following requirements

1. The isotope must be detectable in tracer amounts.
2. It must, if radioactive, have a half-life of several times the total diffusion anneal time.
3. It should not constitute a safety hazard.

Of the two known isotopes of hydrogen, deuterium, H_1^2 , is nearest to hydrogen in properties but is non-radioactive and must be determined by physical methods which are not yet sensitive enough for the experiments envisaged though an activation analysis method has recently been reported in which one mgm. samples of deuterium can be accurately determined.²⁵ The second isotope tritium, H_1^3 , does not occur naturally but is easily prepared by a $Li^6(n, \alpha)T$ nuclear transformation. It is radioactive and disintegrates with the emission of a weak β , 0.018 MeV and has a half-life of 12.3 years making it a suitable isotope for a tracer diffusion study.

An important point arises, however, over the isotope effect. In normal diffusion studies e.g. in metallurgy, this is negligible but the mass difference between tritium and hydrogen is large 3:1 hence an appreciable isotope effect may be observed if the proton diffuses alone. Studying tritium diffusion in a normal and a completely deuterated hydrogen bonded system and comparing the values obtained, however, may help to elucidate the mechanism. Isotope studies in ice²⁵ have shown that the activation energy of conduction is almost unaltered by substituting deuterium for hydrogen.

The choice of the most suitable systems to study was made with reference to the following points.

1. The systems must differentiate between the different types of hydrogen bonding, co-operative and non co-operative so that an assessment can be made of the effect of co-operation on the proton transport properties.
2. They should be thermally stable.
3. They should be obtainable in a high degree of purity.
4. They should have similar properties and crystal structure so that a direct comparison can be made between them.
5. They should not undergo a phase transition between room temperature and the melting point.
6. They should be mechanically stable and should not shatter on application of a shear stress or rapid cooling.
7. Suitable isotopically labelled molecules must be available, also in a high degree of purity.

It was decided that the mono-carboxylic acids would be the most suitable system. All normal mono-carboxylic acids crystallise as cyclic dimers with the exception of the two initial members, formic and acetic acid, which have linear chains of hydrogen bonds extending through the crystal. Two acids were chosen for study each exhibiting one type of hydrogen bonding.

Benzoic acid was chosen as the example of a non co-operative hydrogen bonded system consisting of non interacting cyclic dimers. The advantages of studying benzoic acid were:

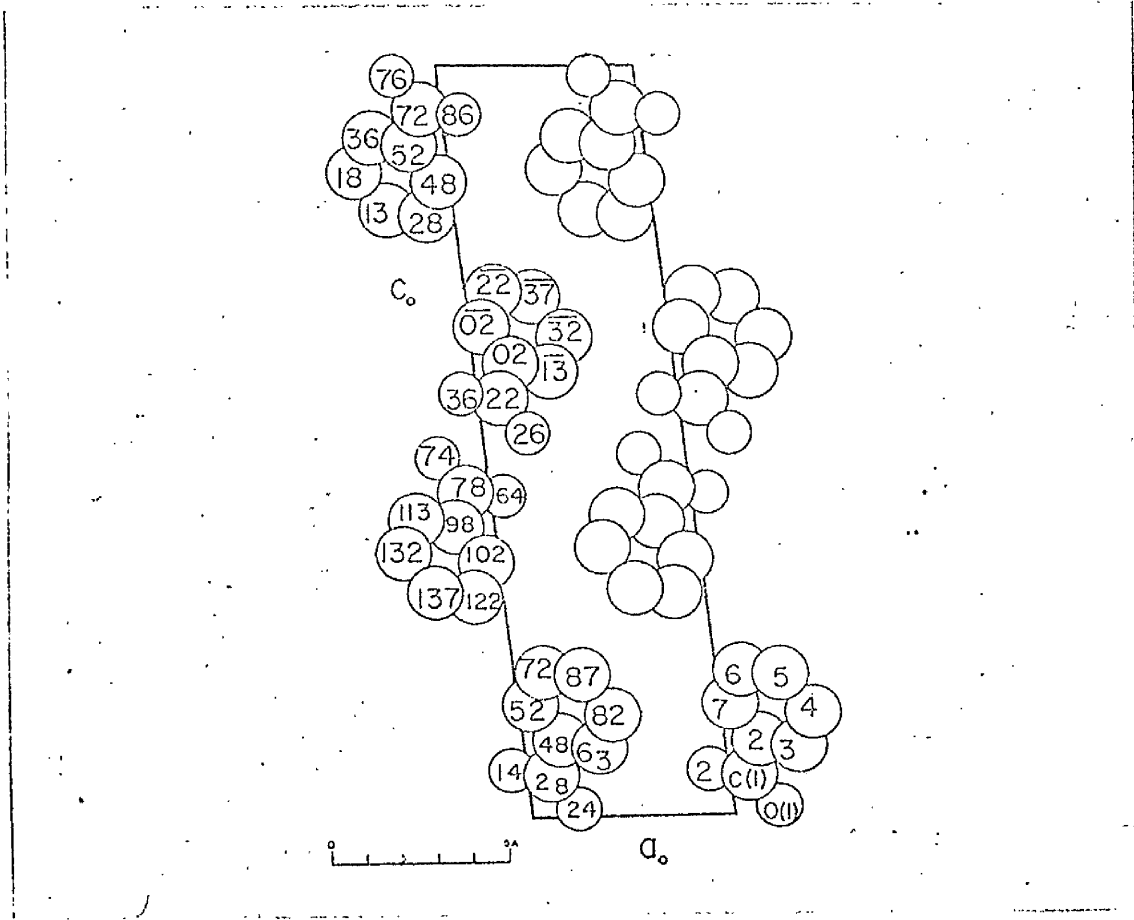


FIG. 1a. UNIT CELL BENZOIC ACID VIEWED ALONG b_0 AXIS.

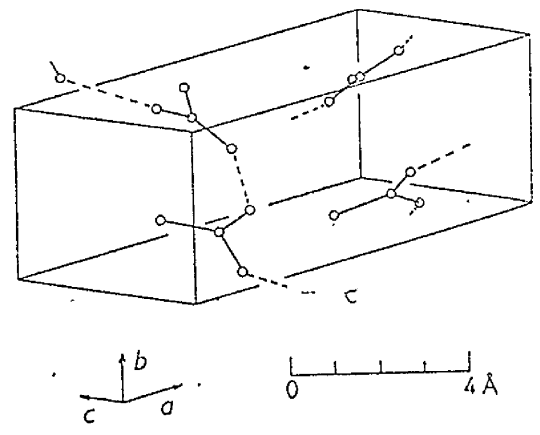


FIG 1b. UNIT CELL ACETIC ACID.

1. It is obtainable in a high degree of purity.
2. It is thermally stable and has no solid state transition.
3. It crystallises in the mono clinic system, space group $P2_1/C_1$ with four molecules per unit cell, fig. 1a with ³⁰ a 5.52Å, b 5.14Å, c 21.9Å and β 97°. ²⁷
4. It has a well defined cleavage plane (001) ²⁸ which facilitates crystal orientation.
5. Tritium and C¹⁴ labelled molecules are readily available.

Acetic acid was chosen as the example of a co-operative hydrogen bonded system and had the following advantages.

1. It is thermally stable with no known transition below the melting point.
2. Its crystal structure has been characterised by Jones and Templeton.²⁹ It is orthorhombic, space group Pna 2₁ with four molecules per unit cell, having a 13.32Å, b 4.08Å and c 7.77Å. Fig 1b
3. Tritium and C¹⁴ labelled molecules are easily prepared.

Disadvantages in using acetic acid are its low melting point of 16.7°C and the fact that it is slightly hygroscopic. It was thought, however, that these points could be overcome by suitable experimental technique.

Both these acids are of similar strength, benzoic acid pKa = 4.2, acetic acid pKa = 4.7, and solidify to give systems containing hydrogen bonds of approximately the same length, benzoic 2.64Å, acetic 2.61Å. The crystal structure of

both is approximately the same as benzoic acid is almost orthorhombic, $\beta = 97^\circ$ and the major difference between these crystals is ^{the} type of hydrogen bonding hence it is to be expected that any difference in the proton transport properties will be directly attributable to this factor.

In both these solids the bulk molecule is large and can be easily labelled with C^{14} hence a comparison can be made between diffusion of the bulk molecule and that of the proton. This will show whether the proton diffuses with the bulk molecule or not. Very little is known of molecular diffusion and this study may help to elucidate bulk diffusion mechanisms in organic solids.

As the defect structure of solids has been shown to have a marked effect on the properties it was thought that additional information could be obtained from a study of the above system by a) Introducing a substitutional chemical impurity and b) introducing gross non equilibrium defects by studying conductivity and diffusion in high purity polycrystalline compacts.

The object of this thesis, therefore, was threefold.

1. To purify and grow large single crystals of hydrogen bonded organic acids.
2. To measure, in these crystals, the conductivity and proton diffusion coefficients, using tritium as tracer, to confirm or disprove the hypothesis that intrinsic

proton conduction can occur in co-operative hydrogen bonded solids and elucidate the mechanism.

3. To examine the effect of introduced imperfections in the above systems.

I 1. INTRODUCTION.

As the defect structure of solids has been shown to exert a marked effect on many solid state phenomena³¹, it is important when embarking on a study of a particular crystalline solid to prepare single crystals with only an equilibrium defect structure. That is to say that non equilibrium defects such as dislocations, grain boundaries and point defects introduced by the incorporation of impurities should be reduced to such a level that they have no effect on the intrinsic property being studied. It is not always possible to attain this equilibrium due to the technical difficulties involved and the method of growing such perfect crystals is still very much an art.

There are three principal ways of growing crystals of which all techniques are simple or sophisticated adaptations.

- (a) Growth from solution.
- (b) Growth from the vapour phase.
- (c) Growth from the melt.

Method (a) is the most generally used industrial method and has been used to grow very large single crystals e.g. a 43 lb. crystal of ammonium dihydrogen phosphate was grown³² by the Bell Telephone Laboratories over a four month period.

This method frequently gives flawless crystals but suffers from the disadvantage that crystal growth is very slow, about 1 mm/day being an average rate, and that the crystals may grow in a particular crystal habit which is experimentally unsuitable. Crystal habit varies with the solvent used and can often be modified to force the crystal to grow in a preferred crystallographic direction. Habit modifiers are frequently dyes³³ which adsorb on a particular crystal plane preventing further growth thereon. As the modifier is usually incorporated in the crystal this may affect the intrinsic property being studied. This method may also introduce microscopic occlusions of solvent which are equally detrimental and hence is not considered particularly suitable for growing high purity crystals with a uniform defect structure. This method, however, is frequently the only suitable method of growing single crystals which either decompose on heating or undergo a phase transition between room temperature and the melting point.

Growth of crystals from the vapour phase is also useful where decomposition on heating or a phase change occurs. This method, however, usually requires a fairly high vapour pressure at the growth temperature although

some organic crystals have been grown at vapour pressures of a few hundred microns Hg.³⁴ Growth rates can vary considerably and can be as high as 1-2 cm/day. Vapour growth gives high purity, flawless crystals but difficulty is experienced in growing crystals larger than a few mm. on edge, predominately due to a large heat of crystallisation coupled with poor heat dissipation caused by the low thermal conductivity of most organic solids. In this method of growth it is also difficult to control the habit of the crystal formed.

Method (c), growth from the melt, was considered the best method of growing crystals of sufficient purity, size and uniformity in the present investigation.

Growth from the melt is essentially a simple one step operation in which a melt of pure material is cooled through the freezing transition at a rate slow enough to allow equilibrium single crystal growth. There are two principle variations of this method.

- a) The Kyropoulos method.³⁵
- b) The Bridgman - Stockbarger method.³⁶

In the Kyropoulos technique a seed crystal is slowly withdrawn from a melt of pure material. Surface tension draws the melt in contact with the seed above the level of

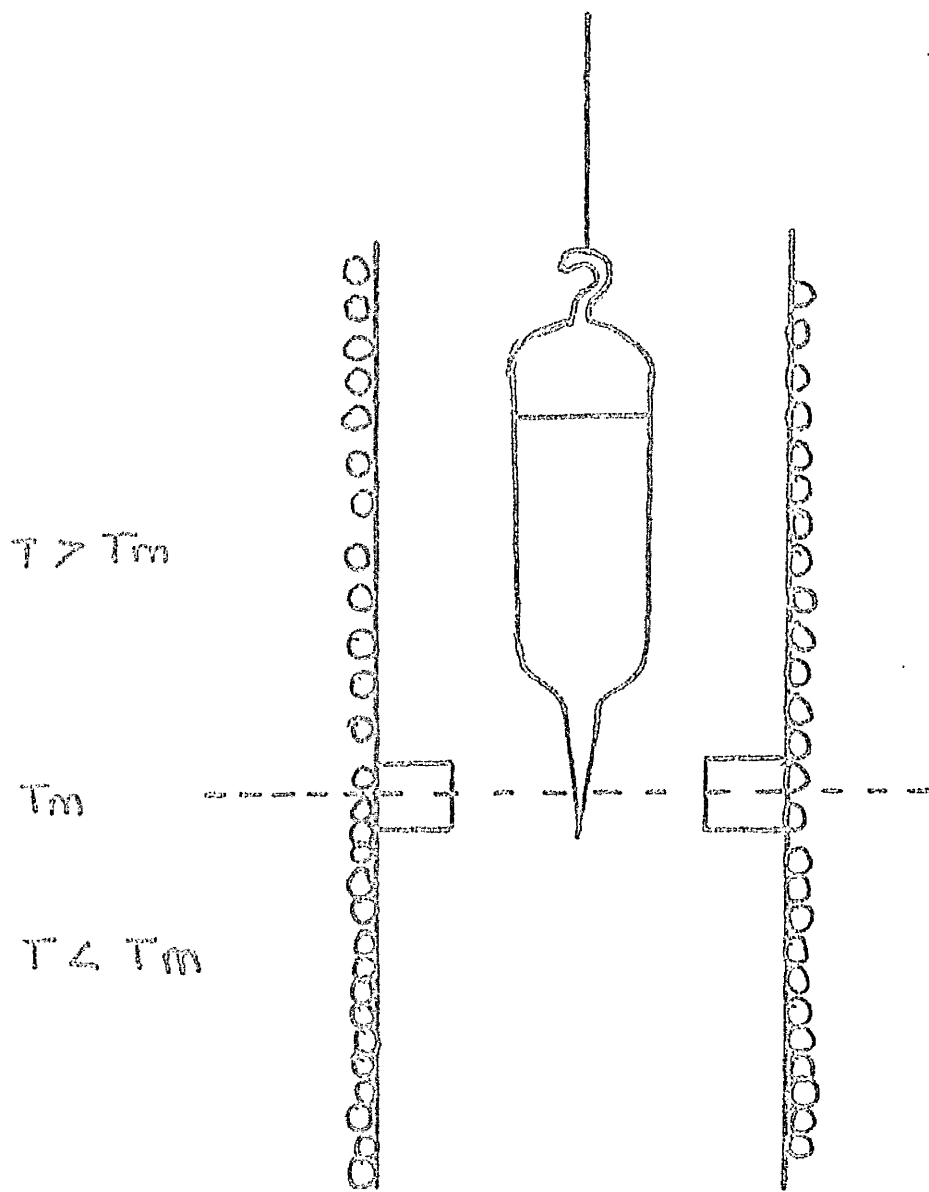


FIG.2 PRINCIPLE OF SINGLE CRYSTAL GROWTH.

the melt where it then crystallises. The rate of withdrawal of the seed is adjusted to give equilibrium freezing and a single crystal is obtained. This method, however, is only suitable for materials which have a low vapour at the melting point and has been successfully used to grow large alkali halide single crystals.³⁷ Unfortunately the organic acids to be grown both have fairly high vapour pressures at the melting, of the order of several mm. Hg, and sublime hence this method was not considered particularly suitable.

The principle of the Bridgman - Stockbarger, or moving vessel technique, is illustrated in fig 2. A vessel A containing the melt is slowly lowered from a high temperature region, $T > T_m$, through the melting point isothermal, T_m , into a low temperature region, $T < T_m$. In order to grow a single crystal a seed crystal must be formed at the lower end of the growing tube from which the melt will crystallise into one single crystal boule. The formation of this preferential seed crystal which controls the whole growth process has taxed the ingenuity of crystal growers in the past and several standard crystal growing vessels have been designed³⁸, all of which start with polycrystalline material formed by spontaneous nucleation on supercooling the melt. The crux of the problem is to preferentially select one of

these crystals and this is usually accomplished by either having a constriction in the growing tube which allows only one crystal through which then controls the subsequent single crystal growth, or by forcing the crystal to grow through a bent capillary. This latter procedure may also control the orientation of the single crystal formed as the growth plane of the crystal formed as it travels up the capillary can be altered by the angle of bend through which it is grown³⁰. In this way the orientation can be altered by 90°.

The Bridgman Stockbarger method was chosen to grow crystals of benzoic and acetic acid for the following reasons.

1. The method is relatively simple.
2. The crystals, which sublime, can be contained in a sealed vessel which also prevents external contamination during growth.
3. Large uniform single crystals can be grown in a few days.
4. It should be possible to grow crystals with different crystallographic orientation.

Before growing the crystals the starting materials were purified by the following procedures.

2. Purification of Benzoic Acid.

Purification of organic materials can be accomplished by a variety of unit operations of which solvent extraction, distillation, sublimation and recrystallisation are the most common.⁴⁰ In the present study benzoic acid was required in as pure a form as possible for the reasons given in the previous section.

The preparation of high purity benzoic acid for use as a standard substance for calorimetry and acidimetry has been studied by Schwab & Wichers⁵⁴. They found that purity greater than 99.98% could be obtained by several methods, recrystallisation from water or benzene, fractional freezing or hydrolysis of benzoyl chloride. Purity of 99.999% was obtained only by recrystallising from benzene eight times or by fractionally freezing twice in a manner similar to the Bridgman technique for growing single crystals. The simplest of these methods was fractional freezing and this was the method chosen to^{grow} single crystals in this investigation.

The starting material used was Analar reagent grade benzoic acid supplied by Messrs. B.D.H. Limited. The specifications of this material guaranteed greater than 99.9% purity with known impurities having the following maximum concentrations, 6 p.p.m. metallic, 0.025% non volatile,

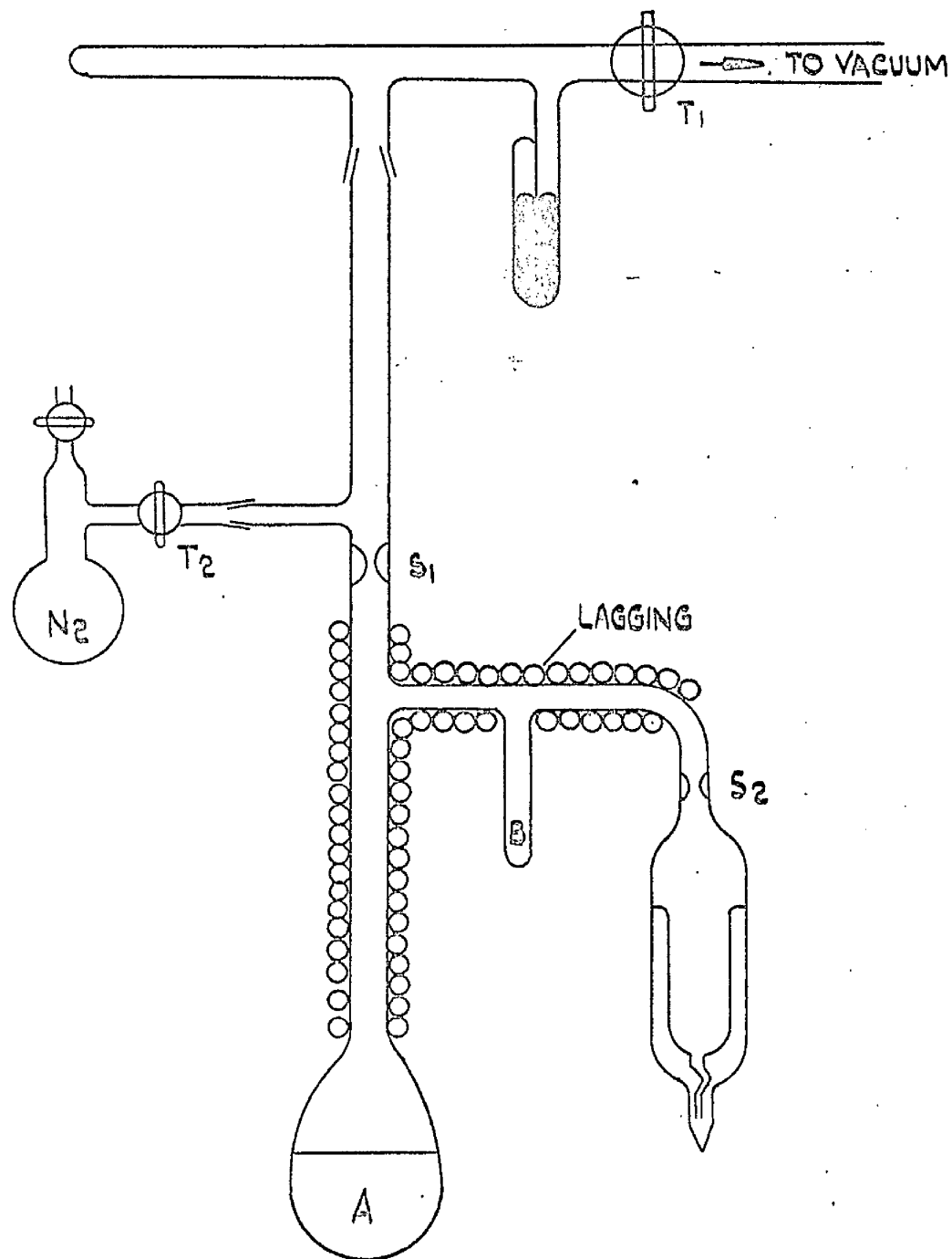


FIG.3. DISTILLATION OF BENZOIC ACID INTO GROWING TUBE.

0.02% chlorine compounds and the remainder probably adsorbed oxygen and water. In a tritium diffusion study water is likely to be the most detrimental impurity but in this case is easily removed by simply evacuating the fused acid.

For the initial purification of benzoic acid prior to single crystal growth, zone refining appeared to be the most suitable technique. As no zone refiner was available it was decided to construct one. During this period benzoic acid was purified by simple distillation under reduced pressure using the following technique.

I 2 a Distillation.

For the initial experimental growth of benzoic acid single crystals the apparatus shown in fig. 3 was used. Approximately 200 gms. of analar benzoic acid was placed in flask A and evacuated for 1-2 hours at 10^{-2} cm. Hg. Tap T_1 was closed and a few cm. of dry nitrogen introduced. The acid was carefully melted and degassed by opening tap T_1 to the vacuum. This procedure removed most of the water and it was swept out of the acid by the dissolved air bubbling out. T_1 was then closed and 10 cm. Hg. pressure of nitrogen introduced. The system was then sealed at S_1 and the acid gently distilled over into the crystal growing vessel, the first 20 ml. of distillate being trapped in

limb B using a liquid nitrogen trap which served to remove any last traces of water. The subsequent 60-80 ml. of distillate sufficed to fill the crystal growing tube to within 1" of the seal S_2 . The distillation was stopped at this point and the growing tube sealed at S_2 . The glass at S_2 was then fashioned into a hook from which the vessel was suspended in the crystal growing oven. The benzoic acid in the growing tube was always crystal clear in the liquid state and crystallised to give a pure white crystalline solid. The benzoic acid left in the distillation tube, however, always had a light brown colouration. This indicated that either some degree of purification had taken place or the acid was decomposing. Experiments by Schwab and Wichers^{4:1} in which they held 3 samples of high purity benzoic acid in sealed capsules for 72 hours at 200°C. under one atmosphere of air and oxygen and under vacuum, gave 0.047, 0.047 and 0.025% impurity respectively. This indicated that the rate of decomposition was very slow and was probably due to oxidation hence it seemed likely that purification was occurring during distillation. A further indication that this brown colouration was a natural impurity was later obtained by zone refining during which a similar brown material was quickly rejected.

This method of purification and tube filling was used successfully until the superior technique of zone refining had been developed.

2.2.b Zone Refining

Since its introduction by Pfann in 1952⁴² zone refining, or zone melting as it is sometimes called, has rapidly become one of the most powerful methods of obtaining materials of super purity i.e. impurity concentrations of parts per million or less. The theoretical and practical development took place simultaneously and was the sine qua non of the semiconductor industry⁴³. The technique is of general application to materials which do not decompose on melting and thus in many cases can be used to prepare organic crystals with contaminants well below the level of analytical detectability.⁴⁴

In principle zone refining is a simple adaptation of the normal freezing method of purification. Its power lies in the speed with which a large number of unit freezing operations can be made coupled with the method of rejection of the impurity. The factor controlling the separation of an impurity between the liquid and solid phase is the

equilibrium distribution coefficient, k_0 ,

$$\text{where } k_0 = \frac{x_s}{x_L}$$

x_s, x_L being the mole fraction of impurity in the solid and liquid respectively. When the impurity is more soluble in the liquid phase then $k_0 < 1$ and the solid becomes progressively purer, when the impurity is more soluble in the solid phase then $k_0 > 1$ and the liquid becomes purer. The theoretical assumption of constant distribution coefficient is only applicable in the case of very dilute solutions and k_0 can be obtained by extrapolation of phase diagrams to zero concentration. In normal zone refining operations equilibrium freezing conditions are not attained and a related parameter is used called the effective distribution coefficient, k .

The practical process of zone refining consists of slowly passing a molten zone of constant length, λ , through a length, L , of the solid to be purified. If the initial concentration throughout is C_0 then the impurity distribution after one pass is given by ^{4.5}.

$$C/C_0 = 1 - (1 - k) \exp \left[- \frac{kx}{\lambda} \right]$$

where C/C_0 is the relative impurity concentration from the top of the sample ($x = 0$). The benefit of zone refining is

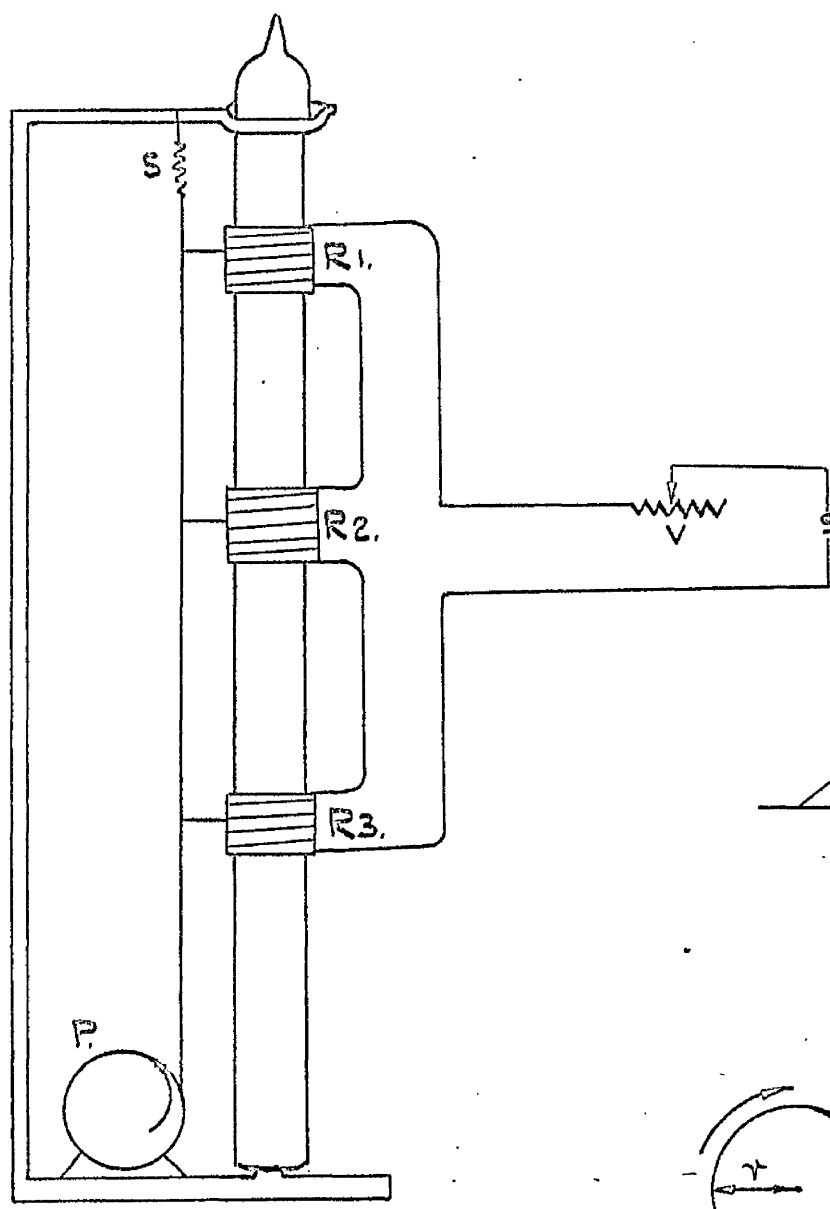
that several molten zones can be passed through the sample at the same time providing that a length of solid exists between them.

The degree of purification using this method is limited, however, and Braun⁴⁶ has calculated the number of passes beyond which no further purification will be obtained. For $0.1 \leq k \leq 0.3$ he calculated the maximum effective number of passes, n , as

$$n = \left[2 \left(\frac{L}{l} \right) + 2 \right]$$

It is possible to further purify this material by extracting the pure fraction of the charge and re-introducing it into a longer, narrower zone refining tube thus giving a larger value of L/l and higher purity. For a further discussion of the many facets of zone refining the standard work on the subject is by Pfann⁴⁷.

The applicability of zone refining to the purification of benzoic acid was demonstrated by Jessup⁴⁸ who increased the purity of a sample of benzoic acid from 99.98% to more than 99.999% by two equilibrium freezing operations. This indicated that the distribution coefficient of normal impurities in benzoic acid is ≤ 1 and that relatively few zone passes were required to give high purity material. It



$R_1 = R_2 = R_3 = 15 \Omega$
 S. SPRING.
 P. SCREWED WHEEL.
 V. "VARIAC" AUTOTRANSFORMER.
 Y. RADIUS OF WHEEL.

FIG. 1.

SCHEMATIC VIEW.

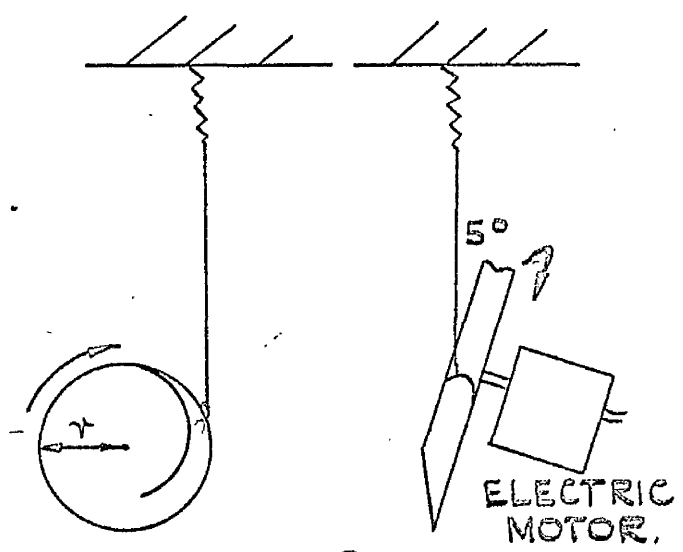


FIG. 2.

RECIPROCATING MECHANISM.

FIG. 4

AUTOMATIC ZONE REFINER.

has also been shown that water does not form solid solutions with benzoic acid^{4r1}, hence this method should also remove the final traces of water.

Design of Zone Refiners.

Two simple zone refining mechanisms were evolved during this period of research.

The first mechanism is shown in fig 4 . It is extremely simple and consisted essentially of a screwed pulley wheel, P, to which a length of copper string was brazed. The other end of the string was fastened to a fixed spring and heaters were attached at suitable equally spaced intervals. The actual mechanism is shown in fig 4 After one revolution of the wheel the string screwed off suddenly and the heaters were returned to their initial position by the tension in the spring. This gave a vertical displacement equal to the circumference of the wheel and thus the heaters were separated by this distance to give the required overlap of the zones. The pulley wheel used was 2.5 cm. dia. and the speed of the drive motor was $\frac{1}{6}$ r.p.h., giving a zone refining speed of 1' cm./hr. which was quite suitable for refining organic solids.

The heaters used were wound with 33 ohm/yd. 'Nichrome' wire on glass formers insulated with asbestos paper and the heating current was controlled through a 'Vaviac' autotransformer. Several sizes of heaters were constructed for use with tubes of varying diameter ranging from one to three cm.

Attempts were made to zone refine benzoic acid using two heaters but it was found that the glass tube containing the acid always fractured due to the large volume expansion on melting, ~~80%~~⁴¹ and even two mm. thick walled glass tubing could not withstand the pressure created. Some success was obtained by using Teflon tubing to contain the acid. This tubing, which is suitable for use at temperatures over 200°C., expanded sufficiently to contain the melt. Unfortunately the heaters frequently stuck to the tubing and melted it at the point of contact. It was decided, therefore, that the zone refining must be carried out in glass tubing in which the acid could be melted, degassed and sealed under vacuum. This meant that only one heater could be used as it had to start at a free surface for every pass to avoid fracture due to the volume change on melting. It was found that even with one heater the tube occasionally fractured if it was exposed to

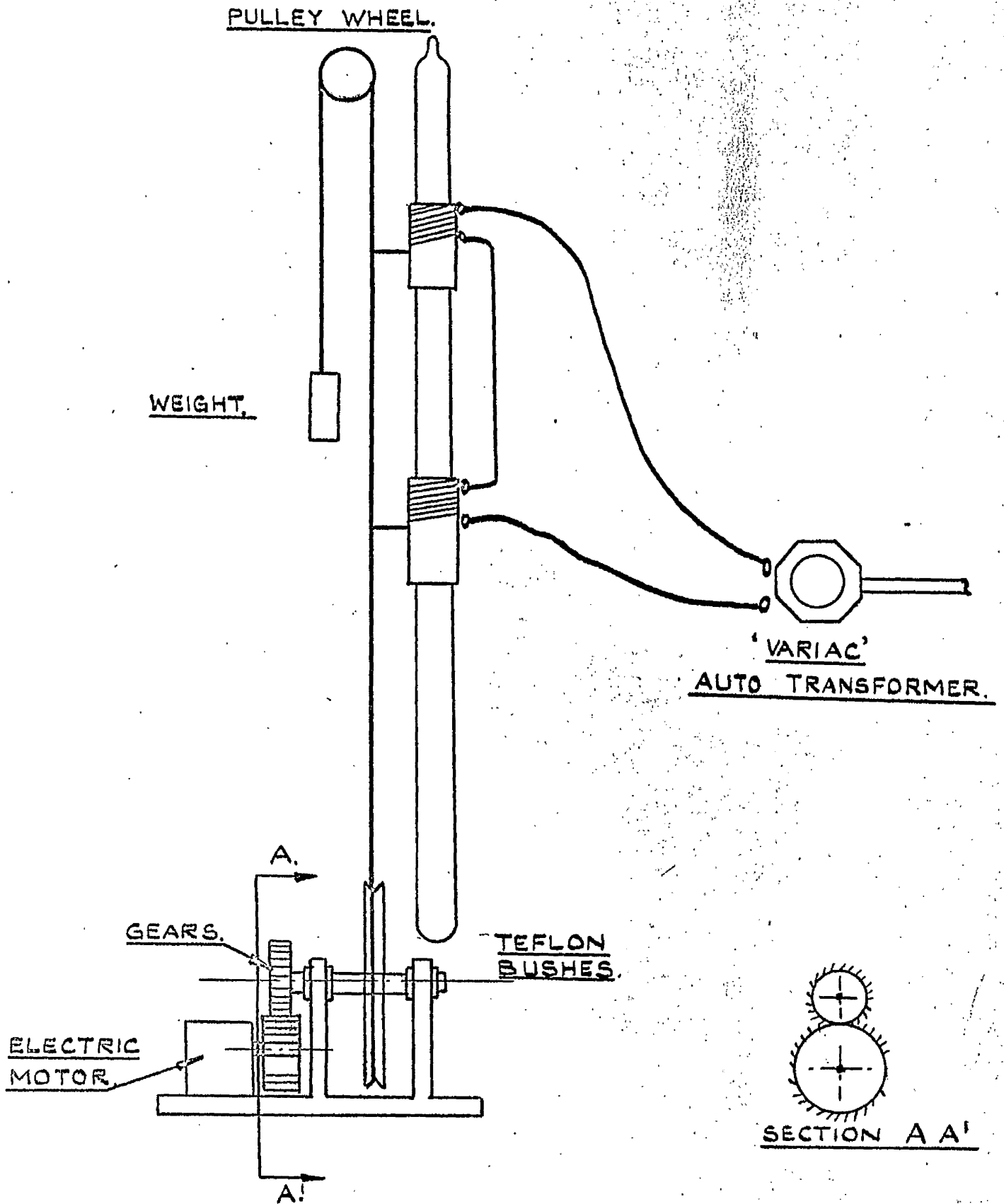


FIG.5. AUTOMATIC ZONE REFINER.

draughts or sudden variations in ambient temperature which altered the zone length, hence it was placed in a draught free position.

This zone refiner was not particularly suitable for a single heater unit as this meant that the heater must travel the full length of the charge and for a length of 30 cm. x 2.5 cm. dia., giving a reasonable charge of 200 gms., the wheel dia. required was 10 cm. and the motor speed $\frac{1}{30}$ r.p.h.

At this time an improved design of zone refiner was evolved, fig. 5 , in which the speed and path length could be easily varied. This refiner was again of simple design and the principle of operation is shown in fig. 5b. A Sangamo Weston motor, $\frac{1}{8}$ r.p.h., drove the lower gear from which several teeth had been removed. This gear drove a second gear wheel attached to a spindle of variable diameter. A cord was attached to this spindle and passed over a pulley wheel at the top of the apparatus terminating in a heavy weight. The heater, of the same constructed as before, was attached to this cord and was slowly pulled down by the drive gear wheel until the gap was reached whereupon the heavy weight returned it to its original position as the spindle was free to rotate in Teflon bushes. The gearing used was in the ratio 2:1 so that the spindle turned twice during every zone pass. In this way a total

pass length of 30 cm. was obtained. The zone refining speed was controlled by varying the electrical input to the motor through a 'Simmerstat' controller. In this way zone refining speeds of 4.5 cm./hr. and under were obtained.

In zone refining benzoic acid the procedure adopted was to use a heater giving a 2-3 cm. molten zone. The total length of charge was 35 cm. and the tube diameter 2.5 cm. 3 or 4 fast passes were initially made at 4.5 cm./hr. which served to remove the major impurity as a brown band of solid which was quickly rejected. This was then followed by a minimum of 20 passes at 2.0 cm./hr. Within two or three passes the acid always started to crystallise as large singular pieces, a sign of high purity. 25 passes were always given to ensure complete removal of impurities.

Two methods of filling the zone refining tubes were used. Initially the zone refining tube was broken open and the top inch and lower third rejected. The remainder was then placed in a large tube glass blown on to the end of a crystal growing tube and connected to the vacuum line. The crystals were then evacuated for half an hour before admitting a little nitrogen and melting into the growing tube. The melt was again degassed before admitting 10 cm. H₂. nitrogen and sealed. At a later stage the crystal growing tube was attached directly to the zone refining

tube as in fig. 11 . The upper inch of crystal was always melted into the top of the refining tube before the subsequent material was melted into the growing tube.

I. 3. Design of Benzoic Acid Crystal Growing Ovens.

The basic principle in constructing an oven suitable for growing crystals by the Bridgman-Stockbarger method is to have two well lagged furnaces, one thermostatted above the melting point of crystal and the other thermostatted below it, separated by a baffle in the middle of which the melting point isothermal should lie.

The major factors controlling the growth of large single crystals by this method are.

- a. The thermal stability of the oven.
- b. The temperature gradient at the freezing transition.
- c. The rate of lowering the crystal through this transition.
- d. The development of a suitably oriented seed crystal.

The most common oven design is to have two electrically heated wire wound furnaces. This is probably because of their widely variable temperature range and the fact that initially this method was used to grow high melting point crystals of metals, ionic salts and semiconducting materials. ⁴⁵

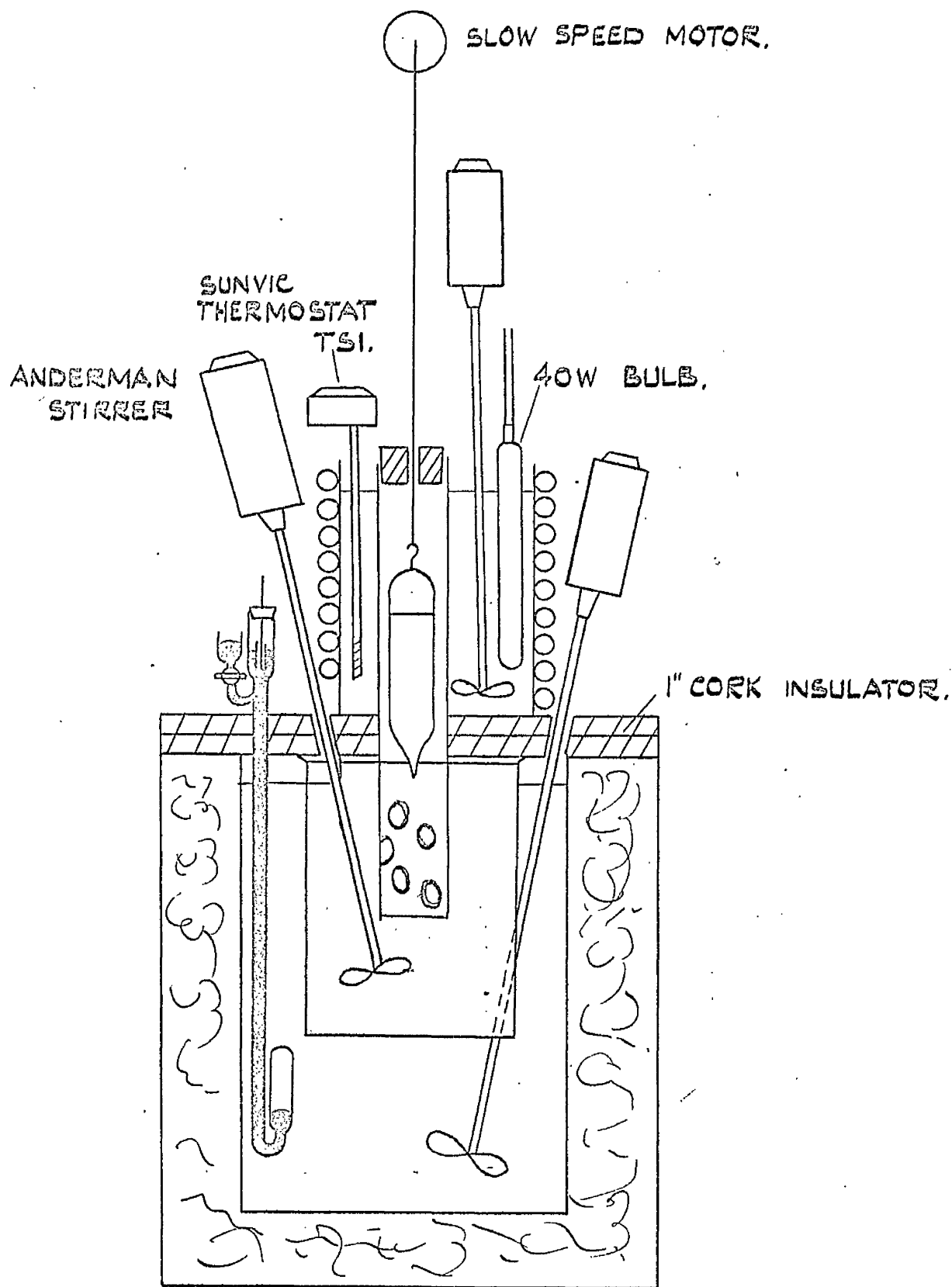


FIG. 6. BENZOIC ACID CRYSTAL GROWING OVEN.

As benzoic acid has a fairly low melting point, 122°C . and as wire wound furnaces do not give a uniform temperature distribution throughout their length it was decided to construct a crystal growing oven in which a much more uniform and stable temperature could be maintained above and below the baffle. To accomplish this thermostatted baths of liquid were used to obtain the two temperatures required.⁵⁰ This type of oven has been constructed by Hood and Sherwood⁵¹ and found satisfactory for growing cyclohexane a low melting point organic 'plastic' crystal.

The design of this oven is illustrated in fig. 6 . The lower bath was enclosed in a 1' x 1' x 1'6" deep plywood box. A large metal drum fitted neatly in this box and was insulated with straw. The drum was filled with water, with a layer of paraffin to suppress evaporation, and thermostatted using a toluene regulator to control a 500w heating element. The lid of this box was a 1' x 1' x $\frac{1}{2}$ " thick plywood board to which a piece of cork of similar dimensions was glued. This gave a 1" thick insulation layer of sufficient strength to support the upper bath. A two litre beaker which effectively formed the lower bath was bolted to this lid and was also filled with water having a paraffin layer on top.

The upper vessel consisted of a copper can $5\frac{1}{2}$ " x 10" dia.

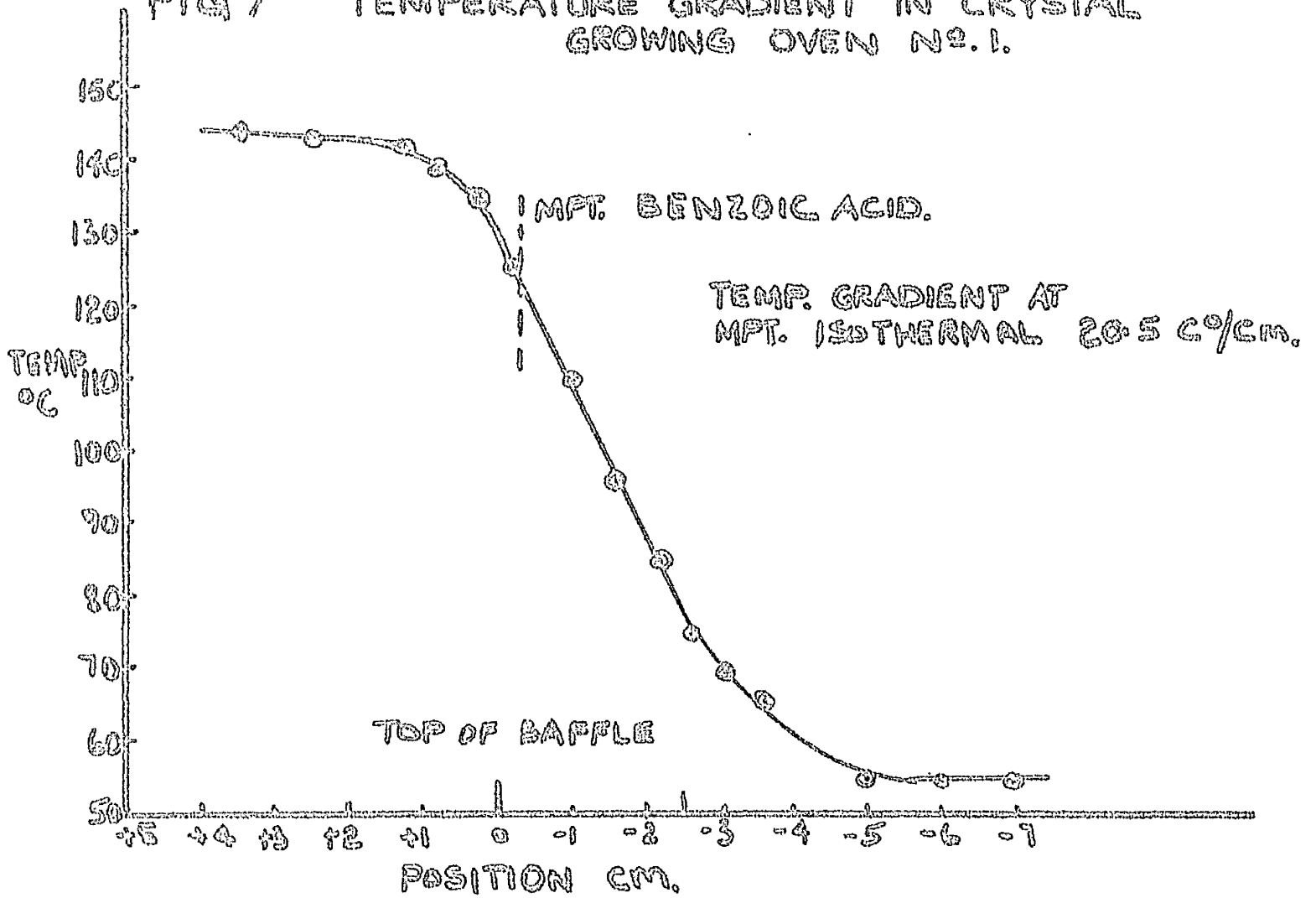
with a 2" dia. hole drilled off-centre in the base, through which a tight fitting pyrex tube was inserted and sealed with 'Araldite' epoxy resin. Holes were blown in the lower section of the tube which projected into the two litre beaker to allow the lower bath to attain rapid thermal equilibrium. The upper bath was filled with glycerol and had a silicone oil layer on top to reduce evaporation. A background heater was wound round the copper can, insulated with asbestos, using 33 ohm/yd. 'Nichrome' wire and lagged with $\frac{1}{4}$ " dia. asbestos rope. It was controlled using a Variac to give a bath temperature 20-30°C. below that required. The final temperature control was obtained using a Sunvic TSI bimetallic strip regulator which controlled a 40w Osram bulb giving a temperature stability of ± 0.10 C° at 140°C.

The optimum rate of lowering at which equilibrium freezing conditions are still maintained is a factor which depends on the material. Metal single crystals can be grown at rates of several cm./hr.⁵² whereas anthracene and naphthalene require growth rates less than 2 mm./hr.⁵³ The rate is also related to the temperature gradient at the freezing point as the heat of crystallisation must be dissipated through the crystal and this increases with increasing temperature gradient. In the case of benzoic

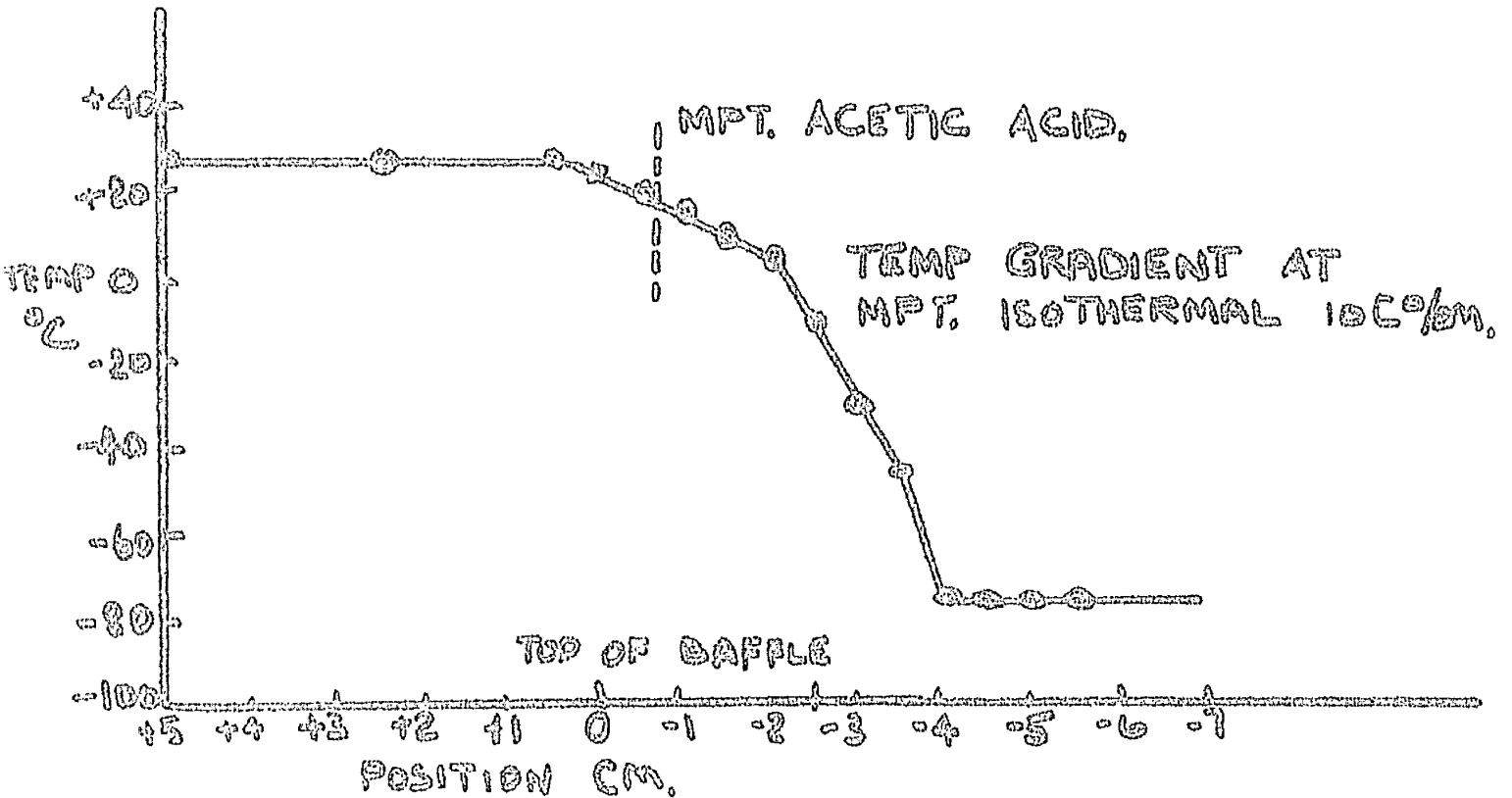
acid the rate was determined by trial and error. It was found that a lowering rate of 2.0 mm./hr. was satisfactory with a temperature gradient of 20 C°/cm. The growing tubes were, therefore, lowered using a Sangamo Weston electric motor rated at $\frac{1}{12}$ r.p.h. for a 30 c.p.s. a.c. supply. The 50 c.p.s. laboratory supply was found to increase the speed proportionally to $\frac{1}{8}$ r.p.h. The spindle dia. was 0.32 cm. and this gave a lowering rate of 1.7 mm./hr. A very fine, strong cotton thread was used to suspend the growing tube. It was found that this occasionally broke in the hot section of the oven and was replaced by a short length of copper 'string' which was tied to the thread above the hot section. This lowering mechanism was independently clamped from the rest of the oven to minimise the effect of any vibration caused by the stirrer.

The problem of the best temperature gradient to use is one in which there are two schools of thought. A sharp temperature gradient is considered to give better and quicker dissipation of the heat of crystallisation and increases the positional stability of the melting point isothermal. In favour of a shallow temperature gradient is the fact that the crystal can anneal as it is formed and will not be subjected to the stresses which occur on rapid cooling. These stresses and the subsequent non-equilibrium defects they introduce can, however, be annealed out by

FIG 7 TEMPERATURE GRADIENT IN CRYSTAL GROWING OVEN N2.1.



TEMPERATURE GRADIENT IN ACETIC ACID CRYSTAL GROWING OVEN



reheating the crystal to just below the melting point for a suitable time period followed by gradual controlled cooling. In this investigation the crystals were grown with a sharp temperature gradient. The temperature profile across the baffle is shown in fig. 7. The upper bath was controlled at 142°C ., 20°C above the melting point and the lower bath at 60°C ., 60°C below the melting point. The temperature gradient obtained across the baffle was $20^{\circ}\text{C}/\text{cm}$. and was found to be quite suitable for growing benzoic acid crystals. The upper bath temperature was limited to a maximum of 150°C . as Schwab and Wichers⁴⁾ found that a slow oxidative degradation occurred at 200°C . and that a reversible dehydration to benzoic anhydride and water occurred in the liquid phase. The extent of this dehydration was small, however, and only occurred when the acid was very dry. It was found to return to its initial value when the material passed through the freezing transition.

When this crystal growing oven was operating properly good crystal boules were obtained which usually consisted of two or three large single crystal pieces growing with the cleavage plane vertical or at an angle of 60° to the horizontal. Unfortunately the system could not always be relied upon and several factors which influenced its

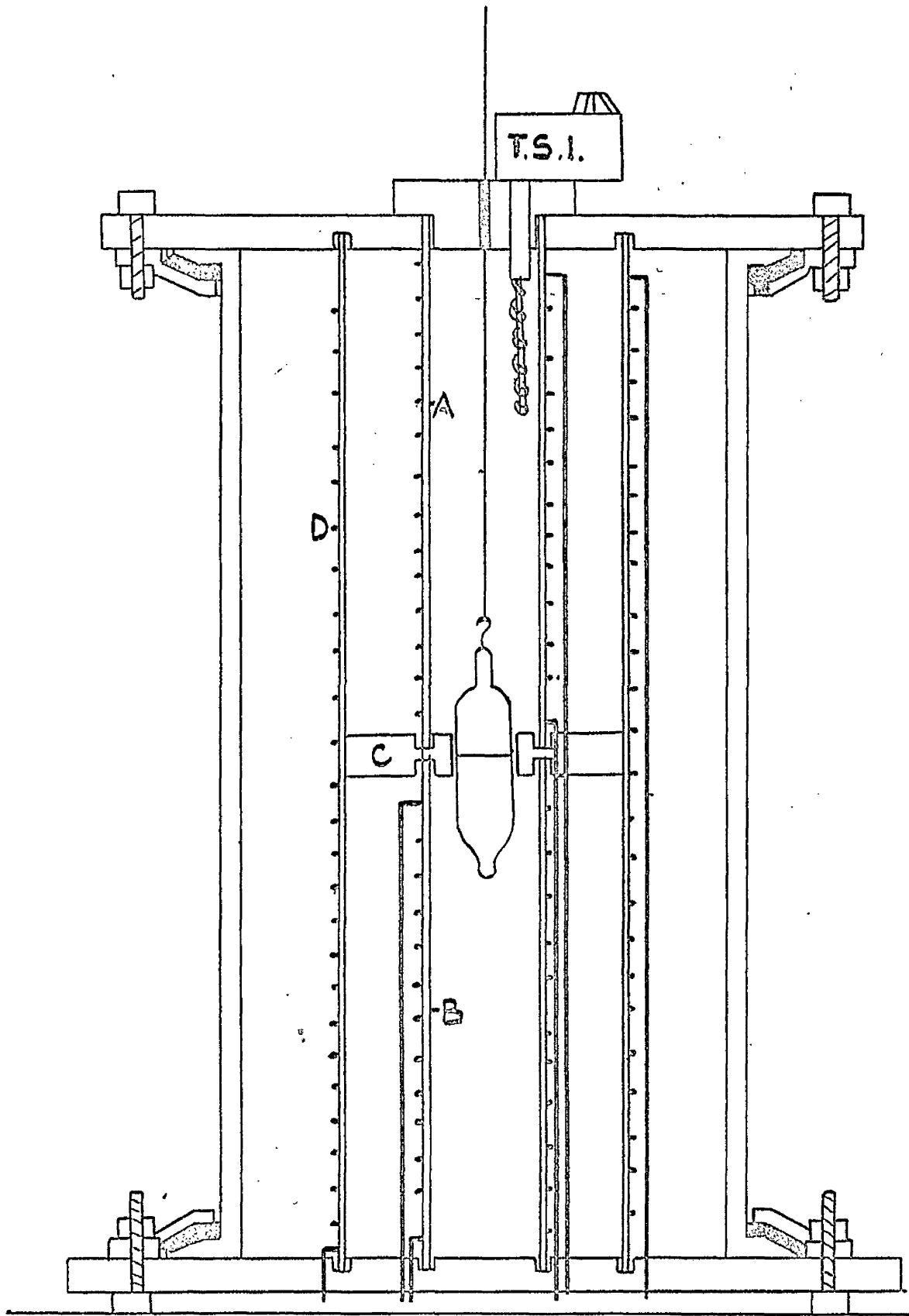


FIG. 8. THE CRYSTAL GROWING OVEN No. 2.

performance were.

- a. The stirrer in the high temperature bath had a tendency to stick occasionally and when this occurred the crystal was restarted.
- b. The stirrers also occasionally caused excessive vibration which affected the crystal growth process.
- c. The crystal could not be observed during the growth process and the crystallisation had to be carried out completely before it was known whether or not the seeding had been successful.
- d. When the string broke or the crystal slipped off the hook, and this happened several times, the oven had to be completely stripped down to remove the tube.

A period occurred during which for a combination of the above reasons unsatisfactory crystals were obtained. At this point it was decided to change the crystal growing oven in an attempt to obtain better crystals.

The new oven used was one constructed by Dr. J. N. ⁵³Sherwood and successfully used to grow anthracene crystals, m.pt. 217°C . This oven, fig. 8 was an all glass oven made in Pyrex which enabled the crystal to be observed at all times during the growth process. A detailed description of the oven has been given elsewhere ⁵³ and only the principle features will be described. Two 'Nichrome'

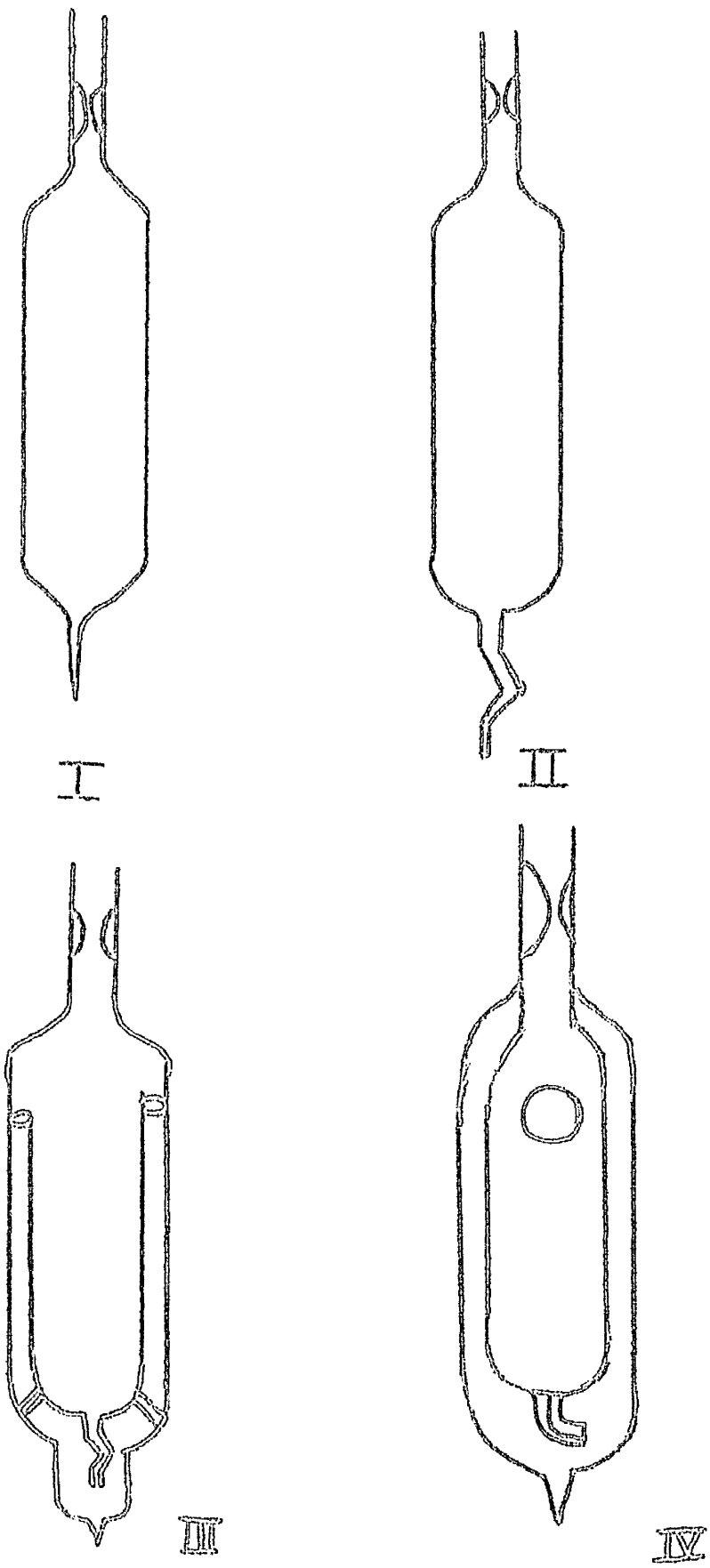


FIG. 9

CRYSTAL GROWING TUBES

heater A & B of resistances 80Ω and 130Ω respectively were wound on pyrex glass tubes and were adjusted to temperatures $10 - 20\text{ C}^\circ$ below those required, (upper heater 130°C lower heater 80°C .) using rheostats in series with the line supply. A heater D, resistance 100Ω , was wound on a concentric pyrex tube 2.6" dia. and the oven was raised to the required temperature and thermostated by controlling the supply to this heater through a 'Sunvic' circuit F 102/3M. which used a Sunvic TSI normally closed thermostat as sensing element. The detailed operation of this circuit is given elsewhere⁵³. As with the previous oven the temperature gradient was adjusted to $20\text{ C}^\circ/\text{cm}$. at the interface but the lower heater was controlled at 95°C . to avoid the larger temperature drop in the other oven. The rate of lowering with this oven was 1 mm./hr. and good quality crystals were obtained when high purity benzoic acid was used.

The Crystal Growing vessels.

The first attempt at crystal growing was made in the vessel shown in fig. 9a. A polycrystalline mass resulted, however, containing some singular pieces which were observed by examining pieces of the crystal boule between

crossed polaroids where four positions of complete extinction were obtained. This indicated the necessity for a better seeding arrangement and the second crystal was grown in the vessel shown in fig. 9b in which a short piece of bent capillary was used to seed the crystal. This crystal was considerably better than the first and gave several singular pieces which had the (001) plane growing vertically. As there were still too many crystals formed the vessel shown in fig. 9c was adopted for all subsequent growing vessels. This vessel, which has been used previously to grow anthracene crystals⁵⁸, gave an insulating layer of the material in the outer vessel which helped to stabilise the melting point isothermal in the inner vessel and was found to improve the quality of the crystal obtained considerably. It was not possible, however, to obtain a monocrystal and usually two or three large single crystal pieces were obtained which grew the whole length of the tube and gave excellent cleavage and extinction between crossed polaroids. Fig. 9d was yet another variation of vessel C which was used in the later stages of crystal growing. Attempts were made to grow crystals with horizontal cleavage in the tube by altering the angle of the capillary³⁹. It was found, however, that this had no effect. Crystals were obtained with cleavage plane vertical and at an angle of 30° and 45° to

the vertical irrespective of the angle at which the tube was bent. The fact that the cleavage plane could be grown at an angle, however, indicated that the growth rate was slow enough for equilibrium freezing conditions otherwise a vertical cleavage would be obtained along the direction of fastest growth. In all the crystals grown the cleavage plane obtained was the (001)²⁸

When crystals were withdrawn from the oven and allowed to cool naturally they always fractured due to the thermal strain induced. When the crystals were withdrawn from the oven they were, therefore, placed in a large, water filled dewar flask at the same temperature as the lower bath, stoppered and allowed to cool naturally.

2.4. Preparation of Doped Benzoic Acid Crystals.

Attempts were made to alter the defect structure of benzoic acid by introducing known impurities into the lattice.

It was thought that the introduction of cations into the lattice would introduce defect sites in the acidic hydrogen lattice which would increase the conductivity and tritium diffusion. Ubbelohde¹⁴ tried to incorporate sodium ions in benzoic acid but found no effect on the

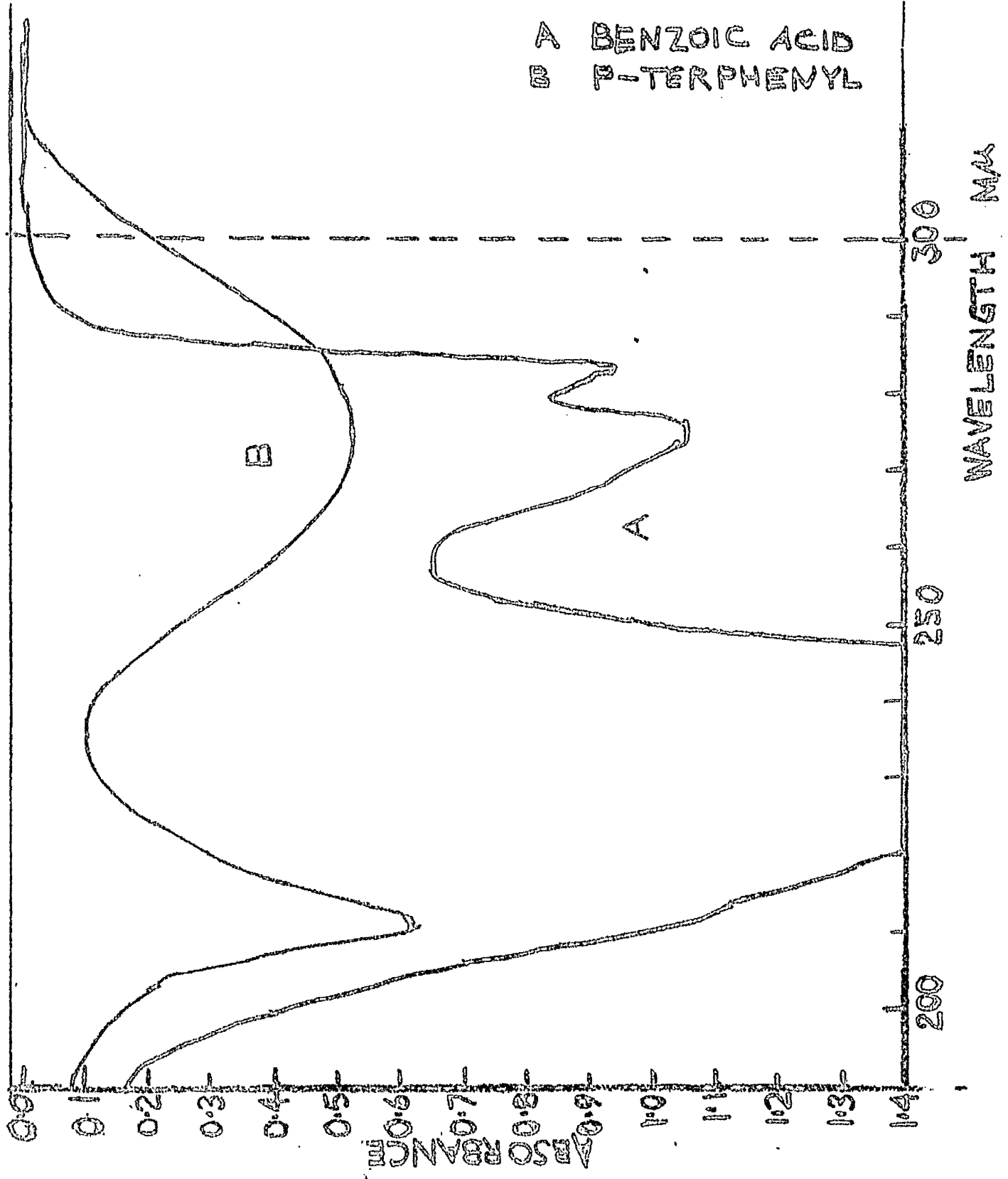
conductivity. It was thought that lithium, being smaller, was more likely to enter the lattice substitutionally. An attempt, therefore, was made to grow a crystal doped with 1:1000 parts by weight of lithium benzoate. The crystal obtained was completely polycrystalline indicating that the lithium did not enter the lattice substitutionally and no further work was attempted on this system.

Another crystal was grown with p-terphenyl as impurity. p-terphenyl is similar in shape to a benzoic acid dimer but slightly shorter and it was thought that it might enter the lattice substitutionally and cause a loosening of the lattice around these substitutional impurity sites with its subsequent effect of increasing the rate of self diffusion.

This crystal was grown in the normal way using zone refined benzoic acid to which 0.105 gms. of scintillation grade p-terphenyl (supplied by messrs. Nuclear Enterprises Ltd.) had been added, giving an impurity concentration of 1:600. This rather high initial concentration was used as it was not known to what extent the p-terphenyl would be incorporated.

When the crystal was removed it was found to have a horizontal cleavage plane, a phenomena which had not been observed with any other crystal. The crystal was transparent with a small ring of brown material rejected at the top. The crystal was not, however, completely singular as only partial

FIG 10 U.V. SPECTRA OF BENZOIC ACID AND P-TERPHEENYL



extinction was observed between crossed polaroids.

The distribution of p-terphenyl through the crystal was obtained by measuring the U.V. absorption on a Perkin Elmer 137 U.V. spectrophotometer. The p-terphenyl concentration was obtained from a calibration graph of p-terphenyl in benzoic acid. P-terphenyl exhibits a broad absorption in the U.V. at λ_{max} 275 m μ with ϵ_{max} 3500 in hexane solution. Unfortunately benzoic acid also absorbs at 275 m μ but gives a much sharper band and the p-terphenyl can be determined from the overlap, see fig.10. A calibration graph was constructed using p-terphenyl/benzoic acid solutions in hexane. The values obtained are tabulate below for a benzoic acid concentration of 1.3 mgm/ml. taking the absorbance at 300 m μ .

p-Terphenyl absorption at 300 m μ .

SAMPLE	ABSORBANCE	CONCENTRATION mgm/ml.
1	0	4.7×10^{-6}
2	0.01	2.15×10^{-4}
3	0.25	2.5×10^{-3}
4	0.44	4.9×10^{-3}
5	0.55	6.9×10^{-3}
6	0.65	8.9×10^{-3}

Four samples of p-terphenyl doped benzoic acid were taken at various positions along the crystal, their U.V. absorption

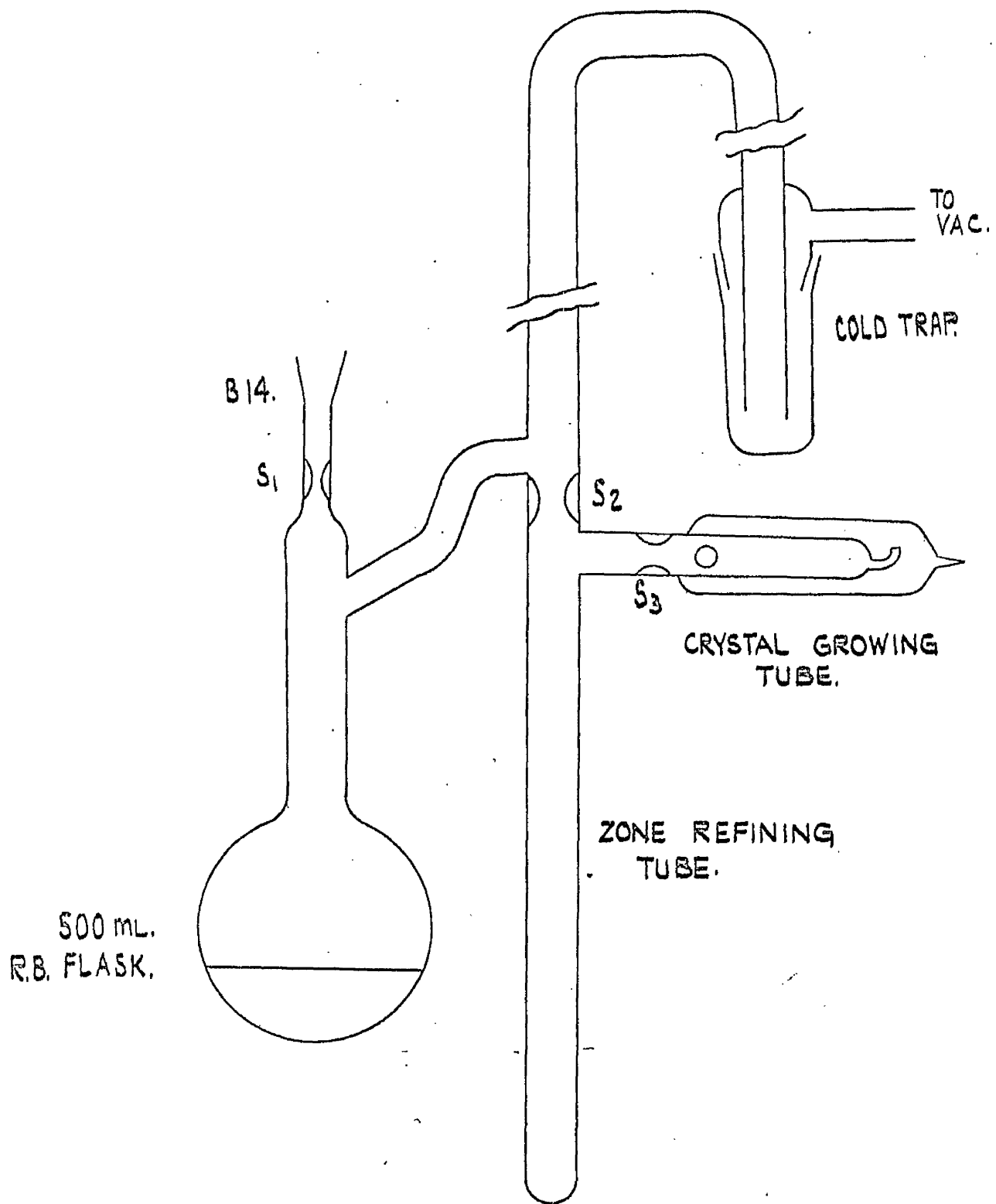


FIG. II. PREPARATION AND PURIFICATION OF DEUTERO-BENZOIC ACID.

spectra measured and the p-terphenyl concentration calculated from the calibration graph. The results are tabulated below:

SAMPLE	POSITION (Base-o) cm.	WEIGHT mgm/25ml.	ABSORBANCE	p-Terphenyl concentration mgm/ mgm. B.A.
1	0	17.74	0.02	2.8×10^{-4}
2	2.5	16.04	0.04	6.2×10^{-4}
3	5.5	14.77	0.09	15.0×10^{-4}
4	8.0	14.15	0.95	350×10^{-4}

The majority of the p-terphenyl was, therefore, rejected although a small amount appears to have been incorporated.

Deuterobenzoic Acid.

In order to study the isotope effect on tritium diffusion in benzoic acid a crystal of benzoic acid- d_1 was grown and the deuteration was carried out by hydrolysing benzoic anhydride with deuterated water following the procedure used by Robertson & Ubbelohde.⁵⁷

120 gms. of reagent grade benzoic anhydride (Messrs. B.D.M. Ltd.) m.pt. 39.5°C . was purified by 10 passes on a zone refiner. The upper 100 gms. of this purified material, m.pt. $42-43^{\circ}\text{C}$., was melted into the r.b. flask in fig ||. 20 ml. of 99.7% D_2O (I.C.I. LTD) , a three fold excess, was introduced and 4 drops of freshly distilled thionyl chloride added to catalyse the hydrolysis. The tube was sealed at S_1 and opened

to air through a Ca Cl_2 tube to prevent entry of normal water vapour into the apparatus. The mixture was refluxed for 8 hrs, using an isomantle, to allow complete hydrolysis. The excess D_2O was removed on evacuation and trapped out using a liquid nitrogen trap. The benzoic acid was then sublimed over, under vacuum, into the 2' long tube above the zone refining tube. The vacuum pump was turned off, a little dry air added and the sublimed acid melted down into the zone refining tube. This procedure was repeated until the zone refining tube was full, approximately 80 gms acid, over a period of 4 hours. The material in the zone refining tube was degassed twice in the melt before sealing at S_2 under a pressure of 10 cm. dry air. The material had a very pale yellow colouration at this stage. The acid was zone refined, 30 passes at 2 cm/hr. Large transparent crystals were obtained with a mustard coloured impurity being rejected. The upper inch of material was melted into the top of the tube and the subsequent 60-70 gms. melted into the crystal growing tube and sealed at S_3 . The crystal was grown in the all glass oven at a lowering rate of 1 mm./hr. The crystal obtained was perfectly transparent, gave a well defined cleavage plane at 30° to the vertical and gave good extinction between crossed polaroids. The crystal was annealed at 120.5°C . for one week. The melting point of this crystal was 119.3°C ., 3° below that of normal benzoic

acid and in good agreement with the value of Robertson & Ubbelohde.

Annealing of Crystals.

All crystals prepared from zone refined material were annealed for one week at 121°C . These crystals were designated ZR1, ZR2 etc. with the exception of the p-Terphenyl doped crystal, p-Ter, and the deuterio benzoic acid, D.B.A. The non zone refined crystals were designated NON Z.R.

Purity of Benzoic Acid.

Although the method used to prepare the benzoic acid should have ensured a purity 99.99 mole % an attempt was made to determine the impurity by:-

- a. Measuring the freezing range.
- b. Measuring the water content.
- c. Estimation of metallic impurities by activation analysis.

a. The Freezing Range.

The freezing point of benzoic acid for use as a standard in thermometry has been determined by Schwab & Wichers⁵⁴ in an exhaustive series of experiments. They found the triple point of pure benzoic acid to be $122.362 \pm 0.002^{\circ}\text{C}$. and 0.013° higher under a pressure of 1 atmosphere of dry air. It was impossible to duplicate their experiments as they used 400 gms of acid in each fixed point cell. Such a large amount was not

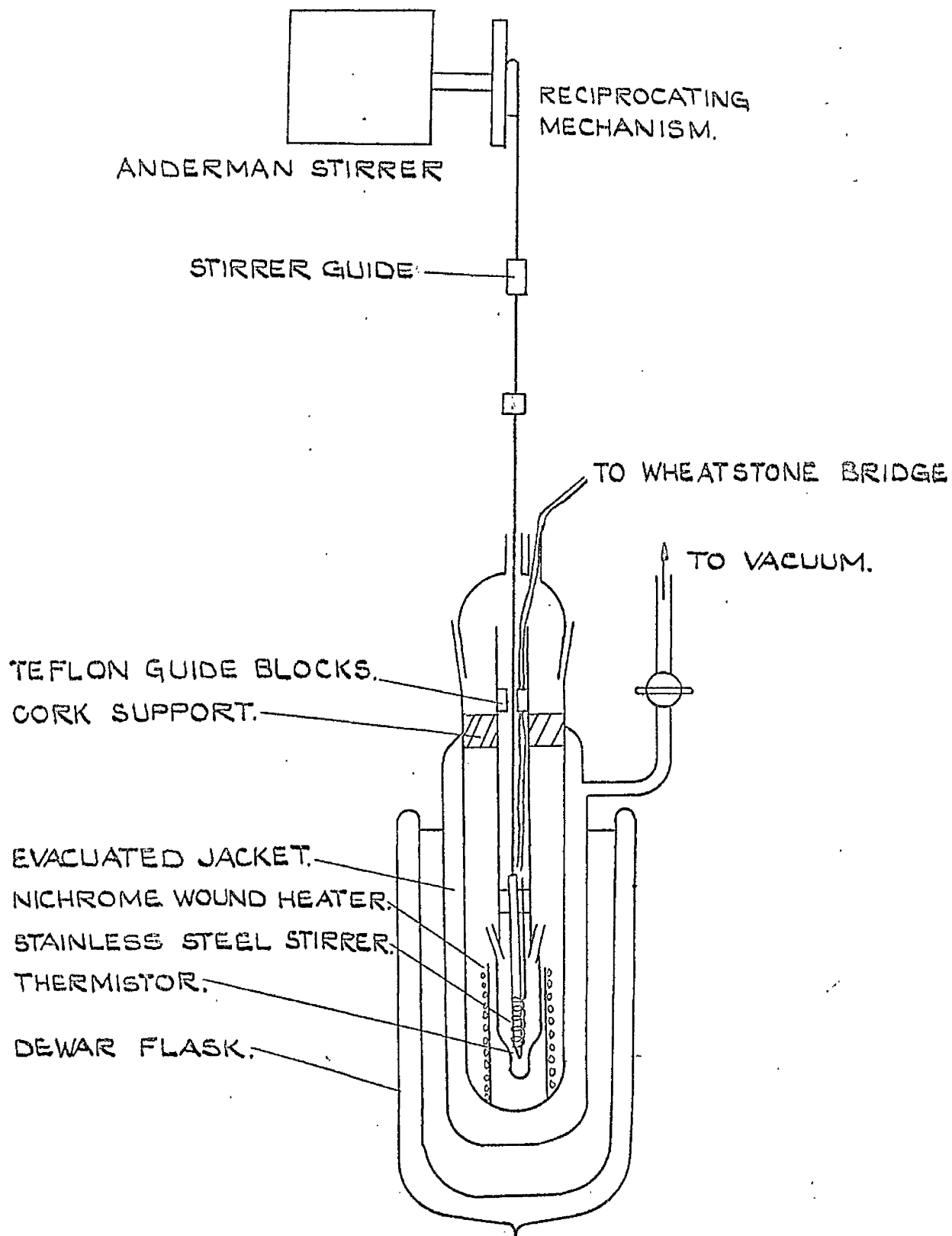


FIG. 12. FREEZING POINT APPARATUS.

available as each crystal grown only weighed 60 gms. An attempt was made to construct an apparatus in which the freezing range of each crystal used in a diffusion experiment could be measured. The final form of this apparatus is shown in fig. 12. It consisted of a small sample holder, sample volume 0.5 ml., attached by a B14 cone and socket to a long glass tube in which two tight fitting teflon inserts acted as guides and supports for a Stantel F15 thermistor and a platinum wire stirrer. The stirrer was adjusted to give a vertical displacement of 1 cm. using an eccentric drive. This tube was surrounded by a glass jacket which could be evacuated. A small 'Nichrome' wound heater controlled through a 2 amp Variac was used to melt the sample and the whole assembly was thermostatted in a glycerol filled Dewar flask.

The procedure used to determine the freezing point was to maintain the outer bath at 75°C . and allow the assembly to equilibrate. The crystal was then melted using the heater, the stirrer started and the temperature obtained by measuring the thermistor resistance on a wheatstone bridge. The outer jacket was then evacuated to minimize the rate of heat extraction. The variation of temperature with time was noted. The thermistor was calibrated against a platinum resistance thermometer and the temperature was accurate to $\pm 0.01^{\circ}\text{C}$.

Attempts were made to measure the freezing point of samples of several single crystal boules. The freezing points obtained,

however, were always lower than expected and it was observed that when the sample was remelted and redetermined the freezing point became progressively lower. e.g. a sample of boule ZR.4 gave melting points 122.30°C ., 122.20°C ., 122.17°C . It was concluded that this progressive decrease in freezing point was due to absorption of moisture in the melt as benzoic acid is significantly hygroscopic in the melt. (Schwab & Wichers⁵⁴ found a 0.15°C decrease in melting point on equilibration with water vapour at a partial pressure of 18 mm. Hg) It was considered that the effect of the stirrer would increase the rate of absorption. On consideration of this fact and the difficulty of obtaining accurate and reproducible results due to the melt supercooling to a variable extent in each determination, this method of purity determination was abandoned in favour of the following more accurate determination.

b. Determination of Water in Benzoic Acid.

The normal method of water determination in acids using the Karl Fisher reagent⁵⁸ was considered but was rejected as the amount of water expected was less than 0.1 μg per 10 μg . Gas-liquid chromatography was considered and a special column of Carbowax 400 on Teflon 6 was prepared. As the benzoic acid was solid it had to be introduced in solution and no water peak could be detected as it was masked by the broad solvent band.

The method used to determine the water content of benzoic acid was that used by Schwab and Wichers⁵⁹ to determine the volatile impurity in high purity benzoic acid which has been

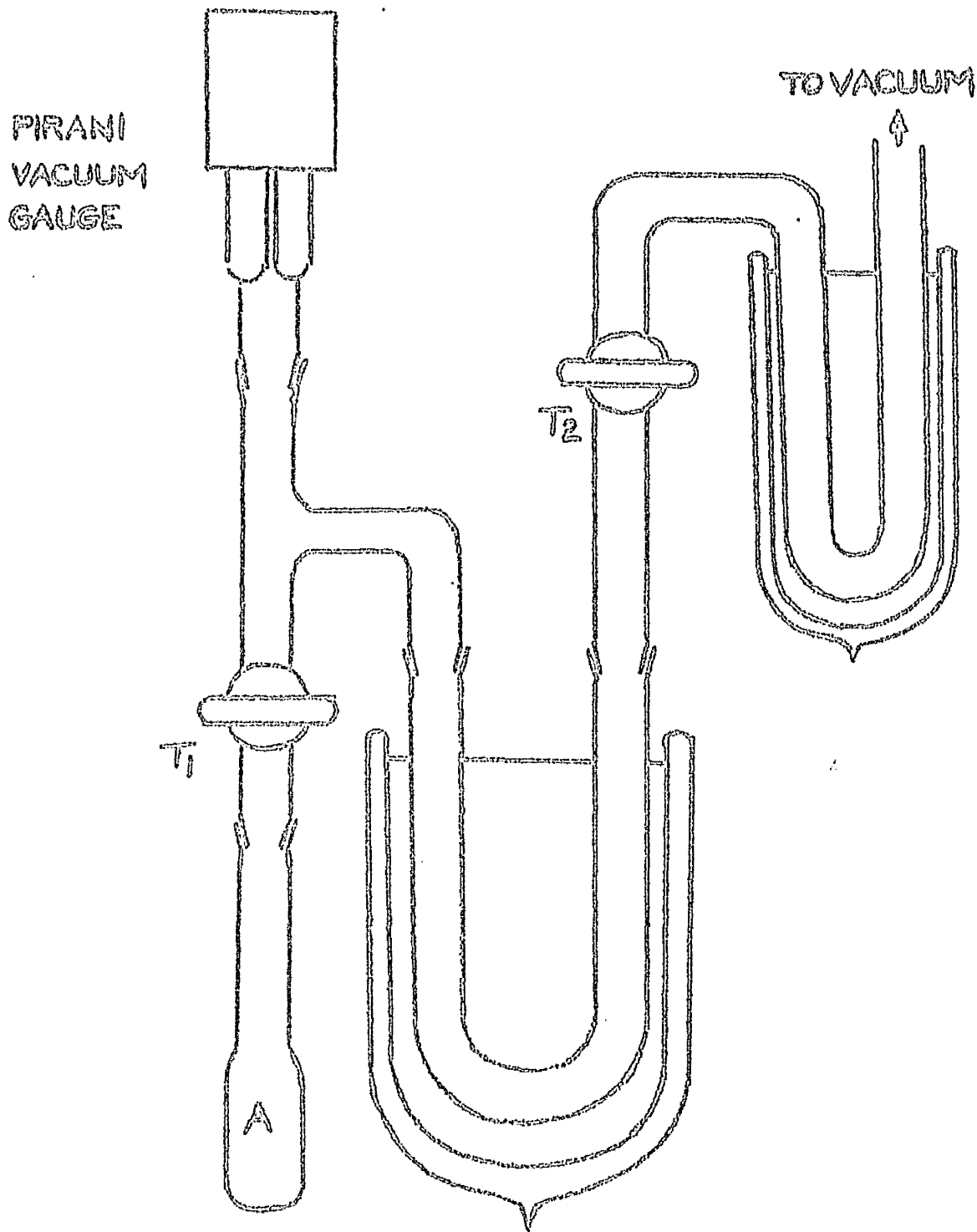


FIG.13 WATER DETERMINATION IN BENZOIC ACID

shown to be almost entirely water. The apparatus is shown in fig. 13. Crystals of benzoic acid were placed in A and degassed for $\frac{1}{2}$ hour to remove any adsorbed moisture. Schwab & Wichers⁵⁹ have demonstrated that the water absorbed by three samples of benzoic acid at 90% relative humidity at 23°C. was 0.0004, 0.0004, 0.0000 mole % on exposure for 45 days. The acid was sublimed in A under continuous vacuum and the volatile impurity trapped in the 'U' tube with liquid oxygen. This tube was calibrated between the two stopcocks, 120 ± 1 ml., and included a Pirani gauge head (Edwards & Co. model GR1) calibrated from 0.1 micron to 1 mm. Hg. When all the acid had been sublimed taps T₁, T₂ were closed and the 'U' tube brought to room temperature using a water bath. The volatile impurity, assumed to be water, exerted its vapour pressure and provided it was less than the saturation vapour pressure at room temperature the amount of water could be determined knowing the pressure and volume of the enclosed system. Blank experiments were performed to determine the pressure increase caused by degassing the sample holder during sublimation.

The pressure in the system after degassing was always 1.5 - 2.0 microns. Two blank determinations increased the pressure to 20 microns. The volatile impurity in three crystals was determined, a non zone refined crystal, a zone refined crystal and the deuterio benzoic acid crystal. In all cases the final pressure was less than the saturation vapour

pressure. It was observed, however, that on standing the pressure slowly decreased due to re-adsorption on the walls of the vessel. The impurity content was therefore calculated from the maximum pressure observed. The weight of crystal, pressure increase and maximum calculated impurity concentration are tabulated below.

CRYSTAL	WT. SAMPLE GMS.	MAXIMUM PRESSURE INCREASE MICRONS.	MOLE % IMPURITY ASSUMED TO BE WATER
NON Z.R.	3.060	120	0.0034
Z.R.7	5.108	90	0.0015
D.B.A.	4.794	110	0.0020

e. Metallic Impurities.

Although the known metallic impurities were low, Fe 0.0002%, Pb 0.0004% alkali metal impurities were unknown and these were determined by activation analysis. ⁶⁰ Samples of nine single crystals and one of Analar Benzoic acid, ranging from 0.3 to 0.5 gms., were activated for one hour in a neutron flux of 10^{12} n.p. cm² (at the Scottish Research Reactor Centre, East Kilbride). Each sample was subsequently analysed on a Laben Multichannel Pulse Height Analyser and a spectrum of each obtained on 128 channels in the range 0.1 - 2.5 MeV. In all cases the Na²⁴ γ peak at 1.37 MeV ⁶¹ was obtained along with its associated background and photopeak at the lower end of the range. A small peak was obtained in the analar acid spectrum at 1.6 - 1.7 MeV presumably due to Cl³⁸ ⁶¹ produced by the reaction

Cl^{37} (n, γ) Cl^{38} . In the single crystals, however, this peak was non-existent or only just detectable indicating that the chlorine concentration was extremely low. The absolute concentration of Na was calculated using the following information. The total counting efficiency for Na γ 's using a 3" x 3" NaI crystal is 28% with a peak to total ratio of 0.37.⁶² The sample was taken to be 3 mm. from the crystal surface. The saturation activity for a 10^{12} neutron flux was 390 mc/gm. Na.⁶¹ The half-life of Na²⁴ was 15.0 hrs.⁶¹ Using the above information all the samples were found to lie within the range 1-3 p.p.m. Hence it is assumed that all other metallic impurities are as small or smaller.

I. 6 Growth of Acetic Acid Crystals.

As in the case of benzoic acid the Bridgman technique was used to grow single crystals of acetic acid. The growing oven used, however, had to be re-designed because of the low melting point of acetic acid ($16.7^{\circ}\text{C}.$)

Crystal Growing Oven.

The oven used was similar to the type designed by Hood and Sherwood⁵¹ for their experimental growth of cyclohexane single crystals. In principle this oven was identical to that shown in fig. 6. the only difference being that the lower metal drum was replaced by a 15 litre Dewar vessel. The lower temperature bath was obtained by packing the Dewar with

an acetone/'Driheld' slurry which maintained a constant temperature of -78°C . for several days and then slowly started to rise. The effect of this slow rise in the lower vessel was only to slow down the rate of crystal growth as the position of melting point isothermal was lowered. The water in the lower 2 litre beaker was replaced by acetone and the glycerol in the upper bath was replaced by water. No background heater was required for the upper bath as it was thermostatted at 30°C . The temperature gradient through the melting point isothermal was measured using a calibrated thermistor and shown in fig. 7. The gradient used was $100^{\circ}/\text{cm}$.

The crystal growing vessels used were those shown in fig. 9 c & d and the lowering rate used was 1.7 mm./hour.

Purification and Crystal Growth.

The starting material used was 'analar' reagent grade acetic acid (Messrs. B.D.H. Ltd.) m.pt. above 16.0°C . (Lit. 16.604°C .)

In the first attempt at crystal growth the acid was simply distilled, the middle fraction, b.pt. 117°C . being collected in the growing tube. The liquid was degassed three times on a vacuum line before sealing under a slight pressure of dry nitrogen. The crystal obtained consisted of many polycrystals all oriented with a vertical cleavage plane and indicated that single crystals could be obtained by this method.

An attempt was made to purify the acid by zone refining in a deep freeze at -20°C . using the zone refiner in fig. 4. The large expansion on melting fractured glass tubing and teflon tubing was used to contain the acid. The acid was purified slowly by this method as the melting point was raised from 16.2 to 16.55°C . after 30 passes. This method was rejected in favour of the following purification procedure recommended by Wiberg.⁶³ As analar acetic acid may contain some acetaldehyde and other oxidisable components $1\frac{1}{2}$ litres was reflux with 2% chromic acid and distilled, 1 litre of the middle fraction, b.pt. $115.5 - 116.5^{\circ}\text{C}$., being retained. This procedure introduced some water as an impurity but this was removed by distillation after treatment with acetyl borate which reacted with the water present to give acetic acid and boric acid which was non volatile. Very pure acetic acid was obtained by this method. The acetyl borate was prepared by heating 1 part Boric acid/5 parts acetic anhydride for one hour at 60°C . On cooling the acetyl borate crystallised out and was filtered off and washed with acetic acid to remove excess anhydride. The chromic distilled acid and the acetyl borate were stored separately until required.

The crystals obtained using this material were of good quality but still produced several single crystal pieces in the boule. The cleavage plane was always obtained vertically. The crystals gave excellent extinction between crossed polaroids

and melted at 16.7°C . An attempt was made to measure the water content of these crystals by gas liquid chromatography. The column used was 10% P.E.G. 400/Teflon 6 on a Griffin and George Mark IIB G.L.C. with a kertharometer detector. Due to the insensitivity of the machine, however, the water content could only be determined to be less than 1:500.

When the crystals were withdrawn from the growing oven they were broken open inside a polythene bag which was subsequently placed in a deep freeze at -20°C . The crystals were then removed and placed in stoppered glass jars and stored in the deep freeze until required. All handling of the crystals was performed in this unit.

Crystal Structure

The acetic acid crystals gave one well defined, easy cleavage plane which from the optical and cleavage studies of Steinmetz⁶⁴ and the x-ray structural analysis of Jones and Templeton²⁹ was concluded to be the (100) plane. Unfortunately this is parallel to the hydrogen bonded chains. As diffusion studies were to be carried out down the hydrogen bonded chains attempts were made to cut the crystals perpendicular to the cleavage plane. The crystals, however, were so hard in this direction that it was very difficult in the direction of growth and almost impossible at right angles to it. The crystals always split along the cleavage plane when this was attempted. As it was impossible to diffuse in the required direction the diffusion and conductivity were studied perpendicular to the cleavage plane.

CHAPTER II

DIFFUSION AND CONDUCTIVITY STUDIES

Ch. II - THE DIFFUSION EXPERIMENTS.

II. 1. Introduction to Diffusion

Diffusion in solids is a kinetic phenomena which can be treated as a macroscopic system without knowledge of the atomic nature of the diffusion process. Diffusion is governed by fundamental laws which were first applied by Adolf Fick and are known as Fick's Laws.⁶⁵

The first of Fick's Laws relates the flux of matter, J , across a given plane to the instantaneous concentration gradient at the plane and perpendicular to it

$$J = -D \left(\frac{\partial c}{\partial x} \right) \quad (1)$$

where D is the constant of proportionality, called the diffusion coefficient and has dimensions $\text{length}^2 \text{sec}^{-1}$

Diffusion problems can be solved by equation (1) only under steady state conditions where $\frac{\partial c}{\partial x}$ is a constant. In many diffusion studies, however, the concentration gradient varies with time and this effect requires the introduction of Fick's second law.

$$\frac{\partial c}{\partial t} = D \frac{\partial^2 c}{\partial x^2} \quad (2)$$

assuming constant D .

Where D is not constant then the second law becomes.

$$\frac{\partial c}{\partial t} = \frac{\partial}{\partial x} \left(D \frac{\partial c}{\partial x} \right) \quad (3)$$

The solution to all diffusion problems can in theory be found by applying the appropriate boundary conditions and solving equation (2) or (3). Usually in self diffusion studies the diffusion coefficient is concentration independent and one diffusion mechanism predominates. In the case of organic crystals the possibility of diffusion anisotropy arises due to the low symmetry of most organic crystals, usually monoclinic or triclinic. This will complicate the diffusion kinetics by introducing 3 diffusion coefficients D_{xx} , D_{yy} , D_{zz} along the x, y, and z axes of the crystal. Previous studies on anthracene⁵³ and naphthalene⁶⁶ have shown no significant variation of diffusion coefficient with crystallographic axes hence it is initially assumed that diffusion in these acids can be treated as isotropic until measurement of the anisotropy have been made.

There are two common methods of measuring diffusion coefficients in solids.

- 1) Non destructive
- 2) Destructive

1) In the non destructive method the rate of penetration of the diffusing species is obtained by monitoring its change of concentration outside the solid either by chemical analysis in the case of impurity diffusion or in the case of self diffusion the activity of a radioactive isotope can be measured

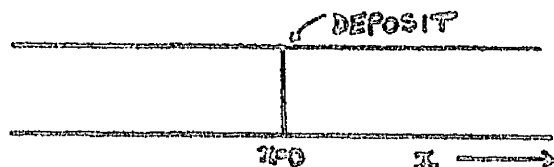
as in the 'surface decrease' method.⁶⁷ The trouble with these methods is that they do not differentiate easily between several concurrent diffusion processes and only an overall diffusion coefficient can be obtained.

2) In the destructive method the solid is sectioned and a concentration profile of the diffusing species is obtained.⁶⁸ The power of this method lies in the fact that concurrent diffusion processes can be observed, though not necessarily measured, and the diffusion coefficient can be obtained to a high degree of accuracy if the experiment is carefully performed.

There are two sectioning methods normally used in diffusion studies.

- 1) Diffusion in an infinite cylinder.
- 2) Diffusion in a semi-infinite cylinder.

Diffusion in an infinite cylinder. In this method an infinitely thin deposit of the diffusing species is placed in the middle of two infinitely long cylinder thus



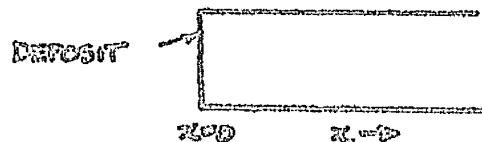
This diffusion couple is then allowed to anneal for a time t_1 after which the cylinder is sectioned on either side of the

interface and the concentration of the diffusing species obtained as a function of distance, x , from the initial deposit at $x=0$. The solution to Fick's law for these boundary conditions is ⁶⁹

$$c(x, t) = \frac{S}{2\sqrt{\pi Dt}} \exp\left[-x^2/4Dt\right] \text{ ---- (4)}$$

where S is the total amount of diffusing species present hence knowing the variation of $c(x)$ with x , the diffusion coefficient can be calculated.

Diffusion in a semi-infinite cylinder is variant of the above method in which an infinitely thin deposit is placed on one end of an infinitely long cylinder.



and allowed to diffuse as before. In this case the solution to Fick's equation is ⁶⁹

$$c(x, t) = \frac{S}{\sqrt{\pi Dt}} \exp\left[-x^2/4Dt\right] \text{ ---- (5)}$$

i.e. twice the concentration obtained in the infinite cylinder method.

The advantages of using the infinite cylinder, are that a check on the diffusion coefficient is given by the symmetry of the concentration profiles. This method also prevents surface diffusion and evaporation losses. In general it is a good method where diffusion coefficients are known to be high and

for examining the Kirkendall effect⁷⁰ in which the initial boundary is found to move. This is only found in impurity (chemical) diffusion and is due to differing diffusion rates of two or more species.

Diffusion rates in molecular crystal have been shown to be fairly low, approximately $1 \times 10^{-10} \text{ cm}^2 \text{ sec}^{-1}$ near the melting point^{53,71} hence this method is considered unsuitable as the two sections of the cylinder would have to be cut and aligned very accurately. In order to minimise these errors the diffusion times necessary would become prohibitively large. The semi-infinite cylinder method has several advantages.

1. A uniform thin deposit can be placed on the surface epitaxially by evaporation or from solution.
2. The crystal can be aligned and sectioned accurately thus allowing diffusion coefficients as low as $10^{-13} \text{ cm}^2 \text{ sec}^{-1}$ to be measured in a reasonable length of time.

The minimum time necessary to measure such a slow diffusion rate can be calculated from equation (5). Assuming a concentration change of 10^4 in a penetration of 30 microns with an initial deposit . approximately one micron thick the time necessary is 600 hrs. i.e. approximately one month. The disadvantage of using this system is possible loss of surface activity by evaporation or surface diffusion. These can be minimised, however, by pressing active faces together, having as small a free volume in the diffusion cell as possible

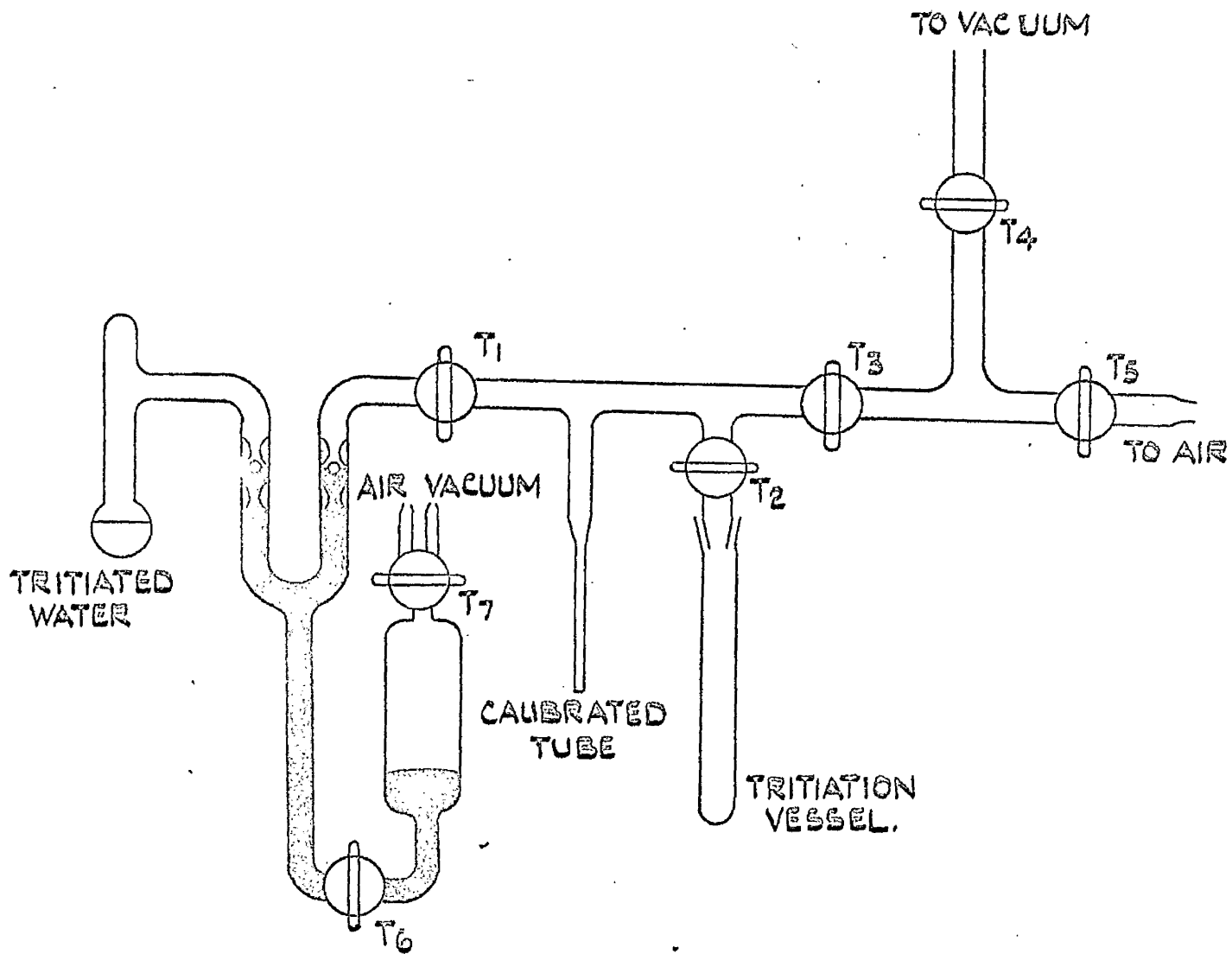


FIG. 14 TRITIATION OF BENZOIC ACID.

and keeping the anneal temperature as constant as possible.

It was decided, therefore, to study the diffusion of tritium and C^{14} in benzoic and acetic acid in this way.

The experimental procedure required the following steps.

1. Preparation of radioactive isotopes.
2. Design and construction of a depositor.
3. Diffusion Anneal conditions.
4. Method of Sectioning the crystal.
5. Radiochemical analysis of the Section.

1.2. Preparation of Radioactive Isotopes.

a. Tritium Labelled Benzoic Acid.

This is one of the simplest preparations of a radioactively labelled molecule, being prepared by a simple exchange reaction between tritiated water and the acidic carboxylic hydrogen of the acid. The activity required was calculated on the basis of a surface activity of 10,000 cps. with a deposit thickness of 2-3 microns and a counting efficiency of 20%. This required a specific activity of approximately 3 micro curies per milligram and this was the tritiation level aimed at.

The apparatus used is shown in fig. 14. 0.35 gms of AnalaR benzoic acid was placed in the tritiation vessel, evacuated to a vacuum of 10^{-5} cm. Hg and taps T_2 and T_3 closed. Tap T_1 was opened and the mercury 'ventil' released to allow tritiated water from the reservoir to be condensed into the calibrated tube using an acetone/'Drikold' mixture. The

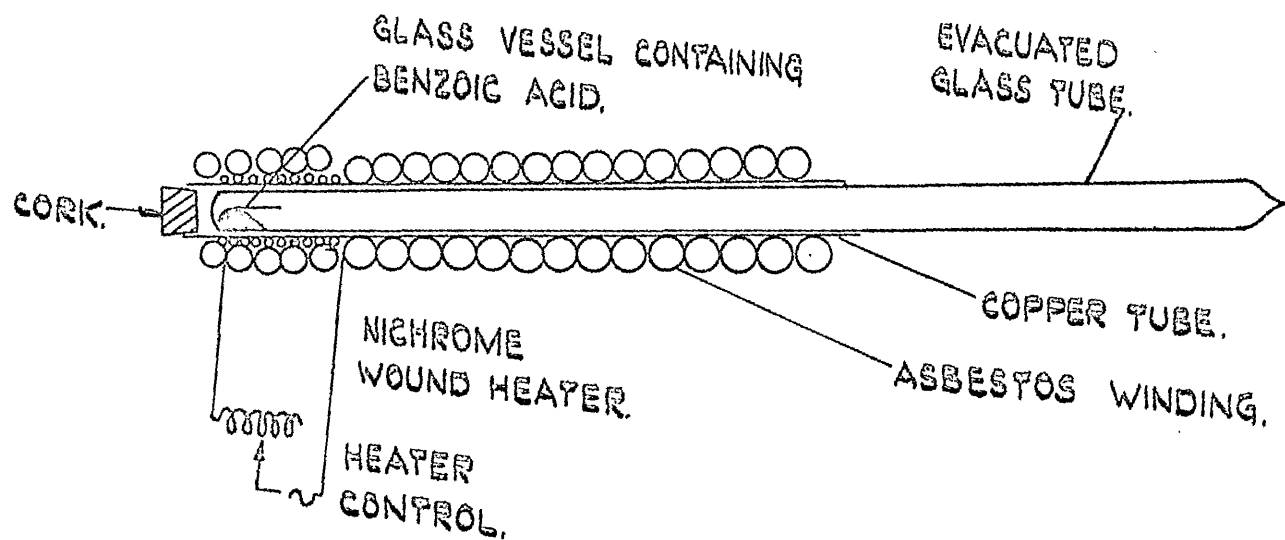


FIG. 15. VACUUM SUBLIMATION APPARATUS.

tritiated water had a specific activity of 1 curie/5 ml. and approximately 1 cm. length of calibrated tube was filled equivalent to 1.5 millicuries of tritium. The 'ventil' and tap T_1 were then closed and the tritiated water distilled into the tritiation vessel where it was left for several days to equilibrate. The excess water was then removed by freezing the water in the reservoir and distilling over the excess with gentle heating of the benzoic acid. After about 1 hour the ventil and T_1 were closed, T_3 , T_4 opened to continuous vacuum and the remaining traces of tritiated water were trapped out in liquid nitrogen cooled traps for another hour. T_4 was then closed and T_5 slowly opened to the atmosphere. The tritiation cell was removed, stoppered with Apiezon grease seal and stored in a fridge at -20°C . until required.

A 50 mgm. sample of this acid was vacuum sublimed in a sublimation tube shown in fig. 15. The tube was evacuated to a pressure of 1-2 microns Hg prior to sealing. The nichrome wound heater had a resistance of 80 ohms and was controlled by a 'Variac' autotransformer. It was found that a 15 v supply gave a temperature of approximately 90°C . at the base of the tube and this was sufficient to give a beautiful zone of small well developed crystals about half way up the tube with a few odd crystals formed at the end of the asbestos winding where there was a sharp temperature drop. The tube was broken open and each of these zones carefully scraped out and placed in stoppered

vials. Approximately 2 mgm. samples of these zones and of the original tritiated benzoic acid were weighed on a microbalance, dissolved in scintillator solution and made up to 25 ml. in a standard flask. One ml. samples of each were taken and counted on the Eeko scintillation counter. The results obtained are shown in the following table.

BENZOIC ACID	WEIGHT mgm	COUNT RATE, R _s cps. per ml.	ACTIVITY cps. per mgm.	ABSOLUTE SPECIFIC ACTIVITY uc/mgm.
ORIGINAL	2.885	378	131.0	0.875
MAJOR ZONE	2.605	340	130.5	0.873
UPPER ZONE	1.892	253	133.5	0.893

These results coupled with the melting point (122-3°C.) show that the benzoic acid is of sufficient chemical and radiochemical purity and the original material was used in the initial tritium diffusion runs even although the specific activity was only one third of that initially aimed at.

It was found, however, that this activity was too low for convenient use as it required long counting times to obtain the required accuracy of 1-3%. A further sample of tritiated benzoic acid was prepared from 1 gm. of zone refined benzoic acid and 0.1 ml. of tritiated water. These were sealed off under a pressure of 10 cm. air in a tube containing a side limb. The benzoic acid was melted and refluxed for 15 mins. after which the excess tritiated water was condensed into the side limb using a liquid nitrogen trap.

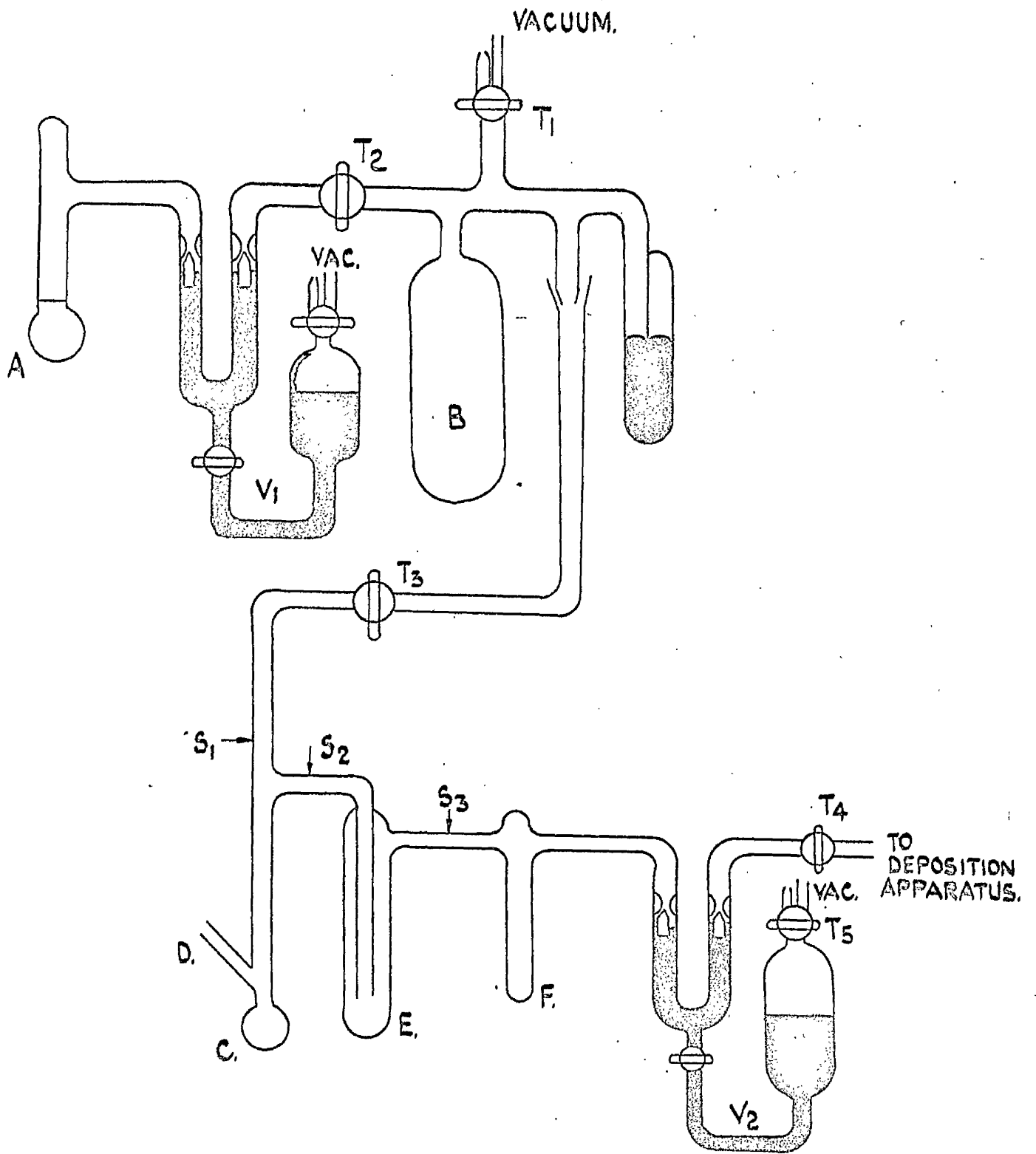


FIG. 16. TRITIATION OF ACETIC ACID.

The benzoic acid was heated until only a white powder remained where upon the side limb was sealed off. The benzoic acid was then removed and placed in a long tube. This tube was then connected to a vacuum line and the benzoic acid sublimed up this tube under a continuous vacuum of 1 micron Hg., the tritiated water again being trapped by liquid nitrogen. The benzoic was then removed and a 100 mgm. sample was resublimed under continuous vacuum. The specific activities of the samples were obtained as for the previous preparation with the exception that the standard solutions were 250 ml. of Analar toluene. The specific activities obtained were 7.45 $\mu\text{c}/\text{mgm.}$ and 7.38 $\mu\text{c}/\text{mgm.}$ respectively thus showing radiochemical purity.

b. C^{14} Labelled Benzoic Acid.

This was obtained direct from the Radiochemical Centre, Amersham as 0.1 millicuries in 2.38 mgm. from batch CFA216/1. As this was much too active to use directly it was diluted by dissolving it in vial containing 2 ml. of scintillation grade toluene along with 36.5 mgm. of zone refined benzoic acid. This was then evaporated to dryness by warming in a draught of hot air with a plug of cotton wool to prevent dust entering the solution. The final activity of the benzoic acid was 2.57 microcuries/mgm. and this was used directly.

c. Tritium Labelled Acetic Acid.

The apparatus used is shown in fig. 16. The tritiated

water in reservoir A was frozen using liquid nitrogen. Approximately 0.75 ml. of Messrs. B.D.H. Analar acetic acid which had been fractionally crystallised three times, m.pt. $16.55 \pm 0.05^{\circ}\text{C}$. and 0.1 gm. of acetyl borate were introduced into vessel C through the side limb D which was then sealed off. Vessel C was then frozen down with liquid oxygen, evacuated to 10^{-2} cm. Hg. and all taps and mercury vents V_1 , V_2 closed. Tap T_2 and vent V_1 were opened and the tritiated water allowed 5 mins to equilibrate to a vapour pressure of 1.8 cm. Hg. Tap T_2 was closed, T_3 opened and the tritiated water was condensed into C using a liquid oxygen trap in approximately 2 minutes. Tap T_3 was closed, T_2 opened and B again filled to 1.8 cm. Hg and condensed into C. T_3 was then closed and C sealed off under vacuum at S_1 . The mixture in C was then boiled gently for a few minutes to allow the acetyl borate to react with the water present. Approx. $\frac{1}{2}$ of the liquid in C was then distilled into E. This was slowly crystallised using ice water until about $\frac{1}{2}$ had crystallised. The supernatant liquid was then 'flash' evaporated into C by placing a liquid oxygen trap around C and sealed at S_2 . The liquid in S_2 melted at $16.55 - 16.70^{\circ}\text{C}$. This liquid was then distilled into F and slowly crystallised and 'flash' evaporated twice before sealing at S_3 . The melting point of the liquid in F was $16.6 - 16.7^{\circ}\text{C}$. The literature value for the melting point of pure acetic acid is 16.67°C . hence the maximum

impurity content is 0.05%.

The volume of section B was 105 c.c. and knowing the vapour pressure of water vapour, 1.8 cm. Hg., the total activity added to 0.75 ml. of Acetic acid was 0.8 millicuries hence making the reasonable assumption of complete equilibration this gave the acetic acid a specific activity of 1 uc/mgm. which was of sufficiently high activity for diffusion studies.

II.3. The Deposition Systems.

a. Benzoic Acid Depositor.

There are two methods of obtaining a thin uniform deposit on a crystal surface, deposition from solution or, if the material is sufficiently volatile, evaporation. As benzoic acid exhibits a sufficiently high vapour pressure, 1 mm. at 90°C. ⁷², it was decided to evaporate radioactive deposits under vacuum. This has the following advantage over deposition from solution.

- 1) Even epitaxial deposits can be obtained.
- 2) The area being deposited can be uniformly masked and varied at will.
- b) The crystal ^{can be} pumped under vacuum for 5 to 10 minutes to clean up the surface before deposition.
- c) The radioactive material undergoes a further purification step during the evaporation.

The disadvantage of this method is that 100% deposition cannot

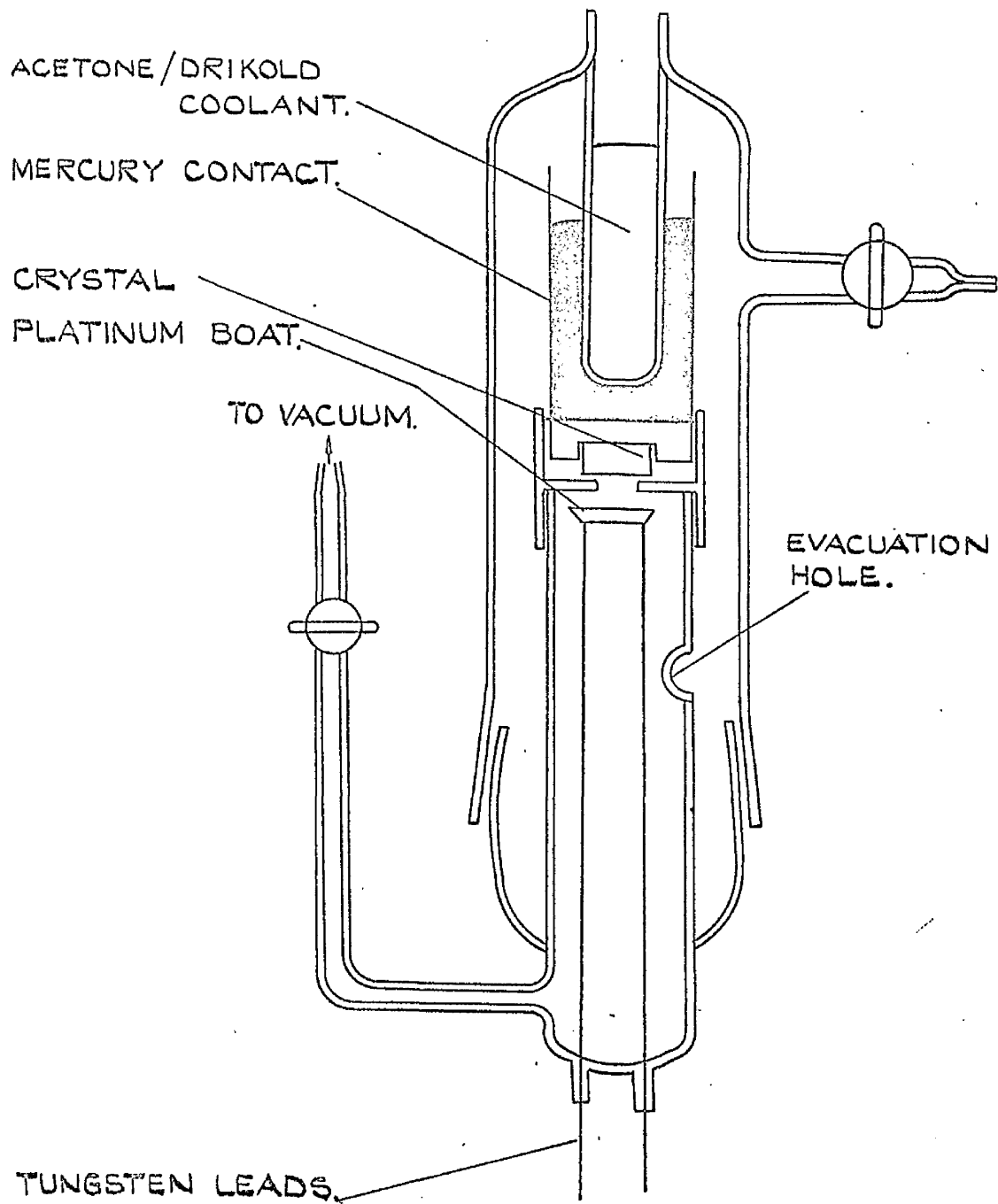


FIG. 17 BENZOIC ACID EVAPORATOR.

be achieved as with deposition from solution but for a well constructed evaporation unit 50% efficiency is not unreasonable. Greater efficiencies can be obtained by cooling the crystal.

The system devised for the evaporation of benzoic acid is shown in fig. 17. It consisted essentially of a small platinum boat contained in a 1.0 cm. i.d. glass tube a few millimetres from the top^{of} whose surface was ground flat. The boat was attached to tungsten leads which were sealed through the glass at the base of this tube. A brass cover piece with a centrally drilled hole 1.0 cm. dia. fitted tightly on top of this tube and the crystal to be deposited was placed over the hole. A brass vessel was then placed over the crystal and fitted tightly into the coverpiece, pressing lightly upon the crystal to give good contact. This upper brass vessel contained mercury which acted as a contact liquid for the glass 'cold finger' which was used to cool the crystal. The system was evacuated through the central tube which had a small hole blown in it to give access to the outer section of the depositor. Before this hole was introduced it was found that the air being evacuated was drawn past the platinum boat so fast that the radioactive material contained in it was blown out.

The thickness of deposit required for the solution to Pick's equation to be applicable should be less than \sqrt{Dt} hence for a diffusion coefficient of $1 \times 10^{-12} \text{ cm.}^2 \text{ sec.}^{-1}$ to be measured in 200 hours the maximum deposit thickness is 8.5u.

The deposit thickness used in all experiments was less than 2-3 microns.

In order to give an even, epitaxial deposit on the crystal surface the evaporation must be carried out fairly quickly to avoid whisker growth, a most undesirable effect which has been observed on evaporating deposits onto organic crystals when the evaporation rate was slow enough to allow preferential crystallization at specific surface sites.⁵⁵ The conditions necessary for good epitaxial deposition were found by experiment. It was found that a heating current of 10 amps passed for 45 to 60 seconds through the platinum boat gave a good deposit. The heating time, however, depended on the vacuum of the system and the amount of material to be deposited. The vacuum achieved varied from deposit to deposit but was always less than 2 microns Hg. The evacuation line used consisted of a 2 stage mercury diffusion pump coupled to an oil filled rotary fore pump. The heating current was obtained using a 6.5v. 20 amp transformer with a Variac controlled means input. The current flowing through the platinum boat was monitored by having an Avometer incorporated in the circuit.

The efficiency of the deposition was measured by evaporating known weights of acid onto 1 cm. dia. glass coverslips and weighing on a microbalance before and after deposition. This was found to give an efficiency of $20 \pm 5\%$. Hence for a deposit of thickness 2 - 3 microns on a surface area of 0.785 cm^2 the weight of acid required in the platinum boat was 1 - 2 μgms . For several diffusion experiments this weight of material was weighed out to ensure that the proper conditions were attained. In others, however, this amount of acid could be judged quite easily. The crystals were cooled in most of the diffusion experiments using an acetone/Drikold mixture taking the crystal temperature down to around 0°C . to increase the efficiency of deposition. This procedure was abandoned in later experiments when it was realised that the cooling was inducing condensation of water vapour onto the crystal surface during the short period between its removal from the depositor and sealing in the diffusion cell which affected the tritium diffusion results quite seriously. The design of the depositor, however, was found to be very successful and was used throughout the series of experiments without modification for the deposition of tritiated and C^{14} labelled benzoic acid.

b. Acetic Acid Depositor.

The acetic acid could not be evaporated in the same way as benzoic acid as it is a liquid at room temperature. Its vapour pressure, 1 cm. Hg. at 17.2°C .⁷², is sufficiently high to allow

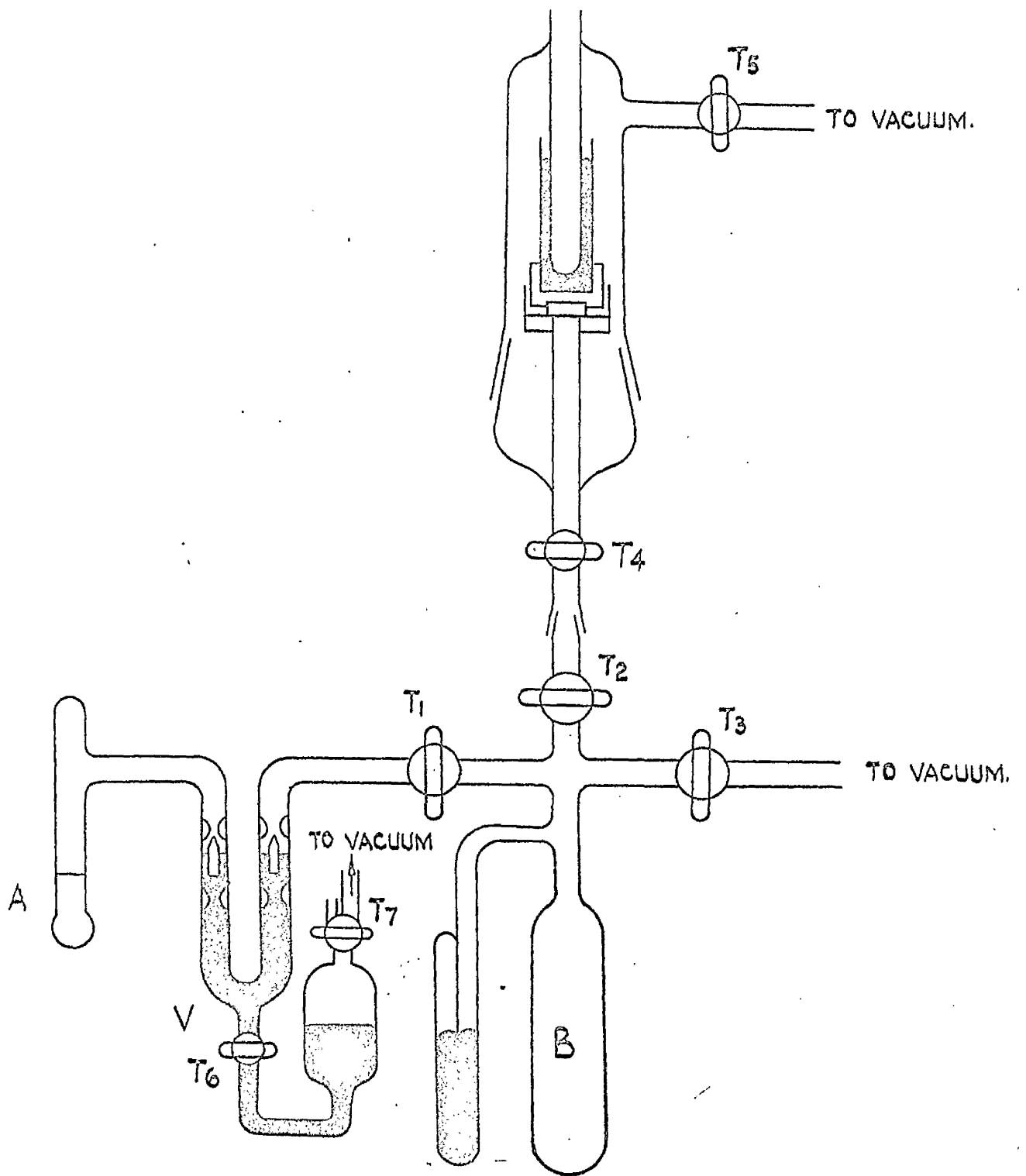
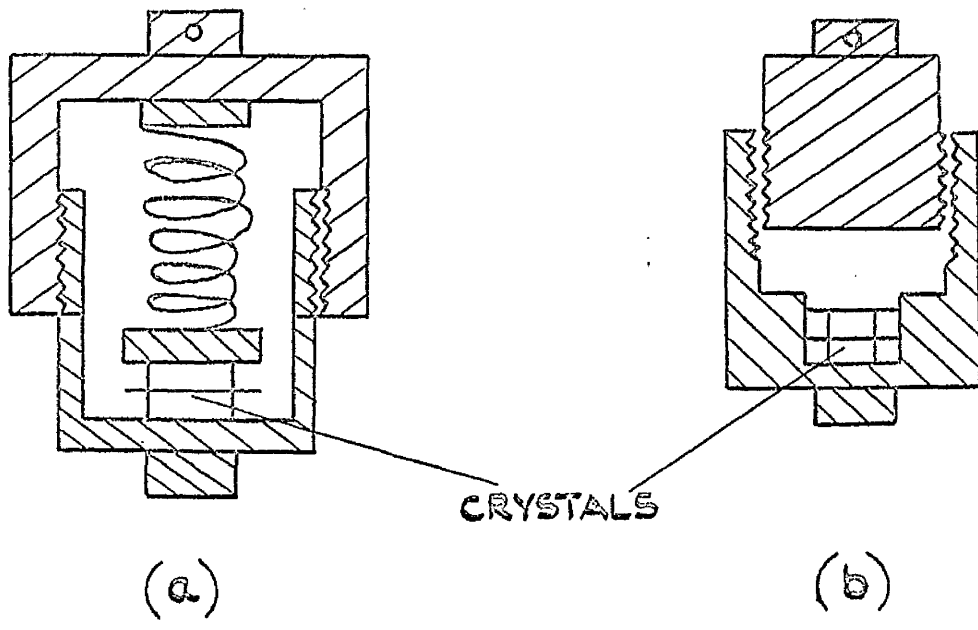


FIG.18. ACETIC ACID DEPOSITION SYSTEM.

a known volume to be filled at room temperature which can be rapidly condensed on a cooled crystal surface. This was the method used.

The apparatus is shown in fig. 18. The crystal holder and cooling section were similar to that used in the benzoic acid evaporator. The lower section was a dosing system in which a known volume B was filled with the saturation vapour pressure of tritiated acetic acid stored in A. This dose was then condensed onto the crystal surface.

The actual procedure finally used to carry out a deposition was as follows. The section above T_2 was removable and the crystal placed in position in a fridge at -20°C . This section was then replaced and the crystal cooled using an acetone/'Drikold' mixture. Taps T_1 , T_4 , T_5 were closed, T_2 , T_3 opened and the known volume B evacuated down to zero pressure on the manometer using a rotary pump. T_2 , T_3 were closed, T_1 opened and the mercury ventill opened and the acetic acid vapour in the system allowed to reach equilibrium, at 20°C . this was 1.1 cm.Hg. T_1 was closed, T_4 , T_5 opened and the upper section pumped down through tap T_5 . T_5 was closed and T_2 slowly opened. The manometer fell rapidly to approximately 0.1 cm. Hg. showing that the acetic acid was condensing out and that the crystal temperature was approximately -20°C . from the residual vapour pressure. T_2 , T_4 were then closed and the upper section returned to the fridge where the crystal was quickly removed



BENZOIC ACID DIFFUSION CELLS.

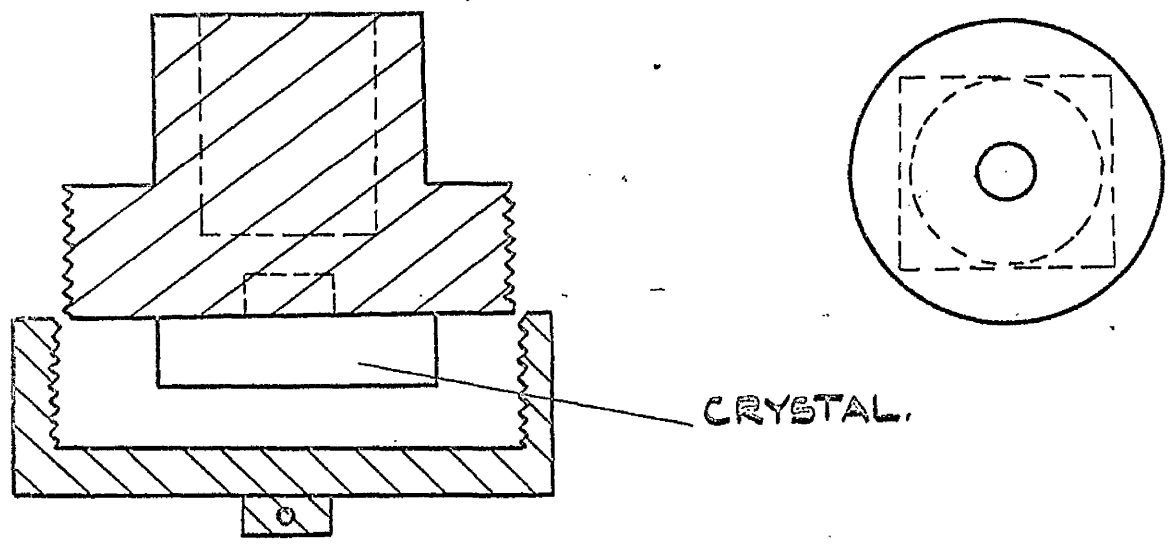


FIG.19. ACETIC ACID DIFFUSION CELL.

and sealed in the diffusion cell. The handling of the crystal in the fridge was the most unsatisfactory feature of the whole operation due to the possible contamination with water vapour (s.v.p. at -20°C ., 0.77 mm.). This was minimised by carrying out these transfer operations as quickly as possible.

4. The Diffusion Anneal Conditions.

a. Benzoic Acid Diffusion Cells.

The diffusion cells used were designed so that several crystals could be diffused simultaneously, the crystals could be pressed against each other with glass or mica spacers and the cell could be sealed air tight. The original cell, fig. (9) was constructed in brass and had a total internal volume of 15 cc., most of which was taken up by the spring used to press the crystals together. This cell was found to be satisfactory for temperatures up to 100°C . above this temperature it was observed that a slight reaction occurred between the brass and benzoic acid and that evaporation of the crystal became a serious objection to their use. A second set of cells was constructed in aluminium fig. (9) in which the free space was cut down to a minimum, the total available space being 3 cc. These were found to be vastly superior with little or no evaporation being observed even at 116°C ., 6°C below the melting point. Both cells were sealed by screwing both halves

together using teflon tape to give a gas tight seal.

Acetic Acid Diffusion Cell.

The simple cell used above was not suitable for acetic acid as the crystals could not be conveniently handled. The cells used in this case are shown in fig. 19 and were constructed in aluminium. An acetic acid crystal was cut to approximately the correct size 1.5 cm. dia. x 0.2 mm. thick. This was then bonded on to the plane surface of the cell using a few drops of pure liquid acetic acid which froze to the crystal and the cell in the fridge. The square end of the cell was clamped in the chuck of the microtome and aligned using the technique described in the next section. The crystal was microtomed for several hundred microns and the sides cut off immediately prior to deposition. The diffusion cell fitted into the depositor and the mercury contact to the cold finger fitted into the hole at the top of the cell as shown in fig. 18. On removal from the depositor the bottom cover of the cell was screwed on using a teflon tape seal. After the diffusion anneal the cell was remounted and aligned on the microtome in the fridge prior to sectioning.

Thermostat Baths.

Benzoic acid diffusion was measured in the range 70 - 116°C. The first bath used was a 5 litre beaker of silicone oil, contained in a large metal drum and insulated with 'Rocksil'.

The thermostat unit was simply a xylene filled toluene regulator which controlled a 250 watt immersion heater through a 'Sunvic' vacuum switch F102/3 . This was found to operate satisfactorily with an accuracy of $\pm 0.1^{\circ}\text{C}$. over short periods of time and $\pm 0.2^{\circ}\text{C}$. over a period of several days. At elevated temperature it was found that the stirrer occasionally stuck and when this happened the run was abandoned as the temperature variations with position in the bath were large. Where long diffusion anneal times were necessary a second annealing oven was constructed. A nichrome winding was made on an insulated brass former 3 " dia. x 1' long having a central hole 1.5" dia. This winding was insulated with asbestos and encased in aluminium with syndanyo end pieces. The temperature was maintained by a thermistor controlled thermostat circuit, fig.20 , the thermistor being located in a 3" well drilled in the central brass former. The temperature stability of this oven was found to be better than $\pm 0.05^{\circ}\text{C}$ using a 50°C Beckman thermometer. The temperature gradient down the oven was measured with a Pt.-Rh thermocouple and found to be constant over a 6 " length at the middle of the oven. Diffusion cells were always placed in this region and their temperature measured with a 0 - 200°C . thermometer which had been standardised against an N.P.I. standardised thermometer.

The acetic acid crystals were annealed in either a Thomson

and Mercer '-70 thermostat bath' accurate to $\pm 0.05^\circ$ or a laboratory constructed low temperature thermostat designed by Dr. J. N. Sherwood for use down to -20°C . with an accuracy of $\pm 0.05^\circ\text{C}$.

II.5. The Sectioning Technique.

The major problem faced in studying diffusion by the semi-infinite solid method is to align the crystal accurately parallel to the initial face and take uniform sections of the crystal perpendicular to this face. There are several possible methods of sectioning.

1. Grinding.
2. Removal using a lathe.
3. Microtoning.
4. Evaporation.
5. Dissolution.

Grinding has been successfully used to measure very low diffusion coefficients in NaCl^{74} of the order of $10^{-14}\text{cm}^2\text{sec}^{-1}$ but a high precision grinding machine was specially constructed and it is not a routine method. Sectioning using a lathe is the normal metallurgical practice and has been applied to the sectioning of Anthracene⁵³. The limiting factor using the lathe, however, is that the minimum section which can be accurately taken is about $\frac{1}{1000}$ " i.e. 25 microns hence the minimum diffusion coefficient which can be measured

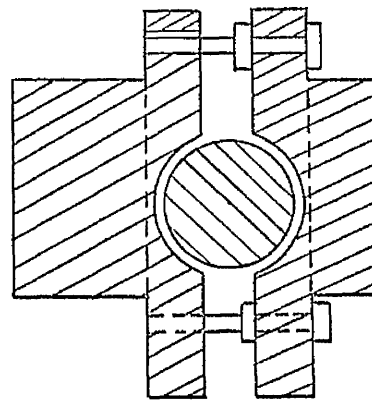
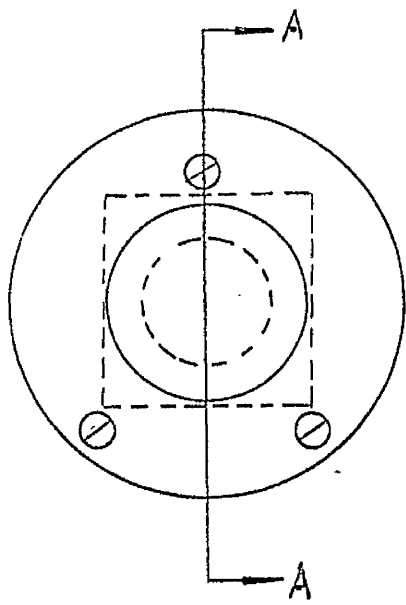
Assuming 6 active sections and a diffusion anneal time of 200 hours is $8 \times 10^{-12} \text{ cm}^2 \text{ sec}^{-1}$. This is not considered sufficiently low for the present study. Sectioning by evaporation is a technique which has been recently used to section ice crystals⁷³ by subliming layers from the crystal held at -80°C . onto a collecting plate at -20°C . This method, however, may preferentially etch crystals down grain boundaries or dislocation pipes and is difficult to ensure uniformity of section thickness and planarity of the crystal face. Diffusion coefficients of $10^{-13} \text{ cm}^2 \text{ sec}^{-1}$ have been quoted using this method. Sectioning by dissolution is a common metallurgical technique and may prove useful in studies in organic material but it is open to the same objections as evaporation. Very low diffusion coefficients of the order of $10^{-19} \text{ cm}^2 \text{ sec}^{-1}$ have been_{measured} by dissolution techniques⁷⁴ but is particular to the case of tantalum. The most satisfactory method appeared to be the microtome. The normal sledge based or rotary microtome can take sections of 1 - 15 microns thick with a high degree of accuracy. Assuming 6 active sections of 5 microns each and a diffusion time of 200 hours a minimum diffusion coefficient of $3 \times 10^{-13} \text{ cm}^2 \text{ sec}^{-1}$ can be measured. This was considered sufficiently accurate for the present experiments. In previous experiments on molecular crystals a diffusion coefficient of around $10^{-10} \text{ cm}^2 \text{ sec}^{-1}$ was obtained at temperatures approaching the melting point. Hence diffusion coefficients should be

measurable over a range of 10^3 which was thought sufficient to allow accurate calculation of the diffusion parameters.

The microtome used was a Beck Rotary microtome model no. 3820/163 which was calibrated to take 1-15 μ sections. In this microtome the crystal is moved in a vertical plane past a knife blade fixed at some slight angle to the vertical. For every rotation of the microtome handle the knife blade moved towards the crystal by the amount set on the calibration dial. The accuracy of the calibration was checked over large distances, hundred of microns, by Dr. G. M. Hood using a travelling microscope and found to be true.⁷⁵ The accuracy of sectioning in the region 5 μ , 10 μ , 15 μ was determined by weighing section of a piece of paraffin wax of known surface area and density. These weighings were carried out on an Oertling microbalance. The overall accuracy of sectioning was found to be 1% with average deviations of 5%, 3%, 3% for 5, 10, and 15 μ slices respectively. These values were considered sufficiently accurate for the experiments. The accuracy of the microtome was also experimentally confirmed for benzoic acid using the sectioning method of collection described later.

Alignment of the Crystal.

As this was the most crucial step in the experiment much thought was given to the best method of alignment. Alignment



SECTION AA.

FIG. 21. FINE ADJUSTMENT CHUCK.

using a travelling microscope was rejected as insufficiently accurate and the method chosen was based on the optical lever. The alignment operation required the construction of a fine adjustment chuck fig 21, as the chuck of the microtome only gave rough positioning. This fine adjustment chuck was held by the microtome chuck and it rotated on a ball joint, the accurate setting of the face being attained using the 3 adjustment screws. A piece of paraffin wax was melted on to this chuck and microtomed to give a smooth face. A small plane mirror made by vacuum depositing silver on a microscope slide was placed on this face and held in position using a strip of 'Sellotape' transparent adhesive. A 'Sealamp' light source was positioned about 3 feet from the microtome and the light reflected from the mirror onto a plain white paper above the lamp. Cross wires were placed on the lamp bulb and their reflection was focussed on the paper. The centre of the cross wires was marked and this acted as the reference point for the plane of the knife blade. The chuck was removed and the crystal stuck on using 'Picene' wax which gave a rigid mount. The mirror was replaced on the face of the crystal and remounted on the chuck. The face of the crystal was then brought into the correct alignment by use of the fine adjustment screws so that the reflection of the cross wires was again at the reference point. The crystal was now aligned parallel to the blade but not at the edge of the blade. The knife blade was

adjusted to almost the correct position at the crystal face by using an adjusting screw on the microtome. This was then locked and sectioning commenced until the blade was just scraping the surface of the crystal. Usually after a diffusion anneal it was found that slight variations had occurred on the crystal surface and the first slice was always suspect due to these variations, slight compression effects and the fact that the position of the crystal surface was not known accurately. Allowance was made for the thickness of the first slice by comparing its weight with the others. It should be noted that when attempts were made to section the crystal with the knife blade vertical the compression effect was so great that the crystal shattered. Experimenting with the angle of the blade showed that at an angle of 15° to the vertical negligible compression was experienced. At all angles, however, in the case of benzoic acid, it was found that on sectioning the acid disintegrated into a powder which had a tendency to 'spark' due to static charge. This sparking occurred only with benzoic acid and not with other organic crystals like anthracene and naphthalene which were found to give a coherent slice which could be readily picked off the knife blade using a single edged razor blade. This fact is in keeping with the greater hardness of benzoic acid which was quite a brittle crystal and when a single crystal was grown it gave a metallic ring when struck. Non-single crystals, however, gave a much

more muted sound.

This problem of slice collection was difficult to achieve completely. A method which had previously been used to collect crystals which disintegrate was to place a strip of adhesive over the crystal face prior to sectioning. On microtoming the section adheres to the adhesive which is simply removed and counted. This method was used by Mapother Crooks and Maurer to section sodium chloride crystals.²⁴ When this procedure was attempted the adhesive always stuck to the knife edge as sectioning started buckling the adhesive and causing distortion of the crystal, hence it was rejected.

The method used was to take a 10 μ section. This powdered and spread out in a fan shape over the knife blade with a fairly thick ridge along the knife edge. A 1" piece of glass capillary was dipped into a vial containing cyclohexane, in which the solubility of benzoic acid is only a few mgm./ml., and capillary attraction filled the tube. The end of this capillary was allowed to touch the knife edge and the cyclohexane immediately flowed out wetting the powdered acid. This small amount of liquid was sufficient to bind the particles together and allowed them to be removed from the knife blade using a single edged razor blade. The acid was immediately transferred to a piece of plain white paper 2" square and the cyclohexane allowed to evaporate off over 5-10 minutes. The section then looked like a white needle about $\frac{1}{2}$ " long. It was subsequently transferred

to a $\frac{1}{2}$ dram glass vial and stoppered prior to weighing on a microbalance which weighed to 0.002 mgms. The weighing procedure was to allow each vial 5-10 minutes to reach equilibrium, the weight was recorded, the vial picked up with tongs and inverted over a filter funnel sitting in an empty scintillation vessel. The vial was given a sharp rap to knock all the acid into the funnel then replaced on the balance and reweighed while 10 ml. of scintillator solution was used to wash the acid into the scintillation vessel. The difference in the two weighings was taken as the weight of acid in the scintillation vessel. Due to the sparking of the acid it was not possible to collect the section in 100% yield and the several operations also involved some loss. The weight per section could vary considerably depending on the amount of sparking. An example of an average run is shown below.

Section 10 μ	Wt. MGM.	% DEVIATION FROM MEAN	SECTION 10 μ	WT. MGM.	% DEVIATION FROM MEAN
1	0.613		10	1.300	11.3
2	0.966	-17	11	1.238	11.1
3	1.311	12.2	12	0.960	-17.8
4	1.135	- 2.8	13	1.173	0.34
5	1.164	- 0.35	14	1.274	9.0
6	1.090	- 4.3	15	1.178	0.85
7	1.064	- 8.9	16	1.194	2.2
8	1.190	1.9	17	1.200	2.7
9	1.207	3.3	18	1.190	1.9

The average weight per 10 μ section = 1.168 mgm.

The weight calculated from a surface area of 1.21 sq. cm. and density 1.32 gm./cc = 1.60 mgm.

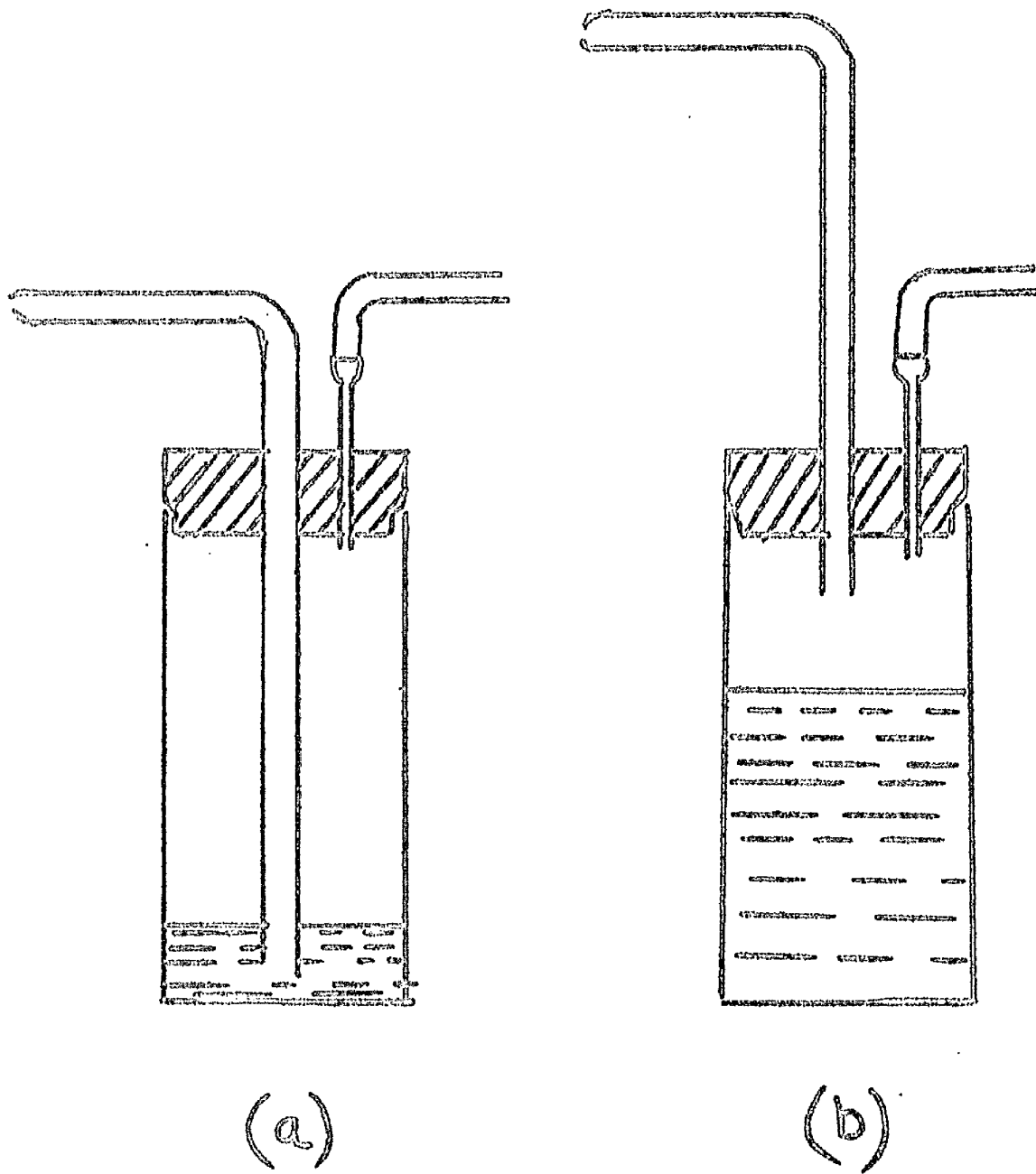


FIG. 22 SUCTION APPARATUS

The average % of slice collected $\frac{1.168}{1.60} \times 100 = 73\%$.

This is typical of the deviations experienced. Fortunately it was not essential to obtain the section in 100% yield as only the specific activity per section was required, i.e. the activity per milligram, to plot the concentration variation with penetration into the crystal. Therefore having shown that the microtome was accurately calibrated the actual penetration was taken from the microtome calibration and the weight per section was only used to determine the specific activity, except for the first slice whose thickness was obtained by comparing it with the average weight per section. This sectioning method was considered suitable for 10 μ slices where weights of about 1 mgm. were obtained to an accuracy of 2% or better. It was found, however, that the diffusion coefficients to be measured required 5 μ slices to be taken as the penetration distances became smaller and the weight of the section fell to 0.4 - 0.5 mgm. for a 1 sq. cm. crystal. Crystals of around 1 sq. cm. were found to be the optimum size for ensuring uniform surface planarity.

A more refined method of section collection was developed based on a suctioning method described by Labes et al.⁷⁶ This enabled the complete section to be collected and smaller crystals to be used. The apparatus was simple and shown in fig. 22. Central holes were drilled in 20 polythene caps for 4 dram glass vials. Right angled pieces of 0.5 cm. dia. x 6"

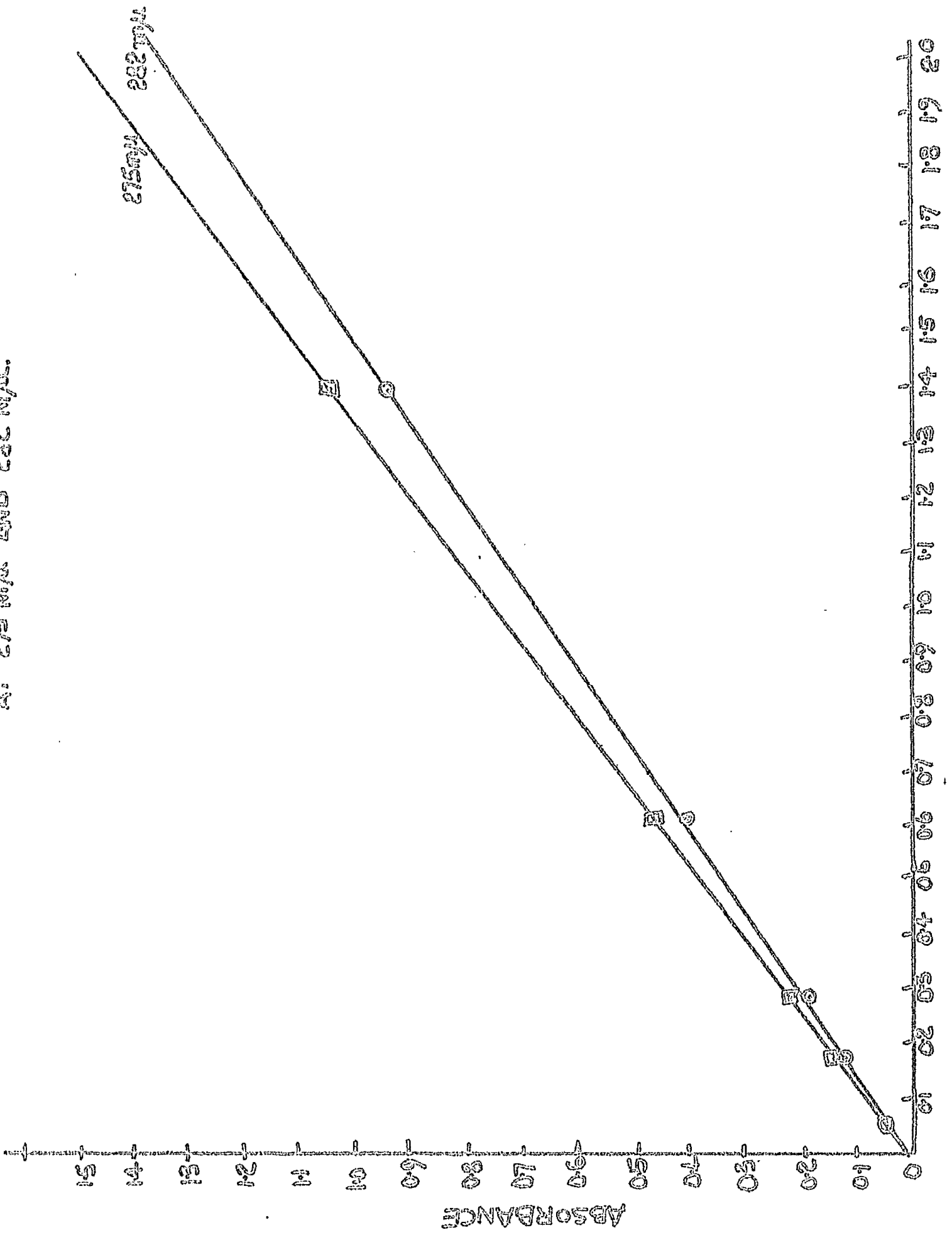
long glass capillary tubing were introduced to give a tight but sliding fit. The protruding edge was rounded off to protect the crystal from scratching. Approximately 0.5 to 1 ml. of a trapping liquid was drawn into the vial by inserting a syringe needle into the polythene cap which was connected to a water pump which gave a vacuum of a few inches Hg. The external end of the capillary was drawn backwards and forwards across the knife edge as the section was taken and when the vacuum was high enough every particle was drawn into the capillary. This enabled the act of cutting to be observed throughout the operation thus ensuring that no part of the surface was being missed. This was especially important at high diffusion temperatures where it was found that distortions of the surface of a few microns could occur. When this happened the procedure adopted was to take the first section and chop off any part of the face not being sectioned using a sharp razor blade. Once the section had been taken the capillary was raised as in fig. 22b and a further amount of liquid drawn through the capillary to wash through any adhering particles.

The accuracy of this technique was checked by taking benzoic acid sections in cyclohexane. These were made up to 10 ml. in a standard flask and their U.V. spectra taken on a Perkin Elmer 137 U.V. Spectrophotometer in 1 cm. cells.

The U.V. spectra of benzoic acid in cyclohexane fig. 10

FIG 23

UV CALIBRATION OF BENZOIC ADD IN CYCLOHEXANE
AT 275 M μ AND 282 M μ .

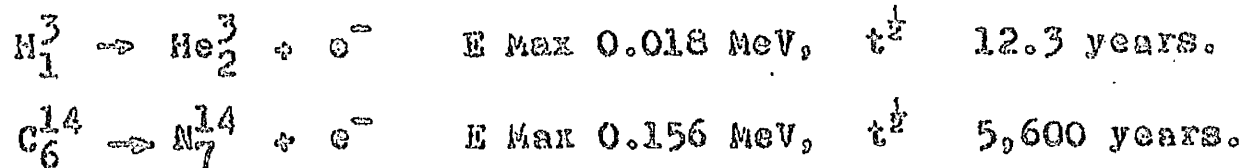


consists of 2 bands in the region 205 - 295 μ known as the B and C bands ⁷⁷ the B band having λ_{\max} 229 - 233 μ with $\log \epsilon_{\max}$ 4.15 and the C band having 2 maxima at λ_{\max} 275 μ and 282 μ with $\log \epsilon_{\max}$ 2.88 and 2.74 respectively. It was found that the C band gave ideal absorbance peaks in the region 0.5 to 1.2 absorbance units for concentrations of 0.5 to 2.0 mgm. per 10 ml. cyclohexane and a calibration graph, fig. 23, of peak height at 275 μ and 282 μ vs acid concentration was constructed using standard solutions of benzoic acid in cyclohexane. The weight per section was then read directly from this graph.

The sectioning procedure developed was to take the first section in cyclohexane to determine its weight and the subsequent sections in scintillator solution. In this case 10 ml. of scintillator was accurately measured into a 50 ml. beaker. Approximately 0.5 to 1 ml. was drawn from this to trap the section. After sectioning the capillary was raised to prevent air bubbling through the solution to minimise oxygen quenching and the remainder of the scintillator drawn in. The special cap was then removed and the vial stoppered giving a 10 ml. solution ready for scintillation counting. By this method a check could be made on the activity as sectioning proceeded. When the sections ceased to be active several 10 μ sections were taken in cyclohexane to determine the average weight per section and the accuracy of sectioning which was normally found to agree with the theoretical weight to within 5%.

6. DETERMINATION OF RADIOACTIVITY IN THE CRYSTAL SECTIONS.

The radioactive isotopes used in this investigation, tritium and carbon -14, have the following decay schemes:-



There is only one step in each decay scheme resulting in the emission of a weak β particle. Both β 's have half-lives long enough to be considered invariant during the course of any experiment.

The low β energies eliminate the use of end window Geiger Muller counting for their detection and require the more sophisticated techniques of internal gas counting⁷⁸ or scintillation counting⁷⁹. The former method requires the combustion of the radioactive sample to a suitable gas, CO₂ or H₂, which can then be counted internally in a G.M. tube. This method gives high counting efficiencies but is very time consuming.

The more rapid method of scintillation counting yields high counting efficiencies with 90% having been recorded for C¹⁴⁸⁰ and 40% for tritium⁸¹. It was decided, therefore, to use scintillation counting to detect both isotopes.

The principle of liquid scintillation counting is as follows. The radioactive sample is dissolved in a suitable

organic solvent containing a scintillating phosphor, known as the scintillator solution, and placed over a photomultiplier tube in a light tight box. The β particle emitted activates the phosphor to an excited state which decays with the emission of a photon, $h\nu$. This photon interacts with the photocathode of the photomultiplier tube which emits an electron. This electron is amplified through the dynode chain of the photomultiplier to give a weak electronic pulse which is subsequently re-amplified to operate a scaling unit or recorder.

Counting Assemblies.

Two liquid scintillation assemblies have been used. Initially the assemblies used for C^{14} and T consisted of the following units. An Ecko head unit, N664B, having a 2" water cooled photomultiplier, was followed by a Nuclear Enterprises non-overloading linear amplifier, NE5202, and Nuclear Enterprises differential pulse height analyser, NE5102. The output from the pulse height analyser actuated a Dynatron scaling unit, type 1009E, coupled to an automatic timing unit N108. The stabilised L.H.T. supply to the head unit was supplied by a Dynatron power unit N103.

This assembly was later replaced by a complete Nuclear Enterprises unit consisting of a head unit, NE5503, having a 1" water cooled photomultiplier, amplifier NE5202, pulse height selector NE5102 and power supply NE5203. The Dynatron

scaling unit, 1009E and timer was also used with this assembly.

Counting Conditions.

The best counting conditions are not necessarily those which give the highest efficiency as this is always associated with a high background count rate which will have a large variation which will prevent accurate determination of low count rates.

The conditions required in this investigation were those which would combine a high counting efficiency (to reduce the counting time) and low background with long term stability during the time taken to count any particular diffusion run. In each case the best conditions were obtained by varying the four parameters E.H.T., amplification factor, pulse height and gatewidth around the values recommended by the manufacturer. The conditions used are tabulated below.

ECKO	EHT VOLTS	AMPLIFICATION FACTOR	P.H. VOLTS	GATE VOLTS	BACKGROUND cps.	EFFICIENCY %
T	1400	5000	6	30	5.0	17
C ¹⁴	1350	10,000	30	20	0.2	66
N.E.						
T	750	5,000	6	30	3.0	15
C ¹⁴	750	5,000	10	30	0.5	60

It was found that the counting conditions altered slightly from day to day when the counter was switched on but they remained

FIG 24 a

EFFECT OF SCINTILLATOR VOLUME ON TRITIUM COUNTING EFFICIENCY.

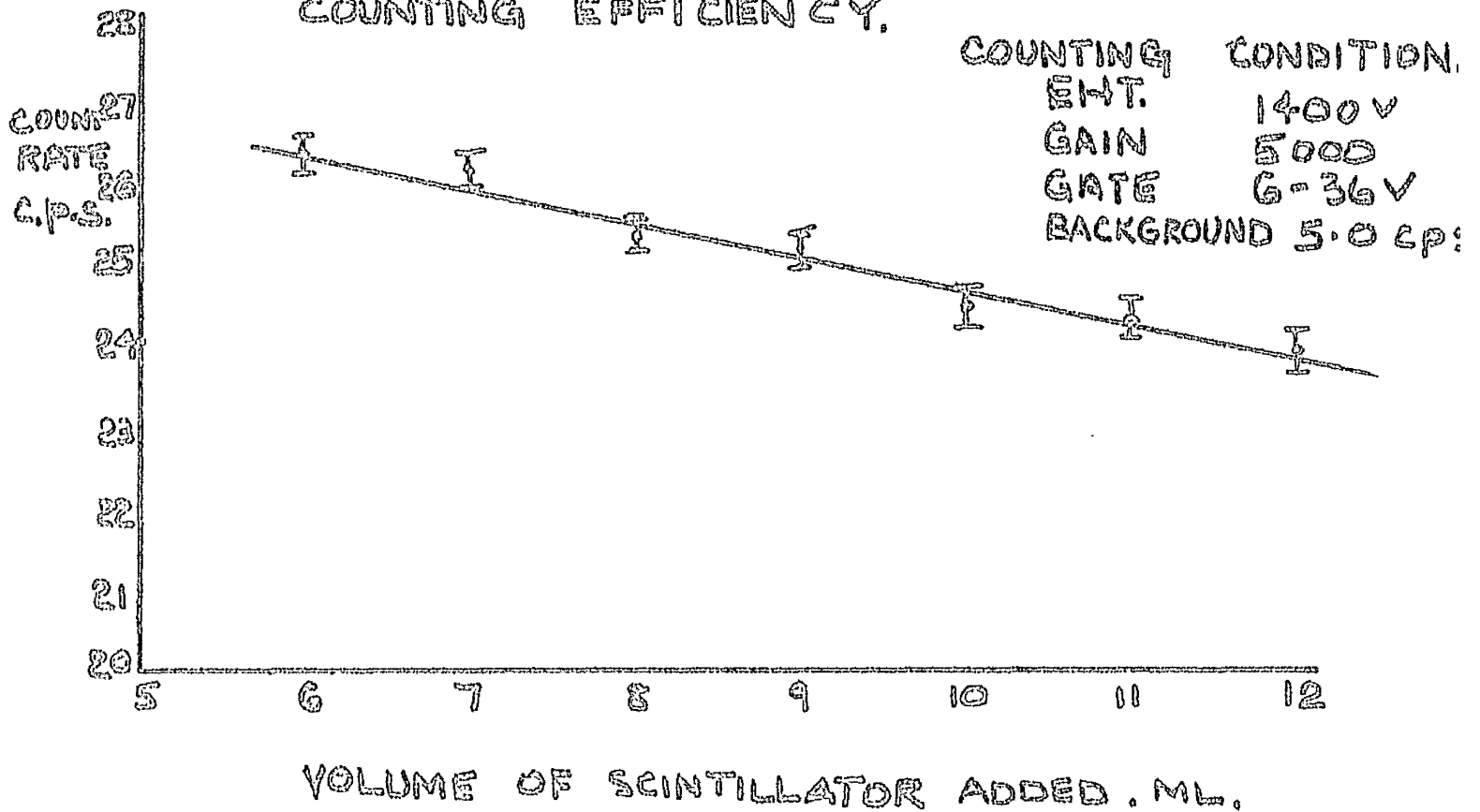
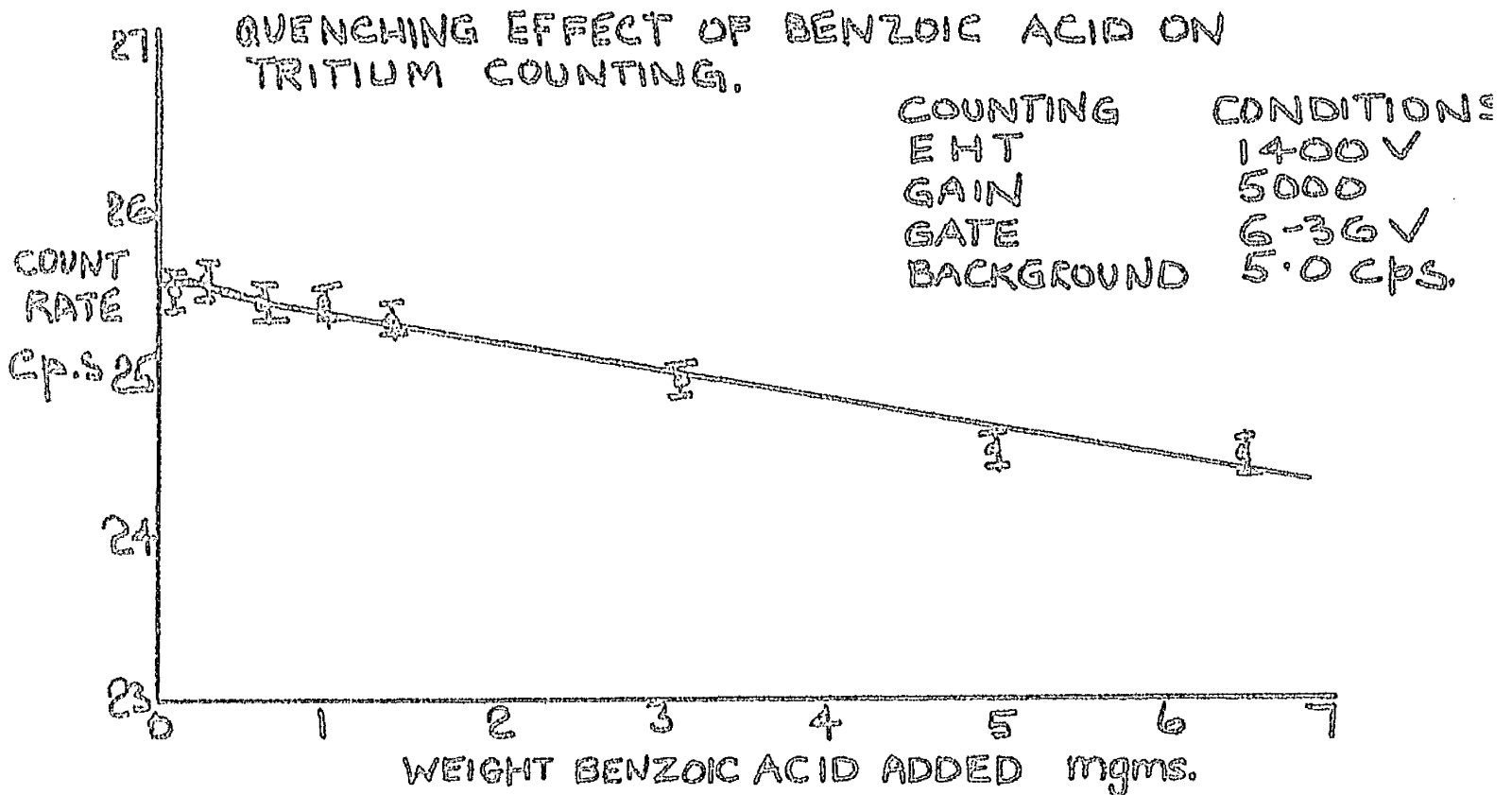


FIG 24 b.

QUENCHING EFFECT OF BENZOIC ACID ON TRITIUM COUNTING.



stable after a 1-2 hour warm up period. A long term drift in stability was observed over a period of months due to the ageing of the photomultiplier and consequently slight changes had to be made in the counting conditions.

Factors Affecting the Counting Efficiency.

a. Volume of Scintillator.

A depth effect was experienced due to the photons being absorbed by the scintillator. This effect is shown in fig. 24a. The efficiency was greatest at small volumes of scintillator but was very dependent on the volume of scintillator. This dependence decreased with increasing scintillator volume. The volume of scintillator used in all samples was 10 ml. and at this level the efficiency only varied by 0.5%/ml. This large amount was also necessary to wash the radioactive sample into the scintillation vial.

b. Quenching.

It has been shown that oxygen containing compounds, especially those containing carboxyl groups, can quench scintillations.²¹ Hayes²² has shown that benzoic acid has no effect on e^{45} counting efficiency in the concentration range 2mg to 1.3 gm/litre. The quenching effect of benzoic acid on this system was checked for the concentration range of interest, 0.2 to 6 gms/litre, see fig. 24b, and a very slow decrease in efficiency was observed amounting to $<1\%/mg$. As sections taken

were of the same size this represented a negligible error. In the case of acetic acid it was found that the addition of up to 10 mgm. had no effect on the counting efficiency of C^{14} or T.

c. The Scintillator.

The counting efficiency of the system was greatly affected by the scintillator solution used. One of the most efficient scintillators is diphenyl oxazole (P.P.O.) dissolved in toluene. The wavelength of the emitted photon, however, does not give maximum efficiency of photocathodic emission. This is overcome by introducing 1,4 - di - 2(5 - Phenyloxazolyl) benzene (P.O.P.O.P.) which acts as a waveshifter to give the wavelength of maximum efficiency. This was the scintillator used and as large amounts of scintillator were required it was prepared in the laboratory from 'scintillation grade' chemicals supplied by Nuclear Enterprises Ltd. The concentrations used were 3.0g/l. P.P.O. and 0.1g./l P.O.P.O.P. This scintillator was found to give the same efficiency as the commercial scintillator NE 213 supplied by Nuclear Enterprises.

d. Dark Adaption and Temperature Variation.

It has been observed⁸² that if the scintillation vial is exposed to light before counting a residual phosphorescence,

or afterglow, may occur which gives spuriously high counts initially. Samples were, therefore, kept in a light tight box prior to counting and it was found that after two or three minutes in the counter reproducible counting was obtained. This period also allowed the sample to temperature adapt to the temperature of the water cooled head unit.

Counting.

All samples were counted to a statistical accuracy of one percent or better where possible. For very low counts, however, this was not possible and an accuracy of 3% was usually obtained. The background count rate and standard count rate was measured periodically during a counting session to ensure that no sudden variations in stability occurred.

3.7. Preparation of Diffusion Samples

Benzoic acid single crystals were readily cleaved along the (001) plane. An excellent, smooth cleavage plane was always obtained with few cleavage steps. These steps, however, prevented the crystal being used directly as the surfaces were not sufficiently planar.

Attempts were initially made to grind the crystal face with carborundum and alumina powders and water. This was followed by polishing on a stretched piece of chamois, using cyclohexane as solvent. The surfaces obtained by this method, however, were not sufficiently uniform and this method of preparation was abandoned.

The method used to prepare the crystal surface was to cleave the crystal, cut it to the approximate shape required with a razor blade, align it on the microtome perpendicular to the cleavage plane and take one micron sections. This resulted in a smooth crystal face with a perfectly uniform and planar surface with little apparent damage. All crystals used in diffusion studies were prepared in this way including the studies on polycrystalline benzoic acid compacts and acetic acid single crystals.

For the studies on benzoic acid parallel to the (001) plane the crystals were cut horizontally from a crystal ZR3, which had a vertical cleavage plane. Great difficulty was experienced in obtaining pieces sufficiently large for diffusion studies as the crystals tended to split along the cleavage plane. Hence few studies were made in this direction.

g. The Diffusion Experiments

Benzoic Acid.

Tritium diffusion was measured perpendicular to the (001) plane in single crystals under a variety of conditions in the following systems

- a) High purity benzoic acid.
- b) p-Terphenyl doped benzoic acid.
- c) Deutero benzoic acid.

The diffusion of C^{14} labelled benzoic acid was measured in high purity benzoic acid and deuterobenzoic acid crystals perpendicular and parallel to the (001) plane.

Tritium and C^{14} diffusion was measured in polycrystalline compacts of high purity benzoic acid.

Acetic Acid.

Tritium diffusion was measured by the sectioning technique in single crystals of acetic acid perpendicular to the (100) cleavage plane.

The experimental conditions used in the above studies are included in the results.

Exchange Experiments

It became apparent that tritium diffusion could be due to an exchange reaction occurring between the tritiated benzoic acid deposit and the small concentration of water vapour present in the diffusion cell followed by diffusion of tritiated water into the crystal. It was decided, therefore, to test this exchange reaction experimentally by monitoring the rate of tritium exchange between tritium labelled benzoic acid crystals and inactive water vapour.

The apparatus used was simple and consisted of a 250 ml. r.b. flask with a long neck sealed with a serum cap. The flask was allowed to equilibrate to the humidity of the room which was measured with a wet and dry bulb thermometer. A known weight of pure, dry tritiated benzoic acid was introduced in a small open dram glass vial and the run started by placing the flask in thermostat bath. The neck of the flask, however, was kept at room temperature and one ml. samples of the vapour were withdrawn with a syringe through the serum cap at time intervals which depended on the exchange temperature. The vapour in the syringe was slowly bubbled through a scintillation vial containing 10 ml of scintillator to trap the tritiated water formed by exchange and this was subsequently counted on the NE5504 tritium counting assembly. Usually about 15 samples were taken. This volume represented less than 5% of the total volume of the system, 320 ml. and it was thought

that this would not influence the exchange characteristics significantly.

The effect of the vapour pressure of benzoic acid on the activity of the vapour was checked by carrying out 'blank' runs in which C^{14} labelled benzoic acid, specific activity $257\mu\text{c}/\text{mgm}$, was used. At 38°C no C^{14} could be detected in the vapour phase over a seven hour period. At 71°C the C^{14} activity rose to a small value within 5 minutes and remained constant thereafter within the accuracy of the experiment.

The temperature range in which this experiment can be carried out is limited as the acid will sublime to the cold neck of the tube when the vapour pressure is great enough and this will affect the exchange kinetics.

A total of 8 exchange runs were made covering the temperature range $20 - 75^{\circ}\text{C}$.

10 Conductivity Studies.

In ionic conductors it has been shown that if the mobility of a diffusing particle, μ , is known then its diffusion coefficient, D , can be calculated by means of the Nernst-Einstein relation.

$$D \cong \mu k T. \quad \text{where } k \text{ is Boltzmann's const.} \\ T \text{ the absolute temperature.}$$

If the measured conductivity, σ , is due to one species then it is related to the mobility thus

$$\sigma = n z^2 e^2 \mu \quad \text{where } n \text{ is the number of the diffusing} \\ \text{species per c.c.}$$

ze is the charge on the ion hence the diffusion coefficient and conductivity are related thus.

$$\frac{\sigma}{D} = \frac{n z^2 e^2}{RT}$$

If the same mechanism is responsible for both conductivity and tracer diffusion then the above equation should hold. If this equation holds over a range of temperature then the same activation energy should be obtained from Arrhenius plots of diffusion and conductivity.

In order to verify whether or not the conductivity of hydrogen bonded organic acids is due to proton migration the conductivity of benzoic acid and acetic acid were measured and their temperature dependence obtained using both A.C. and D.C. techniques. A further study was made of the conductivity of oxalic acid dihydrate to compare it with previous experimental results and determine the effect of water of crystallisation in

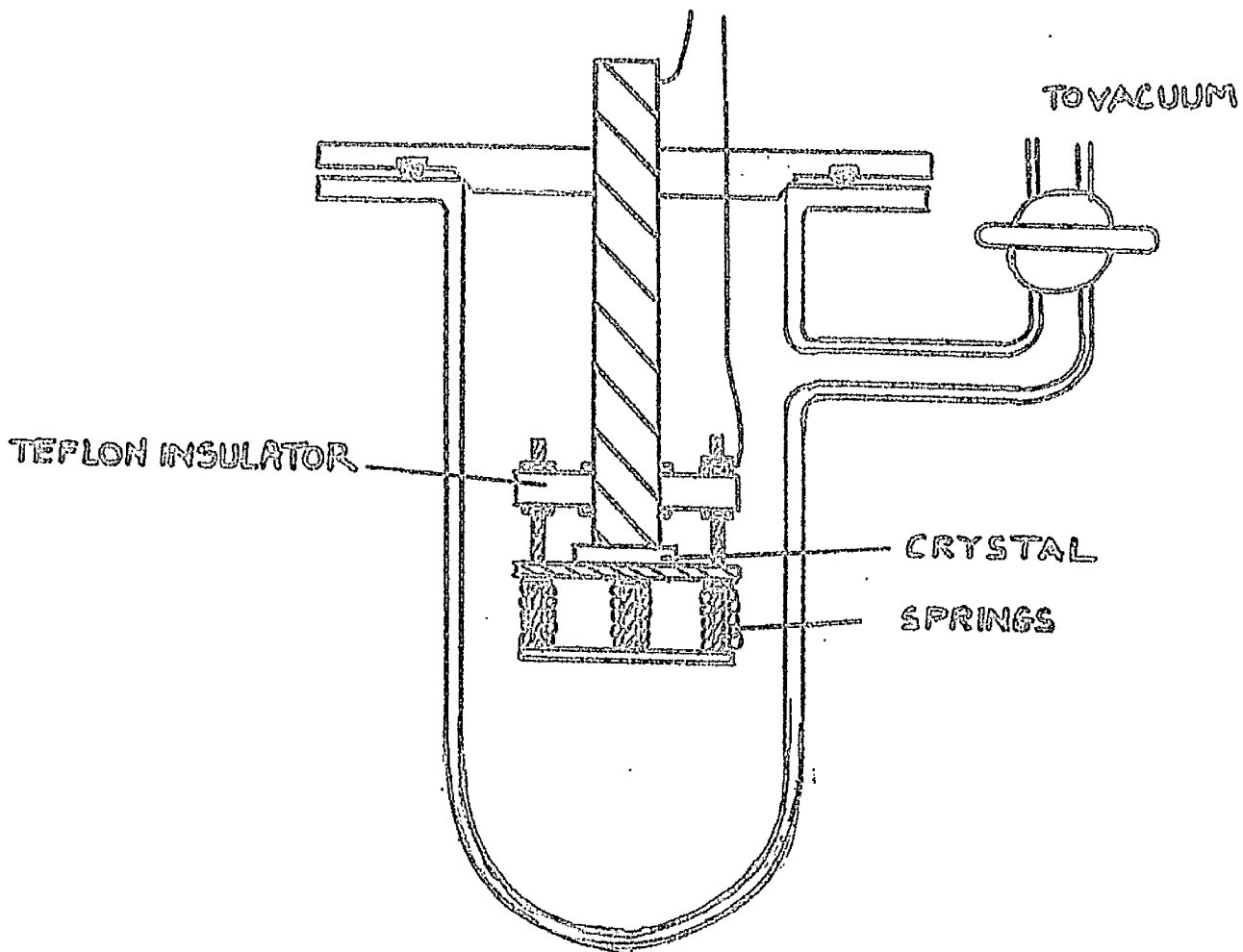
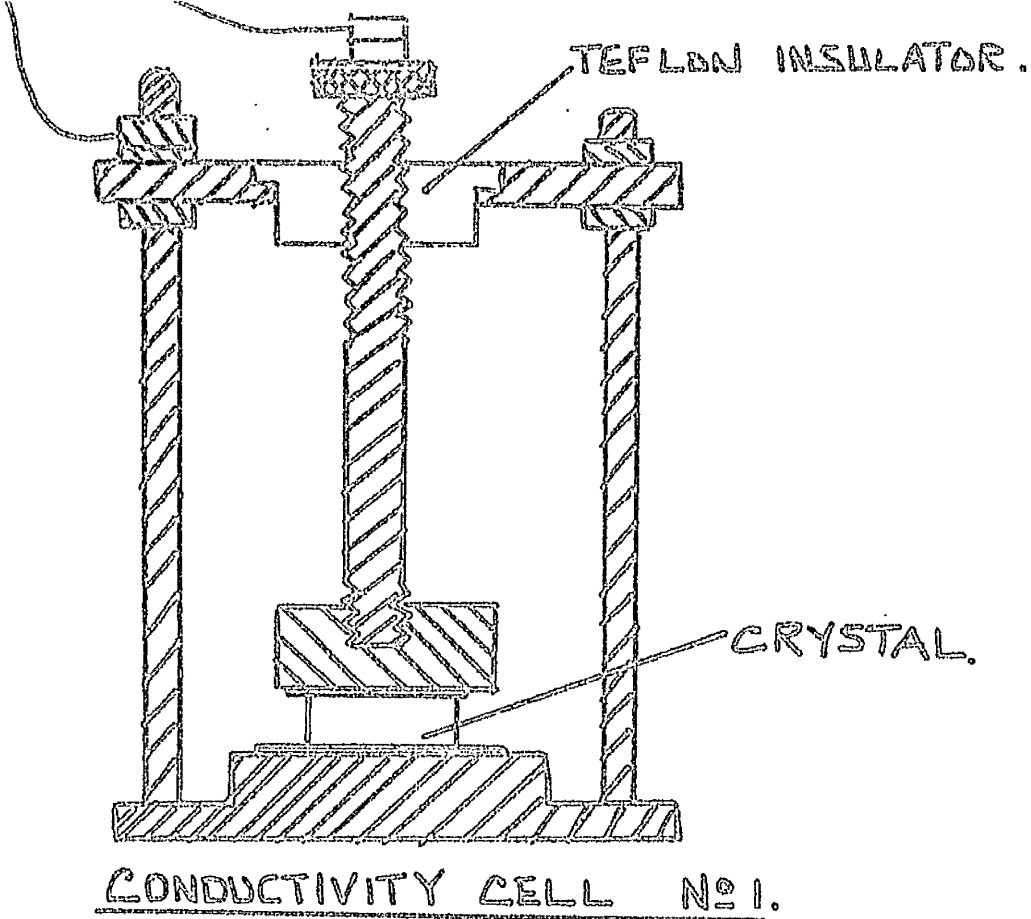


FIG 25

CONDUCTIVITY CELL No 2

the hydrogen bonded chains on the conductivity.

Conductivity Cells.

The conductivity was measured using a simple two probe technique. The cell used to measure the conductivity of benzoic acid and oxalic acid dihydrate is shown in fig. 25, cell No. 1. This was an all brass cell, 2" dia. x 3" long, in which a crystal or compact was placed between two platinum electrodes, the upper of which screwed down through a teflon insulator to give good electrical contact with the crystal. The cell was placed in a glass furnace which was electrically screened and which had a non inductively wound nichrome heater controlled through a Variac. The temperature of the crystal was measured with a Stantel F15 thermistor which projected through the bottom of the furnace and through a hole drilled in the lower electrode to within one mm. of the crystal surface.

In order to measure the conductivity of acetic acid a different cell design was required due to the low melting point and hygroscopic nature of the crystal. The cell is shown in fig. 25, cell No.2. The electrodes were stainless steel, the upper being of accurate dimensions 0.25" dia. and the lower being a larger plate 1" dia. which was kept in good contact with crystal by the lower compression springs. The cell could be evacuated and the temperature of the crystal measured using a 'Stantel' F15 thermistor which was located in a centrally drilled hole in the upper electrode. Teflon insulation was used throughout.

Electrodes.

Two types of electrodes were used. Graphite electrodes were applied as a colloidal suspension in water, 'Aquadag' and the water evaporated off in an oven at 80°C. Silver electrodes were applied as a suspension of colloidal silver in methyl isobutyl ketone which evaporated off rapidly on standing. Both these electrodes were found to give satisfactory contact.

A.C. Conductivity.

The A.C. conductivity was measured using a Wayne Kerr Universal Bridge. The conductivity was obtained directly in mhos and the smallest conductivity detectable was 2×10^{-11} mho. The specific conductivity, σ , was obtained from the equation

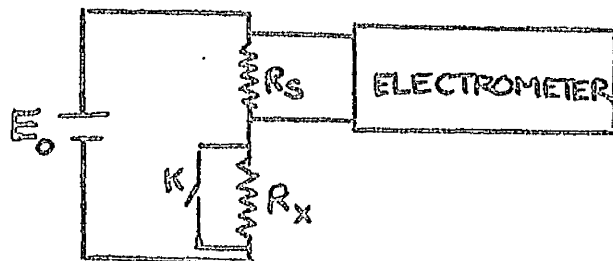
$$\sigma' = \frac{l}{A} \sigma \quad \text{where } l \text{ is the thickness of the crystal.}$$

A the cross section area of the crystal.

σ the measured conductivity.

D.C. Conductivity.

The D.C. conductivity was measured using the following circuit.



The apparatus used was an Ecko vibrating reed electrometer, model N616B. A 105 volt high stability D.C. output from the electrometer was passed through a potential divider and a voltage E_0 selected and applied across the standard resistor, R_s , with key, K , closed. A backing off voltage was applied to the

electrometer from a Pye Precision Decade Potentiometer and using the electrometer as a null point detector the voltage E_0 was accurately obtained. K was then opened and the voltage drop over the resistance R_S measured using the electrometer. The unknown resistance, R_X , i.e. the crystal resistance, was then obtained from the equation

$$R_X = R_S \cdot \left(\frac{E_0}{E_1} - 1 \right)$$

The largest standard resistor used was 10^{12} ohms and an applied voltage of 1 volt was used to minimise polarisation effects. The maximum resistance measurable, therefore was 10^{15} ohms assuming that a voltage E_1 of 1 mV could be accurately measured.

Preparation of Crystals and Compacts.

Benzoic acid compacts were prepared in two ways. Initially one inch dia. compacts were pressed at 700 p.s.i. and 4000 p.s.i. for one minute using analar reagent acid. A second batch of compacts were prepared for conductivity and diffusion studies from benzoic acid purified by single crystal growth. This material was powdered and compressed under vacuum at 5000 p.s.i. into $\frac{1}{2}$ " dia. pellets. These pellets, 14 in all, were annealed at 116°C . for seven days and allowed to cool slowly. Their density was measured and found to be $1.32 \pm .01 \text{ gm.cm}^{-3}$, identical to that of single crystals.

Pieces of benzoic acid were cut from single crystals both parallel and perpendicular to the (001) plane. These pieces

were cut to a suitable size and ground planar on a glass plate with fine carborundum and water and subsequently polished on stretched chamois using cyclohexane as solvent.

Oxalic acid compacts were pressed at 700 p.s.i. and 4000 p.s.i. using analar reagent grade material. Single crystals were grown from aqueous solution using recrystallised analar acid. These were cut and polished similar to the benzoic acid crystals.

Acetic acid crystals were cut in the fridge from single crystal boules using a razor blade. Due to the cleavage properties thin crystals were obtained with planar surfaces which required no polishing and were used directly.

CHAPTER III

THE RESULTS AND THEIR INTERPRETATION

Layout

This chapter has been subdivided into the following six sections.

- a. Tritium and C^{14} diffusion in benzoic acid single crystals.
- b. Tritium and C^{14} diffusion in polycrystalline benzoic acid.
- c. Tritium exchange between benzoic acid and water vapour.
- d. Tritium diffusion in acetic acid single crystals.
- e. Conductivity studies in organic acids.
- f. Tabulated results.

Each section has been treated separately with respect to interpretation of the results though experimental results for all sections are included in section f in tabulated form. . -

III a. Tritium and C^{14} Diffusion in Benzoic Acid Single Crystals.

1. Interpretation of results.

The experimental arrangement used in these diffusion studies was that of an infinitely thin deposit being allowed to diffuse through an infinitely thick crystal perpendicular to a known plane face. When diffusion occurs by a single mechanism the following solution has been derived for the case of constant D ⁶⁹

$$C = \frac{Q}{(\pi Dt)^{\frac{1}{2}}} \cdot \exp \left[-\frac{x^2}{4 Dt} \right] \text{-----} \quad (1)$$

taking logarithms to the base 10 of each side gives

$$\log_{10} C = \log_{10} \frac{C_0}{(\pi D t)^{1/2}} - \frac{x^2}{2.303 \cdot 4 D t}$$

CONCENTRATION OF THE

hence a plot of the logarithm of the Δ diffusing species at a penetration depth x versus the square of that depth (x^2) should give a straight line of gradient

$$m = - \frac{x^2}{2.303 \cdot 4 D t}$$

Thus if the anneal time, t , at a temperature T is known the diffusion coefficient at that temperature can be calculated from this gradient. This solution assumes that there is no loss from the surface other than that due to bulk diffusion.

The results of tritium and C^{14} diffusion in benzoic acid are shown in graphical form in figs. 26 to 34, from which it can be observed that in most cases straight lines of $\log_{10} A$ vs. x^2 were obtained, though in the case of C^{14} diffusion 'tails' were observed due to a secondary diffusion mechanism. These graphs indicated that the solution given by equation (1) was the appropriate one to use.

2. Tritium Diffusion Perpendicular to the (001) Plane.

In this system it was discovered that variable results could be obtained depending on the experimental conditions used. The results, therefore, are tabulated under the conditions used.

The initial tritium diffusion studies were carried out in

large brass vessels, fig 19. The results of these experiments are tabulated in section f and plots of $\log_{10} A$ vs x^2 are shown in fig. 26. All these diffusion runs were carried out on benzoic acid crystals purified by distillation. The diffusion coefficients calculated from equation (1) by the method of least mean squares, see appendix I, are tabulated below. A sample calculation is given in appendix II.

TABLE I. TRITIUM DIFFUSION $D^T(001)$ IN NON ZONE REFINED BENZOIC ACID (LARGE VESSELS).

Diffusion Run No.	Time hours	Temp. °C.	$1/T^{\circ}A$ $\times 10^5$	D $cm^2 \cdot sec^{-1}$ $\times 10^{-12}$	$\log_{10} D$ $+12$
DR7	18.5	88.8	2.762	23.9 ± 2.6	1.379
DH8	24.0	93.2	2.729	19.6 ± 2.0	1.292
DR9	24.0	93.5	2.727	24.0 ± 1.0	1.380
DR10	25.0	104.5	2.651	43.1 ± 1.0	1.635
DR13	19.0	108.0	2.623	100 ± 5.0	2.000
DR14	16.0	108.0	2.623	83.0 ± 4.0	1.920
DR16	235.5	78.5	2.843	7.50 ± 0.15	0.876
DR17	334.0	93.4	2.721	19.2 ± 3.0	1.284
DR18	165.7	100.0	2.680	48.0 ± 2.0	1.681

A plot of $\log_{10} D$ vs $1/T$, line A fig. 27, was found to be linear and followed the Arrhenius equation

$$D = 175 \cdot 10^{+2,000} \cdot \exp \left[- \frac{21,200 \pm 2,000}{RT} \right] \cdot 10^{-163}$$

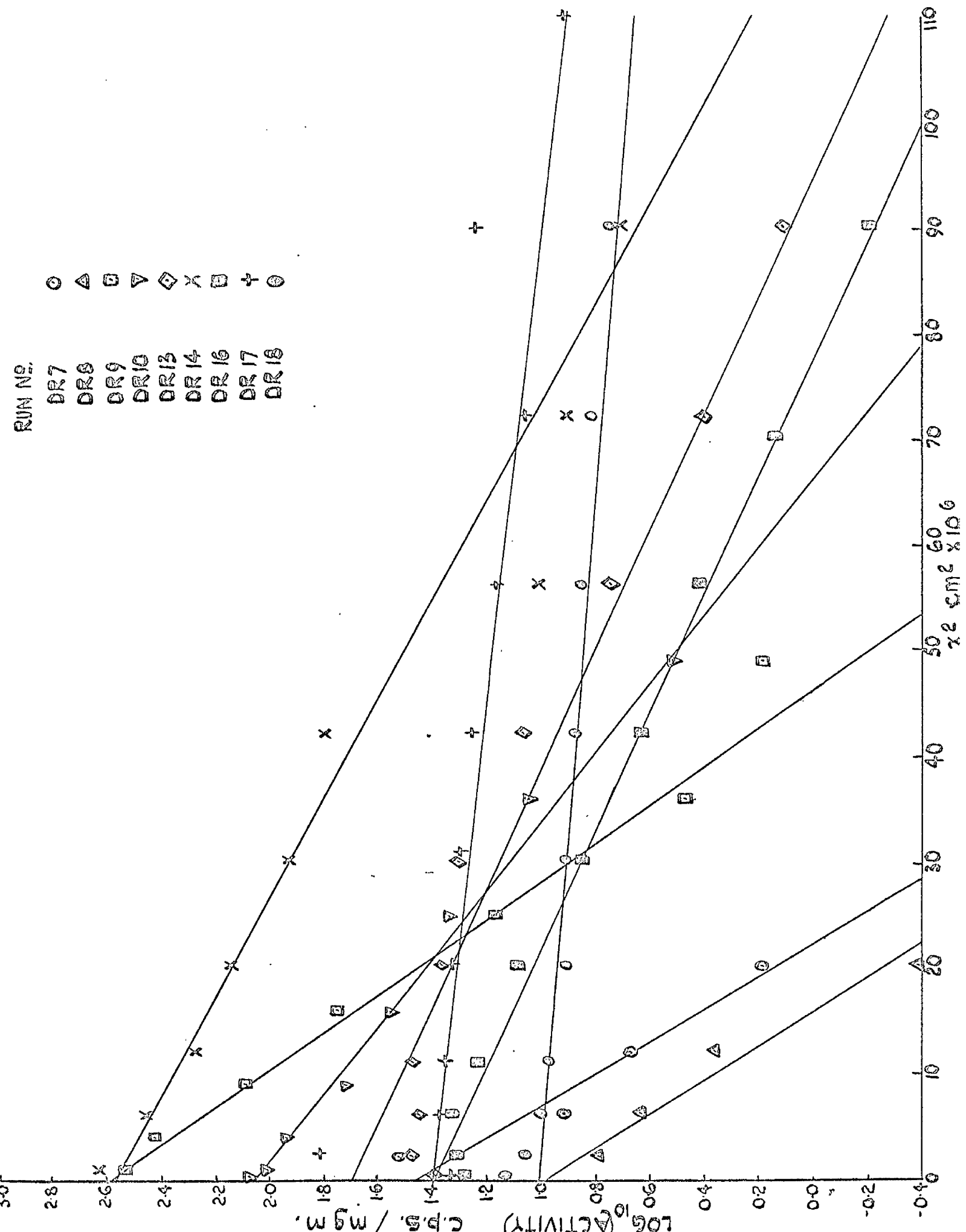
This line was obtained by the method of least mean squares and the calculation is shown in appendix III.

From these results it appeared that the diffusion coefficient was independent of time, concentration and crystal perfection.

IN BENZOIC ACID (LARGE VESSELS).

RUN NO.
 DR7
 DR8
 DR9
 DR10
 DR13
 DR14
 DR16
 DR17
 DR18

○ △ □ ▽ ◆ × ⊞ ⊕ ⊙



The scatter obtained was due to the inaccuracy of sectioning and the fact that some sublimation of the crystal occurred which prevented long diffusion anneals.

In an effort to cut down sublimation and avoid the slight tarnishing reaction which occurred at high temperatures in the brass vessel, diffusion runs were carried out in small aluminium vessels.

The results of these experiments are shown in figs. 28, 29 and the diffusion coefficients obtained tabulated below.

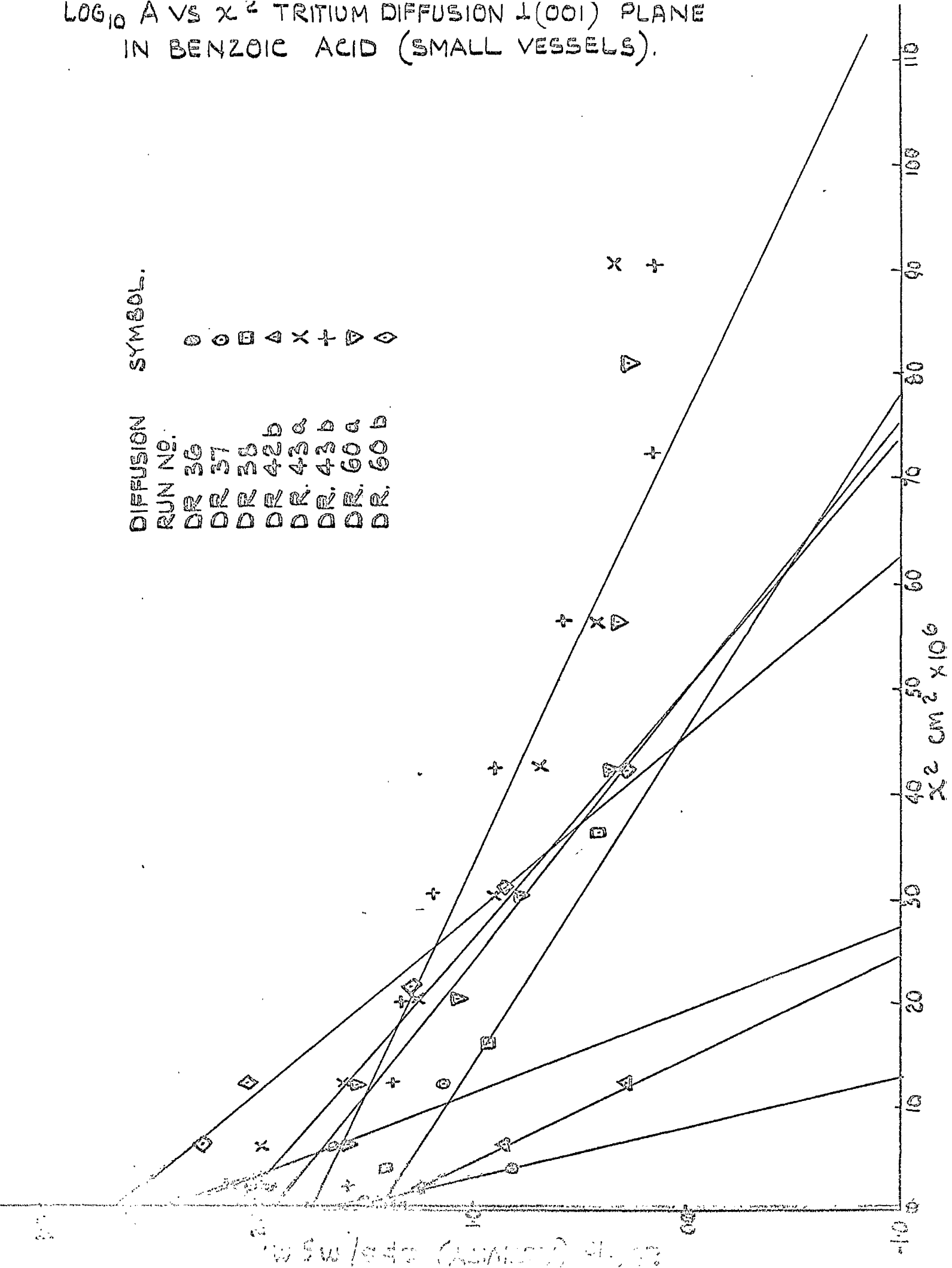
TABLE II TRITIUM DIFFUSION Δ^V (OOL) IN BENZOIC ACID (SMALL VESSELS)

DIFFUSION RUN No.	TIME hours	TEMP. °C	$1/T^{\circ A}$ $\times 10^3$	D $\text{cm}^2 \cdot \text{sec}^{-1}$ $\times 10^{12}$	Log D 10 +12	CRYSTAL SOURCE
DR. 36	116	105.5	2.640	1.4 ± 0.7	0.146	ZR.5
DR. 37	137	105.5	2.640	1.7 ± 0.3	0.230	ZR.5
DR. 38	240	110.8	2.602	3.7 ± 0.3	0.568	NOM Z.R.
DR. 42b	148	99.5	2.682	2.0 ± 0.4	0.301	ZR.4
DR. 43a	166	99.5	2.682	6.0	0.779	ZR.4
DR. 43b	166	99.5	2.682	7.1 ± 0.3	0.852	ZR.4
DR. 60a	160	115.0	2.576	4.85 ± 0.4	0.686	NOM Z.R.
DR. 60b	160	115.0	2.576	3.33 ± 0.2	0.523	NOM Z.R.
DR. 62	72	110.0	2.6095	6.26 ± 0.3	0.798	NOM Z.R.
DR. 63a	160	115.0	2.576	4.06 ± 0.1	0.610	ZR.7
DR. 63b	160	115.0	2.576	3.30 ± 0.1	0.519	ZR.7
DR. 69	134	98.5	2.6905	1.00 ± 0.1	0.00	ZR.7
DR. 76a	324	110.5	2.606	2.74 ± 0.1	0.437	NOM Z.R.
DR. 76b	324	110.5	2.606	3.24 ± 0.1	0.510	NOM Z.R.
DR. 84a	222	115.0	2.576	2.93 ± 0.15	0.467	ZR.5
DR. 84b	220	115.0	2.576	2.66 ± 0.2	0.426	ZR.7
DR. 85a	255	103.0	2.658	1.45 ± 0.05	0.163	ZR.4
DR. 85b	255	103.0	2.658	1.56 ± 0.07	0.194	ZR.5

A $\text{Log}_{10} A$ vs \bar{x}^2 plot for these results is shown in fig. 27 points \odot on line B and \triangle above it. A large experimental

LOG₁₀ A VS x² TRITIUM DIFFUSION ⊥(001) PLANE
 IN BENZOIC ACID (SMALL VESSELS).

DIFFUSION RUN NO.	SYMBOL.
DR 36	○
DR 37	◐
DR 38	◑
DR 42b	◒
DR 43a	◓
DR 43b	×
DR 60a	+
DR 60b	▽

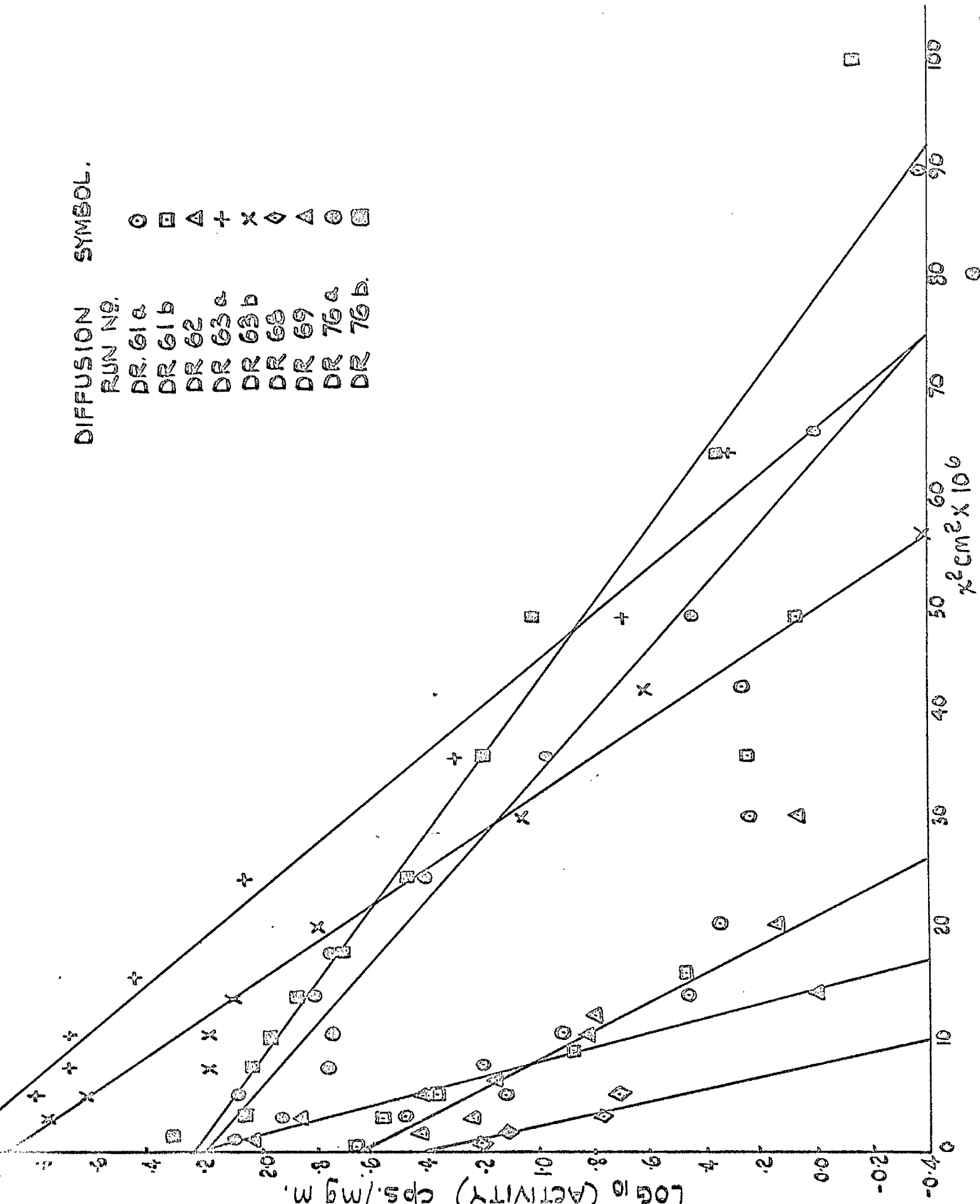


LOG₁₀ A vs x² TRITIUM DIFFUSION ⊥ (001) PLANE
 IN BENZOIC ACID (SMALL VESSELS).

FIG. 100

DIFFUSION SYMBOL.

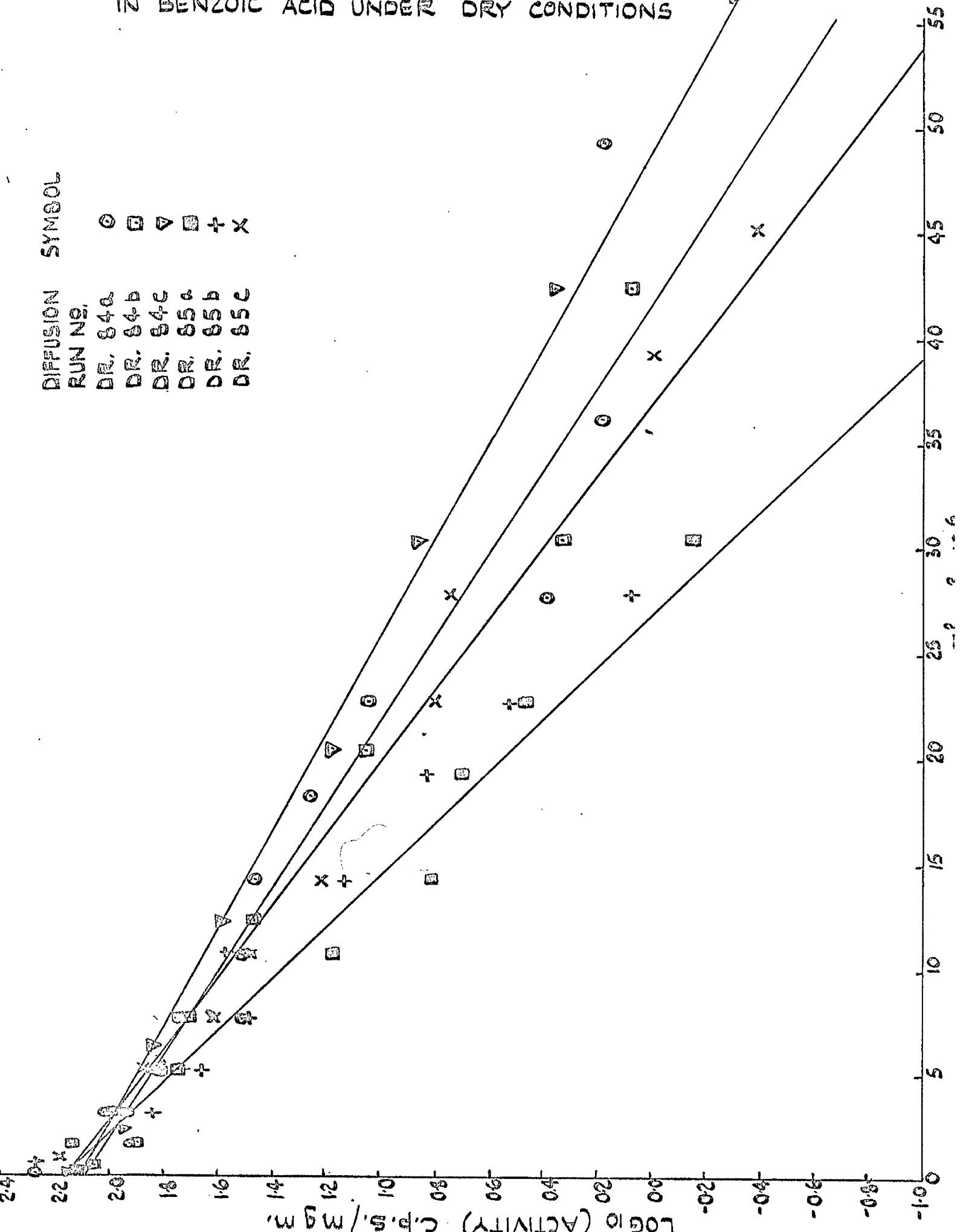
RUN NO.	SYMBOL
DR. 61a	○
DR. 61b	□
DR. 62	△
DR. 63a	+
DR. 63b	x
DR. 68	◇
DR. 69	▲
DR. 76a	⊙
DR. 76b	■



LOG₁₀ A VS X² FOR TRITIUM DIFFUSION 1 (001) PLANE
 IN BENZOIC ACID UNDER DRY CONDITIONS

FIG 29

DIFFUSION RUN NO.	SYMBOL
DR. 84a	○
DR. 84b	□
DR. 84c	▽
DR. 85a	+
DR. 85b	×
DR. 85c	•



scatter was initially observed but all results were at least an order of magnitude below the diffusion coefficients in the large vessels. Initially it was thought that it was due to crystal perfection. The results shown in Table II, however, proved that this was not the case. It was found that lower diffusion coefficients were obtained when the crystal was not cooled during deposition. This indicated that the diffusion coefficient depended on the water vapour concentration in the diffusion cell.

When the crystals were not cooled during deposition the diffusion coefficients were found to lie on line B fig. 27. A special effort was made to thoroughly dry the crystals and diffusion cells in DR.84, 85 by enclosing them in P_2O_5 cell in a dry box for 24 hours prior to the diffusion anneal. The diffusion coefficients obtained ^{see fig 29} also fell on line B indicating that this represented a lower limit to tritium diffusion in these crystals.

Line B obeyed the following Arrhenius equation

$$D = 0.5^{+2.0}_{-0.4} \text{ EXP } \left[- \frac{20,000 \pm 1,300}{RT} \right]$$

The results of tritium diffusion experiments in p-terphenyl doped benzoic acid ^{shown in fig 30 and} are tabulated below. These were carried out in aluminium vessels without cooling the crystal.

LOG₁₀ A VS X FOR TRITIUM DIFFUSION I (001) PLANE
 IN DEUTEROBENZOIC ACID AND p-TERPHENYL DOPED
 BENZOIC ACID.

FIG. 50

SYMBOL.

RUN NO.

CRYSTAL

p-TERPHENYL DOPED

DEUTERO BENZOIC
ACID

○	DR. 67a	"
◻	DR. 67b	"
△	DR. 68	"
⊙	DR. 80c	"
◻	DR. 80d	"
▽	DR. 47	DEUTERO BENZOIC
◇	DR. 52	ACID
x	DR. 80e	"
+	DR. 80b	"

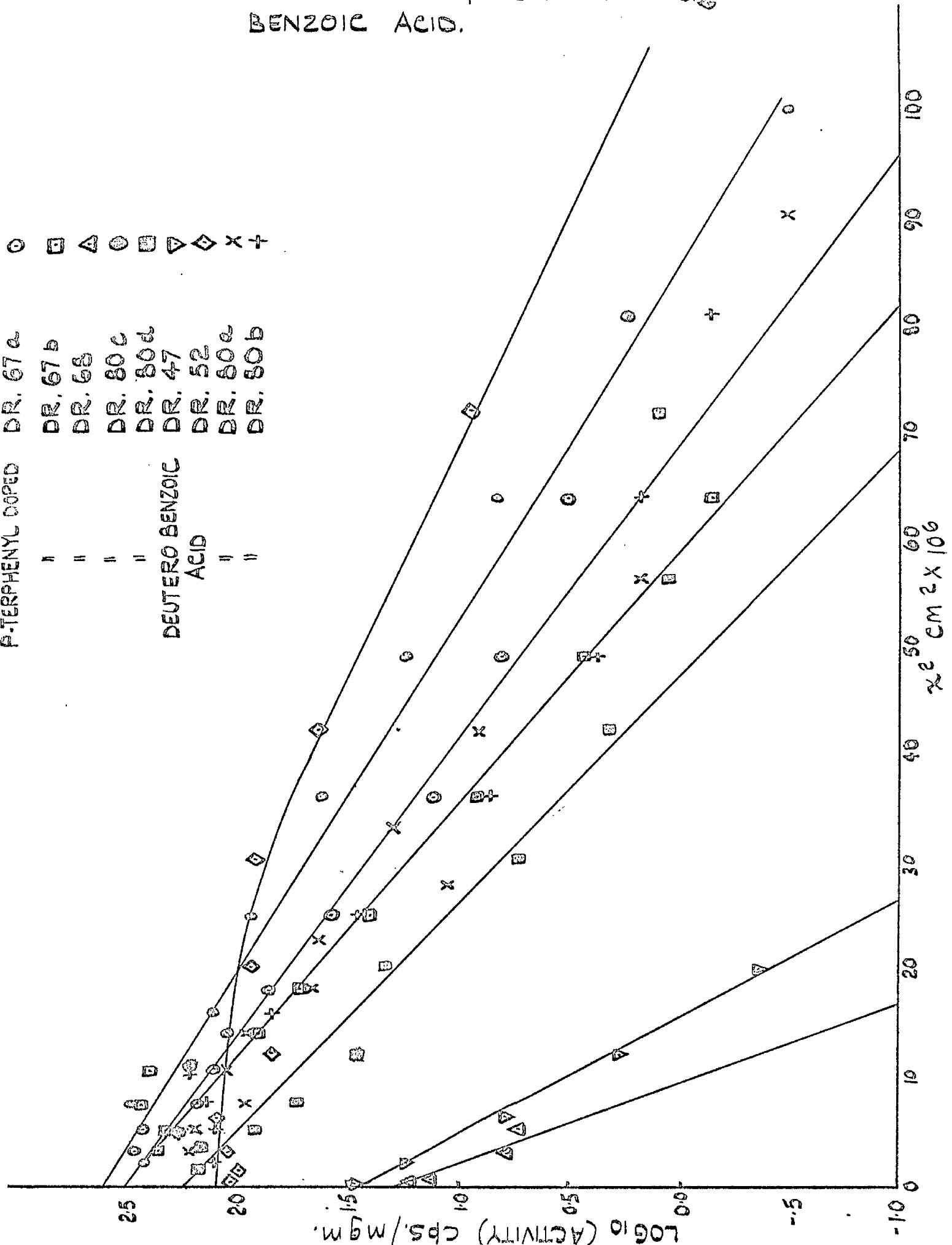


TABLE III. TRITIUM DIFFUSION \perp^r (001) IN P-TERPHENYL DOPED BENZOIC ACID (SMALL VESSELS).

DIFFUSION RUN No.	TIME hours	TEMP. °C.	$\frac{1}{T^{\circ}A} \times 10^3$	$\frac{D}{\text{cm}^2 \cdot \text{sec}^{-1}} \times 10^{12}$	$\text{Log}_{10} D + 12$
DR.67a	256	100.5	2.676	3.15 ± 0.1	0.500
DR.67b	256	100.5	2.676	2.50 ± 0.1	0.400
DR.68	169	90.0	2.7535	1.50 ± 0.22	0.177
DR.80c	250	115.0	2.576	4.01 ± 0.05	0.604
DR.80d	250	115.0	2.576	2.60 ± 0.12	0.415
DR.85c	255	103.0	2.658	2.26 ± 0.1	0.355

A $\text{Log}_{10} D$ vs $1/T$ plot of these results is shown in fig.27, points A, line D. The Arrhenius equation was obtained by the least mean squares method to yield

$$D = \left(4.7 \begin{array}{c} +75 \\ -4.4 \end{array} \right) \times 10^{-8} \cdot \text{EXP} \left[- \frac{7,450 \pm 2,200}{RT} \right]$$

A series of diffusion runs were made on deuterobenzoic acid to determine the isotope effect on diffusion. The results are tabulated in section f and $\text{log}_{10} A$ vs x^2 plots in fig.30. The calculated diffusion coefficients are tabulated below.

TABLE IV TRITIUM DIFFUSION D^D (001) IN DEUTEROBENZOIC ACID.

DIFFUSION RUN No.	TIME hours	TEMP. °C.	$\frac{1}{T^0 A}$ $\times 10^3$	$\frac{D^D}{cm. sec.}$ $\times 10^{12}$	$\log_{10} D^D$ +12	VESSEL USED.
DR. 47	120	100.0	2.679	2.81 ± 0.1	0.449	SMALL
DR. 52	112	115.5	2.573	11.0	1.05	"
DR. 61a	67.5	115.0	2.576	6.9 ± 1.4	0.836	"
DR. 61b	67.5	115.0	2.576	5.9 ± 1.5	0.771	"
DR. 72a	204	110.5	2.606	37.6 ± 0.7	1.575	LARGE
DR. 72b	204	110.5	2.606	36.0 ± 1.4	1.556	"
DR. 80a	250	115.0	2.576	3.17 ± 0.15	0.502	SMALL
DR. 80b	250	115.0	2.576	3.33 ± 0.1	0.522	"

A plot of $\log_{10} D^D$ vs $\frac{1}{T}$ is included in fig. 27.

The analysis of these results is complicated by the fact that in DR. 47, 52, and 61 the crystals were cooled during deposition thus explaining the large variation observed. This meant that an Arrhenius expression could not be obtained.

DR. 61, 72 and 80 illustrate the fact that crystals annealed in the same cell under the same conditions give almost identical diffusion coefficients though the actual values vary widely.

The isotope effect on tritium diffusion was obtained by carrying out diffusion runs on normal benzoic acid and deuterobenzoic acid in the same cell. The results are tabulated below.

TABLE V TRITIUM DIFFUSION IN BENZOIC ACID AND DEUTEROBENZOIC ACID SIMULTANEOUSLY.

DIFFUSION RUN No.	CRYSTAL	D cm ² sec. ⁻¹ x 10 ¹²	AVERAGE D _H /D _D
DR.72a	D.B.A.	37.6	1.21
DR.72b	D.B.A.	36.0	
DR.73a	B.A.	41.0	1.015
DR.73b	B.A.	48.0	
DR.80a	D.B.A.	3.17	1.015
DR.80b	D.B.A.	3.33	
DR.80c	B.A.	4.01	
DR.80d	B.A.	2.60	
DR.82a	B.A.	10.9	0.73
DR.82b	D.B.A.	15.0	

To determine the effect of the size of vessel used in the diffusion anneal a diffusion run was repeated in a large vessel. The crystals were not cooled on deposition and they were wrapped in aluminium foil to suppress sublimation. The results are tabulated in section 7 and fig. 3). The diffusion coefficients obtained are tabulated below.

TABLE VI TRITIUM DIFFUSION D^v (001) IN ZONE REFINED BENZOIC ACID (LARGE VESSEL).

DIFFUSION RUN No.	TIME hours	TEMP. °C.	$1/T^0 A$ x 10 ³	D cm ² sec. ⁻¹ x 10 ¹²	Log ₁₀ D
DR.73a	204	110.5	2.6095	41.0 ± 1.2	12.612
DR.73b	204	110.5	2.6095	48.0 ± 1.7	11.682

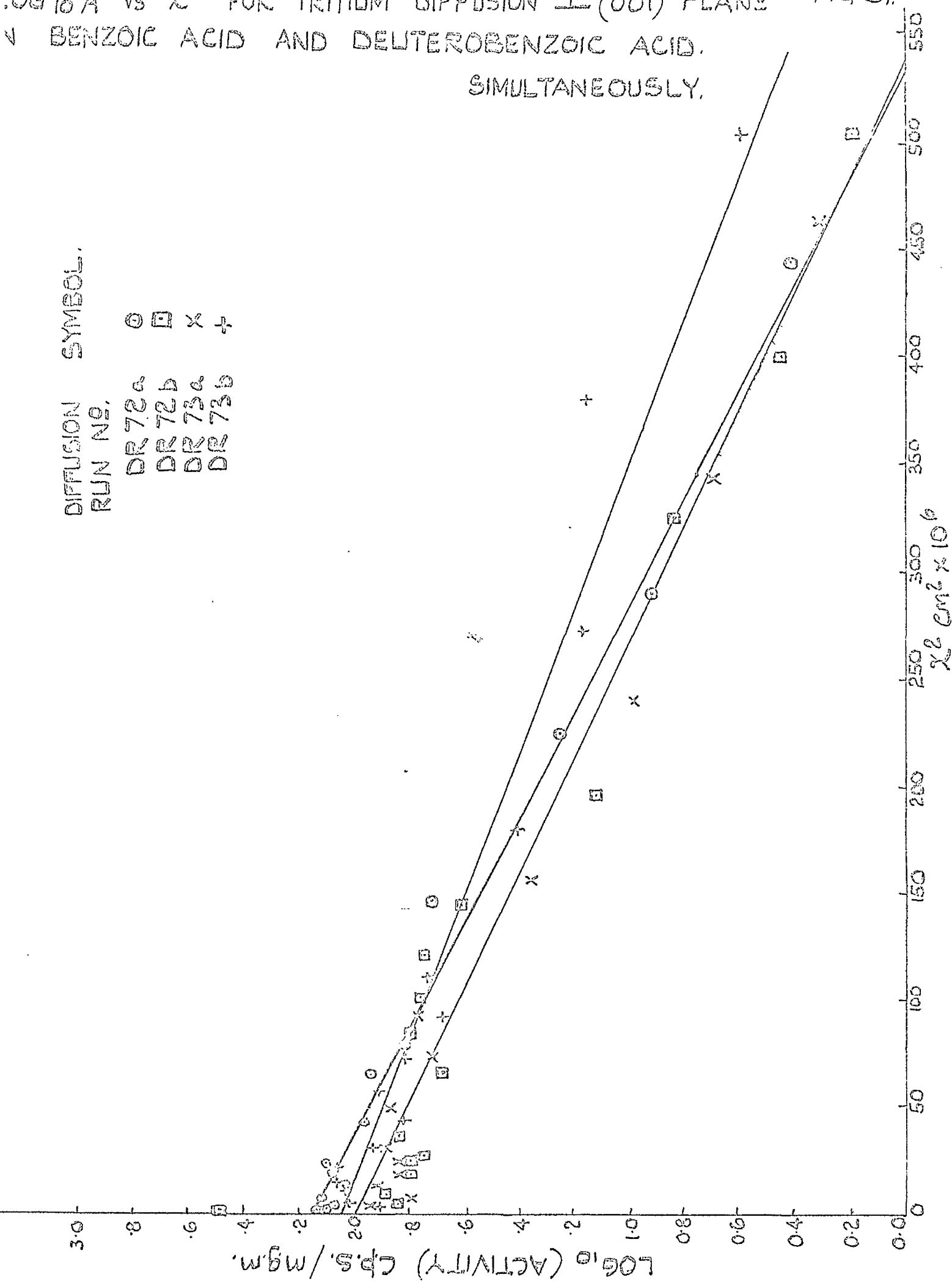
$\log_{10} A$ vs x^2 FOR TRITIUM DIFFUSION \perp (001) PLANE

FIG. 51.

IN BENZOIC ACID AND DEUTEROBENZOIC ACID.

SIMULTANEOUSLY.

DIFFUSION SYMBOL.
RUN NO. ○ □ × +
DR 72^a ○ □ × +
DR 72^b ○ □ × +
DR 73^a ○ □ × +
DR 73^b ○ □ × +



The results of DR.72 also carried out in this cell is tabulated in Table IV. A plot of $\log_{10} D$ vs $1/T$ of these results is shown in fig. 27, points \odot .

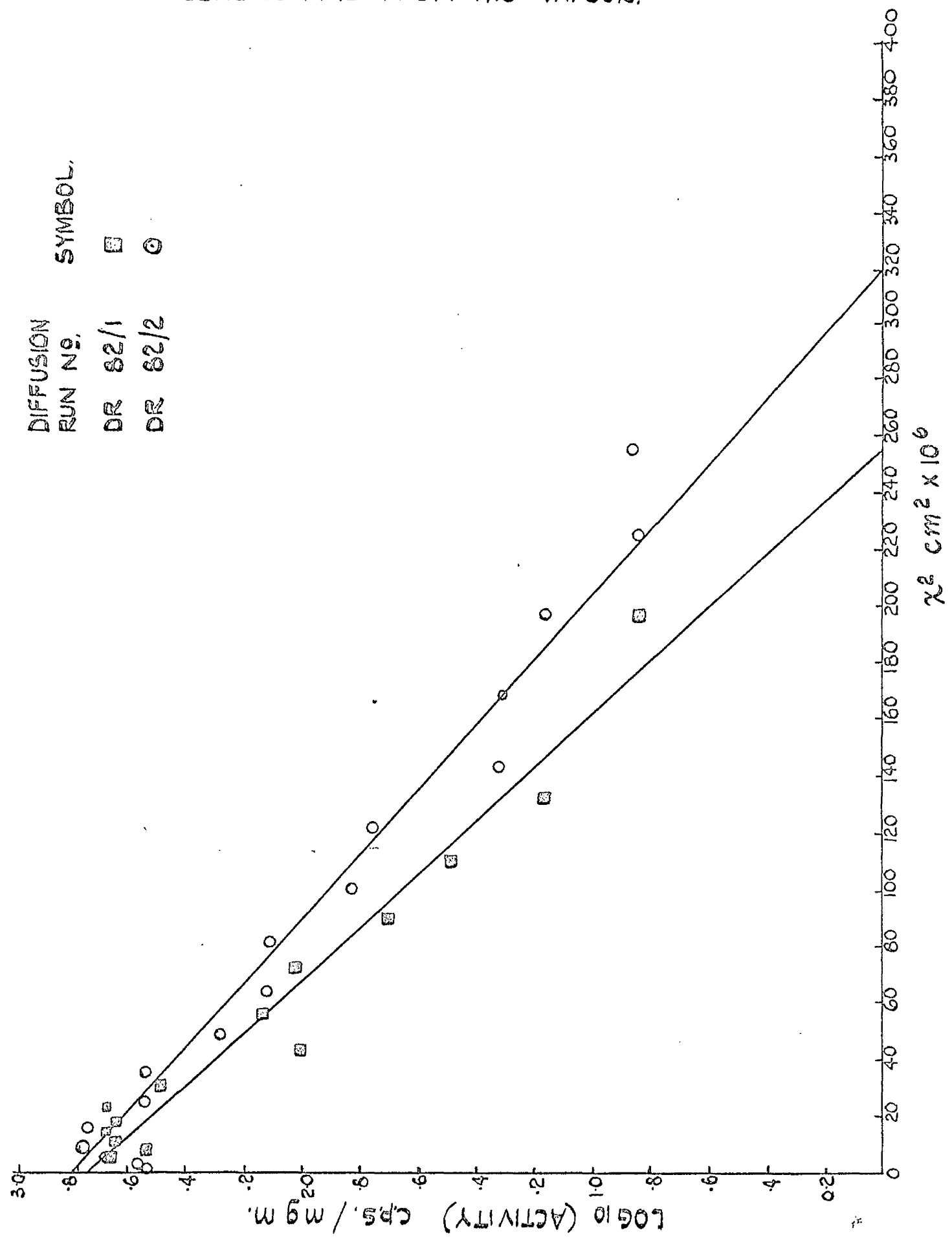
These diffusion coefficients lie almost on the upper line. The lower values are considered due to the fact that the crystals were not cooled on deposition and subsequently contain less water vapour.

An experiment was performed to observe the tritium diffusion rate in benzoic acid crystals in the presence of THO vapour. Inactive crystals were prepared in the usual way. They were placed in a glass tube, evacuated, and a little THO vapour introduced. A small amount of dry nitrogen was introduced and the tube sealed under reduced pressure. The crystals were annealed and sectioned in the usual way. The results are tabulated in section f and shown in fig. 32. The diffusion coefficients obtained are tabulated below.

TABLE VII TRITIUM DIFFUSION \perp^r (001) IN BENZOIC ACID IN CONTACT WITH TRITIATED WATER. (GLASS VESSEL).

DIFFUSION RUN No.	TIME hours	TEMP. °C.	$1/T^{\circ}A$ $\times 10^3$	D $cm^2 \cdot sec^{-1}$ $\times 10^{12}$	$\log_{10} D$ + 12	CRYSTAL SOURCE
DR. 82a	250	115.0	2.576	10.9 ± 0.4	1.036	ZR.7
DR. 82b	250	115.0	2.576	15.0 ± 0.5	1.176	D.B.A.

LOG₁₀ A VS X² FOR TRITIUM DIFFUSION ⊥ (001) PLANE
IN BENZOIC ACID FROM THO VAPOUR.



These results indicated that the THO exchanged easily with the benzoic acid and diffused in a similar way to all other tritium diffusion runs. The diffusion coefficients obtained were 3-4 times greater than those obtained under dry conditions.

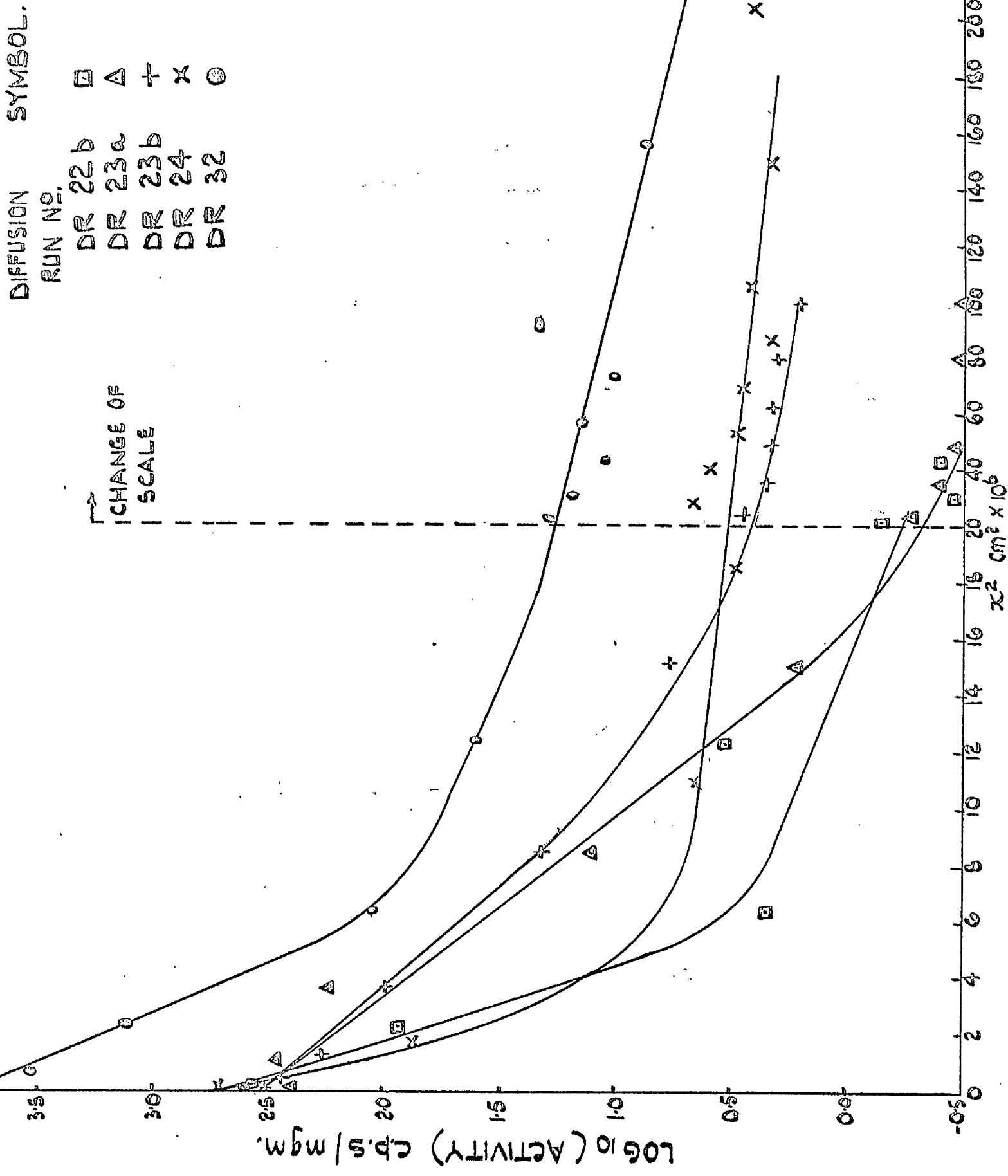
Diffusion of Benzoic Acid - C^{14} $\underline{11}$ (001) Plane in Benzoic Acid.

The results of this study are tabulated in section f and $\log_{10} A$ vs \bar{x}^2 plots in figs 33a and b. In all cases two distinct lines were obtained indicating that diffusion was occurring by two different mechanisms. The slow initial diffusion was considered to be due to bulk diffusion of the benzoic acid molecule and the fast process due to diffusion of benzoic acid molecules down dislocations or other structural defect.

The bulk diffusion coefficient was obtained by assuming that the diffusion profile represented the superposition of two independent processes. The plot of $\log_{10} A$ vs \bar{x}^2 for the bulk process was obtained by projecting the 'fast' diffusion line back to $\bar{x}^2 = 0$ and subtracting the contribution due to it from the total activity of each section. The diffusion coefficients were calculated as for tritium diffusion and are tabulated below.

LOG₁₀ A VS X FOR C₁₂ DIFFUSION IN (001) PLANE
IN BENZOIC ACID.

FIG. 55A



LOG₁₀ A VS X² C¹⁴ DIFFUSION L(001) PLANE
 BENZOIC ACID.

DIFFUSION SYMBOL.
 RUN NO. ○ □ ▲ ▼ ●

DR. 78a ○
 DR. 78b □
 DR. 79 ▲
 DR. 77b ▼
 DR. 77c ●

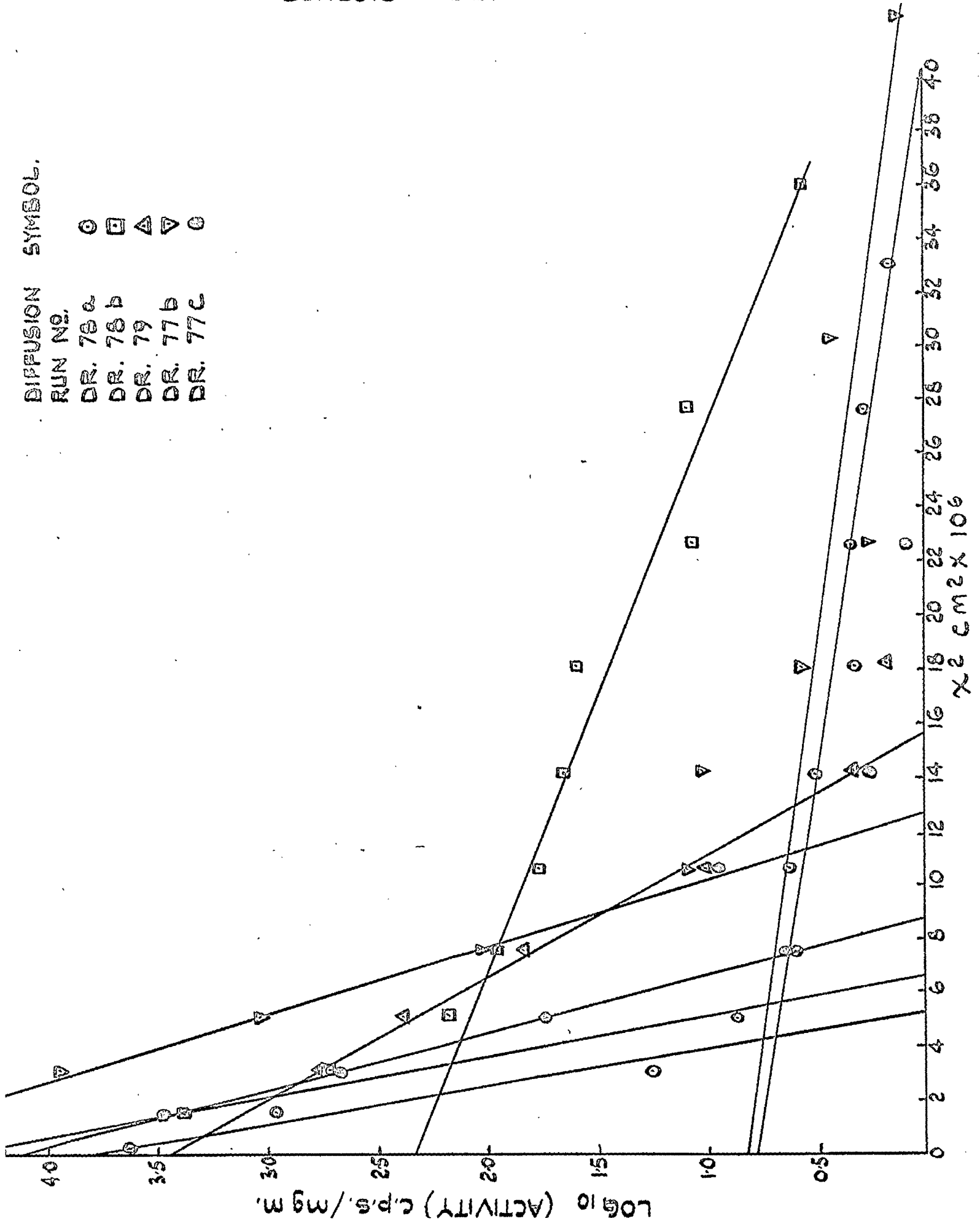


TABLE VIII BENZOIC ACID - C¹⁴ BULK DIFFUSION \perp (001) IN BENZOIC ACID.

DIFFUSION RUN No.	TIME hours	TEMP. °C.	$1/T^{\circ}A \times 10^3$	D cm ² .sec ⁻¹ $\times 10^{14}$	Log ₁₀ D + 14	CRYSTAL SOURCE:
DR.22b	403	105.2	2.6425	20.0 ± 10.0	1.740	NON Z.R.
DR.23a	329	116.5	2.566	55.0 ± 5.0	1.740	NON Z.R.
DR.23b	329	116.5	2.566	69 -	1.848	NON Z.R.
DR.24	547	110.5	2.605	13 ± 5	1.114	NON Z.R.
DR.32	172	110.0	2.610	50 -	1.700	Z.R.5
DR.77b	236	110.5	2.606	32 ± 2	1.502	Z.R.4
DR.77c	236	110.5	2.606	27 ± 0.5	1.434	D.B.A.
DR.78a	496	103.5	2.655	8.6 ± 1.0	0.936	Z.R.4.
DR.78b	496	103.5	2.655	11.0 ± 0.3	1.037	NON Z.R.
DR.79b	202	115.0	2.576	66.0 ± 1.5	1.820	Z.R.5

A plot of $\log_{10}D$ vs \bar{x}^2 is shown in fig. 27, points \square and \dagger . These diffusion coefficients are exceptionally low and approach the limit of the sectioning method. Diffusion runs DR.22 - 32 were carried out using the original sectioning technique (see p. 72) and are less accurate than DR.77-79 which were carried out using the suction technique (p. 74). Within the accuracy of the experiment the bulk diffusion was independent of crystal source and the data excluding DR.22, 32, were found to fit the Arrhenius equation.

$$D = \left(1.8 \begin{matrix} +7.6 \times 10^2 \\ -1.79 \end{matrix} \right) \times 10^{12} \cdot \text{EXP} \left[- \frac{44,000 \pm 4,400}{RT} \right]$$

Benzoic Acid - C¹⁴ Diffusion \perp (001) Benzoic Acid.

The result of two attempts to measure diffusion parallel to the cleavage plane are tabulated in section f and $\log_{10}A$ vs

x^2 plots shown in fig. 34 . The profile obtained was similar to that for diffusion perpendicular to the cleavage plane and diffusion coefficients were calculated by the same procedure and tabulated below.

TABLE IX ¹⁴ C DIFFUSION 11 (001) BENZOIC ACID.

DIFFUSION RUN No.	TIME hours	TEMP. °C.	$1/T^{\circ}A \times 10^3$	$D \text{ cm}^2.\text{sec}^{-1} \times 14$	$\text{Log}_{10} D + 14$	CRYSTAL SOURCE
33	182	109.8	2.611	45	1.65	ZR.3
34	162	100.5	2.678	25	1.40	ZR.3

Due to the small crystals used, surface area 0.5 cm^2 , and the subsequent short diffusion anneal these results are not considered particularly accurate. They serve to indicate, however, that diffusion in this direction is very low and approaches that obtained perpendicular to the (001) plane.

The 'Fast' Diffusion Process in Benzoic Acid.

This process was found to vary with the crystal used. The diffusion coefficients ^{were} calculated assuming that the profile was linear and could be calculated as for the bulk diffusion, gave values in the range 1×10^{-12} to $5 \times 10^{-11} \text{ cm}^2.\text{sec}^{-1}$ but there was no pattern evident in a $\text{log}_{10} D$ vs $1/T$ plot. It was assumed that the diffusion was due to a dislocation or other structural crystal defect mechanism and no further work was attempted on this system.

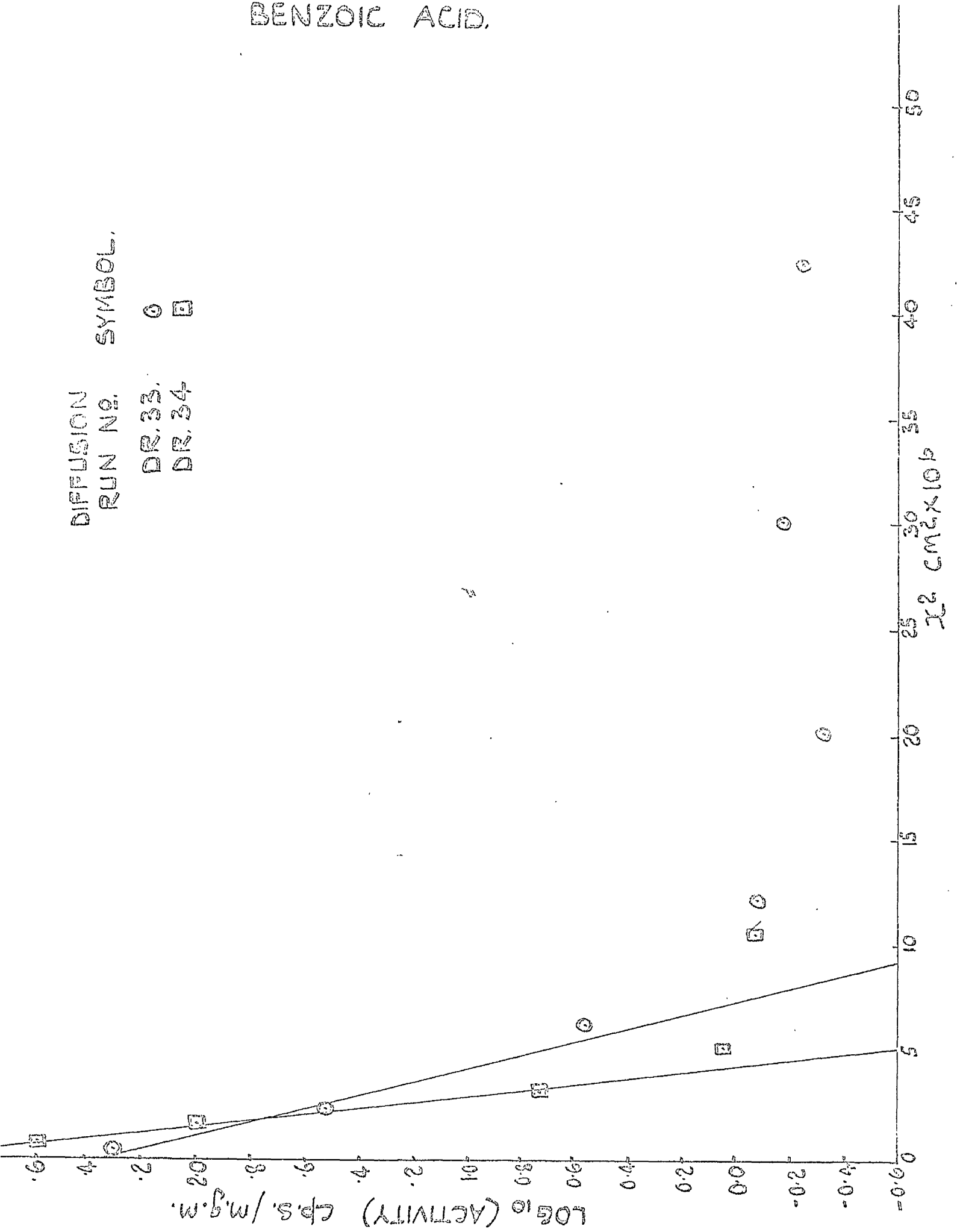
LOG₁₀ A VS \bar{x}^2 C¹⁴ II (001) PLANE
 BENZOIC ACID.

FIG. 34

DIFFUSION
 RUN NO. SYMBOL.

DR. 33. ○

DR. 34. □



Surface Diffusion in Benzoic Acid.

In several tritium diffusion experiments the back face of the crystal was removed by scraping it off with a razor blade after the diffusion anneal. The section was weighed and counted. In all cases it was found that within the experimental error the activity of the back face was the same as the front face indicating that there was a rapid surface equilibrium of tritiated benzoic acid caused either by a surface diffusion or vapour exchange process.

The C^{14} diffusion, however, gave a different result. In this case the surface activity was monitored using a portable G.M. counter. The surface activities obtained are tabulated below.

TABLE X

DIFFUSION RUN No.	ANNEAL TIME hours.	COUNT RATE FRONT SURFACE c.p.s.	COUNT RATE BACK SURFACE c.p.s.
77a	236	350	220
77b	"	360	220
77c	"	500	220
77d	"	500	220
78a	496	500	250
78b	"	500	100
79	202	500	300

These results show that surface migration of benzoic acid - C^{14} is much slower than tritiated benzoic acid and must go by a different mechanism.

GRAIN BOUNDARY DIFFUSION OF TRITIUM AND C^{14} IN
POLYCRYSTALLINE BENZOIC ACID.

The first quantitative attempt to solve the problem of grain boundary diffusion was made by Fisher.⁸³ His solution was approximate but simple to apply to experimental results. The exact solution was published by Whipple⁸⁴ but was in a form that was difficult to apply to experimental results and hence until recently the Fisher solution was the one commonly used.

A comparison of the two solutions has been made by Le Claire⁸⁵ who has published in graphical form some numerical evaluations of the Whipple solution. This enables estimates to be made of the error involved in using the Fisher solution.

The mathematical model used in the analysis is to represent the grain boundary as an isotropic slab of material of width δ within which diffusion occurs according to Fick's laws, with a coefficient D^1 much greater than D , the coefficient of bulk diffusion on either side of the boundary.

With the boundary conditions

$$C(x, y, t) = C_0 \quad ; \quad t \geq 0 \quad ; \quad y = 0$$

where y is the direction of the grain, x the direction at right angles to the grain, C_0 the constant surface concentration and t the time of diffusion Fisher's solution is

$$C/C_0 = \text{Exp.} \left(-\pi^{1/2} \eta \beta^{-1/2} \right) \text{erfc} \frac{1}{2} \xi \quad (2)$$

where η , β and ξ are the reduced dimension less quantities.

$$\eta = \frac{y}{(Dt)^{1/2}} \quad ; \quad \beta = \frac{D'}{D} \frac{\delta/2}{(Dt)^{1/2}} \quad ; \quad \xi = \frac{x - \delta/2}{(Dt)^{1/2}}$$

where δ is the width of the grain boundary and this is only valid for very large values of η .

In the sectioning technique the concentration of the diffusant, \bar{c} , in a number of thin slices cut parallel to the initial surface, is determined as a function of y . The general solution is

$$D^1 \delta = \left(\frac{\ln \bar{c}}{\partial y} \right)^{-2} \left(\frac{4D}{t} \right)^{1/2} \left[\frac{\partial \ln \bar{c}}{\partial (\eta \beta^{-1/2})} \right]^2 \quad (3)$$

In the Fisher solution the last term is a const, $\pi^{-1/4}$ hence a plot of $\ln \bar{c}$ vs y should be linear and a value of $D^1 \delta$ easily obtained.

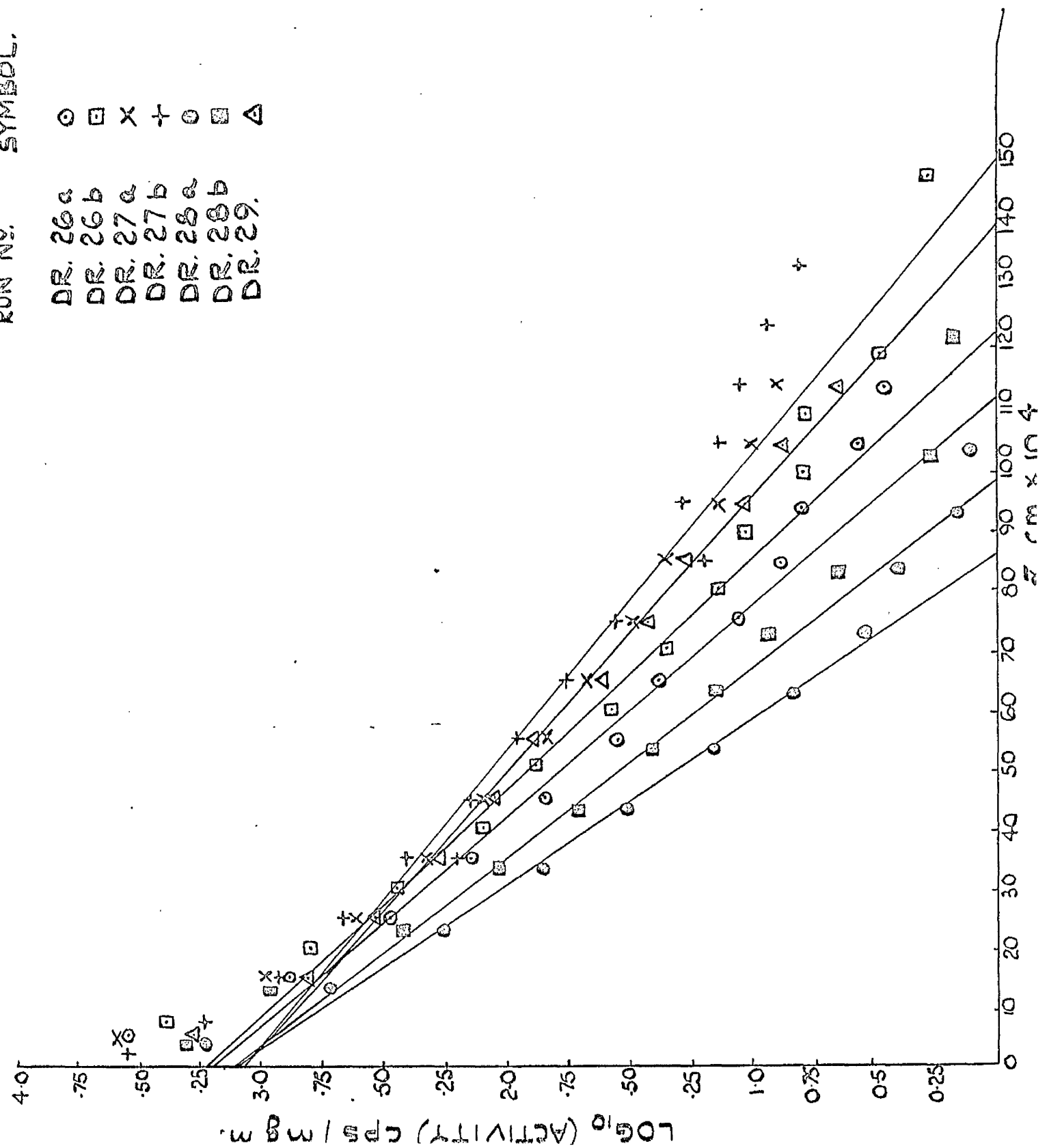
LeClaire has evaluated $\frac{\partial \ln \bar{c}}{\partial (\eta \beta^{-1/2})}$ as a function of $\eta \beta^{-1/2}$ for various values of β and presented it in graphical form thus allowing the Whipple diffusion coefficient to be evaluated.

The results of the diffusion of C^{14} Benzoic Acid and tritiated benzoic acid in polycrystalline compacts are shown in the form of \log_{10} (specific activity) vs. \bar{x} the penetration into the crystal in figs 35, 36 respectively. According to the Fisher analysis these should be linear except for the high point at the surface. The curves are essentially

DIFFUSION BENZOIC ACID
 COMPACTS.

DIFFUSION
 RUN NO. SYMBOL.

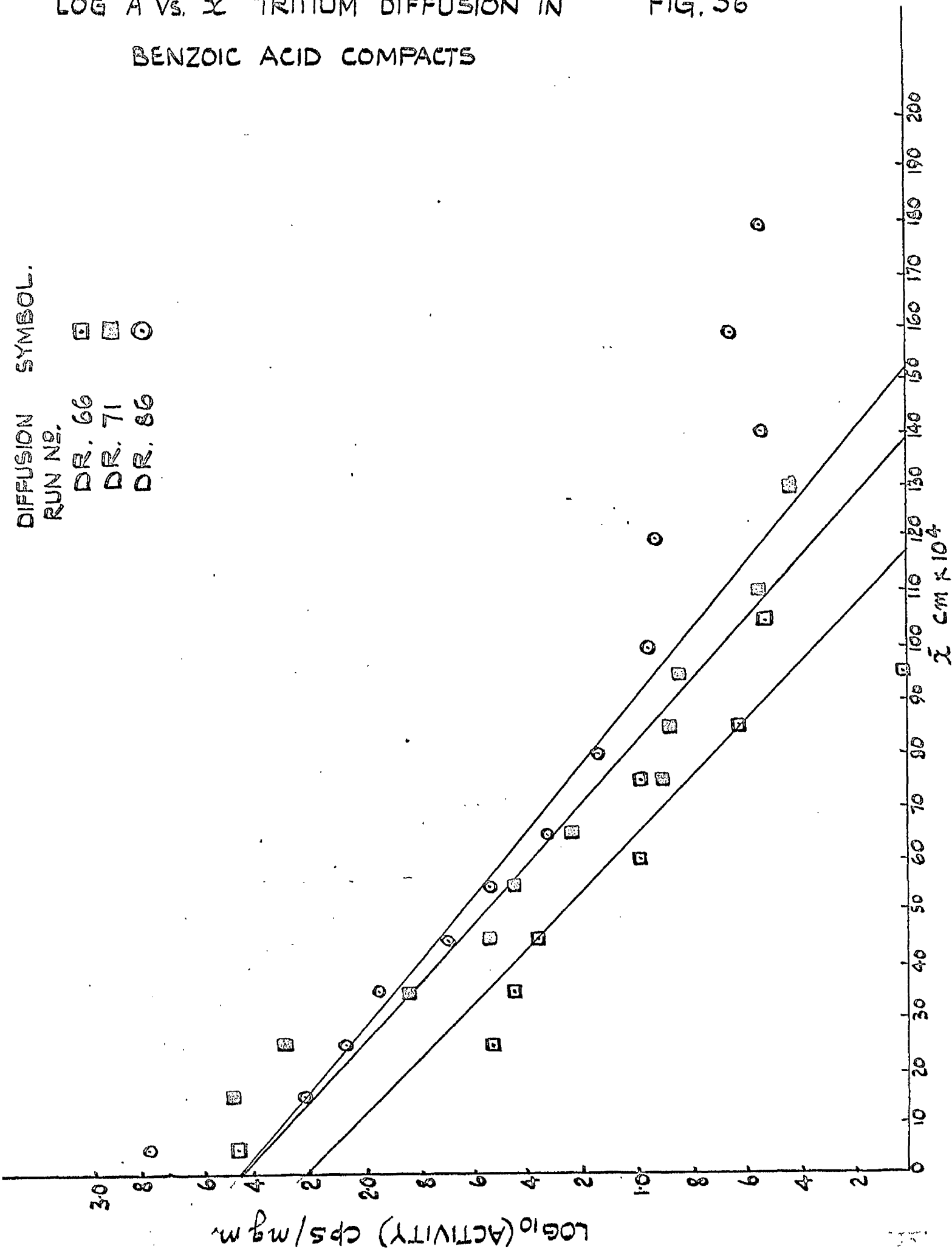
DR. 26a ○
 DR. 26b □
 DR. 27a ×
 DR. 27b +
 DR. 28a ◊
 DR. 28b ◻
 DR. 29. △



LOG A vs. \bar{x} TRITIUM DIFFUSION IN
 BENZOIC ACID COMPACTS

FIG. 36

DIFFUSION SYMBOL.
 RUN NO. DR. 66 DR. 71 DR. 86
 □ □ ○



linear with some 'tailing' occurring at deep penetrations. This curvature is in agreement with that predicted by the Whipple solution.

The grain boundary diffusion coefficients were calculated from the Fisher equation.

$$\bar{c} = c_0 \exp \left[-\frac{2^{\frac{1}{2}}}{\pi^{\frac{1}{2}}} \cdot \frac{y}{\delta} \cdot \left(\frac{D}{D'} \right)^{\frac{1}{2}} \cdot \left(\frac{\xi^2}{D t} \right)^{\frac{1}{4}} \right] \operatorname{erfc} \xi \quad (4)$$

assuming $\operatorname{erfc} \xi = 1$

using the linear part of the curve to obtain $\frac{d \ln \bar{c}}{dy}$. The values of D used were calculated from the bulk diffusion equation (see p. 101) obtained in this investigation. The value of ξ to be used was the only unknown quantity.

Other grain boundary studies have shown that ξ is of the order of 2 - 3 lattice spacings⁸⁶ hence a value of $\xi = 25\text{\AA}$ was assumed. The gradients were calculated by the least mean square method and the diffusion coefficients obtained tabulated in table XI

The Whipple diffusion coefficients were then obtained by calculating η and β to give $\eta\beta^{-\frac{1}{2}}$ from which the value of $\frac{d(\ln \bar{c})}{d(\eta\beta^{-\frac{1}{2}})}$ ($= A$) was calculated from LeClaires graph. The values used in these calculations are shown in table XII. The calculated values of the Whipple diffusion coefficients are also included in table XI.

TABLE XI C^{14} AND TRITIUM GRAIN BOUNDARY DIFFUSION IN BENZOIC ACID.

DIFFUSION RUN No.	TEMP. °C.	$1/T^{\circ}A \times 10^3$	D^1_{Fisher} $cm^2 \cdot sec^{-1} \times 10^{10}$	$Log_{10} D^1_{Fisher} + 10$	$D^1_{Whipple}$ $cm^2 \cdot sec^{-1} \times 10^{10}$	$Log_{10} D^1_{Whipple} + 10$
DR. 26a	91.0	2.746	38.4 ± 2	1.59	102	2.008
26b	91.0	2.746	55 ± 4	1.75	147	2.167
27a	103.5	2.655	260 ± 20	2.42	415	2.618
27b	103.5	2.655	260 ± 20	2.42	415	2.618
28a	78.6	2.843	5.7 ± 0.2	0.756	12.9	1.110
28b	78.6	2.843	7.4 ± 0.6	0.780	16.7	1.223
29	83.3	2.805	29 ± 1	1.47	66	1.820
TRITIUM						
66	101.0	2.673	243 ± 60	2.386	350	2.545
71	78.5	2.843	20 ± 2.5	1.301	34	1.532
86	96.1	2.708	115 ± 10	2.061	198	2.297

TABLE XII CALCULATION OF LECLAIRE PARAMETER 'A'.

DIFFUSION RUN	$(Dt)^{1/2} \times 10^5 \text{ cm.}$	$\gamma \times 10^4 \text{ cm.}$	η	β	$\eta\beta^{-1/2}$	A
DR. 26	3.63	68	187	385	9.5	2.01
27	8.15	100	123	4000	1.95	1.10
28	2.19	56	256	1800	6.05	1.30
29	2.60	96	370	3500	6.25	1.31
66	3.88	120	310	7830	3.50	1.20
71	2.21	100	453	5650	6.40	1.30
86	8.26	120	146	554	6.20	1.31

Plots of $\log_{10} D$ VS $1/T$ for both sets of diffusion coefficients are shown in figure 37. Both Fisher and Whipple lines are approximately linear and fit the Arrhenius equation $D = D_0 \exp \left[\frac{-EA}{RT} \right]$ where the individual parameters are given by the following equations.

⁴ Diffusion

$$\text{Fisher} = (7.3 \pm 3.5) \times 10^{13} \cdot \text{EXP} \left[- \frac{37,100 \pm 2,200}{RT} \right] \\ -7.0$$

$$\text{Whipple} = (1.0 \pm 24) \times 10^{12} \cdot \text{EXP} \left[- \frac{33,500 \pm 2,500}{RT} \right] \\ - 0.97$$

Tritium Diffusion

$$\text{Whipple} = (1.8 \pm 40) \times 10^8 \cdot \text{EXP} \left[- \frac{27,100 \pm 700}{RT} \right] \\ -1.0$$

These results show that within the experimental accuracy tritium and C^{14} diffuse by the same mechanism.

The decrease in activation energy obtained on applying the Claire analysis is in agreement with that predicted.⁸⁵

A combination of the tritium and C^{14} Whipple data fitted following Arrhenius equation.

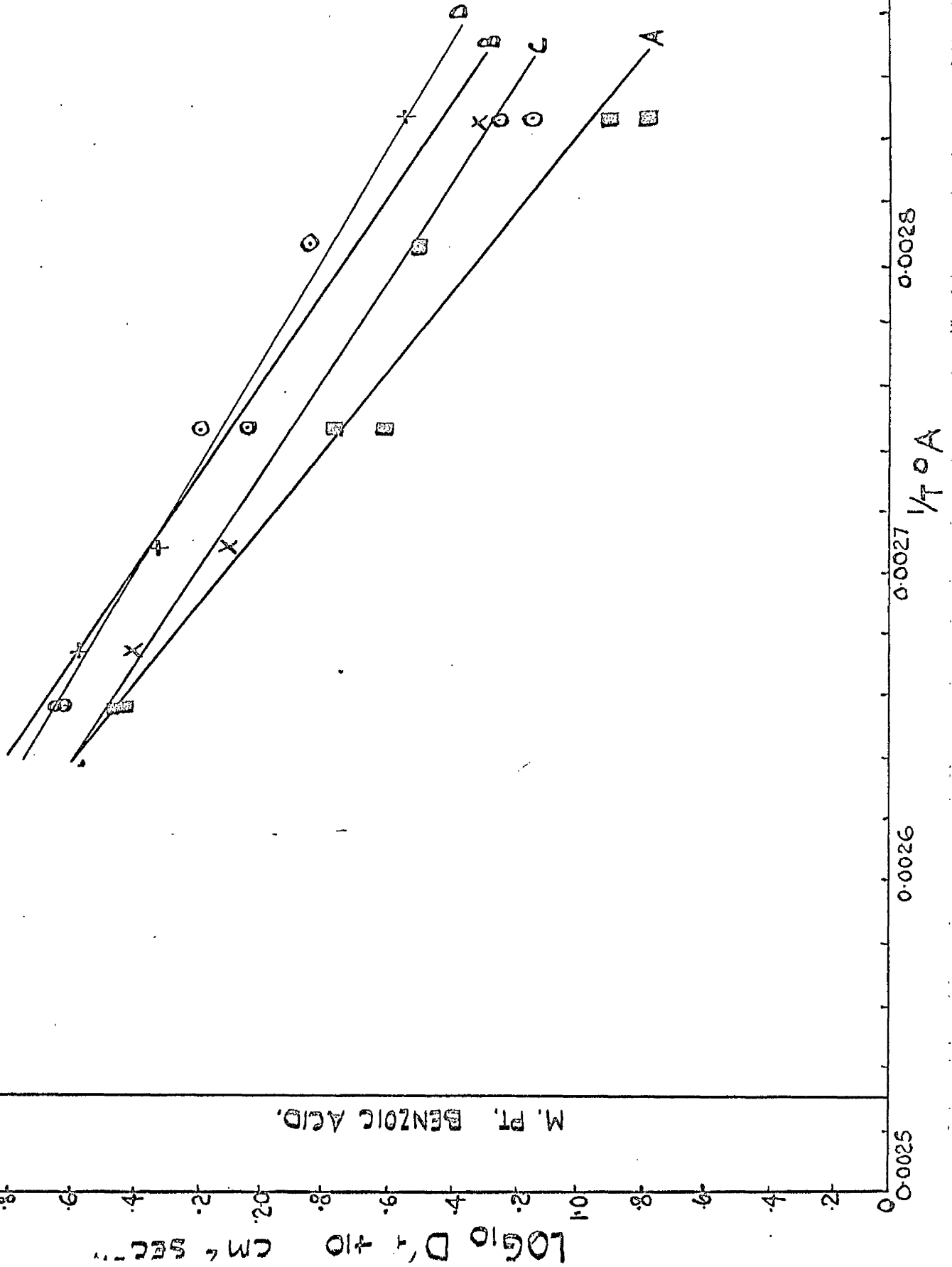
$$\left(1.0 \pm 13 \right) \times 10^{11} \cdot \text{EXP} \left[- \frac{31,800 \pm 2,000}{RT} \right] \\ -0.93$$

ARRHENIUS PLOT FOR GRAIN BOUNDARY

DIFFUSION IN BENZOIC ACID COMPACTS.

FIG. 51

A	□	D6B	FISHER	} C ¹⁴
B	○	D6B	WHIPPLE	
C	X	D6B	FISHER	} TRITIUM
D	+	D6B	WHIPPLE.	



c. Exchange Reaction Between Tritiated Benzoic Acid and Water Vapour

It was found that when tritiated benzoic acid and inactive water vapour were in contact an exchange reaction took place and the water vapour became radioactive.

The reaction was found to obey neither first nor second order kinetics but instead gave linear plots of radioactive concentration in the vapour vs. square root of exchange time. This indicated diffusion controlled kinetics similar to that obtained by Feitknecht in inorganic hydroxides⁸⁷ with the exception that no initial rapid surface exchange was observed.

The exchange equation must, therefore, have the following form.

$$\frac{R_t}{R_{\infty}} = A \cdot (Dt)^{\frac{1}{2}} \quad (5)$$

where R_t is the vapour phase activity at time t , R_{∞} is equilibrium activity of the vapour, A is a constant depending on the surface area and geometry of the crystals, D the diffusion coefficient.

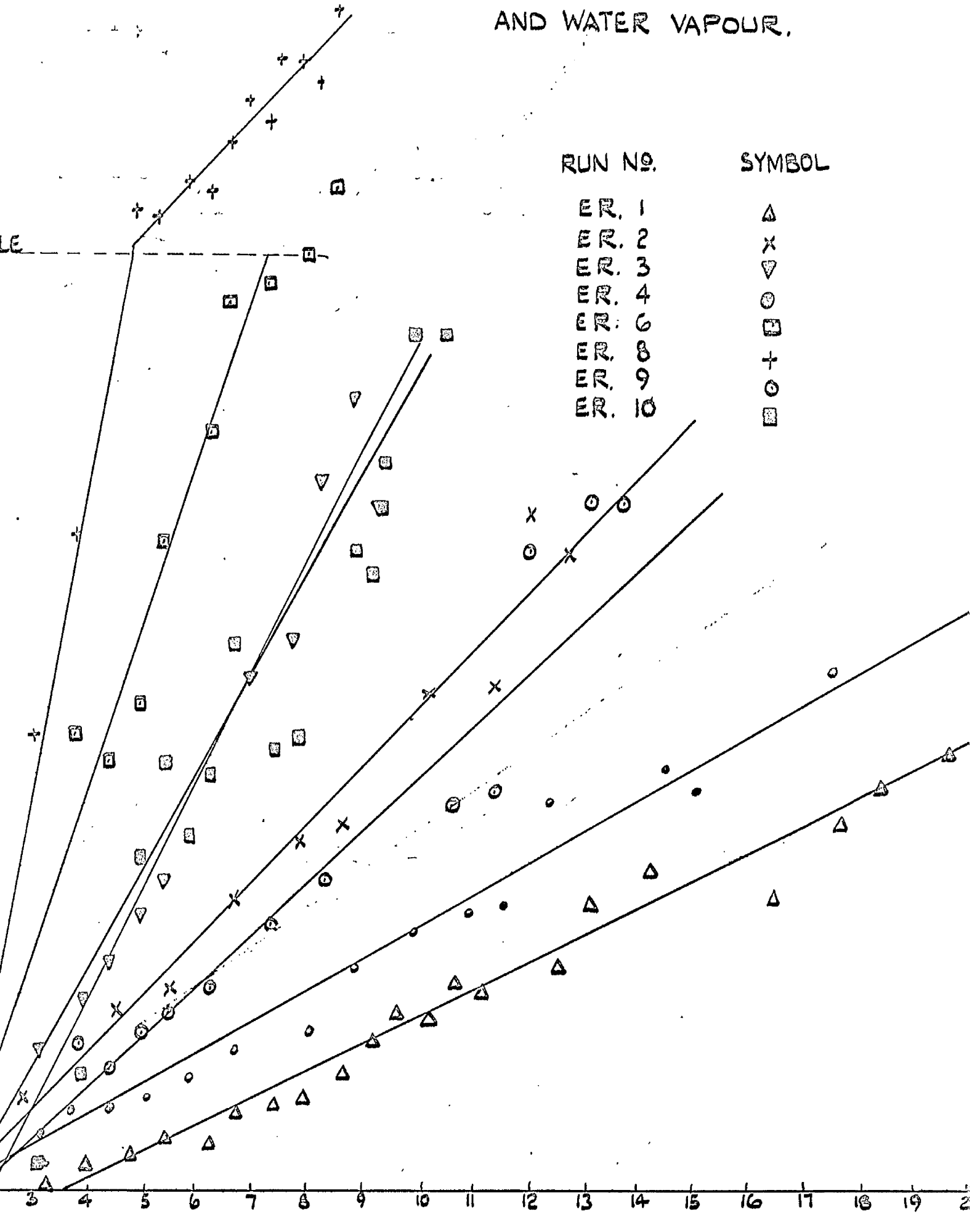
The results of the exchange experiments are tabulated in section f, ER1 to ER10. Plots of R_t vs. \sqrt{t} are shown in fig 38. Although there is some scatter due to inaccuracy in the sampling method (p.85) a linear relation is apparent indicating that equation (5) is the correct solution.

The gradient, m , of these slopes is given by

$$m = R_{\infty} \cdot A \cdot D^{\frac{1}{2}}$$

i.e. $\frac{m}{R_{\infty}} \propto D^{\frac{1}{2}}$

ACTIVITY OF VAPOUR R_s VS \sqrt{z} FOR EXCHANGE REACTION BETWEEN TRITIATED BENZOIC ACID AND WATER VAPOUR. FIG. 38



Values of m were obtained by the method of least mean squares.

Values of R_{00} were calculated from the volume of the cell, water vapour pressure and Weight of sample. Values of $m' = \frac{m}{R_{00}}$ were calculated and are tabulated below.

TABLE XIII RELATIVE DIFFUSION COEFFICIENTS OBTAINED FROM EXCHANGE EXPERIMENTS.

E. R.	TEMP. °C	$\frac{W}{T}$	WT. TBA. mgm	H Vapour H Solid	Total Activity μ	R_{00}	m	m' $\times 1000$	$\log_{10} m'$
1	22.0	3.388	6.40	8.45	47.4	545	0.976	1.79	0.253
2	53.0	3.059	5.50	9.85	40.7	475	2.114	4.45	0.649
3	66.0	2.947	5.00	10.8	37.0	435	3.59	8.25	0.917
4	38.0	3.213	4.90	11.0	36.3	428	1.20	2.80	0.448
5	71.0	2.905	5.50	9.85	40.7	556	6.22	11.20	1.050
6	76.5	2.860	5.70	9.5	42.2	575	11.15	19.1	1.282
7	43.0	3.162	5.05	10.8	30.7	545	1.97	3.62	0.558
10	60.2	3.000	4.90	11.0	36.3	545	4.00	7.35	0.866

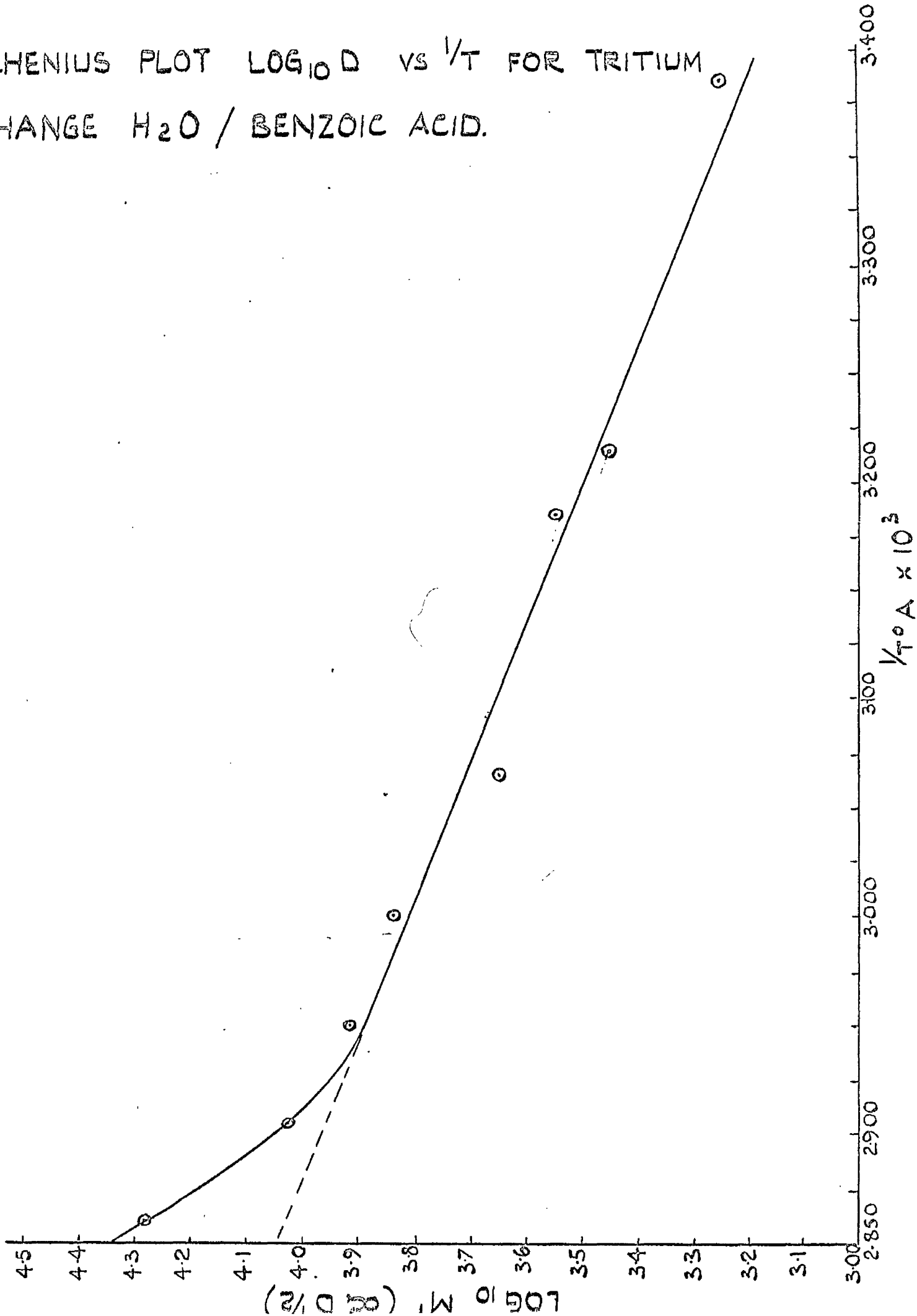
A plot of $\log_{10} m' (\propto D_i)$ vs. $\frac{1}{T}$ is shown in figure 39. This

plot is essentially linear in the range 20 - 70°C hence the process can be represented by the following Arrhenius equation.

$$D = D_0 \exp \left[- \frac{14,000 \pm 700}{RT} \right]$$

As these are relative diffusion coefficients a pre-exponential factor cannot be calculated. This activation energy represents a maximum value as the increasing diffusion coefficient at high temperature is due to the superposition of another exchange process which, from the linear plots also obtained, indicate that this is due to another diffusion mechanism. This may be the bulk diffusion of benzoic acid molecules.

ARRHENIUS PLOT $\text{LOG}_{10} D$ VS $1/T$ FOR TRITIUM
 EXCHANGE H_2O / BENZOIC ACID.



113

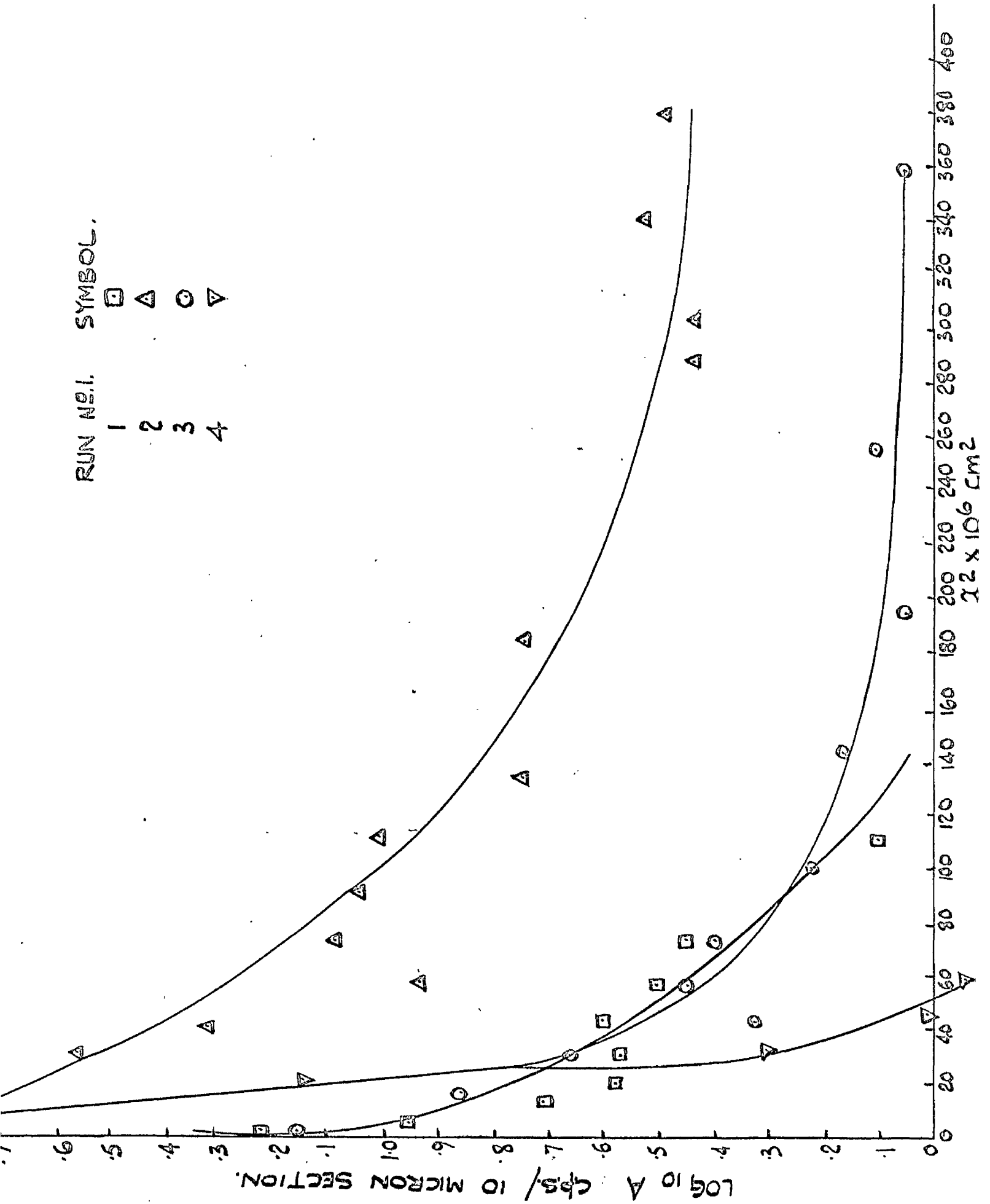
Tritium diffusion perpendicular to the (100) plane in acetic acid.

This system was found to be very difficult to handle as all operations had to be carried out in a deep freeze at -20°C . The diffusion experiments were carried out in an identical manner to the benzoic acid system.

A total of 15 diffusion runs were attempted over the temperature range $+10$ to -15°C of which only 4 gave reasonable results. The other eleven runs were lost due to the poor alignment or very uneven surface after the diffusion anneal, the crystals splitting when the sides were cut off prior to sectioning and lack of activity.

Due to difficulty in obtaining the weight of each section it was assumed that the microtome was accurate and the specific activity was obtained as counts per second per 10 micron section. The results of the acceptable diffusion runs are shown in figure 40 as plots of $\log_{10} A$ vs \bar{x}^2 . There is considerable scatter in the experimental points but the diffusion profiles are obvious curves in all cases, except run 4, indicating that equation (1) is not the correct solution to this problem. If, as with C^{14} diffusion in benzoic acid, these curves represent the superposition of two diffusion processes then an estimate of the bulk diffusion coefficient can be made from the initial slope of the curve.

TRITIUM DIFFUSION + (100) PLANE IN ACETIC ACID, FIG. 40



The diffusion coefficients so calculated, which will represent a maximum value of the bulk diffusion coefficient, are tabulated below.

TABLE XIV TRITIUM DIFFUSION IN ACETIC ACID.

RUN	TEMP. °C	TIME hours	MAXIMUM BULK DIFFUSION COEFFICIENT
1	0.8 ± .05	25.0	1.3×10^{-10}
2	-13.5 ± .05	23.0	1.7×10^{-10}
3	-5.2 ± .05	48.0	6×10^{-11}
4	0.0 ± .05	48.0	1×10^{-11}

Inspection of these results shows that there is no apparent correlation between diffusion coefficient and temperature.

It is believed that the variation in these results is due to variable amounts of water vapour being absorbed on the crystals prior to the diffusion anneal. It has been shown that the conductivity of acetic acid is very dependent on adsorbed water (p 103) and also that diffusion in benzoic acid is very dependent on the water vapour in the diffusion cell. Hence it was concluded that a similar phenomena was occurring in this system. Due to the difficulties involved in improving the diffusion technique this system was abandoned. The intrinsic diffusion coefficient of tritium in acetic acid \perp (100) plane was concluded to be less than $1 \times 10^{-11} \text{ cm}^2 \text{ sec}^{-1}$ at 0°C.

o Conductivity Studies

1. Conductivity in benzoic acid

The results of A.C. conductivity measurements on analar benzoic acid compacts are shown in figure 41. These results were obtained on the same compact using a heating rate of $0.50^{\circ}/\text{min}$. In the first run, run 1, transient effects were observed in the region $20 - 50^{\circ}\text{C}$ which were not evident in the subsequent runs. The conductivity was found to decrease with each run probably due to a sintering reaction taking place which is indicated by the curvature of the Arrhenius plots above 100°C . In the temperature range $40 - 100^{\circ}\text{C}$ runs 2 and 3 had the same activation energy and run 3 can be represented by the following Arrhenius equation.

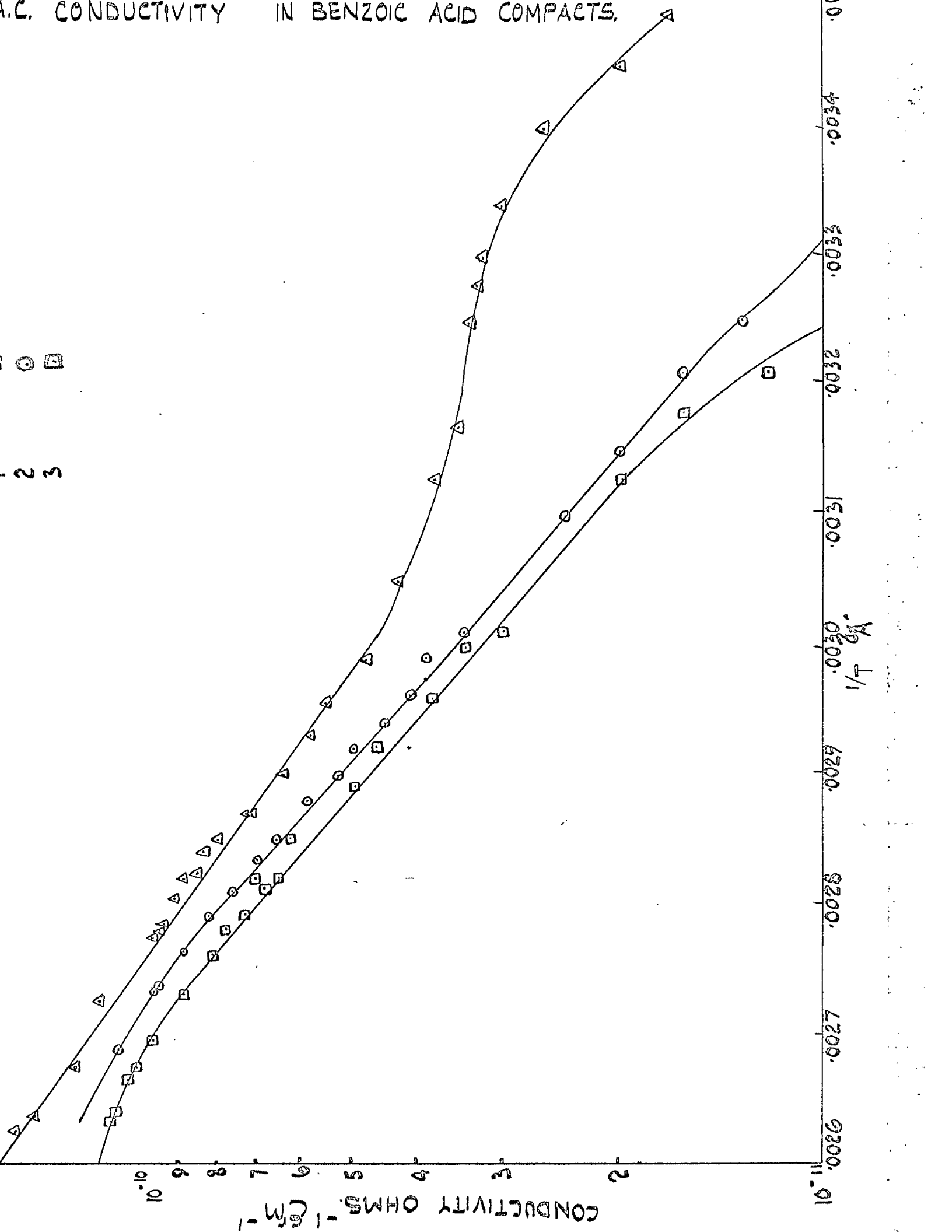
$$\sigma = 3 \times 10^{-6} \exp \left[\frac{-7,600}{RT} \right]$$

Attempts to measure A.C. conductivity in compacts of high purity benzoic acid (p 89) were unsuccessful as only transient effects were observed on the very lowest scale of the instrument. This indicated that the bulk conductivity was less than $10^{-11} \text{ohm}^{-1} \text{cm}^{-1}$.

Attempts to measure D.C. conductivity in single crystals and polycrystals was also unsuccessful which indicated that the bulk conductivity was less than $10^{-14} \text{ohm}^{-1} \text{cm}^{-1}$, 7°C below the melting point. These results suggest that the conductivity in the analar compacts are due to an impurity of which the most likely is water as no attempts were made to dry this material prior to pelleting.

A.C. CONDUCTIVITY IN BENZOIC ACID COMPACTS.

○ □
2 3



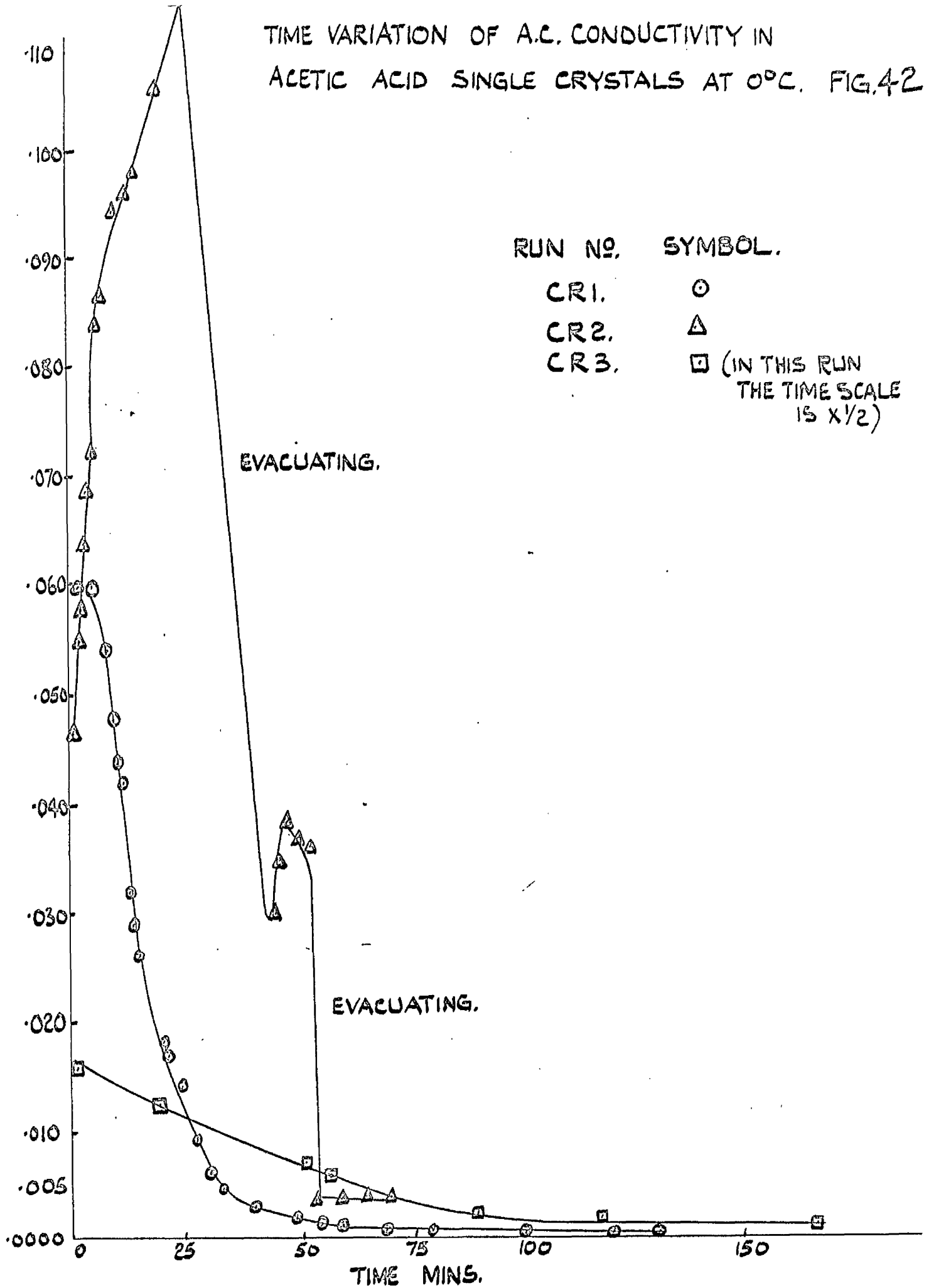
2. Conductivity in acetic acid.

As the conductivity could not be measured down the hydrogen bonded chains (p48) an attempt was made to measure it at right angles to them down the (100) plane. The conductivity of single crystals of acetic acid was measured at 0°C with P₂O₅ present at the base of the conductivity cell, figure 25. The A.C. conductivity was found to vary with time and the experimental results are shown graphically in figure 42. The crystals were placed in the conductivity cell at -20°C in a fridge and then inserted in the thermostat bath.

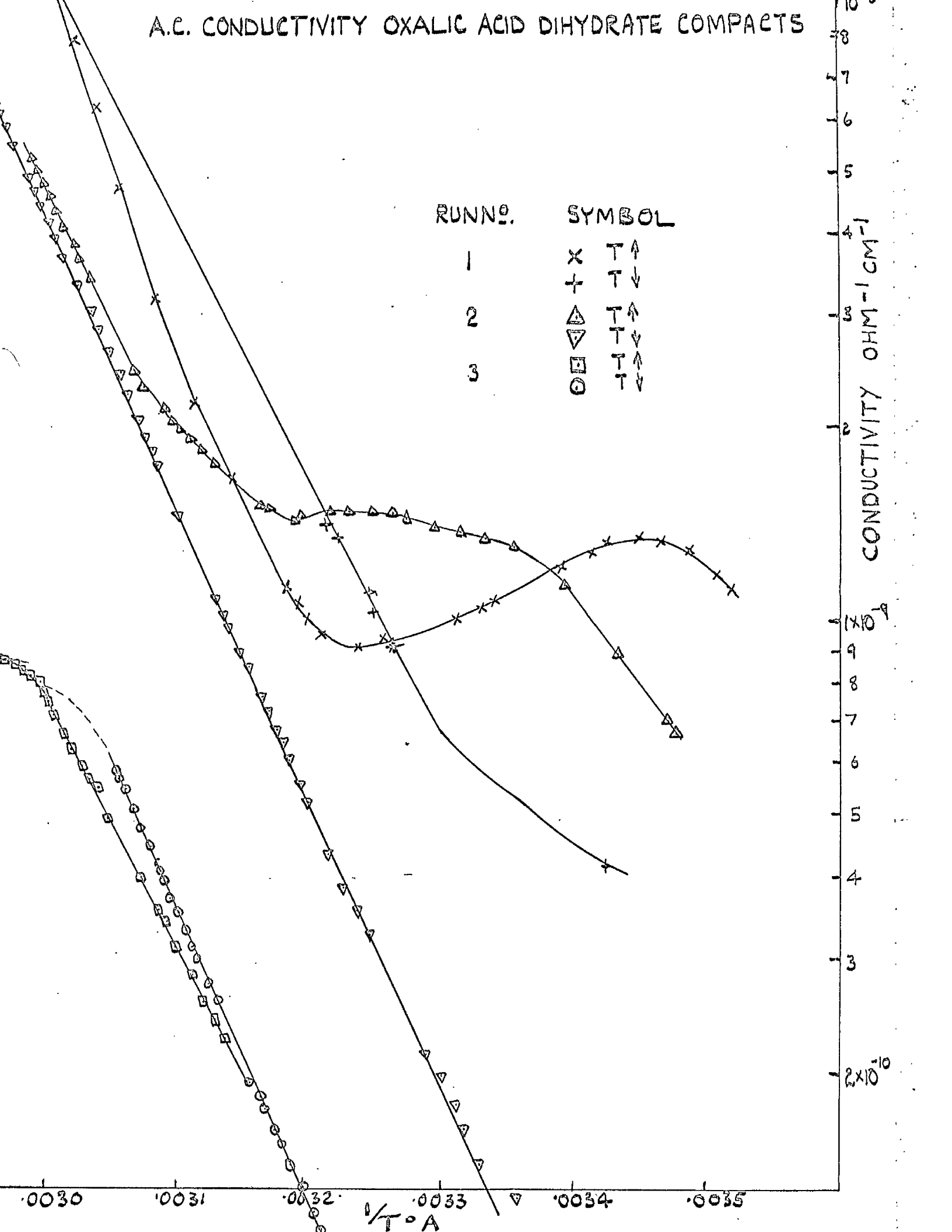
In run CR1 the conductivity rose to 6×10^{-8} mho then decreased with time as shown to 2×10^{-10} mho after 2 hours. The temperature was allowed to warm up slowly to 10°C over a further 2 hour period but the conductivity remained unaltered. This was the limit of detection of the instrument hence it was concluded that the bulk conductivity was less than 2×10^{-10} ohm⁻¹cm⁻¹ as the cell constant was approximately one.

In CR2 the cell was not dried thoroughly prior to inserting the crystal and some water droplets were observed on the side of the cell. In this case the P₂O₅ was not sufficient to absorb all the moisture and a rapid increase in conductivity was observed due to adsorption of water on the crystal. On pumping the crystal to remove the water a rapid decrease in conductivity was observed and the conductivity again fell to a very low value.

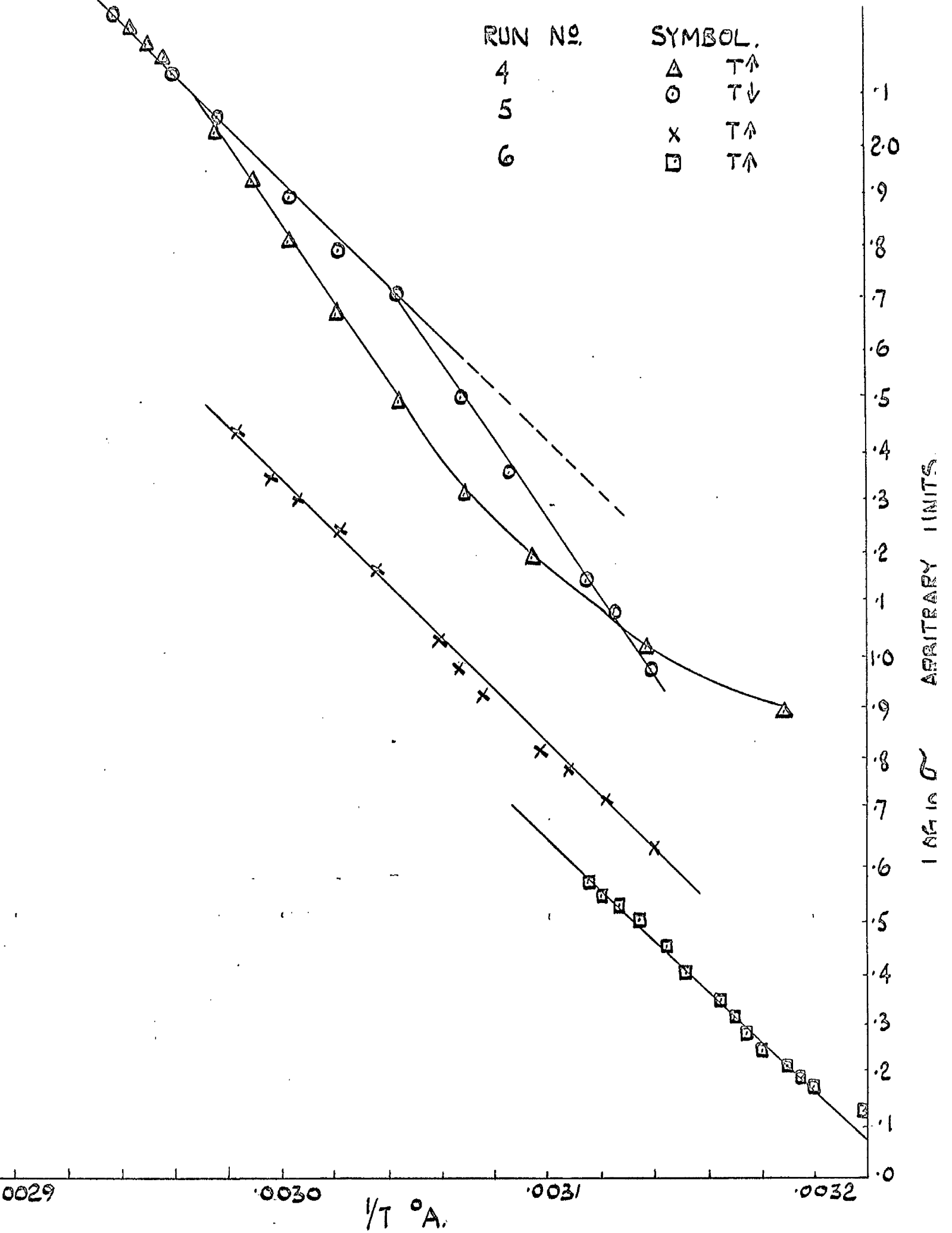
TIME VARIATION OF A.C. CONDUCTIVITY IN ACETIC ACID SINGLE CRYSTALS AT 0°C. FIG. 42



A.C. CONDUCTIVITY OXALIC ACID DIHYDRATE COMPACTS



RUN NO.	SYMBOL.
4	△ T↑
5	○ T↓
6	x T↑
	□ T↑



f. Tabulated Results.

This section includes the results of all successful diffusion runs attempted in benzoic acid. The runs are numbered and tabulated in the order that they were performed and range from DR7 to DR86.

These results are followed by the results of the exchange reaction between tritiated benzoic acid and water vapour and are numbered ER1 to ER10.

Nomenclature - The nomenclature used for the diffusion results is as follows.

R_s Total activity of the section, counts per second.

A Specific activity of the section, counts per second per mgm.

x Penetration depth to the end of each section, microns.

\bar{x}^2 Square of the penetration to the middle of each section,
 $\text{cm}^2 \times 10^6$

\bar{x} Penetration to the middle of each section, microns.

DIFFUSION RUN DR7

18.50 hours at $88.8 \pm 0.1^\circ\text{C}$.

Section	R_s	Log A	x	\bar{x}^2
1	-	-	10	0.25
2	17.89	1.513	20	2.25
3	7.09	0.913	30	6.25
4	4.65	0.661	40	12.20
5	1.49	0.184	50	20.30
6	0.	-	60	30.20

DIFFUSION RUN DR8

24.0 hours at $93.2 \pm 0.1^\circ\text{C}$.

Section	R_s	Log A	x	\bar{x}^2
1	-	-	10	0.25
2	4.84	0.782	20	2.25
3	3.26	0.623	30	6.25
4	1.59	0.367	40	12.20
5	0.30	-0.380	50	20.20

DIFFUSION RUN DR9

24.0 hours at $93.5 \pm 0.2^\circ\text{C}$.

Section	R_s	Log A	x	\bar{x}^2
1	-	-	5	0.0625
2	221.0	2.533	15	1.00
3	262.0	2.42	25	1.56
4	75.46	2.096	35	2.10
5	62.48	1.796	45	3.04
6	7.58	1.378	55	3.04
7	2.2	1.34	65	4.23
8	1.1	1.1	75	5.63

DIFFUSION RUN DR10

23.0 hours at $104.2 \pm 0.2^{\circ}\text{C}$.

Section	R_s	Log A	x	\bar{x}^2
1	56.2	2.070	5	0.0625
2	61.8	2.019	15	1.000
3	68.6	1.940	25	4.00
4	40.0	1.724	35	9.00
5	35.5	1.548	45	16.00
6	21.1	1.340	55	25.00
7	10.3	1.038	65	36.00
8	3.10	0.498	75	49.00

DIFFUSION RUN DR13

19.0 hours at $108 \pm 1.0^{\circ}\text{C}$.

Section	R_s	Log A	x	\bar{x}^2
1	30.0	1.388	10	0.25
2	27.4	1.490	20	2.25
3	23.15	1.45	30	6.25
4	31.7	1.48	40	12.20
5	22.8	1.366	50	20.30
6	21.0	1.315	60	30.20
7	11.7	1.066	70	42.30
8	6.43	0.735	80	56.20
9	2.40	0.394	90	72.30
10	1.26	0.104	100	90.20

DIFFUSION RUN DRL4

16.0 hours at $108.0 \pm 0.2^{\circ}\text{C}$.

Section	R_s	Log A	x	x^2
1	750.0	2.630	20	1.00
2	191.5	2.455	30	6.25
3	101.5	2.272	40	12.20
4	99.6	2.140	50	20.30
5	65.8	1.924	60	30.20
6	35.7	1.586	70	42.30
7	6.2	1.007	80	56.20
8	4.42	0.898	90	72.30
9	5.08	0.722	100	90.20

DIFFUSION RUN DRL6

235.5 hours at $78.5 \pm 0.2^{\circ}\text{C}$.

Section	R_s	Log A	x	x^2
1	10.60	1.287	10	0.25
2	13.50	1.318	20	2.25
3	19.80	1.338	30	6.25
4	14.65	1.227	40	12.20
5	8.50	1.089	50	20.30
6	5.60	0.839	60	30.20
7	3.30	0.62	70	42.30
8	2.10	0.41	80	56.20
9	1.20	0.134	90	72.30
10	0.50	-0.210	100	90.20

DIFFUSION RUN DR17

334.0 hours at $94.3 \pm 0.2^\circ\text{C}$.

Section	R_s cps.	Log A	x microns	$x^{-2} \times 10^{-6} \text{cm}^2$
1	11.17	1.356	10	0.25
2	13.47	1.813	20	2.25
3	8.14	1.370	30	6.25
4	8.57	1.344	40	12.2
5	11.87	1.330	50	20.3
6	9.67	1.302	60	30.2
7	9.26	1.250	70	42.3
8	7.00	1.148	80	56.3
9	7.32	1.061	90	72.3
10	7.59	1.232	100	90.3
11	5.73	0.911	110	110.2

DIFFUSION RUN DR18

165.7 hours at $100.0 \pm 0.2^\circ\text{C}$.

Section	R_s	Log A	x	x^{-2}
1	9.46	1.129	10	0.25
2	10.11	1.056	20	2.25
3	11.13	1.000	30	6.25
4	4.05	0.964	40	12.2
5	4.13	0.908	50	20.3
6	4.61	0.910	60	30.2
7	3.92	0.878	70	42.3
8	4.05	0.849	80	56.3
9	4.06	0.812	90	72.2
10	3.56	0.723	100	90.2
12	2.67	0.383	120	132.
14	1.74	0.432	140	182
16	0.87	0.137	160	240

DIFFUSION RUN 23a

329 hours at $116.5 \pm 0.05^{\circ}\text{C}$.

Section	R_s	Log A	x	\bar{x}^2
1	192	2.402	6	0.09
2	260	2.476	14	1.00
3	238	2.239	24	3.61
4	9.92	1.106	34	8.40
5	2.02	0.217	44	15.2
6	0.73	-0.27	54	24.0
7	0.45	-0.40	64	34.8
8	0.45	-0.47	74	47.6
9	0.28	-0.67	84	62.5
10	0.40	-0.50	94	79.2
11	0.46	-0.50	104	98.0

DIFFUSION RUN DR22b

403 hours at $105.2 \pm 0.2^{\circ}\text{C}$.

Section	R_s	Log A	x	\bar{x}^2
1	291	2.562	10	0.25
2	68.0	1.926	20	2.25
3	2.36	0.344	30	6.25
4	3.27	0.520	40	12.2
5	0.88	-0.15	50	20.3
6	0.53	-0.46	60	30.2
7	0.57	-0.40	70	42.3

DIFFUSION RUN DR23b

329 hours at $116.5 \pm 0.05^{\circ}\text{C}$.

Section	R_g	Log A	x	\bar{x}^2
1	238	2.567	4	0.04
2	156	2.431	8	0.36
3	155	2.263	14	1.21
4	128	1.986	24	3.61
5	29.5	1.323	34	8.40
6	8.72	0.764	44	15.2
7	3.90	0.454	54	24.0
8	3.63	0.347	64	34.8
9	3.04	0.331	74	47.6
10	3.36	0.334	84	62.5
11	3.37	0.302	94	79.2
12	2.60	0.205	104	98.0

DIFFUSION RUN DR24

547 hours at $110.5 \pm 0.2^{\circ}\text{C}$.

Section	R_g	Log A	x	\bar{x}^2
1	376	2.710	8	0.16
2	69.0	1.868	18	1.69
3	7.33	0.874	28	5.30
4	3.94	0.659	38	10.90
5	2.79	0.484	48	18.5
6	4.70	0.669	58	28.1
7	3.86	0.595	68	39.7
8	3.33	0.468	78	53.2
9	2.64	0.404	88	69.0
10	2.60	0.322	98	86.6
11	2.78	0.412	108	106
13	2.35	0.312	128	151
15	2.74	0.414	148	204

DIFFUSION RUN DR26a

23 hours at $91.0 \pm 0.05^\circ\text{C}$.

Section	R_B	Log A	\bar{x}
1	3450	3.530	5
2	580	2.896	15
3	350	2.476	25
4	152	2.146	35
5	53.5	1.831	45
6	43.3	1.501	55
7	25.5	1.178	65
8	13.7	1.020	75
9	10.8	0.891	85
10	7.23	0.732	95
11	5.14	0.575	105
12	3.90	0.467	115

DIFFUSION RUN DR26b

Section	R_B	Log A	\bar{x}
1	4260	3.376	7.5
2	800	2.796	20
3	274	2.434	30
4	150.5	2.123	40
5	105.5	1.874	50
6	45.6	1.572	60
7	32.0	1.345	70
8	17.2	1.139	80
9	14.4	1.043	90
10	7.66	0.785	100
11	7.52	0.782	110
12	4.24	0.490	120
13	4.44	0.537	130
15	2.70	0.272	150

DIFFUSION RUN DR27a

16.5 hours at 103.5 ± 0.05°C.

Section	R_g	Log A	\bar{x}
1	3570	3.553	5
2	862	2.991	15
3	478	2.619	25
4	178	2.316	35
5	147	2.116	45
6	90.8	1.853	55
7	41.8	1.670	65
8	35.9	1.470	75
9	24.8	1.344	85
10	18.4	1.151	95
11	11.8	1.010	105
12	8.24	0.892	115

DIFFUSION RUN DR27b

Section	R_g	Log A	\bar{x}
1	1550	3.534	2.5
2	1500	3.227	7.5
3	830	2.910	15
4	622	2.642	25
5	283.5	2.402	35
6	162.0	2.118	45
7	93.9	1.936	55
8	59.2	1.746	65
9	40.9	1.559	75
10	25.6	1.143	85
11	23.8	1.293	95
12	15.25	1.116	105
13	12.5	1.052	115
14	10.05	0.916	125
15	7.5	0.810	135

DIFFUSION RUN DR28a

67 hours at $78.6 \pm 0.05^{\circ}\text{C}$.

Section	R_s	Log A	\bar{x}
1	1407	3.214	4
2	642	2.721	13
3	219	2.257	23
4	92.5	1.854	33
5	44.5	1.506	43
6	14.5	1.152	53
7	9.25	0.824	63
8	4.04	0.55	73
9	2.86	0.40	83
10	2.16	0.20	93
11	1.77	0.11	103
12	1.45	-0.24	113

DIFFUSION RUN DR28b

Section	R_s	Log A	\bar{x}
1	1515	3.292	4
2	1000	2.956	13
3	286	2.428	23
4	138	2.033	33
5	67.9	1.711	43
6	27.4	1.396	53
7	17.1	1.154	63
8	11.3	0.918	73
9	6.40	0.663	83
11	2.64	0.294	103
13	2.13	0.193	123

DIFFUSION RUN DR29

42 hours at $84.3 \pm 0.05^\circ\text{C}$.

Section	R_s	Log A	\bar{x}
1	2635	3.255	5
2	742	2.787	15
3	420	2.542	25
4	247.5	2.300	35
5	152	2.081	45
6	81.3	1.886	55
7	38.0	1.605	65
8	32.8	1.450	75
9	24.0	1.256	85
10	13.55	1.041	95
11	7.08	0.87	105
12	4.40	0.64	115

DIFFUSION RUN DR32

172 hours at 110.0 ± 0.05

Section	R_B	Log A	x	\bar{x}^2
1	2517	3.799	5	0.0625
2	1619	3.526	10	0.562
3	815	3.109	20	2.25
4	104.5	2.074	30	6.25
5	34.2	1.620	40	12.2
6	14.7	1.305	50	20.3
7	15.7	1.200	60	30.2
8	11.0	1.052	70	42.3
9	14.8	1.183	80	56.3
10	7.8	1.014	90	72.2
11	15.8	1.342	100	90.2
12-16	20.9	0.888	150	156
17-21	9.2	0.424	200	306

DIFFUSION RUN DR33

182 hours at $109.8 \pm 0.5^{\circ}\text{C}$.

Section	R_s	Log A	x	\bar{x}^2
1 } 2 }	72.7	2.313	10	0.25
3	15.50	1.537	20	2.25
4	2.10	0.558	30	6.25
5	0.29	-0.084	40	12.2
6	0.21	-0.32	50	20.3
7	0.35	-0.17	60	30.2
8	0.18	-0.25	70	42.3
9	0.50	0.075	80	56.3
10	0.26	-0.10	90	72.2
11	0.45	0.018	100	90.1
12	0.25	-0.30		
13	0.18	-0.32		

DIFFUSION RUN DR34

162 hours at 100.5°C .

Section	R_s	Log A	x	\bar{x}^2
1	332.3	2.996	5	0.0625
2	109.0	2.594	10	0.56
3	27.5	1.983	15	1.56
4	1.26	0.704	20	3.06
5	0.46	0.05	25	5.06
7	0.12	-0.07	35	10.6

DIFFUSION RUN DR36

116 hours at $105.5 \pm 0.1^{\circ}\text{C}$.

Section	R_g	Log A	x	\bar{x}^2
1	17.73	1.462	5	0.0625
2	29.88	1.490	15	1.00
3	8.54	0.814	25	4.00
4	0.1	-1.00	35	9.00

DIFFUSION RUN DR37

137 hours at $105.5 \pm 0.1^{\circ}\text{C}$.

Section	R_g	Log A	x	\bar{x}^2
1	260.5	2.369	10	0.25
2	95.0	2.020	20	2.25
3	43.8	1.650	30	6.25
4	14.5	1.136	40	12.2
5	0	-	50	20.3

DIFFUSION RUN DR38

240 hours at $110.8 \pm 0.05^{\circ}\text{C}$.

Section	R_g	Log A	x	\bar{x}^2
1	8.3	1.393	5	0.0625
3	20.9	1.398	25	4.00
5	8.4	0.925	45	16.0
7	3.5	0.408	65	36.0
9	0	-		64.0

DIFFUSION RUN DR42b

148 hours at $99.5 \pm 0.05^{\circ}\text{C}$.

Section	R_g	Log A	x	\bar{x}^2
1)	27.3	1.403	10	0.25
2)				
3	16.3	1.236	20	2.25
4	7.4	0.840	30	6.25
5	1.9	0.279	40	12.2
6	0	-	50	20.3

DIFFUSION RUN DR43a

166 hours at $99.5 \pm 0.05^{\circ}\text{C}$.

Section	R_g	Log A	x	\bar{x}^2
1	122	1.978	10	0.25
2	195	2.105	20	2.25
3	96.9	1.960	30	6.25
4	44.4	1.587	40	12.2
5	19.3	1.258	50	20.3
6	8.4	0.882	60	30.2
7	5.54	0.670	70	42.3
8	2.80	0.406	80	56.3
10	2.10	0.318	100	90.2
12	1.4	0.123	120	132
14	0.6	-0.28	140	182

DIFFUSION RUN DR52

112 hours at 115.5 ± 0.05°C.

Section	R_s	Log A	x	\bar{x}^2
1	58.0	2.031	10	0.25
2	32.2	1.991	15	1.56
3	35.9	2.037	20	3.06
4	56.4	2.091	30	6.25
5	45.2	1.848	40	12.2
6	52.0	1.936	50	20.3
7	66.1	1.904	60	30.2
8	21.3	1.622	70	42.3
10	8.0	0.938	90	72.2
12	1.2	0.135	100	110
14	0	-	120	132

DIFFUSION RUN DR60a

160.0 hours at 115.0°C.

Section	R_s	Log A	x	\bar{x}^2
1	-	-	10	0.25
2	58.0	1.954	20	2.25
3	28.8	1.585	30	6.25
4	26.5	1.549	40	12.2
5	8.40	1.050	50	20.3
6	4.45	0.784	60	30.2
7	1.70	0.356	70	42.3
8	1.55	0.316	80	56.4
9	2.70	0.256	100	81

DIFFUSION RUN DR60b

Section	R_s	Log A	x	\bar{x}^2
1	-	-	20	1.00
2	177.5	2.249	30	6.25
3	109.5	2.040	40	12.2
4	18.3	1.263	50	20.3
5	6.5	0.814	60	30.2
6	2.1	0.322	70	42.3

DIFFUSION RUN DR61a

67.5 hours at $115.0 \pm 0.05^\circ\text{C}$.

Section	R_s	Log A	x	\bar{x}^2
1	-	-	10	0.25
2	-	-	15	1.56
3	24.9	1.494	20	3.06
4	11.0	1.138	25	5.06
5	12.9	1.207	30	7.56
6	6.70	0.923	35	10.6
7	2.35	0.468	40	14.1
8	3.7	0.365	50	20.3
9	2.9	0.258	60	30.2
10	3.0	0.274	70	42.3
14	0.7	-0.40	110	90.2

DIFFUSION RUN DR61b

Section	R_s	Log A	x	\bar{x}^2
1	64.8	1.664	15	0.56
2	12.3	1.578	20	3.06
3	11.4	1.380	25	5.06
4	5.8	0.895	35	9.0
5	1.90	0.485	45	16.0
6	-	-	-	25.0
7	1.90	0.247	65	36.0
8	1.20	0.077	75	49.0
9	-	-	-	64.0
10	0	-	95	81.0

DIFFUSION RUN DR62

72.0 hours at $110.0 \pm 0.05^{\circ}\text{C}$.

Section	R_s	Log A	x	\bar{x}^2
1	-	-	10	0.25
2	13.60	1.435	15	1.56
3	8.80	1.246	20	3.06
4	14.7	1.167	30	6.25
5	6.3	0.800	40	12.2
6	1.4	0.146	50	20.3
7	1.2	0.079	60	30.2
8	0	-	70	42.3

DIFFUSION RUN 63a

160 hours at 115.0°C .

Section	R_s	Log A	x	\bar{x}^2
1	-	-	20	1.00
2	325	2.813	25	5.06
3	247.5	2.697	30	7.56
4	249.5	2.699	35	10.6
5	287.5	2.459	45	16.0
6	116.3	2.064	55	25.0
7	20.0	1.301	65	36.0
8	5.1	0.700	75	49.0
9	2.1	0.32	95	64.0

DIFFUSION RUN DR63b

Section	R_s	Log A	x	\bar{x}^2
1	-	-	15	0.56
2	357	2.775	20	3.06
3	258	2.634	25	5.06
4	93.4	2.192	30	7.56
5	93.2	2.192	35	10.6
6	76.3	2.104	40	14.1
7	75.4	1.798	50	20.3
8	13.9	1.064	60	30.2
9	5.0	0.620	70	42.3
10	0.5	-0.4	80	56.3

DIFFUSION RUN DR66a

42.0 hours at $101.0 \pm 0.2^\circ\text{C}$.

Section	R_s	Log A	\bar{x}^2
1	(300)	(2.50)	5
2	-	-	15
3	34.2	1.534	25
4	28.4	1.454	35
5	23.1	1.364	45
6	19.6	0.992	60
7	9.7	0.987	75
8	9.2	0.624	85
9	1.0	0.00	95
10	3.3	0.520	105
11	0	-	115

DIFFUSION RUN DR67a
 DIFFUSION RUN DR67a
 256 hours at 100.5°C.

Section	R_s	Log A	x	\bar{x}^2
1	-	-	10	0.25
2	-	-	15	1.56
3	130.0	2.453	20	3.06
4	127.7	2.425	25	5.06
5	71.0	2.170	30	7.56
6	60.4	2.100	35	10.6
7	51.5	2.031	40	14.1
8	25.9	1.732	45	18.1
9	36.0	1.575	55	25.0
10	12.4	1.111	65	36.0
11	6.10	0.804	75	49.0
12	3.20	0.524	85	64.0
13	4.00	0.320	110	100.0
17	0	-	165	272

DIFFUSION RUN DR67b

Section	R_s	Log A	x	\bar{x}^2
1	-	-	10	0.25
2	-	-	15	1.56
3	132.3	2.352	20	3.06
4	122.2	2.317	25	5.06
5	161.0	2.435	30	7.56
6	145.9	2.393	35	10.6
7	50.0	1.929	40	14.1
8	30.0	1.706	45	18.1
9	30.5	1.416	55	25.0
10	9.72	0.920	65	36.0
11	3.05	0.420	75	49.0
12	0.80	-0.16	85	64.0

DIFFUSION RUN DR68

169.0 hours at 90.0°C.

Section	R_g	Log A	x	\bar{x}^2
1	-	-	5	0.0625
2	4.6	1.216	10	0.56
3	3.8	1.153	15	1.56
4	1.7	0.784	20	3.06
5	1.5	0.730	25	5.06
6	0	-	30	7.56

DIFFUSION RUN DR69b

134.0 hours at 98.5 ± 0.2°C.

Section	R_g	Log A	x	\bar{x}^2
1	-	-	5	0.0625
2	-	-	10	0.56
3	55.4	2.044	15	1.56
4	37.5	1.876	20	3.06
5	13.17	1.421	25	5.06
6	3.44	0.838	30	7.56
7	0.50	0.00	35	10.6
8	0	-	40	14.1

DIFFUSION RUN DR71

68.0 hours at 78.5°C.

Section	R_s	Log A	\bar{x}
1	-	-	5.0
2	343.6	2.494	15.0
3	219.6	2.300	25.0
4	77.0	1.846	35.0
5	38.4	1.543	45.0
6	30.7	1.446	55.0
7	19.0	1.238	65.0
8	8.75	0.900	75.0
9	8.25	0.876	85.0
10	7.60	0.840	95.0
11	7.55	0.536	110
12	6.00	0.417	130
13	-	-	145
14	-	-	155
15	2.05	-0.30	170

DIFFUSION RUN DR72a
204 hours at 110.5°C.

Section	R_g	Log A	x	\bar{x}^2
1	-	-	10	0.25
2	61.8	2.128	15	1.56
3	57.5	2.097	20	3.06
4	55.9	2.075	25	5.06
5	59.6	2.113	30	7.56
6	99.4	2.033	40	12.2
7				
8	54.9	2.077	45	18.1
9	57.4	2.097	50	22.6
10	48.4	2.022	55	27.6
11	158.1	1.961	75	42.3
12				
13	79.4	1.936	85	64.0
14	59.7	1.813	95	81.0
17	47.8	1.716	125	144
20	16.3	1.248	155	225
23	7.70	0.923	185	289
26	2.40	0.417	215	441
29	1.20	0.116	245	576
35	0			

DIFFUSION RUN DR72b

Section	H_g	Log A	x	\bar{x}^2
1	743	2.489	15	0.56
2	94.5	1.830	25	4.00
3	115.9	1.890	35	9.00
4	92.6	1.797	45	16.0
5	84.7	1.758	55	25.0
6	99.7	1.829	65	36.0
7	92.3	1.795	75	49.0
8	69.9	1.675	85	64.0
9	95.9	1.803	95	81.0
10	86.9	1.769	105	100
11	81.7	1.742	115	121
12	61.0	1.614	125	144
14	18.9	1.106	145	196
15	16.8	1.055	155	225
18	10.2	0.838	185	324
20	4.10	0.443	205	400
22	2.30	0.190	225	505
24	0.3	-0.70	245	600

DIFFUSION RUN DR73a

204 hours at 110.5°C.

Section	H_g	Log A	x	\bar{x}^2
1	-	-	15	0.56
2	37.8	1.934	20	3.06
3	53.9	1.786	30	6.25
4	68.3	1.910	40	12.2
5	29.8	1.831	45	18.1
6	30.0	1.834	50	22.6
7	64.0	1.883	60	30.2
8	127.2	1.860	80	49.0
9	45.2	1.711	90	72.2
10	49.9	1.754	100	90.1
11	20.0	1.356	130	156
12	8.30	0.975	160	240
13	4.40	0.700	190	342
14	1.80	0.310	220	463
15	11.0	0.055	250	600

DIFFUSION RUN DR73b

Section	R_s	Log A	x	\bar{x}^2
1	-	-	10	0.25
2	80.4	1.992	20	2.25
3	83.4	2.007	30	6.25
4	44.2	2.032	35	10.6
5	47.9	2.067	40	14.1
6	86.2	2.077	50	20.2
7	65.1	1.900	60	30.2
8	53.3	1.813	70	42.3
9	65.4	1.902	80	56.2
10	53.1	1.812	90	72.2
11	39.0	1.677	100	90.1
12	44.2	1.732	110	110.2
13	20.5	1.400	140	182
14	12.2	1.172	170	272
15	10.7	1.116	200	380
16	3.2	0.592	230	506

DIFFUSION RUN DR76a

324 hours at 110.5°C.

Section	R_s	Log A	x	\bar{x}^2
1	-	-	10	0.25
2	54.3	2.106	15	1.56
3	36.2	1.934	20	3.06
4	53.1	2.096	25	5.06
5	25.0	1.769	30	7.56
6	24.8	1.766	35	10.6
7	27.8	1.813	40	14.1
8	24.5	1.762	45	18.1
9	22.3	1.420	55	25.0
10	8.10	0.979	65	36.0
11	2.37	0.446	75	49.0
12	0.84	0.00	85	64.0
13	0.2	-0.6	95	81.0

DIFFUSION RUN DR 76b

Section	R_g	Log A	x	\bar{x}^2
1	-	-	10	0.25
2	87.8	2.331	15	1.56
3	47.9	2.068	20	3.06
4	42.5	2.016	25	5.06
5	45.1	2.042	30	7.56
6	37.7	1.964	35	10.6
7	30.1	1.866	40	14.1
8	23.6	1.760	45	18.1
9	24.0	1.472	55	25.0
10	13.0	1.200	65	36.0
11	8.85	1.033	75	49.0
12	1.75	0.33	85	64.0
13	-	-	95	81.0
14	0.60	-0.14	105	100

DIFFUSION RUN DR77b

236 hours at 110.5°C.

Section	R_g	Log A	x	\bar{x}^2
1	-	-	15	0.56
2	2.000	3.933	20	3.06
3	372.7	3.027	25	5.06
4	36.2	2.014	30	7.56
5	4.10	1.069	35	10.6
6	3.70	1.024	40	14.1
7	1.26	0.557	45	18.1
8	0.63	0.256	50	22.6
9	1.88	0.430	60	30.2
10	1.00	0.155	70	42.3
11	0.90	0.11	80	56.2
12	-	-	90	72.2
13	0.80	0.058	100	90.1
14	0.65	-0.3	150	210

DIFFUSION RUN DR77c

Section	R_g	Log A	x	\bar{x}^2
1	(10,000)	(4.0)	10	0.25
2	814.7	3.464	15	1.56
3	129.7	2.666	20	3.06
4	15.3	1.736	25	5.06
5	1.15	0.614	30	7.56
6	1.63	0.766	35	10.6
7	2.45	0.942	40	14.1
8	0.50	0.254	45	18.1
9	0.35	0.097	50	22.6

DIFFUSION RUN DR78a

496 hours at 103.5°C.

Section	R_g	Log A	x	\bar{x}^2
1	4000	3.616	10	0.25
2	31.2	2.963	15	1.56
3	5.94	1.242	20	3.06
4	2.50	0.867	25	5.06
5	1.32	0.590	30	7.56
6	1.34	0.596	35	10.6
7	1.07	0.498	40	14.1
8	0.71	0.320	45	18.1
9	0.79	0.366	50	22.6
10	0.67	0.295	55	27.6
11	0.49	0.158	60	33.0

DIFFUSION RUN DR78b

Section	R_s	Log A	x	\bar{x}^2
1	11,540	4.223	10	0.25
2	790	3.380	15	1.56
3	172.5	2.719	20	3.06
4	49.9	2.180	25	5.06
5	28.9	1.943	30	7.56
6	18.8	1.756	35	10.6
7	14.4	1.640	40	14.1
8	12.44	1.577	45	18.1
9	3.70	1.050	50	22.6
10	4.00	1.083	55	27.6
11	2.32	0.546	65	36.0
12	2.44	0.568	75	49.0
13	1.45	0.342	85	64.0
14	3.10	0.973	95	81.0
15	1.12	0.230	135	169

DIFFUSION RUN DR79

202 hours at $115.0 \pm 0.05^\circ\text{C}$.

Section	R_s	Log A	x	\bar{x}^2
1	(5000)	(4.0)	15	0.56
2	141.5	2.754	20	3.06
3	59.0	2.374	25	5.06
4	16.8	1.828	30	7.56
5	2.53	1.00	35	10.6
6	0.53	0.327	40	14.1
7	0.36	0.158	45	18.1
8	0.25	0.00	50	22.6
9	0.2	-0.1	55	27.6
10	0.1	-0.4	60	33.0

DIFFUSION RUN DR80B

250 hours at $115.0 \pm 0.05^\circ\text{C}$.

Section	R_B	Log A	x	\bar{x}^2
1	-	-	15	0.56
2	50.7	2.207	20	3.06
3	47.2	2.176	25	5.06
4	28.7	1.960	30	7.56
5	35.0	2.046	35	10.6
6	27.3	1.938	40	14.1
7	14.4	1.660	45	18.1
8	13.0	1.616	50	22.6
9	3.40	1.034	55	27.6
10	6.00	1.280	60	33.0
11	2.48	0.896	70	42.3
12	0.45	0.154	80	56.3
14	0.2	-0.5	100	90.2

DIFFUSION RUN DR80B

Section	R_B	Log A	x	\bar{x}^2
1	-	-	10	0.25
2	124.5	2.095	20	2.25
3	61.5	2.090	25	5.06
4	78.8	2.197	30	7.56
5	79.8	2.203	35	10.6
6	69.0	1.840	45	16.0
7	26.7	1.427	55	25.0
8	7.10	0.852	65	36.0
9	2.30	0.362	75	49.0
10	1.90	0.280	85	64.0
11	0.70	-0.15	95	81.0

DIFFUSION RUN DR80c

Section	R_g	Log A	x	\bar{x}^2
1	-	-	10	0.25
2	275.8	2.441	20	2.25
3	96.8	2.287	25	5.06
4	150.8	2.480	30	7.56
5	83.1	2.221	35	10.6
6	127.3	2.105	45	16.0
7	85.8	1.934	55	25.0
8	41.2	1.616	65	36.0
9	10.55	1.024	75	49.0
10	6.60	0.820	85	64.0
11	1.70	0.230	95	81.0
12	0.3	-0.5	105	100.0

DIFFUSION RUN DR80d

Section	R_g	Log A	x	\bar{x}^2
1	-	-	10	0.25
2	74.6	2.174	15	1.56
3	72.8	2.162	20	3.06
4	40.8	1.912	25	5.06
5	26.1	1.718	30	7.56
6	29.2	1.466	40	12.2
7	21.0	1.322	50	20.3
8	5.30	0.724	60	30.2
9	2.00	0.301	70	42.3
10	1.10	0.040	80	56.3
11	1.20	0.080	90	72.2
12	0.7	-0.25	100	90.1
13	0.3	-0.52	120	132

DIFFUSION RUN DN82a

250 hours at $115.0 \pm 0.05^\circ\text{C}$.

Section	R_g	Log A	x	\bar{x}^2
1	-	-	20	1.00
2	68.3	2.658	25	5.06
3	50.4	2.527	30	7.56
4	65.9	2.643	35	10.6
5	72.1	2.682	40	14.1
6	66.1	2.644	45	18.1
7	70.3	2.671	50	22.6
8	92.2	2.489	60	30.2
9	29.8	1.598	70	42.3
10	41.6	2.142	80	56.3
11	31.3	2.020	90	72.2
12	15.2	1.705	100	90.1
13	9.10	1.482	110	110
14	4.30	1.156	120	132
15	2.10	0.846	130	196

DIFFUSION RUN DR82b

Section	R_B	Log A	x	\bar{x}^2
1	-	-	10	0.25
2	131	2.538	15	1.56
3	139	2.563	20	3.06
4	178	2.672	25	5.06
5	427	2.750	35	9.00
6	407	2.729	45	16.0
7	260	2.535	55	25.0
8	261.7	2.537	65	36.0
9	151	2.288	75	49.0
10	99.7	2.114	85	64.0
11	97.2	2.107	95	81.0
12	50.7	1.825	105	100
13	43.1	1.755	115	121
14	16.1	1.326	125	144
15	15.0	1.295	135	169
16	11.0	1.160	145	196
17	5.30	0.844	155	225
18	5.60	0.868	165	256
20	3.20	0.624	185	324
23	0.6	-0.1	215	441

DIFFUSION RUN DR84a
222 hours at 115.0°C.

Section	R_s	Log A	x	\bar{x}^2
1	388.5	2.290	10	0.25
2	86.0	1.955	15	1.56
3	107.0	2.029	20	3.06
4	71.8	1.857	25	5.06
5	33.2	1.522	30	7.56
6	33.3	1.523	35	10.6
7	29.8	1.475	40	14.1
8	18.8	1.274	45	18.1
9	11.4	1.057	50	22.6
10	2.50	0.398	55	27.6
11	3.10	0.19	65	36.0
12	3.1	0.19	75	49.0
13	0.8	-0.4	85	64.0
14	0	-	95	81.0

DIFFUSION RUN DR84b

Section	R_s	Log A	x	\bar{x}^2
1	413.3	2.616	5	0.0625
2	117.3	2.070	10	0.56
3	83.5	1.922	15	1.56
4	131.9	2.012	20	3.06
5	57.4	1.759	25	5.06
6	52.0	1.716	30	7.56
7	60.0	1.478	40	12.2
8	23.0	1.061	50	20.3
9	4.20	0.322	60	30.2
10	1.20	0.08	70	42.3

DIFFUSION RUN DR84g

Section	R_g	Log A	x	\bar{x}^2
1	147	2.168	10	0.25
2	90.6	1.958	20	2.25
3	70.8	1.850	30	6.25
4	40.4	1.606	40	12.2
5	15.8	1.199	50	20.3
6	7.70	0.887	60	30.2
7	2.30	0.362	70	42.3
8	0.5	-0.30	80	56.3

DIFFUSION RUN DR85a

255 hours at 103.0°C.

Section	R_g	Log A	x	\bar{x}^2
1	282.6	2.157	10	0.25
2	143.1	2.155	15	1.56
3	88.9	1.950	20	3.06
4	69.6	1.843	25	5.06
5	55.1	1.742	30	7.56
6	15.4	1.188	35	10.6
7	6.5	0.813	40	14.1
8	5.20	0.716	45	18.1
9	3.00	0.477	50	22.6
10	1.40	-0.154	60	30.2
11	0.8	-0.4	70	42.3

DIFFUSION RUN DR85b

Section	R_s	Log A	x	\bar{x}^2
1	577	2.284	15	0.56
2	68.2	1.854	20	3.06
3	46.2	1.665	25	5.06
4	32.2	1.508	30	7.56
5	38.8	1.589	35	10.6
6	14.1	1.149	40	14.1
7	6.90	0.839	45	18.1
8	3.30	0.519	50	22.6
9	1.20	0.079	55	27.6
10	0.3	-	60	33.0

DIFFUSION RUN DR85c

Section	R_s	Log A	x	\bar{x}^2
1	417	2.018	20	1.00
2	72.5	1.861	25	5.06
3	42.3	1.627	30	7.56
4	31.2	1.494	35	10.6
5	17.0	1.231	40	14.1
6	20.3	1.308	45	18.1
7	6.60	0.820	50	22.6
8	5.70	0.756	55	27.6
9	-	-	60	33.0
10	1.00	0.00	65	39.1
11	0.4	-0.22	70	45.6

DIFFUSION RUN DR66

60.0 hours at 96.1 ± 0.05°C.

Section	R _B	Log A	\bar{x}
1	617	2.791	5
2	172	2.236	15
3	121.7	2.085	25
4	88.1	1.946	35
5	49.5	1.695	45
6	34.2	1.534	55
7	20.7	1.316	65
8	27.4	1.136	80
9	18.0	0.955	100
10	16.8	0.925	120
11	6.6	0.519	140
12	9.1	0.658	160
13	6.8	0.532	180

EXCHANGE RUN ER1

Temperature $22.0 \pm 1.0^{\circ}\text{C}$.Wt. Tritiated Benzole
Acid 6.40 mgm.

Sample	$t^{\frac{1}{2}}$ mins	Count Rate R_g cps/ml.
1	3.16	0.2
2	4.00	1.0
3	4.80	1.3
4	5.38	1.9
5	6.25	1.8
6	6.70	2.9
7	7.42	3.1
8	7.93	3.4
9	8.65	4.3
10	9.22	5.56
11	9.74	6.6
12	10.25	6.35
13	10.72	7.7
14	11.19	7.65
15	12.64	9.3
16	13.22	10.6
17	14.32	11.86
18	16.50	10.9
19	17.74	13.6
20	18.48	14.9
21	19.75	16.1
22	20.65	18.0
23	24.3	19.3
24	39.0	34.6

EXCHANGE RUN ER2

Temperature $53.0 \pm 1.0^{\circ}\text{C}$.

Wt. T.D.A. 5.50 mgm.

Sample	$t^{\frac{1}{2}}$ mins	Count Rate R_g cps/ml.
1	1.41	3.0
2	2.83	3.5
3	3.61	4.1
4	4.56	6.75
5	5.48	7.5
6	6.70	10.9
7	7.87	12.9
8	8.71	13.6
9	10.25	18.4
10	11.40	18.8
11	12.12	25.2
12	12.85	23.6

EXCHANGE RUN ER3

Temperature 66.0 \pm 0.5°C.

Wt. T.B.A. 5.00 mgm.

Sample	$t^{\frac{1}{2}}$ mins	Count Rate R_g cps/ml.
1	1.41	0.8
2	2.24	2.0
3	3.16	5.3
4	3.87	7.1
5	4.47	8.6
6	5.00	10.3
7	5.47	11.5
8	6.32	14.05
9	7.06	19.1
10	7.75	20.6
11	8.36	26.4
12	8.94	29.5
13	9.48	25.3

EXCHANGE RUN ER4

Temperature 38.0 \pm 0.5°C.

Wt. T.B.A. 4.90 mgm.

Sample	$t^{\frac{1}{2}}$ mins	Count Rate R_g cps/ml.
1	2.235	1.5
2	3.16	2.0
3	3.87	2.7
4	4.46	3.1
5	5.10	3.3
6	5.91	4.2
7	6.70	5.2
8	8.06	5.9
9	8.89	8.2
10	10.00	9.7
11	10.96	11.4
12	11.61	11.6
13	12.45	14.4
14	14.55	15.6
15	15.17	14.7
16	17.60	19.2
17	21.10	22.7

EXCHANGE RUN ER5

Temperature $38.0 \pm 0.05^\circ\text{C}$.Wt. C^{14} B.A. 1.35 mgm.No measurable exchange
during a 7 hour period.

EXCHANGE RUN ER6

Temperature $71.0 \pm 0.05^\circ\text{C}$.

Wt. T.B.A. 5.50 mgm.

Sample	$t^{\frac{1}{2}}$ mins	Count Rate R_s cps/ml.
1	2.235	4.4
2	3.16	8.9
3	3.875	17.0
4	4.46	16.0
5	5.00	18.1
6	5.46	24.0
7	5.91	26.0
8	6.31	28.2
9	6.70	33.0
10	7.41	33.7
11	8.05	34.7
12	8.65	45.8

EXCHANGE RUN ER7

Temperature $71.0 \pm 0.5^\circ\text{C}$.Wt. $\text{C}^{14}\text{B.A.}$ 1.90 mgm.

Sample	$t^{\frac{1}{2}}$ mins	Count Rate R_s cps/ml.
1	5	10.0
2	10	8.0
3	15	7.5
4	20	7.0
5	25	7.2
6	30	6.0
7	40	6.4

EXCHANGE RUN ER8

Temperature $76.5 \pm 0.5^\circ\text{C}$.

Wt. T.B.A. 5.70 mgm.

Sample	$t^{\frac{1}{2}}$ mins	Count Rate R_s cps/ml.
1	1.41	1.7
2	2.24	4.6
3	3.16	17.0
4	3.87	24.4
5	4.46	-
6	5.00	43.2
7	5.46	42.4
8	5.91	49.7
9	6.32	45.7
10	6.70	54.7
11	7.06	63.4
12	7.41	59.7
13	7.75	71.9
14	8.06	70.0
15	8.36	66.7
16	8.66	79.9

EXCHANGE RUN ER9

Temperature $43.0 \pm 0.5^\circ\text{C}$.

Wt. T.B.A. 5.05 mgm.

Sample	$t^{\frac{1}{2}}$ mins	Count Rate R_g cps/ml.
1	2.24	2.7
2	3.16	3.5
3	3.87	5.5
4	4.47	4.6
5	5.00	5.9
6	5.48	6.7
7	6.32	7.6
8	7.40	9.8
9	8.35	11.5
10	9.22	7.7
11	10.0	11.1
12	10.71	14.4
13	11.40	14.8
14	12.07	23.9
15	13.22	25.7
16	13.80	25.7

EXCHANGE RUN ER10

Temperature $60.0 \pm 0.5^\circ\text{C}$.

Wt. T.B.A. 4.90 mgm.

Sample	$t^{\frac{1}{2}}$ mins.	Count Rate R_g cps/ml.
1	2.24	0.6
2	3.16	1.0
3	3.87	4.3
4	5.00	12.6
5	5.47	15.9
6	5.91	13.1
7	6.32	15.5
8	6.70	20.3
9	7.41	16.2
10	8.06	16.9
11	8.94	23.9
12	9.21	22.9
13	9.48	27.0
14	10.00	31.9
15	10.50	31.9

CHAPTER IV

DISCUSSION OF THE RESULTS

IV a. Proton Transfer in Hydrogen Bonded Solids.

i. Previous Work.

Evidence for proton transport in co-operatively hydrogen bonded organic solids has been obtained from

a. Diffusion studies.

b. Conductivity studies.

a. Diffusion studies. There have, until this work, been no direct diffusion measurements in hydrogen bonded organic crystals. The nearest approach has been exchange studies in hydrogen bonded inorganic crystals.

In 1959 Wei and Bernstein²⁸ observed proton diffusion occurring in boehmite, α -alumina monohydrate. They studied the exchange of D_2O^{18} vapour with polycrystalline boehmite from 87-150°C. and found that after an initial surface exchange a diffusion controlled reaction took place between the deuterium and the crystal which had the following Arrhenius dependence.

$$D_{\max} = 5 \times 10^{-9} \exp \left[- \frac{12,900 \pm 800}{RT} \right]$$

where D_{\max} is the highest possible diffusion coefficient as the surface area of the crystals was not accurately known. O^{18} diffusion was found to be very much slower than deuterium indicating that a fast proton mechanism was operating. They also found that proton mobility in bayerite, β - $Al(OH)_3$, was an order of magnitude greater than this.

A similar study was made by Feitknecht et al²⁷ of tritium diffusion from water vapour into $Ni(OH)_2$ and α - $FeOOH$ and their

deuterated analogues and the same diffusion controlled exchange kinetics were obtained as in boehmite and satisfied the following Arrhenius equations.

$$\text{Ni(OH)}_2 \quad D = 2 \times 10^{-7} \quad \exp \left[\frac{-23,000}{RT} \right]$$

$$\text{FeOOH} \quad D = 2 \times 10^{-11} \quad \exp \left[\frac{-16,500}{RT} \right]$$

Several interesting points arise from these studies. Proton diffusion is considerably faster than metal ions at the same low temperature. All these systems have in their structure a co-operative system of hydrogen bonds. All give very small pre-exponential factors, indicating a negative entropy of activation which Bernstein suggests may be a function of a protonic mechanism. The activation energies of these processes are all of the order of the activation energies found in hydrogen bonded solids exhibiting proton conductivity¹⁴ (. . .)

The only co-operatively hydrogen bonded system in which a direct diffusion study has been attempted is ice. The first measurement was made in 1958 by Kuhn and Thurkauf⁷¹ who observed the diffusion rate of deuterium and oxygen-18 in polycrystalline ice and found the same diffusion coefficient for each $1.0 \pm 0.2 \times 10^{-10} \text{ cm}^2 \cdot \text{sec}^{-1}$ indicating that at this temperature diffusion was due to migration of an entire water molecule. This measurement was made at one temperature only and no Arrhenius equation was obtained for the process. It was thought possible, however, that this bulk diffusion could be due to a premelting phenomena

as the measurement was made so near the melting point. This would mask a slower proton conduction mechanism.

During the course of this investigation two other studies were made on ice by Dengel and Riehl⁷³ and Itagaki⁸⁹ in which tritium diffusion was measured in single crystals of ice as a function of temperature and the following Arrhenius equations obtained

$$D = 2 \exp\left[-\frac{13,500}{RT}\right] \quad \text{Dengel and Riehl}$$

$$D = 2.8 \times 10^2 \exp\left[-\frac{15,700}{RT}\right] \quad \text{Itagaki}$$

Riehl has also measured the diffusion of O^{18} in ice and tritium diffusion in ice crystals doped with HF^{90} and found that in all cases the activation energy was the same.

These results appear to confirm that in the case of ice the proton diffusion associated with the measured proton conductivity is masked by a rapid diffusion of neutral water molecules in the lattice. The mechanism of this bulk diffusion process has been examined theoretically and vacancy⁹¹ and interstitial mechanisms^{92,93} proposed. The most likely mechanism is that proposed by Onsager and Runnels⁹³ of a 'free' interstitial mechanism in which a water molecule travels through several interstitial positions before occupying a vacant lattice site. Granicher⁹¹ has suggested, however, that as the activation energy for tritium diffusion agrees with that for D.C. conductivity, hydrogen diffusion may proceed by the same mechanism in both cases.

Conductivity Studies.

Conductivity studies have been made in a large number of organic and inorganic hydrogen bonded solids and mechanisms based on proton migration along co-operative chains of hydrogen bonds have been proposed.

¹⁴ Pollock and Ubbelohde made an interesting study on a series of organic acids, acetylenedicarboxylic acid and its dihydrate, oxalic acid and its dihydrate, benzoic acid and furoic acid, and found that the conductivity increased and activation energy decreased in that order with the hydrates exhibiting greater conductivity than the parent acid. They concluded that the conductivity was protonic and, as the order above was one of decreasing co-operation, that the conductivity depended on the degree of co-operative hydrogen bonding present. They did not, however, verify the nature of the charge carriers and their studies were made on polycrystalline compacts well below the melting point.

The most exhaustive series of conductivity studies in hydrogen bonded solids has been made by Eley and his co-workers¹⁵ on synthetic and naturally occurring solids containing the $-N-H\cdots O=$ hydrogen bond. In all cases a definite conductivity was found in the dry state which in general was found to be electronic in nature with energy gaps determined from the temperature variation of conductance in the region 2-4eV which is of the order of band gap calculated for repeat units of the

type $\text{NH---O} = \text{C}^{13}$ and Eley suggested that these are intrinsic semiconductors due to electron mobility in the CO---NH system. In the case of polyamides,^{9,4} it was observed that at low temperatures the conductivity was low and electronic with a band gap of 2.5eV. At high temperature, however, the conductivity became protonic with conductivities 10^4 times greater than the electronic conductors and a much smaller activation energy of conduction, 1.1-1.3eV was obtained. They concluded that this was due to the rotation of the amide group and that self-ionisation was the rate determining step of the conduction mechanism.

Eley⁵ has also found that the conductivity of these systems can be greatly influenced by adsorbed water¹⁶ and he has shown that in the case of haemoglobin 7% adsorbed water increases the electronic conductivity.¹⁸ It has also been shown that proton conductivity can be obtained on adsorption of water¹⁷ and it has been suggested that the water acts as a plasticiser which facilitates the reorientation of the hydrogen bonded chain.¹⁸

The model substance of a co-operatively hydrogen bonded lattice is ice and a proton conduction mechanism has been proved beyond doubt^{19,20,21} in which the rate determining step appears to be the ionisation of the water molecule. For a static conductivity to be observed in a co-operatively hydrogen bonded solid it is necessary for each hydrogen bonded chain to re-orient to its original state before another charge can pass

along it. In the case of ice neutral orientational defects known as Bjerrum defects⁹⁵ in which one hydrogen bond is doubly occupied and another unoccupied have been proposed to explain this reorientation which must occur in all hydrogen bonded solids which are proton conductors.

The conductivity of another hydrogen bonded crystal, ammonium dihydrogen phosphate has recently been reported by Murphy⁹⁶ in which proton conductivity has been shown to exist and it was proposed that the mechanism was analogous to conduction in ice.

ii Conductivity Results.

The conductivity of benzoic acid was found to be very low. The conductivity of analar benzoic acid compacts was found to obey the following Arrhenius equation in the temperature range 40-100°C.

$$\sigma = 1 \times 10^{-6} \exp \left[\frac{-7,600}{RT} \right]$$

In high purity compacts and single crystals both perpendicular and parallel to the (001) plane the conductivity was not measurable and must be less than $2 \times 10^{-14} \text{ ohm}^{-1} \text{ cm}^{-1}$ within 7°C of the melting point. This agrees with the value recently found by Eley⁹⁷ et al of $1 \times 10^{-15} \text{ ohm}^{-1} \text{ cm}^{-1}$ two degrees below the melting point.

The conductivity of acetic acid perpendicular to the (100) plane was found to vary with the amount of adsorbed water and fell to an unmeasurable value on drying. The bulk conductivity,

therefore, was concluded to be less than 10^{-10} ohm⁻¹cm⁻¹ at 0°C.

The conductivity of oxalic acid dihydrate both as compacts and single crystals gave linear Arrhenius plots having the same activation energy 21-24 K cal/mole but which varied in absolute conductivity by an order of 10^3 .

A comparison of conductivity studies in organic acids is shown in table XVI

TABLE XVI CONDUCTIVITY IN ORGANIC ACIDS.

TYPE	EXAMPLE	EA Kcal/mole	σ (50°C) ohm ⁻¹ cm ⁻¹	REFERENCE
CYCLIC DIMER	BENZOIC ACID			
	compacts	48.9	1.8×10^{-9}	UBBELOHDE ¹⁴
	Analar compacts	7.6	$< 2 \times 10^{-11}$	THIS WORK
	pure compacts	-	$< 2 \times 10^{-14}$	THIS WORK
	single crystal $\perp(001)$	-	$< 2 \times 10^{-14}$	THIS WORK
	" " $\parallel(001)$	-	$< 2 \times 10^{-14}$	THIS WORK
	single crystal	-	1×10^{-15} (at 120°C.)	ELEY ⁹⁷
	FUROIC ACID			
	compact	68.4	1.8×10^{-9}	UBBELOHDE ¹⁴
	PIVALIC ACID	-	5×10^{-13} (at 35°C.)	KONDO AND ODA ⁹⁷
-Bonded chains	OXALIC ACID .2H ₂ O			
	compacts	23.5	2.2×10^{-8}	UBBELOHDE ¹⁴
	compacts	21-24	3.5×10^{-10}	THIS WORK
	single crystal	22.0	1.5×10^{-12}	THIS WORK
	oxalic Acid - compact	40.5	1.1×10^{-9}	UBBELOHDE ¹⁴

TYPE	EXAMPLE	E_A Kcal/mole	σ (50°C) ohm ⁻¹ cm ⁻¹	REFERENCE
ACETYLENE DICARBOXYLIC ACID	compact	12.3	7.1×10^7	UBBELOHDE ¹⁴
	ACETIC ACID			
	Single Crystal <u>1</u> (100)	-	$< 10^{-10}$	THIS WORK

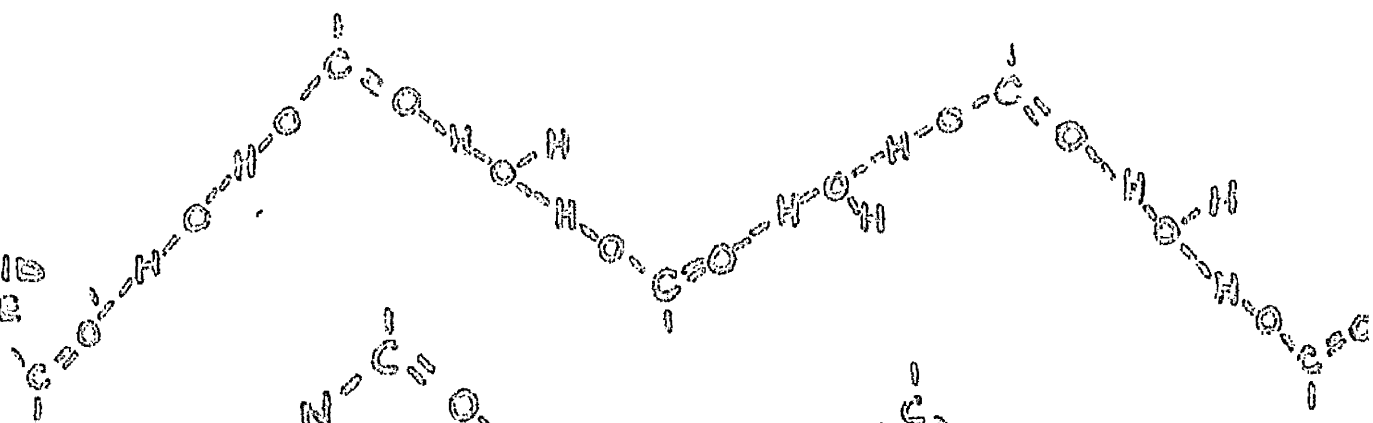
Several conclusions can be drawn from the above table.

1. The conductivity in crystals having cyclic dimers is very much lower than in crystals which have co-operative chains of hydrogen bonds.
2. The conductivity varies considerably with the degree of compaction and much lower conductivities are obtained in single crystals.
3. The effect of water on the crystals is to increase the conductivity.
4. The conductivities are so low in single crystals that the proton diffusion coefficient as calculated from the Nernst - Einstein equation would not be measurable by a tracer diffusion study using a sectioning technique.

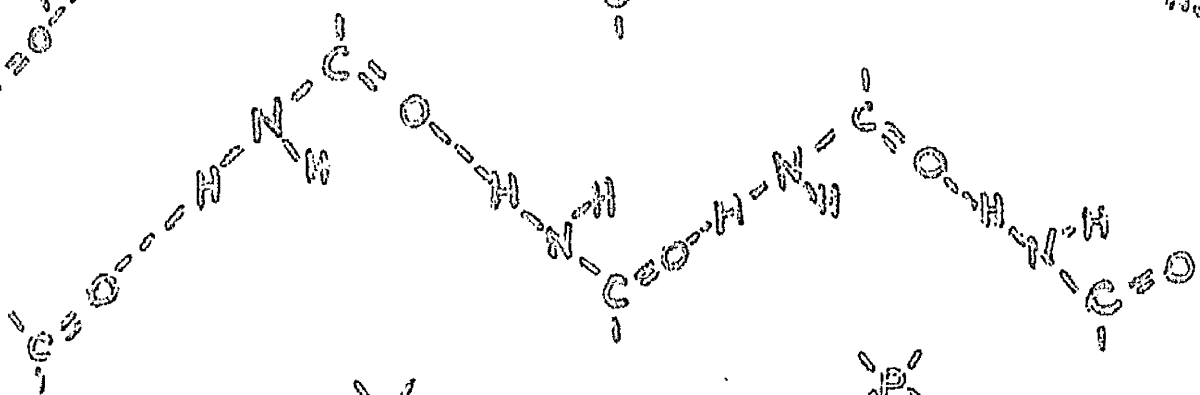
The low conductivity obtained in this work for analar benzoic acid does not compare favourably with Ubbelohde's values. It is possible that his result is due to transient effects which can occur at the low temperature (see e.g. Fig 4, run 1) at which he was working, 20-50°C., and to the fact that he was working near the insulation limit of his cell, tufool, 10^{10} ohms cm.

1. The first part of the document is a list of names and their corresponding addresses. The names are listed in a column on the left, and the addresses are listed in a column on the right. The names are: John Doe, Jane Smith, and Bob Johnson. The addresses are: 123 Main St, 456 Elm St, and 789 Oak St.

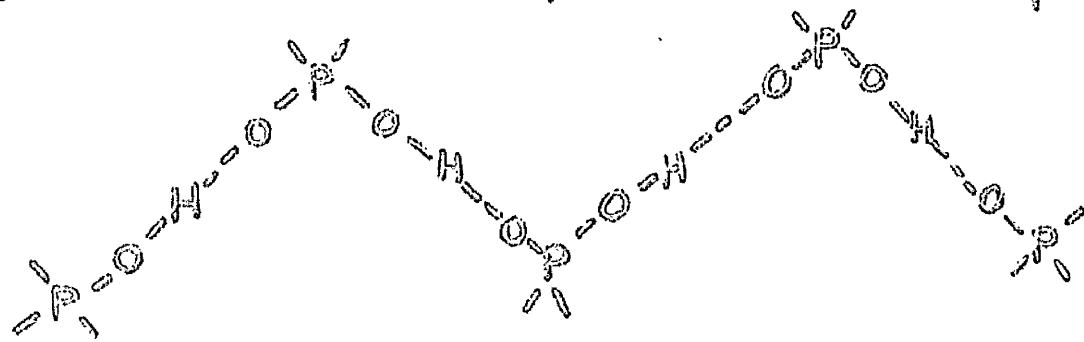
OXALIC ACID
DIHYDRATE



POLYAMIDES



AMMONIUM
DIHYDROGEN
PHOSPHATE



ICE

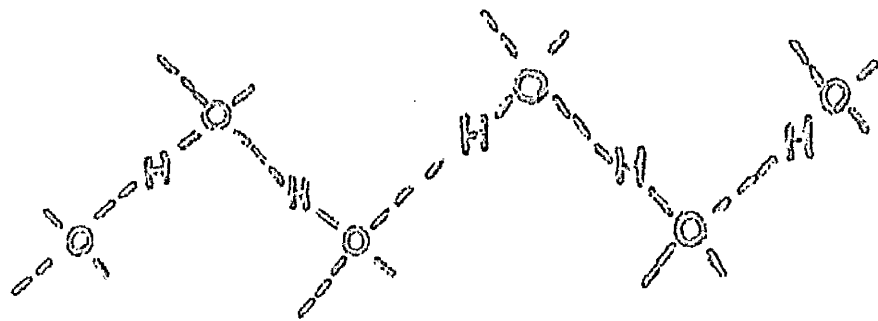


FIG. 44. SCHEMATIC VIEW OF CO-OPERATIVE HYDROGEN BONDED CHAINS IN CRYSTALS.

The conductivity found in this study is believed due to the presence of adsorbed moisture in the analar acid as no attempt was made to dry it. It may be significant that the activation energy of this process 7.6Kcals/mole is approximately the same as the activation energy of mobility of water diffusing in benzoic acid single crystals (see p 140).

The conductivity of oxalic acid dihydrate is interesting in that the same activation energy is always obtained. This result can be compared with conductivity studies in other hydrogen bonded systems in which proton conduction has been found.

TABLE XVII

CRYSTAL	σ $\text{ohm}^{-1}\text{cm}^{-1}$	E_A Kcal/mole	σ (50°C) $\text{ohm}^{-1}\text{cm}^{-1}$	W_D Kcal/mole	W_A Kcal/mole	REF
OXALIC ACID 2H ₂ O	6.3×10^2	22	1.5×10^{12}	(20)	(12)	THIS WORK
POLYAMIDES	2×10^4	25	4×10^{13} *	(30)	(10)	ELEY ⁹⁴
AMMONIUM DIHYDROGEN PHOSPHATE	6.5×10^3	20.4	1×10^{-10}	19.8	10.5	MURPHY ⁹⁶
ICE (1)	1.2	11.0		22	0	EIGEN ²⁶
(2)	2.1×10^2	14.0	1×10^{-7} *	22	3	GRANICHER ⁹¹
					3.9	SPERNOL ⁹⁹

*EXTRAPOLATED VALUES.

A schematic view of the hydrogen bonded chains occurring in the above crystals is shown in fig.44. Only in ice are adjacent hydrogen bonds connected through the same atom.

Murphy has analysed his results for ammonium dihydrogen phosphate⁹⁶ and has explained them in terms of ionic conduction in

23

solid dielectrics where the activation energy E_A consists of two terms.

$$E_A = \frac{1}{2} \cdot W_D + W_A$$

where W_D is the energy for dissociation into ion pairs and W_A the activation energy of mobility. Murphy obtained W_A for ammonium dihydrogen phosphate by studying doped crystals and obtained a value of 10.5 Kcal/mole hence $W_D = 19.8$ Kcals/mole. A similar value has been obtained for ice, $W_D = 22$ Kcal/mole²⁴ hence it does not seem unreasonable to accord a similar value to oxalic acid dihydrate which has the same O-H --- O bond. In the case of polyamides a higher value has been proposed $W_D = 30$ Kcals/mole.⁹⁴ A large variation exists between the activation energy of ice and the other crystals which is due to the lower activation energy of migration in ice. This is due to the hydrogen bonds in ice being in juxtaposition whereas in the other crystals they are separated by a three atom system which subsequently requires a much greater energy for re-orientation of the chains into a suitable orientation for conduction.

An interesting observation was made by Murphy⁹⁶ who found that after overheating the crystals of ammonium dihydrogen phosphate an increase in the conductivity of pure crystals by a factor of 100 could be obtained which gave the same activation energy. This could only be explained in terms of structural change which increased the equilibrium concentration of intrinsic ions and it was suggested that internal surfaces were formed. A similar explanation may hold for the variation observed in oxalic acid dihydrate.

IV b. Diffusion in Benzoic Acid.

1. Summary of Results.

Molecular self-diffusion was observed in benzoic acid single crystals by the sectioning technique using C¹⁴ labelled benzoic acid as tracer. Two diffusion mechanisms were observed, a fast process and a slow process. The slow process was believed due to bulk diffusion and was found to satisfy the following Arrhenius equation perpendicular to the (001) plane.

$$D = \left(1.8 \begin{matrix} +7.6 \\ -1.79 \end{matrix} \times 10^2 \right) \times 10^{12} \cdot \exp \left[- \frac{44,000 \pm 4,400}{RT} \right] \dots (6)$$

The 'fast' process varied with the crystal used and is believed due to non-equilibrium structural defects in the crystals.

Tritium diffusion in single crystals of benzoic acid \perp (001) was found to be much greater than C¹⁴ diffusion and ^bvary with the water vapour content of the diffusion cell. Under dry conditions a lower limit for diffusion was observed which obeyed the following Arrhenius equation.

$$D = 0.5 \begin{matrix} +2 \\ -0.4 \end{matrix} \cdot \exp \left[- \frac{20,000 \pm 1,300}{RT} \right] \dots (7)$$

Within experimental error tritium was also found to diffuse at the same rate in single crystals of benzoic acid - d₁.

Tritium diffusion in benzoic acid single crystals doped with p-terphenyl under dry conditions were found to obey the following Arrhenius equation

$$D = \left(4.7 \begin{matrix} +75 \\ -4.4 \end{matrix} \right) \times 10^8 \cdot \exp \left[- \frac{7,450 \pm 2,200}{RT} \right] \dots (8)$$

Tritium and C^{14} diffusion in polycrystalline benzoic acid compacts were found to be the same within experimental accuracy and satisfied the following Arrhenius equation

$$D = \left(1.0 \begin{matrix} +13 \\ -0.93 \end{matrix} \right) \times 10^{11} \cdot \exp \left[- \frac{31,800 \pm 2,00}{RT} \right] \quad \text{--- (9)}$$

An exchange reaction was observed between polycrystalline tritiated benzoic acid and inactive water vapour which had diffusion controlled kinetics. The rate controlling process was found to obey the Arrhenius equation

$$D = D_0 \cdot \exp \left[- \frac{14,000 \pm 700}{RT} \right] \quad \text{--- (10)}$$

in the temperature range 20-700°C.

b. 1. Molecular Diffusion.

Diffusion of C^{14} labelled benzoic acid was much slower than that of tritium and appeared to have two distinct diffusion mechanisms operating simultaneously whereas with tritium only one diffusion process was observed. Similar diffusion profiles have been obtained in other diffusion studies in crystalline solids, ^{74,100,101} and it has been concluded that the slow process is due to bulk or lattice diffusion and the 'fast' process due to structural diffusion. This latter process may vary considerably in rate as the type of structural defect present in any crystal will depend on the impurities present and the non equilibrium defects introduced during crystal growth. The large variation found in the 'fast' diffusion process agrees with ^{this} reasoning.

The bulk diffusion process is very slow compared to previous studies on molecular solids ^{71,100} in which bulk diffusion coefficients at the melting point were found to be approximately $1 \times 10^{-10} \text{ cm}^2 \text{ sec}^{-1}$ compared with $2.5 \times 10^{-12} \text{ cm}^2 \text{ sec}^{-1}$ in this study. Several studies have recently been made on anthracene ^{101,102,103} and naphthalene ¹⁰³ and much lower values have been obtained which are of the order found in this study.

A comparison can be made between the Arrhenius diffusion parameter in benzoic acid and other molecular crystals and these are shown in table XVIII

TABLE VIII SELF DIFFUSION IN MOLECULAR CRYSTALS

<u>PLASTIC CRYSTALS</u>	D_0 $\text{cm}^2\text{sec}^{-1}$	EA Kcal/mole	ΔH_s Kcal/mole	Reference
Cyclohexane	3.9×10^6	16.3	8.5	Hood & Sherwood. ¹⁰⁴
Pivalic Acid	2.25	10.0	10.0	Hood. ⁷⁵
Argon	3.5×10^2	4.15	1.85	Berne Et Al. ¹⁰⁵
<u>ORGANIC CRYSTALS</u>				
Anthracene I	6.5×10^{10}	42.4	23.3	Sherwood & Thomson. ¹⁰⁰
II	5×10^{16}	60		White. ¹⁰³
III	2	22		Labes. ¹⁰²
Naphthalene	2.5×10^{15}	42.7	17	White. ⁶⁶
Benzoic Acid	1.8×10^{12}	44.0	21.8	This Work.
<u>INORGANIC CRYSTALS</u>				
α -Phosphorus a	1×10^3	9.4	14.0	Nachtrieb & Handler. ¹⁰⁶
b	2×10^{46}	80.6		
Sulphur I a	8×10^{-2}	3.1		Cuddeback & Drickamer. ¹⁰⁷
b	1.8×10^{36}	78		
II	2.8×10^{13}	46.8		Hauffe. ¹⁰⁸
Hydrogen	10^{-7}	0.79	0.46	Cremer. ¹⁰⁹

From this table it can be seen that, in general, diffusion is characterized by large pre-exponential factors and activation energies which are of the order of twice the latent heat of sublimation, ΔH_s . In the case of organic crystals there are two large discrepancies in this statement, pivalic acid and anthracene III. In pivalic acid, however, it is believed that molecular self diffusion was not being measured (p143). In anthracene III it is believed by the author that this result

was due to the quality of the crystals used as the diffusion profiles obtained were similar to those found in polycrystalline naphthalene.¹⁰²

Large pre-exponential factors are associated with large entropies of activation for the diffusion process which in turn is indicative of a co-operative phenomena in which more than one molecule is involved in the diffusion process. From the atomic theory of diffusion the pre-exponential factor, D_0 , can be expressed as¹¹⁰

$$D_0 = \gamma a^2 \nu \exp \frac{\Delta S^{\ddagger}}{R} \quad \dots \quad (11)$$

where γ is a constant depending on the diffusion mechanism, a is the jump distance in the atomic (or molecular) process, ν is a frequency which is approximately the mean vibrational frequency of an atom about its equilibrium site, R is the gas constant and ΔS^{\ddagger} is activation entropy for the diffusion process.

A value of ΔS^{\ddagger} can, therefore, be calculated for benzoic acid, if γ , a and ν are known. γ is a small constant not far from unity. a the jump distance in the benzoic acid lattice down the (001) plane is 5.47 \AA , ν is normally taken as the Debye frequency of the lattice, ν_m which can be obtained from the Debye temperature θ_D , from the equation

$$\nu_m = \frac{3}{4} \frac{k \theta_D}{h}$$

The Debye frequency of benzoic acid is 116°K ¹¹¹

$$\therefore \nu_m = \frac{3 \times 1.38 \times 10^{-16} \times 116}{4 \times 6.62 \times 10^{-27}} = 1.82 \times 10^{12} \text{ sec}^{-1}$$

Substituting these values in equation (11) and using the value of D_0 in equation (6)

$$\begin{aligned} \text{EXP } \frac{\Delta S^*}{R} &= \frac{1.8 \times 10^{12}}{1.82 \times 10^{12} \times (5.47 \times 10^8)^2} \\ &= 3.3 \times 10^{14} \\ \therefore \Delta S^* &= 2.303 \times 2 \times 14.52 \\ &= 67 \text{ e.u.} \end{aligned}$$

This large activation entropy is larger than expected from a simple vacancy mechanism if compared with systems in which such mechanism have been well established¹¹² and indicates a mechanism in which several molecules are involved.

The theoretical energy of formation of a vacancy in a molecular solid is approximately equal to the latent heat of sublimation.¹¹³ Experimental evidence has been obtained from specific heat measurements in solid argon which indicate that $\Delta H_v = 1.1 - 1.4 \times H_g$.^{114,115} This suggests that a value of approximately twice the latent heat of sublimation, ΔH_g , is not an unreasonable value for a vacancy process as $E_A = \Delta H_v + \Delta H_m$, where ΔH_m is the enthalpy of migration. This value is also of the order found in metal vacancy diffusion studies. In metals, however, there is little relaxation of the surrounding lattice on vacancy formation due to their electronic structure whereas in molecular crystals due to their weak Van der Waals binding a relaxation of up to 50% has been suggested thus giving a small region around the vacancy in which the molecules are mobile and tend in the

limit towards liquid like behaviour. This type of defect would be expected to have a large entropy change associated with the relaxation of the surrounding molecules. Migration could then take place by a molecule melting into this cluster as another freezes out with the lower limit of the activation energy of migration being of the order of the latent heat of fusion, L_f .

This mechanism has been proposed by Nachtrieb and Handler ¹¹⁶ to explain self diffusion in alkali metals and by Hood and Sherwood ¹¹⁵ for self diffusion in cyclohexane. It was suggested that the number of molecules associated with each relaxed vacancy or 'relaxion', n , was given by the equation

$$\Delta S_v = \frac{n L_f}{RT_m} \quad \text{where } T_m \text{ is the melting point}$$

i.e.

ΔS_v the entropy of formation of a vacancy

i.e.

$$\Delta S_v = n \Delta S_f$$

ΔS_f entropy of fusion.

The overall activation entropy ΔS^* is given by

$$\Delta S^* = \Delta S_v + \Delta S_m \quad \text{where } \Delta S_m \text{ is the entropy of migration}$$

hence ΔS_m must be known before ΔS_v can be calculated.

From the preceding theory however ΔS_m should be very small

compared to ΔS_v $\therefore \Delta S^* \approx \Delta S_v$

$$\therefore n = \frac{\Delta S^*}{\Delta S_f}$$

In the case of benzoic acid the entropy of fusion, ΔS_f , is 16.4 eu. therefore in this case $n \approx 6-7$ molecules. This number

is small compared with cyclohexane where $n = 20$ and it seems unlikely that a liquid like region exists in benzoic acid. Similar values of n were obtained for anthracene ($n = 5-6$)¹⁰⁰ and naphthalene ($n = 5-6$)¹⁰³. The minimum activation energy predicted by this theory is

$$E_A = \Delta H_s + I_f$$

which for benzoic acid = $21.85^{107} + 4.15 = 27.0$ Kcals/mole

The observed activation energy, however, is 44.0 Kcals/mole which suggests that in such a small 'relaxion' there is no liquid like behaviour and that a considerable activation energy of migration is still required. The diffusion mechanism for molecular diffusion in benzoic acid, therefore, appears to be one of vacancy diffusion through relaxed vacancies.

Grain Boundary Diffusion.

Both tritium and C^{14} diffusion in polycrystalline benzoic acid were found to give approximately the same Arrhenius equations when analysed for the Whipple solution to the grain boundary problem by the method of LeClair (p. 104). This solution was much superior to the Fisher solution and lowered the C^{14} diffusion activation energy by 10%

The fact that the same diffusion parameters were obtained means that the same mechanism is responsible for both phenomena. The activation energy of grain boundary diffusion is normally less than that for bulk diffusion hence from the tritium diffusion studies in single crystals of benzoic acid the activation

energy should be less than 20 Kcal/mole. As it is very much greater this indicates that same mechanism does not operate under grain boundary diffusion conditions and hence it is concluded that both isotopes migrate by molecular diffusion.

A comparison with other systems in which bulk and grain boundary diffusion have been measured is shown below.

TABLE XIX
MOLECULE

MOLECULE	$E_{A L}$ BULK KCal/mole	$E_{A B}$ G. B. KCal/mole	$\frac{E_{A B}}{E_{A L}}$	REFERENCE
Ag	45	21.5	0.48	86
Zn	23	14	0.61	86
Cd	18.5	13	0.71	86
Fe	64	40	0.63	86
Benzoic Acid	44.0	31.8	0.72	THIS WORK
Naphthalene	42.7	29.6	0.69	103

From these results it appears that molecular diffusion has characteristics similar to metal crystals and suggests that a relaxed vacancy diffusion process is not unreasonable in these molecular crystals.

It is interesting to note that the activation energy of the grain boundary diffusion process, 31.8 Kcal/mole, approximates to the value expected from the liquid like 'relaxion' theory predicted for bulk diffusion where the minimum activation energy predicted was 27 Kcal/mole. This suggests that in non plastic crystals this theory may find application in the more highly disordered regions in grain boundaries.

iii Tritium Diffusion in Benzoic Acid Single Crystals.

In the initial tritium and C^{14} diffusion studies tritium was found to diffuse faster than C^{14} by a factor of 100 and it was thought that this was due to a proton transfer mechanism. It was soon realised, however, that this was impossible as the corresponding conductivity was found to be less than $2 \times 10^{14} \text{ ohm}^{-1} \text{ cm}^{-1}$ a few degrees below the melting point. If this were due to proton conduction the corresponding proton diffusion coefficient obtained by applying the Nernst-Einstein equation is $< 10^{-21} \text{ cm}^2 \text{ sec}^{-1}$. As the tritium diffusion coefficients obtained were of the order of $10^{-11} \text{ cm}^2 \text{ sec}^{-1}$ proton conductivity in this system is negligible and another diffusion mechanism must be occurring.

There appear to be only two possible diffusion mechanisms.

- 1) The hydrogen diffuses by itself by a neutral switching mechanism. This could involve breaking the four hydrogen bonds of two cyclic dimers, reorienting two benzoic acid molecules, reformation of a new dimer and translation of the hydrogen across the hydrogen bond. The activation energy necessary for such a process, however, may be prohibitively large.
- 2) Diffusion of an impurity molecule in the lattice.

Several pieces of experimental evidence were obtained from which a possible mechanism was deduced.

The tritium diffusion coefficient was found to vary with the

water content in the diffusion cell. A lower limit to the diffusion coefficient was obtained which remained unaltered on drying the cells prior to the diffusion anneal. When the diffusion cell contained approximately a constant water vapour content the tritium diffusion was found to obey an Arrhenius equation having the same activation energy as diffusion under dry conditions. These facts indicated that tritium diffuses by an impurity mechanism which may be diffusion of water molecules in the benzoic acid lattice.

Tritium diffusion was found to have approximately the same diffusion coefficient in deuterobenzoic acid and normal benzoic acid when carried out in the same diffusion cell. If the diffusion were due to a neutral diffusion of hydrogen as suggested in 1) above then a large isotope effect would be expected which could range from 1.41 according to classical kinetic theory to a maximum of 3.3 from statistical rate theory according to Bigeleisen.⁽¹⁸⁾ The fact that this was not observed indicates that the hydrogen is diffusing as part of some larger species which may be a water molecule.

From the grain boundary diffusion studies in polycrystalline benzoic acid it was found that tritium and C^{14} diffused at the same rate. This shows that under these conditions tritium diffuses with the bulk molecule, a further indication that in the single crystals an impurity mechanism is operating which is swamped by the increased bulk diffusion in grain boundaries.

The rapid exchange reaction found between tritiated benzoic acid and inactive water vapour shows that in the diffusion anneal cell in the temperature range used, 80-115°C, equilibrium between THO and tritiated benzoic acid will be rapidly attained. This indicated that diffusion of tritiated water in benzoic acid may occur under the conditions used.

From the above information it was concluded that under the experimental conditions used tritium diffusion in benzoic acid occurs by diffusion of water molecules through the crystal lattice and that the lower limit of the diffusion coefficient found was due to water trapped in the crystal during growth.

There are two mechanisms by which this impurity diffusion can occur, either by an interstitial or vacancy mechanism.

If water diffuses through vacancies in the benzoic acid lattice then the activation energy of the process $E_A = \Delta H_V + \Delta H_M$. From the experimental studies on argon it has been shown that $\Delta H_V = 1.1 - 1.4 \times \Delta H_B$ ^{114, 115}. Hence for benzoic acid $\Delta H_V = 24-31$ Kcal/mole as $\Delta H_B = 21.8$ Kcal/mole.¹¹⁷ The energy of migration, ΔH_M , of a water molecule will be small but nevertheless it appears that the energy required for such a mechanism is much larger than that found experimentally, 20 Kcal/mole. Hence this suggests that an interstitial diffusion mechanism is more likely.

Evidence for an interstitial mechanism was obtained from the tritium diffusion studies in p-terphenyl doped crystals under 'dry' conditions in which a much lower activation energy was

obtained, 7.5 Kcal/mole. p-terphenyl was not expected to introduce vacancies in the lattice but due to it being smaller than the benzoic acid it was thought that it could give rise to interstitial holes through which water molecules could diffuse. If this can be regarded as similar to the case of e.g. NaCl doped with CdCl_2 in which a non equilibrium vacancy concentration is introduced, then an extrinsic diffusion may be observed with $E_A = H_M$. If this analogy is valid then ΔH_M for water diffusion in benzoic acid = 7.5 Kcal/mole $\therefore \Delta H_1 = 20 - 7.5 = 12.5$ Kcal/mole where ΔH_1 is the energy required to form the interstitial hole. Estimates of the entropies of formation and migration may also be calculated using equation (11) for D_0 .

For tritium diffusion, line B fig.27 the activation entropy ΔS^* for this mechanism can be calculated if the same values of γ , α and ν are assumed. ΔS^* is not, however, markedly dependent on these values and the approximate value is

$$0.5 = (5.47 \times 10^{-8})^2 \times 1.82 \times 10^{12} \exp \frac{\Delta S^*}{R}$$

$$\therefore \Delta S^* = 9.0 \text{ e.u.}$$

This value is much lower than that for bulk diffusion and is not unreasonable for an interstitial mechanism.

For the tritium diffusion in the p-terphenyl doped crystals $\Delta S^* = -23.3$ e.u. According to the above reasoning this should represent, ΔS_M .

This large negative value was unexpected but may be quite genuine as other diffusion studies of small molecules in crystals

of larger molecules have yielded negative entropies of activation
 e.g. H_2/Ni , $\Delta S^* = -5.3$ e.u.; $NH_3/Analcite$, -4.85 e.u.; and
 calculated values of ΔS_m for diffusion of H_2 and argon through
 polyvinyl acetate were -2.2 and -7.8 e.u. respectively.

The entropy of formation of the defect, ΔS_1 , therefore is
 given by

$$\begin{aligned} \Delta S_1 &= \Delta S_{\text{pure}}^* - \Delta S_{\text{doped}}^* \\ &= 9.0 - (-23.3) \\ &= 32.3 \text{ e.u.} \end{aligned}$$

Again this is reasonable value being about half the activation
 entropy for bulk diffusion.

Another factor which indicated interstitial diffusion was the
 variation of tritium diffusion with water content in the cell.
 This phenomena was not recognised at the time and no quantitative
 data is available, hence only a qualitative discussion can be made.

Concentration dependent diffusion has been observed for
 vapours diffusing in polymers but it was thought that a more
 comparable system was the diffusion of Zn in ZnO which has been
 observed by Secco and Moore to vary according to the equation
 $D = A p_{Zn}^{0.65}$ where A is a temp. dependent constant and p_{Zn} is the
 pressure of Zn vapour above the crystal. This was similar to
 the relation expected for interstitial diffusion of Zn and the
 diffusion coefficient could be expressed as

$$D = p_{Zn}^{0.5} \cdot \exp\left[-\frac{\Delta G_0}{RT}\right] \cdot \frac{kT}{h} d^2 \cdot \exp\left[-\frac{\Delta G_1}{RT}\right]$$

where ΔG_0 is the energy of formation of the interstitial Zn
 transition, ΔG_1 the energy of formation of the interstitial Zn

defect, and d , the atomic jump distance. Hence under conditions of constant pressure linear Arrhenius plots would be expected giving a constant activation energy. A similar effect has also been observed in diffusion of cobalt in CoO as a function of oxygen pressure but in this case the exponent of the pressure was found to vary slightly with temperature.¹²⁴ The variation of tritium diffusion with water vapour appears to fit a similar type of mechanism.

In this case there are two activation free energies to be explained ΔG_0 and ΔG_1 . From the above discussion ΔG_1 or rather $\Delta H_1 = E_A = 20.0$ Kcal/mole for the intrinsic diffusion process, therefore, an estimate of $\Delta H_0 (= \Delta G_0 + T\Delta S_0)$ the enthalpy of formation of the defect which in this case is presumed to be a water molecule on an interstitial defect site can be obtained from the activation energy of the diffusion process under a constant water vapour content, i.e. figure 27 line A.

$$\begin{aligned} \therefore \Delta H_0 &= E_{A \text{ line A}} - \Delta H_1 \\ &= 21.2 \pm 2 - 20.0 \pm 1.2 \\ &= 1.2 \pm 3.2 \text{ Kcal/mole.} \end{aligned}$$

i.e. the enthalpy of formation of the defect is very small. A rough calculation shows this to be true. The processes involved in making this defect are a) the creation of an interstitial hole, an endothermic process, for which $\Delta H_v = 12.5$ Kcal/mole

and b) removal of a water molecule from the vapour and replacing it in this interstitial position, an exothermic process which will be of the order of the latent heat of condensation of water, L_c , ~ 10 Kcal/mole. The energy of formation of the defect ΔH_0 , therefore, is $12.5 - 10 = 2.5$ Kcal/mole, in approximate agreement with the value found experimentally. It is believed that the evidence given above is conclusive proof of an interstitial migration of water in benzoic acid crystals.

A comparison can be made with other systems in which tritium diffusion has been measured by a sectioning technique and are shown below.

TABLE XX

MOLECULE	E_A Kcal/mole	D_0 $\text{cm}^2\text{sec}^{-1}$	ΔH_s Kcal/mole	$\frac{E_A}{\Delta H_s}$	ΔS^\ddagger	Ref.
BENZOIC ACID	20.0	0.5	21.8	0.92	9.0	THIS WORK
PIVALIC ACID	10.0	2.25	10.0	1.00	12.3	75
ICE I	13.5	2.0	11.3	1.19	15	73
II	15.7	2.8×10^2		1.39		89

In all three crystals a close correlation exists between the parameters of the diffusion equation and it is possible that the same diffusion mechanism is operating.

In the pivalic acid diffusion study the acidic hydrogen was tritium labelled. It was believed that bulk diffusion was being measured as the acid had been shown to have a very low conductivity in the solid and thus the tritium would remain firmly bound to the bulk molecule. The result obtained, however, did not agree with

other measurements on plastic crystals (see table XV(1)). A possible explanation is to be found in the purity of the crystals used which were known to have 0.04 mole % impurity, probably water which is known to be very difficult to remove.⁹⁸ Hence the author suggests that the diffusion mechanism is one of interstitial diffusion of water molecules trapped in the lattice during crystal growth. Experiments are being conducted at present in this laboratory to determine the molecular diffusion parameters using C¹⁴ labelled acid.

The fact that similar diffusion characteristics were obtained in ice, in which it has been conclusively proved that the diffusion occurs by migration of the bulk molecule, suggests that in this system diffusion may indeed occur by the 'free' interstitial mechanism proposed by Onsager and Kunnels.⁹³

c. Diffusion in Acetic Acid.

Due to the cleavage properties of the crystals diffusion could not be measured along the hydrogen bonded chains and was, therefore, attempted perpendicular to them. Large variations in tritium diffusion rates were obtained, however, which were believed due to water adsorbed on the crystals as it had been shown in the previous section that this can greatly influence tritium diffusion in benzoic acid. The lowest diffusion co-efficient obtained was $1 \times 10^{-11} \text{ cm}^2 \text{ sec}^{-1}$ at 0°C hence this must represent an upper limit for bulk or intrinsic proton diffusion.

Due to the difficulties involved in handling this system it was abandoned.

d. Conclusions.

Proton transport is greatly enhanced in systems having co-operatively hydrogen bonded chains due to the low energy migration pathways they provide. The presence of moisture in all types of hydrogen bonded solids, however, can affect the observed proton migration process.

Attempted proton diffusion studies in benzoic acid single crystals using a tracer sectioning technique resulted in the discovery of a concentration dependent diffusion process which was concluded to be diffusion of impurity water molecules in the lattice by an interstitial mechanism. A lower limit for this process was observed which obeyed the Arrhenius equation.

$$D = 0.5^{\pm 2}_{-0.4} \exp \left[- \frac{20,000 \pm 1,300}{RT} \right]$$

This is believed due to intrinsic diffusion of water molecules trapped in the crystal during growth.

Bulk diffusion in benzoic acid obeyed the following Arrhenius equation

$$D = \left(1.8 \begin{array}{c} +7.6 \times 10^2 \\ -1.79 \end{array} \right) \times 10^{12} \exp \left[- \frac{44,000 \pm 4,000}{RT} \right]$$

from which it was concluded that a vacancy mechanism was operating in which molecular diffusion occurred through relaxed vacancies.

Diffusion and conductivity studies in acetic acid were found to

be very dependent on the water vapour present in the surrounding atmosphere.

These results indicate that the physical properties of systems containing hydrogen bonds may be greatly influenced by the presence of traces of moisture and that great care must be taken when intrinsic properties of such systems are being studied.

V e. Future Work

A logical extension of this work would be to determine the exact dependence of the tritium diffusion coefficient on water vapour by carrying out a series of diffusion experiments under controlled water vapour pressures. Due to the slow diffusion rate this may be more easily performed by a water vapour exchange technique.

An extension of this study to other hydrogen bonded solids is desirable to verify that such an interstitial diffusion of water in a regular close packed lattice is not confined to organic acids.

Verification of proton diffusion by a tracer technique should be attempted in a system which exhibits a sufficiently high conductivity for proton diffusion to be measurable by a tracer sectioning technique. A suitable crystal for such a study might be Ammonium dihydrogen phosphate.

REFERENCES

1. F. Seitz, "The Modern Theory of Solids"; McGraw-Hill N.Y. 1940
2. J.J. Brophy and J.W. Buttrely (EDS) "Organic Semiconductors"
McMillan N.Y. 1962
3. H. Kallman and M. Silver (EDS) "Symposium on Electrical
Conductivity in Organic Solids" Duke University 1960
Interscience N.Y. 1961.
4. R.G. Kepler, Phys. Rev. 1960 119 1226
5. N. Riehl, Ref. 3 p. 61.
6. D.D. Eley, D.G. Parfitt, M.J. Perry and D.H. Taysum, Trans.
Faraday Soc. 1953 49 79
7. A.I. Kitaigorodskii "Organic Chem. Crystallography" p. 55 Consultant
Bureau ~~is~~ 1961
8. G.C. Pimental and A. L. McClellan, "The hydrogen bond"
Freeman 1960.
9. A.R. Ubbelohde and K.J. Gallacher, Acta Cryst. 1955 3 71
10. M. Eigen and L. De Meyer, Proc. Roy. Soc. 1958 A247 505
11. R. A. Horne, J. Inorg. Nuclear Chem. 1963 25 1139
12. Y. Kakiuchi, H. Komatsu and S. Kyoya, J. Chem. Phys. 1951 19 132
13. C.P. Smyth in "Physics and Chemistry of the Organic Solid State".
(Fox, Labes and Weissberger, (EDS)) Vol.1. p.728 Interscience
1963.
14. J. McC. Pollock and A.R. Ubbelohde. Trans. Faraday Soc. 1956
92 112
15. M.H. Cardow and D.D. Eley. Disc. Faraday Soc. 1959 27 115
16. D.D. Eley and R.B. Leslie "Adsorption of Water on Solid Protein".
Advances in Chemical Physics V7 p.238 (Machesno ED) Interscience
1960.
17. G. King and J. A. Medley. J. Coll. Sci. 1949 4 9
18. D.D. Eley and D. Spivey. Nature 1960 186 725
19. J.C. Decroly, H. Granicher, C. Jaccard, Helv. Phys. Acta
1957 30 465
20. A. Steinmann. Helv. Phys. Acta 1957 30 581
21. C. Jaccard, Helv. Phys. Acta 1959 32 89
22. G.P. Brown and S. Aftergut Ref. 2 p.69.
23. H.B. Liddiard "Handbuch Der Physik" V20 S. Flugge ED.
Springer-Verlag Berlin 1957
24. D. Mapother, H.N. Crooks and R. Maurer, J. Chem. Phys. 1950
18 1231

25. E. Fabbri, E. Lazzarini and V. Sanguist, Int. J. Applied
Rad.I. 1964 15 437
26. M. Eigen, L. De Meyer and H. C. Spatz, "Colloquium on the
Physics of Ice Crystals" Erlenbach-Zurich 1962.
27. G.A. Sim, J.M. Robertson and T. H. Goodwin Acta Cryst. 1955 8 157
28. A.N. Winchell "Optical Properties of Organic Crystals".
University of Wisconsin Press. 1943.
29. R.E. Jones and D. Templeton. Acta Cryst. 1958 11 487
30. R. G. W. Wyckoff "Crystal Structures" Fig. XI VA, 30a,
Interscience 1960.
31. F. A. Kröger, "The Chemistry of Imperfect Crystals". North-
Holland Publishing Co. Amsterdam 1964.
32. H. E. Buckley. "Crystal Growth", p.54 Wiley N.Y. 1952.
33. Ibid. p.339.
34. G. E. Gottlieb, J. Electrochem. Soc. 1965. 112 903
35. S. Kyropoulos, Z. Anorg, Chem. 1926 154 308
36. P. W. Bridgman. Proc. Amer. Acad. Arts. Sci. 1925 60 305
37. H. C. Kremers, J. Opt. Soc. Am. 1947 37 337
38. J. N. Sherwood and S. J. Thomson, J. Sci. Inst. 1961 37 242
39. K.T.B. Scott, S. K. Hutchinson and R. Lapage, A.W.R.E.
Report No. O-4/53.
40. K. E. Wiberg "Laboratory Techniques in Organic Chemistry".
McGraw-Hill 1960.
41. P. W. Schwab and E. Wichers, J. Research N.B.S. 1940 25 747
42. W. G. Pfann, J. Metals 1952 4 747
43. N. B. Hannay (ED) "Semiconductors". Reinhold N.Y. 1959.
44. H. C. Wolf and H. P. Deutsch. Naturwiss. 1954 41 423
45. G.J. Sloan in "Physics and Chemistry of the Organic Solid State",
Volume I (ED. D. Fox. M. M. Labes and A. Weissberger.) p.179
Interscience N.Y. 1963.
46. I. Braun. Brit. J. Appl. Phys. 1957 8 457
47. W. G. Pfann "Zone Melting". Wiley. N.Y. 1958.

48. R. Jessup. Quoted in Ref. 11.
49. W. D. Lawson and S. Nielsen "Preparation of Single Crystals"
Butterworth London 1958.
50. S. K. Hutchinson and R. Lapage. A.W.R.E. Report No. O-73/54.
51. G. M. Hood and J. N. Sherwood. Brit. J. Appl. Physics. 1963 14 21
52. A. J. Goss and S. Weintraub Nature 1951 167 349.
53. J. N. Sherwood. Ph. D. Thesis. University of Durham. 1959.
54. F. W. Schwab and E. Wichers. J. Research N. B. S. 1945 34 333
55. L. W. Pickett. Proc. Roy. Soc. 1933 A.142 333.
56. A. E. Gilliam. D. H. Hey, A. Lambert, J. Chem. Soc. 1941 364.
57. J. M. Robertson and A. R. Ubbelohde. Proc. Roy. Soc (London)
1939 A170 222
58. J. Mitchell, D. M. Smith. "Aquometry" Interscience 1956.
59. F. W. Schwab, E. Wichers, J. Research N.B.S. 1944 33 121
60. L. Lyons, "Guide to Activation Analysis" Van Nostrand 1964.
61. "The Radiochemical manual" Part 1. p.18 and 56, The radiochemical
Centre. Amersham. England. 1962.
62. G. E. Crouthamel "Gamma Ray Spectrometry".
63. ref. 40 P.249
64. H. Steinmetz, Z. Kristallogr. 1921 56 160
65. F. G. Shewmon "Diffusion in Solids". McGraw-Hill 1963.
66. J. N. Sherwood and D. J. White "International Symposium on
Organic Crystals". Chicago. May 1965.
67. C. Leymonie "Traceur Radioactifs En Metallurgie Physique".
Dunod. Paris 1960
68. W. Jost "Diffusion" Academic Press. N.Y. 1960.
69. Ibid. P.16.
70. A. Smigelskas and E. Kirkendall. Trans. A.I.M.E. 1947 171 130
71. W. Kuhn and M. Thurkauf, Helv. Chim. Acta 1958 41 938
72. Handbook of Chemistry and Physics, 43rd Edition. p.2403,2420
Chemical Rubber Publishing Co. 1961-2.
73. O. Dengel and N. Riehl, "Colloquium on the Physics of Ice Crystals"
Erlenbach - Zurich 1962.

74. R. E. Pawel and T. S. Lundy, J. Phys. Chem. Solids 1965 26 937
75. G. M. Hood. Ph. D. Thesis. University of Glasgow 1963.
76. C. H. Lee, H. K. Kevorkian, P. S. Reucroft and M. M. Labes
J. Chem. Phys. 1965 42 1406
77. H. E. Ungnade and R. W. Lamb. J. Amer. Chem. Soc. 1962 74 3789
78. M. L. Eidenhoff, Anal. Chem. 1950 22 529
79. C. G. Bell and N. F. Hayes "Liquid Scintillation Counting"
Pergamon 1958.
80. J. D. Davidson and P. Feigelson. Int. J. Applied Rad'n. I. 1957 2 1
81. E. Schram, "Organic Scintillation Detectors". p 86 Elsevier
1963.
82. D. L. Williams, F. N. Hayes, R. J. K'Ardeh and W. M. Roger,
Nuceonics 1956 14 62
83. J. C. Fisher. J. Applied Phys. 1951 1 74
84. R. T. Whipple. Phil Mag. 1954 45 1225
85. A. D. Le Claire "Conference on Diffusion and Mass Transport
in Solids", Reading 1962. Brit. J. Applied Physics 1962 13 433
86. P. G. Shewmon. Ref. 65 p.171.
87. W. Feltknecht, A. Wyttenbach, W. Buser, "Reactivity of
Solids", (De Boers, ED) p.234. Elsevier 1961
88. Y. Wei and R. B. Bernstein. J. Phys. Chem. 1959 63 738
89. K. Itagaki. J. Phys. Soc. Japan. 1964 19 1081
90. N. Riehl. Private Communication.
91. H. Granicher, Phys. Kondens. Materie. 1963 1 1
92. C. Mass. Phys. Letters 1962 3 126
93. L. Onsager and L. K. Runnels. Proc. Nat. Acad. Sci. 1963 50 208
94. D. D. Eley and D. I. Spivey. Trans. Faraday Soc. 1961 57 2280
95. N. Bjerrum. Science A52 115 385
96. E. J. Murphy. J. Applied. Phys. 1964 35 2609
97. D. D. Eley. A. S. Fawcett and M. R. Willis. Nature 1963
200 255
98. S. Kondc and T. Oda. Bull. Chem. Soc. Japan. 1964 27 567
99. A. Spagnol, Z. Electrochem. 1955 59 31.
100. J.N. Sherwood and S.J. Thomson. Trans. Faraday Soc. 1960 56 1443

101. R.C. Jarnagin and J.N. Sherwood "International Symposium on Organic Crystals" Chicago 1965.
102. C.H. Lee, H.K. Kevorkian, P.S. Reucroft and M.M. Labes, J. Chem. Phys. 1965 42 1406
103. D.J. White, Private Communication.
104. G.M. Hood and J.N. Sherwood, "Conference on Molecular Motions and Phase Transitions in Molecular Crystals" Paris June 1965
To be published in J. Chim Phys.
105. A. Berne, G. Boato and M. de Pas, Il Nuovo Cimento 1962 24 1179
106. N.H. Nachtrieb and G.S. Handler, J. Chem. Phys. 1961 41 974
107. R.B. Cuddeback and H.G. Drickamer, J. Chem. Phys. 1951 19 790
108. K. Hoffe, 'Reactionen in und an Festen Stoffen' Berlin 1955
109. E. Cremer, Z. Physik Chem. 1938 B39 445
110. Ref. 65 Chapter 2. 1951 47 256
111. G.T. Furukawa, R.E. McCoskey and G.T. King, J. Research N.B.S.
112. D. Lazarus, Solid State Physics 10 116 Academic Press 1960
113. Ref. 68 p.116 1961 78 1449
114. P. Flubacher, A.J. Leadbetter and J.A. Morrison, Proc.Phys.Soc.
115. G.M. Hood and J.N. Sherwood, Molecular Crystals 1 (1966)
116. N.H. Nachtrieb and G.S. Handler, J.Chem.Phys. 1955 23 1187
117. M. Davies and J.I. Jones Trans. Faraday Soc. 1954 50 1042
118. L. Bigeleisen, Brookhaven Conference Report "Isotopic Exchange Reactions and Chemical Kinetics" Brookhaven National Laboratory (Long Island) N.Y.
119. Ref.65 p.147
120. R.M. Barrer, Trans. Faraday Soc. 1942 38 78
121. P. Meares, J. Amer. Chem. Soc. 1954 76 3415
122. P. Meares, Polymers : Structure and Bulk Properties Ch. 12
Van Nostrand London 1965.
123. E.A. Secco and W.J. Moore, J. Chem. Phys. 1957, 26 946
124. R.E. Carter and F.D. Richardson, J. Metals 1954 6 1244
125. Margeneau and Murphy 'Mathematics of Physics and Chemistry'
p.159 Van Nostrand N.Y. 1956.

APPENDIX I

The parameters m and c in the equation,

$$y = mx + c$$

were calculated by the method of least mean squares.¹²⁵

For a given set of n co-ordinated $x_1, y_1, x_2, y_2, \dots, x_n, y_n$

The gradient, m , is given by

$$m = \frac{\sum x \sum y - n \sum xy}{(\sum x)^2 - n \sum x^2}$$

and

$$c = \frac{\sum x \sum xy - \sum y \sum x^2}{(\sum x)^2 - n \sum x^2}$$

The error in m , pm , and the error in c , pc , can be calculated as follows.

The deviation of each point from the L.M.S. line, d , is

$$d = y_n - (m \cdot x_n + c)$$

The error in m is given by

$$pm = 0.6745 \left(\frac{\sum d^2}{n-2} \right)^{1/2} \left[(\sum x)^2 - n \sum x^2 \right]^{1/2}$$

The error in c is given by $pc = 0.6745 \left(\frac{\sum d^2}{n-2} \right)^{1/2} \left[\frac{\sum x^2}{(\sum x)^2 - n \sum x^2} \right]$

A computer programme was devised to calculate m , c , pm , pc .

This programme was used to calculate both diffusion coefficients and the parameters of the Arrhenius equation D_0 and E_a .

The computer used was a Ferranti 'Sirius'.

APPENDIX II

Calculation of the Diffusion Coefficient.

The solution of Fick's equation for the conditions used was

$$c/c_0 = \frac{1}{\sqrt{\pi Dt}} \cdot \exp \left[-\frac{x^2}{4Dt} \right]$$

$$\log_{10} c/c_0 = \log_{10} \frac{1}{\sqrt{\pi Dt}} - \frac{x^2}{2.303 \times 4Dt} = \log_{10} A$$

Hence the diffusion coefficient can be obtained from the gradient, m , of a plot of $\log_{10} A$ vs x^2

$$\therefore D = \frac{1}{2.303 \times m \times 4 \times t}$$

The gradient, m , was obtained by the method of least mean squares in Appendix I.

e.g. DR18 with $x = x^2 \times 10^6 \text{ cm}^2$, $Y = \log_{10} A$ (c.p.s./mg.)

x	Y	x^2	XY
0.25	1.129	0.0625	0.2823
2.25	1.056	5.0625	2.3760
6.25	1.000	39.0625	6.2500
12.20	0.964	148.8400	11.7608
20.30	0.908	412.0900	18.4324
30.20	0.910	912.0400	27.4820
42.30	0.878	1789.2900	37.1394
56.20	0.849	3158.4400	47.7138
72.30	0.812	5227.2900	58.7076
90.20	0.723	8136.0400	65.2146
132.00	0.383	17420.4000	50.5560
182.00	0.432	33120.4000	78.6240
240.00	0.137	57600.0000	32.8800
$\Sigma x = 886.45$	$\Sigma y = 10.181$	$\Sigma x^2 = 127900.7622$	$\Sigma xy = 437.4189$

$$m = 0.003803 \pm 0.000171$$

$$D = \frac{10^{-6}}{2.303 \times 4 \times (0.003803 \pm 0.000171) \times 165.7 \times 3600}$$

$$= 4.8 \pm .2 \times 10^{-11} \text{ cm}^2 \cdot \text{sec}^{-1}$$

APPENDIX III

Calculation of the Parameters of the Arrhenius Equation

$$D = D_0 \cdot \exp \left[-\frac{E_A}{RT} \right]$$

$$\log_{10} D = \log_{10} D_0 - \frac{E_A}{2.303 RT}$$

A plot of $\log_{10} D$ vs $1/T$ gives a straight line of gradient

$$m = -\frac{E_A}{2.303R} \quad \text{and intercept, } c = \log_{10} D_0$$

The gradient, intercept and their errors were obtained by the least mean squares computer programme.

For Tritium Diffusion in Benzoic Acid Fig.27 line A.

$$m = (4.710 \pm 0.370) \times 10^3$$

$$c = 2.244 \pm 0.994$$

$$\therefore E_A = 2.303 \times 1.98 \times (4.710 \pm 0.370) \times 10^3$$

$$= 21,200 \pm 2000 \text{ Kcal/mole}$$

$$D_0 = 175_{-157}^{+1,600}$$